Neutrinos and Some Aspects of Physics Beyond the Standard Model

By

Manimala Mitra
Harish-Chandra Research Institute, Allahabad

A Thesis submitted to the
Board of Studies in Physical Science Discipline
In partial fulfilment of requirements
For the degree of
DOCTOR OF PHILOSOPHY
of
Homi Bhabha National Institute

October, 2010

Certificate

This is to certify that the Ph.D. thesis titled "**Neutrinos and Some Aspects of Physics Beyond the Standard Model**" submitted by Manimala Mitra is a record of bona fide research work done under my supervision. It is further certified that the thesis represents independent work by the candidate and collaboration was necessitated by the nature and scope of the problems dealt with.

Date: **Dr. Sandhya Choubey**

Thesis Adviser

Declaration

This thesis is a presentation of my original research work. Whenever contributions of others are involved, every effort is made to indicate this clearly, with due reference to the literature and acknowledgement of collaborative research and discussions.

The work is original and has not been submitted earlier as a whole or in part for a degree or diploma at this or any other Institution or University.

This work was done under guidance of Dr. Sandhya Choubey, at Harish-Chandra Research Institute, Allahabad.

Date: **Manimala Mitra**

Ph.D. Candidate

To My Parents....

Acknowledgments

First and foremost, I would like to thank my adviser Dr. Sandhya Choubey for her able guidance and support during my Ph.D at Harish-Chandra Research Institute, Allahabad. She has constantly given me encouragement, has been very patient throughout my Ph.D years and motivated me for independent thinking. It has been a wonderful experience for me to learn physics from her and as well as to learn the technical minute details, which are essential parts of solving a research problem.

I would like to give my heartful thanks to Prof. Amitava Raychaudhuri and Prof. Ashoke sen, with whom I have discussed a lot on several intricate physics issues and clarified my doubts, whenever it was required. Learning physics from them has always been an enchanting experience. I am indebted to Dr. Srubabati Goswami for her active support, suggestions and the very enjoyable physics discussions. She has provided me with her insightful advice, whenever I needed. My special thanks goes to Prof. Raj Gandhi, it has been an excellent experience for me to come across his knowledge, deep physics insight and rigorous way of thinking during the last few years. I am grateful to Prof. Biswaup Mukhopadhyaya and Dr. Asesh Krishna Datta for several intense physics discussions, which has helped me a lot to get the clarification for the different subtle physics issues. It is a great pleasure to thank Prof. V. Ravindran. I have gained a lot of knowledge from him during my coursework and project. I would also like to thank Dr. Andreas Nyffeler.

My special thanks goes to Prof. Ashoke Sen and Rajesh Gopakumar for the excellent courses they have given. I am also grateful to the other course instructors of HRI, who have taught me the basic as well as several advanced subjects during my two years coursework period at HRI. I am indebted to Prof. Pinaki Majumdar for his support, which helped me a lot during my Ph.D years. The several talks and the intense discussions of our Pheno Lunch journal club has given me the exposure to different fields of research, which has broadened my research perspective.

I would like to convey my heartful thanks to all those who helped and advised me to carry out my research forward. Among them, I would like to specially mention my collaborators Prof. Steve F. King from University of Southampton and Dr. Biswajoy Brahmachari. On several occasions, I have discussed with Prof. Anjan Joshipura, Dr. Sudhir Vempati, Dr. Sourov Roy, Dr. Amol Dighe, Prof. Feruglio, Prof. Borut Bajc and Prof. Francesco Vissani and have been benefitted by their knowledge and physics insight. My thanks goes to all of them. I would also like to thank all the course and tutorial instructors of SERC 2008 school, held in IIT Mumbai, from which I have learned many good physics.

It has always been an enjoyable experience to discuss physics and even non-physics with students and post-docs of HRI. I have been extremely benefitted by the physics discussions with my collaborator Dr. Priyotosh Bandyopadhyaya. I would also like to mention Ramlal Awasthi. Physics discussion has always been enjoyable with him. I would like to thank Rajesh Kumar Gupta, Santosh Kumar Singh, Dr. Pomita Ghoshal, Anushree Ghosh, Atri Bhattacharya, Sanjoy Biswas, Satyanarayan Mukhopadhyay, Joydeep Chakraborty, Akhilesh Nautiyal, M C Kumar, Nishita Desai, Abhijit Bandyopadhyaya, Subhaditya Bhattacharya and Dr. Paramita Dey for very enjoyable physics as well as non-physics discussions. My special thanks goes to Archana S. Morye, Dr. Anupama Panigrahi and Atashi Das. Because of them, my five years stay at HRI has become much more enjoyable and meaningful. I would also like to thank all the students, post-docs and my friends of HRI with whom I have interacted, specially Shankha, Akansha, Shrobona, Swapnomoy, Nyayabanta, Arjun da, Nabamita di, Suvankar da, Arijit da, Siddhartha da, Shamik, Ushoshi, Shweta, Rachna, Sini and Bobo. A very heartful thanks goes to our music teacher Mr. Hanuman Prasad Gupta, Dr. Rukmini Dey and all the participants of our "Music and Poetry Session". My stay at HRI has become much more colourful because of them. My special thanks goes to Seema and Archana Madam. Spires, arXiv, Google, HRI computer and cluster section helped me in a significant way to carry out my research forward.

I express my deep gratitude to my parents and acknowledge with pleasure that without their love, affection and support, it would never have been possible for me to pursue my Ph.D work. I would also like to thank my close friends and relatives for being extremely supportive during my Ph.D years. I dedicate this thesis to my parents.

Synopsis

The standard model of particle physics which is based on the local gauge invariance of the gauge group $\mathrm{SU(3)_C} \times \mathrm{SU(2)_L} \times \mathrm{U(1)_Y}$ has been extremely successful in describing the electromagnetic, weak and strong interactions between elementary particles. The theory has been verified to a high degree of accuracy in collider experiments such as the Large Electron-Positron Collider (LEP) at CERN in Europe and the Tevatron at Fermilab, USA. The other very profound characteristic of the standard model of particle physics is renormalizibility, which emerges because of its underlying quantum field theoretical description. However, although this theory gives a number of correct predictions, there are still certain issues which it is unable to explain, hence the standard model is considered a low energy description of some fundamental theory. The standard model of particle physics cannot explain the observed small neutrino mass and the peculiar mixing. It does not give any candidate for the dark matter of the Universe. It also fails to explain the observed matter-antimatter asymmetry of the Universe. In addition, one of its major theoretical drawback is the hierarchy or the naturalness problem. The Higgs particle which is an essential ingredient of the standard model is not stable under quantum corrections. There is no symmetry to protect its mass and hence the mass of the Higgs gets a quantum correction $\delta m_h \sim 10^{18}$ GeV, assuming the validity of the standard model up to the Planck scale. Beyond standard model physics such as supersymmetry gives a very natural solution to the hierarchy problem. In the minimal supersymmetric extension of the standard model, every standard model fermion/scalar is accompanied by its scalar/fermionic superpartner and hence the scalar and fermionic contributions mutually cancel each other, stabilizing the Higgs mass. Other than this, standard model does not give gauge coupling unification. It unifies electromagnetic and weak interaction, but fails to unify the electroweak and strong interactions. Also, it does not include gravity.

Apart from these drawbacks, the mass hierarchy between the standard model particles is itself a puzzle. In the standard model, the left and right handed fermions interact with the Higgs via the gauge invariant Yukawa Lagrangian and their masses are generated when the Higgs takes a non-zero vacuum expectation value. The nonzero vacuum expectation value of the Higgs field breaks the $\mathrm{SU(2)_L} \times \mathrm{U(1)_Y}$ symmetry of the standard model down to $\mathrm{U(1)_{em}}$. The fermion masses in the standard model is determined by this nonzero vacuum expectation value and the Yukawa couplings. Although the mass generation mechanism is the same for all the standard model fermions, still there exist a $\mathcal{O}(10^6)$ hierarchy between the top and electron masses. With the inclusion of neutrino mass, the hierarchy gets much enhanced. A series of outstanding experiments like solar and atmospheric neutrino experiments, KamLAND, K2K, MINOS provide information about the standard model neutrino mass splittings and its very peculiar mixing angles. Combined with cosmological bound specially from WMAP data, the sum of the light neutrino masses are bounded within 0.19 eV while the observed solar and atmospheric mass splitting are $\Delta m^2_{21} \sim 7.59 \times 10^{-5}$ eV^{2}and $\Delta m^2_{23} \sim 10^{-3}$ eV^2 respectively. This extremely small neutrino masses ($<$ eV) point towards a 10^{12} order mass hierarchy between the top quark and the neutrino. Unlike the mixing in the quark sector, in the leptonic sector two of the mixing angles θ_{12} and θ_{23} are quite large ($\sin^2\theta_{12} \sim 0.32$, $\sin^2\theta_{23} \sim 0.46$) while at present there is an upper bound on the third mixing angle θ_{13} as $\sin^2\theta_{13} < 0.05$. The observed mixing angles are in very close agreement with the tribimaximal mixing pattern where the solar mixing angle is $\sin^2\theta_{12} = 0.33$, reactor mixing angle $\sin^2\theta_{13} = 0.0$ and the atmospheric mixing angle is maximal $\sin^2\theta_{23} = 0.5$. The maximal mixing angle θ_{23} and $\theta_{13} = 0$ point towards a possible $\mu - \tau$ symmetry in the neutrino sector. As mentioned before, standard model of particle physics does not shed any light if there is any fundamental principle governing this extremely small neutrino masses as well as the peculiar mixing. It is possible to extend the standard model by introducing gauge singlet neutrinos and to explain the observed neutrino mass as a consequence of the Dirac type of Yukawa interaction between this gauge singlet neutrinos, lepton doublet and the Higgs. However to explain the eV-neutrino mass one eventually will need a Yukawa coupling which is $\mathcal{O}(10^{12})$ order of magnitude suppressed as compared to the top Yukawa coupling, thereby again leading to another fine-tuning problem. All of these above mentioned problems including the necessity for the "natural explanation" of the small neutrino masses and mixing set the motivation to look for beyond standard model physics scenario.

Going beyond the standard model, seesaw mechanism can explain small neutrino masses very naturally, without fine tuning of Yukawa couplings to extremely small values. Considering the standard model as an effective low energy description, the only dimension-5 operator allowed by the standard model gauge symmetry is $y^2\frac{LLHH}{M}$. The dimension-5 operator involving the lepton doublets and the Higgs field is generated when the heavy modes of the fundamental theory get integrated out. After the electroweak symmetry breaking, this dimension-5 operator gives rise to the Majorana mass term $\frac{y^2v^2}{M}$ of the standard model neutrino. Since suppressed by the mass scale of the integrated-out heavy modes M, eV neutrino masses can be very naturally obtained even with large value of the Yukawa coupling y. Seesaw mechanism in its simplest version is of three types, depending on the heavy states which has been integrated out. type-I seesaw requires additional standard model gauge singlet Majorana neutrino, while type-II and type-III seesaw require SU(2) triplet Higgs and fermionic field ($\mathrm{SU(3)_C}$ singlet) with hypercharge $Y = 2$ and $Y = 0$ respectively. While the neutrino mass generation mechanism are identical for type-I and type-III seesaw, in type-II seesaw the neutrino mass ($\frac{y\mu v^2}{M^2}$) has an additional suppression due to the small lepton number violating coupling μ. The seesaw mechanism is well-fitted in the framework of grand unified theories. The other seesaw mechanisms such as inverse seesaw and double seesaw require additional particles as well as symmetries to justify the appropriate neutrino mass matrix.

In [1] we have build a model on type-III seesaw and have studied its detail phenomenology. The triplet fermions which transform as an adjoint representation of SU(2), contain two charged fermionic states ($\Sigma^{\pm}$) and one charge neutral Majorana fermionic states (Σ^0). Since the type-I and type-III seesaw use different $\mathrm{SU(2)_L} \times \mathrm{U(1)_Y}$ representations as the heavy modes, they offer distinct phenomenology. The gauge singlet right handed neutrino field of type-I seesaw interacts with the lepton and Higgs via the Yukawa Lagrangian, while its interaction with the gauge bosons is suppressed by the standard model neutrino-gauge singlet right handed neutrino mixing. Compared to this, the $\mathrm{SU(2)_L}$ triplet fermion interacts directly with the standard model gauge bosons through their kinetic term, as well as with the leptons and the Higgs via the Yukawa Lagrangian. Hence for the 100 GeV mass range, the triplet fermions can be produced copiously at LHC, opening up the possibility to test the seesaw at LHC. This 100 GeV triplet fermions can be accommodated within the SU(5) grand unified framework, where their SU(5) origin could be identified with 24_F representation of SU(5). Non-observation of proton decay and successful unification with this 24_F demand that the SU(2) triplet component of this 24_F should be of the order of few hundred GeV. Since the standard model neutrino masses are $M_\nu \simeq -Y_\Sigma^T M^{-1} Y_\Sigma v^2$, hence for triplet fermion mass $M = \mathcal{O}(10^2)$ GeV, the Yukawa coupling Y_Σ between the triplet fermions-Higgs doublet-leptonic doublet gets constrained as $Y_\Sigma \sim 10^{-6}$ by the eV neutrino mass. We show that the large Yukawa coupling and few hundred GeV triplet fermions are still possible with the addition of another $\mathrm{SU(2)_L}\times\mathrm{U(1)_Y}$ Higgs doublet to this existing setup [1].

In our model we have considered three sets of right handed triplet fermionic fields Σ_i, and one additional Higgs doublet Φ_2. In addition, we also have introduced one discrete Z_2 symmetry, softly broken by the Higgs potential. The additional Higgs field Φ_2 (Z_2 odd) has the same SU(2) and $\mathrm{U(1)_Y}$ transformations as the standard model Higgs doublet Φ_1(Z_2 even), only differing in its Z_2 charge assignment. Hence in the Yukawa Lagrangian, the additional Higgs field Φ_2 interacts only with the standard model leptons (Z_2 even) and the triplet fermions (Z_2 odd), whereas the standard model Higgs Φ_1 interacts with all other standard model fermionic fields. Due to the very specific nature of the Yukawa Lagrangian, the standard model neutrino and the triplet fermionic neutral component mixing is governed by the vacuum expectation value v' of the additional Higgs doublet. Hence small vacuum expectation value $v' \sim 10^{-4}$ GeV generates eV neutrino mass, even with large $\mathcal{O}(1)$ Yukawa coupling Y_Σ. In the charged lepton sector, the mixing between the standard model charged leptons and the triplet fermions is governed by the Yukawa coupling Y_Σ and the VEV v', however the standard model charged lepton masses are determined by the large vacuum expectation value $v \sim 100$ GeV of the standard model Higgs doublet. In this model the quark sector remains the same as the standard model and the quark masses are governed by the same vacuum expectation value v. The choice of the small vacuum expectation value of the additional Higgs field has a significant impact on determining the Higgs mass spectra and the mixing angle between the neutral Higgses. With two Higgs doublets the Higgs sector in our model is enriched with five physical degrees of freedom (H^0, h^0, A^0, $H^{\pm}$). Working within the framework of a softly broken Z_2 symmetry, the mass of the light Higgs h^0 is determined by the standard model Higgs vacuum expectation value ($v \sim 10^2$ GeV) as well as by the extent of the Z_2 symmetry breaking coupling λ_5, whereas all the other Higgs masses are governed by the standard model Higgs vacuum expectation value v. Hence, in our model it is possible to accommodate a light Higgs state h^0. However, the presence of the light Higgs does not violate the LEP bound, due to the vanishing $Z - Z - h^0$ coupling. Due to the order of magnitude difference between the two vacuum expectation values v and v', the mixing angle α between the two neutral Higgs h^0 and H^0 is proportional to the ratio of the two vacuum expectation values ($\tan\beta = \frac{v'}{v}$) and is extremely small $\tan 2\alpha \sim \tan\beta \sim 10^{-6}$.

As compared to the type-I seesaw, type-III seesaw offers much richer phenomenology due to its direct interactions with the leptons, Higgs and also with the gauge bosons. Triplet fermion production at the LHC is mostly governed by the gauge boson mediated partonic subprocesses. Once produced, the triplet fermion can decay to different final state particles such as to a lepton+Higgs or to a lepton+ gauge boson. In our model, due to the large Yukawa coupling Y_Σ and small value of the mixing angle α as well as $\tan\beta$, the triplet fermions ($\Sigma^\pm$, Σ^0) decay predominantly into standard model leptons along with the neutral and charged Higgses h^0, A^0, $H^\pm$. The other decay modes where triplet fermions decay into a standard model lepton along with the neutral Higgs H^0 or the standard model gauge bosons is highly suppressed. The dominant decay of the triplet fermion into a standard model lepton and a Higgs h^0, A^0, $H^\pm$ is 10^{11} times larger compared to the one Higgs doublet type-III seesaw scenario. Another feature of our model is that it is possible to relate the neutrino phenomenology with the triplet fermions decay. In particular, the exact or approximate $\mu - \tau$ symmetry in the neutrino sector distinguishes among the different leptonic states when the triplet fermion decays into a standard model lepton and a Higgs. The $\mu - \tau$ symmetry in the neutrino sector provide equal opportunity to μ and τ states to be the leptonic final states, whereas it forbids the electron state e. In the Higgs sector, the different Higgs decay modes are governed by the Yukawa couplings and also by the small mixing angle α as well as $\tan\beta$. The neutral Higgs predominantly decays to $2b$ while the dominant decay mode for the charged Higgs $H^\pm$ is $H^\pm \to W^\pm h^0$. Other than this, a distinctive feature of our model is the displaced vertex of the Higgs h^0. Unlike the type-III seesaw with one Higgs doublet, in our model the triplet fermions do not have any displaced vertex. The type-III seesaw with two Higgs doublet can be verified at LHC via the different collider signatures which this model offers.

The observed data on solar and atmospheric neutrino mass splitting constraint the number of triplet fermion generation to be minimally two. However the R-parity violating supersymmetric framework enables a viable description of the neutrino mass and mixing even with one generation of triplet matter chiral superfield which has R-parity -1 [2]. R-parity which is a discrete symmetry is defined as $R_p = (-1)^{3(B-L)+2S}$ and has been implemented in the minimal supersymmetric extension of the standard model to forbid the baryon number ($\hat{U}^c\hat{D}^c\hat{D}^c$) and the lepton number violating ($\hat{L}\hat{L}\hat{E}^c$, $\hat{L}\hat{Q}\hat{D}^c$) operators.

Non-observation of proton decay constraints the simultaneous presence of lepton and baryon number violation, however leaving some space for the individual presence of either of these two. To accommodate the Majorana mass term of the standard model neutrino, lepton number violation is required. Spontaneous violation of R-parity meets both ends, it generates neutrino mass and satisfies the proton decay constraint, as in this scheme, the R-parity violating operators are generated very selectively. In our model R-parity is spontaneously broken by the vacuum expectation value of the different sneutrino fields. As a consequence, only the lepton number violating bilinear operators are generated while working in the weak basis. Sticking to the framework of the perturbative renormalizable field theory, the baryon number violating operators ($\hat{U}^c\hat{D}^c\hat{D}^c$) would never be generated, hence naturally satisfying the proton decay constraint. Because of the R-parity violation, the standard model neutrinos ν_i mix with the triplet fermion Σ^0, as well as with the Higgsino $\tilde{h}_u^0$ and gauginos $\tilde{\lambda}_{3,0}^0$. Hence, in our model we have a 8×8 color and charge neutral fermionic mass matrix. With one generation of the triplet matter chiral superfield and the R-parity violation, two of the standard model neutrino masses can be generated as a consequence of the conventional seesaw along with the gaugino seesaw, while the third neutrino still remains massless. Hence, in this scenario viable neutrino masses and mixings are possible to achieve. In addition, the standard model charged leptons ($l^{\pm}$), triplet fermions ($\Sigma^{\pm}$) and the charginos ($\tilde{\lambda}^{\pm}, \tilde{h}_{u,d}^{\pm}$) mixing is also determined by the different R-parity violating vacuum expectation values, as well as the different couplings of the superpotential. Hence, the charged lepton mass matrix is an extended 6×6 matrix. In our model the spontaneous violation of R-parity is not associated with any global U(1) lepton number breaking. Hence, the spontaneous R-parity violation does not bring any problem of Majoron.

While the smallness of the neutrino mass can be explained via the seesaw mechanism, the very particular mixing of the standard model neutrinos can be well explained by invoking a suitable flavor symmetry. Among the widely used flavor symmetry groups, A_4 and S_3 are very promising ones. A_4 is an alternating group where the group elements correspond to even permutation of four objects. This symmetry group has three different one dimensional (1,$1'$ and $1''$) and two three dimensional irreducible representations, and has one Z_2 and Z_3 subgroups. The symmetry group A_4 can be used to produce the tribimaximal mixing and viable neutrino mass splitting by introducing additional standard model gauge singlet Higgs fields, which transform as three as well as one dimensional irreducible representation of A_4 [3]. These gauge singlet Higgs fields which are charged under the flavor symmetry group are denoted as flavon. In our model [3] we have two flavon fields $\phi_{S,T}$ which transform as three dimensional irreducible representation of the group A_4. In addition, we also have three other flavons ξ, ξ', ξ'' which transform as 1, $1'$ and $1''$ respectively. The Lagrangian describing the Yukawa interaction between the different standard model leptons, Higgs and the flavons follows the effective field theoretical description. The different flavon fields take the vacuum expectation values, thereby resulting in a spontaneous breaking of the symmetry group A_4. The A_4 triplet field ϕ_S can alone generate the tribimaximal mixing in the neutrino sector if all the vacuum expectation values v_{s_i} of its component fields are equal. However it gives the atmospheric mass splitting $\Delta m^2_{31} = 0$, and hence is clearly incompatible with the neutrino oscillation data. To generate viable neutrino mass splittings in association with tribimaximal mixing, the one dimensional representations has to be included. Although the representation 1 is the minimalistic choice to recover the correct mass, this particular choice ends up with a severe fine-tuning between the different parameters of the theory. Other than this, the normal hierarchy ($\Delta m^2_{31} > 0$) between the standard model neutrino masses is the only allowed possibility. The fine-tuning between the parameters can be reduced by introducing additional one dimensional flavon fields ξ' and ξ''. Along with the triplet ϕ_S, the combination of the one dimensional flavon fields (ξ', ξ'') and (ξ, ξ', ξ''), and with certain relations between the different vacuum expectation values and Yukawa couplings generate tribimaximal mixing as well as viable mass splittings. In this set up both normal ($\Delta m^2_{31} > 0$) and inverted ($\Delta m^2_{31} < 0$) hierarchies are possible. Deviation from the particular relations between the different Higgs vacuum expectation values and Yukawa couplings will lead to deviation from tribimaximal mixing. In the charged lepton sector the diagonal charged lepton mass matrix emerges as a consequence of an additional discrete symmetry Z_3, as well as the vacuum alignment of the flavon field ϕ_T.

The symmetry group S_3 is a permutation group of three objects and is the smallest non-abelian symmetry group. This group has two distinct one dimensional and one two dimensional irreducible representations, along with one Z_3 and three Z_2 subgroups. In [4] we have constructed a flavor model based on the symmetry group S_3, which reproduces the observed neutrino mass and mixing, as well as the standard model charged lepton mass hierarchy. We use two SU(2) Higgs triplets (Δ) with hypercharge $Y = 2$, arranged in a doublet of S_3, and the standard model singlet Higgs (ϕ_e, ξ) which are also put as doublets of S_3. Due to the appropriate charge assignment under additional discrete symmetry groups Z_4 and Z_3, the flavon ϕ_e enters only in the charged lepton Yukaw Lagrangian, whereas the other flavon ξ enters both in the neutrino as well as in the charged lepton Yukawa interaction. The Higgs triplets Δ and the flavon field ξ take vacuum expectation value, and generate standard model neutrino masses. To reproduce the observed lepton masses and mixings, the symmetry group S_3 has to be broken such that the neutrino sector contains the exact/approximate Z_2 symmetry along the $\nu_\mu - \nu_\tau$ direction, while it is broken down maximally in the charged lepton sector. This particular feature is achieved by the vacuum alignments of the different Higgs fields Δ, ϕ_e and ξ. Exact $\mu - \tau$ symmetry in the neutrino mass matrix is achieved as a consequence of the vacuum alignments $\langle \Delta_1 \rangle = \langle \Delta_2 \rangle$ and $\langle \xi_1 \rangle = \langle \xi_2 \rangle$, otherwise resulting in mildly broken $\mu - \tau$ symmetry. These vacuum alignments have been discussed in the scalar potential. The mild breaking $\mu - \tau$ symmetry opens up the possibility of CP violation in the leptonic sector. The charged lepton sector offers very tiny contribution to the physically observed PMNS mixing matrix, while the main contribution comes from the neutrino mixing matrix. In the neutrino sector both normal and inverted hierarchy are allowed possibilities. Since the Higgs triplet Δ

interacts with the gauge bosons via their kinetic terms, they can be produced at the LHC and then can be traced via their subsequent decays. The doubly charged Higgs can decay to different states such as dileptons, gauge bosons, singly charged Higgs H^+. In our model the mixing between the two doubly charged Higgs is very closely related with the extent of the $\mu - \tau$ symmetry in the neutrino sector. In the exact $\mu - \tau$ limit the mixing angle θ between the two doubly charged Higgs is $\theta = \frac{\pi}{4}$, whereas mild breaking of the $\mu - \tau$ symmetry results in a mild deviation $\theta \sim \frac{\pi}{4}$. This close connection between the $\mu - \tau$ symmetry and the doubly charged mixing angle significantly effects the doubly charged Higgs-dileptonic vertices. In the exact $\mu - \tau$ limit, the vertex factors $H_2^{++} - \mu - \tau$ and $H_2^{++} - e - e$ are zero, hence the doubly charged Higgs H_2^{++} never decays to $\mu^+ + \tau^+$ or to $2e^+$ states. Other than this, the non observation of the $e\mu$ and $e\tau$ states in the dileptonic decay of the doubly charged Higgs would possibly disfavor the inverted mass hierarchy of the standard model neutrino. We have very briefly commented about lepton flavor violation in our model.

Bibliography

[1] **Two Higgs doublet type III seesaw with $\mu - \tau$ symmetry at LHC,**
P. Bandyopadhyay, S. Choubey and M. Mitra,
JHEP **0910**, 012 (2009) [arXiv:0906.5330 [hep-ph]].

[2] **Spontaneous R-parity violating type III seesaw,**
S. Choubey and M. Mitra,
JHEP **1005**, 021 (2010) [arXiv:0911.2030 [hep-ph]].

[3] **$\mathbf{A_4}$ flavor symmetry and neutrino phenomenology,**
B. Brahmachari, S. Choubey and M. Mitra,
Phys. Rev. D **77**, 073008 (2008) [arXiv:0801.3554 [hep-ph]].

[4] **Lepton masses in a minimal model with triplet Higgs bosons and S_3 flavor symmetry,**
M. Mitra and S. Choubey,
Phys. Rev. D **78**, 115014 (2008) [arXiv:0806.3254 [hep-ph]].

Publication and Preprints

1. **Two Higgs doublet type III seesaw with $\mu - \tau$ symmetry at LHC,**
   P. Bandyopadhyay, S. Choubey and M. Mitra,
   JHEP **0910**, 012 (2009) [arXiv:0906.5330 [hep-ph]].

2. **Spontaneous R-parity violating type III seesaw,**
   S. Choubey and M. Mitra,
   JHEP **1005**, 021 (2010) [arXiv:0911.2030 [hep-ph]].

3. **$\mathbf{A_4}$ flavor symmetry and neutrino phenomenology,**
   B. Brahmachari, S. Choubey and M. Mitra,
   Phys. Rev. D **77**, 073008 (2008) [arXiv:0801.3554 [hep-ph]].

4. **Lepton masses in a minimal model with triplet Higgs bosons and S_3 flavor symmetry,**
   M. Mitra and S. Choubey,
   Phys. Rev. D **78**, 115014 (2008) [arXiv:0806.3254 [hep-ph]].

5. **Spontaneous R-Parity Violation, A_4 Flavor Symmetry and Tribimaximal Mixing [1],** *M. Mitra*, arXiv:0912.5291 [hep-ph].

[1] Not included in the thesis

Contents

Chapter 1

Introduction

1.1 Standard Model of Particle Physics

The standard model of particle physics, established by Glashow-Weinberg-Salam [1, 2] in the 1960's has been extremely successful in decscribing the microscopic nature of the elementary particles. The model is based on the gauge group $\mathrm{SU}(3)_C\times$ $\mathrm{SU}(2)_L\times$ $\mathrm{U}(1)_Y$ and successfully unifies the electromagnetic and weak interaction of nature. The fermionic particle contents of the standard model and their transformation properties under the standard model gauge group are the following,
$Q_L = \begin{pmatrix} u_L \\ d_L \end{pmatrix} \equiv (3, 2, \frac{1}{3})$, $u_R \equiv (3, 1, \frac{4}{3})$, $d_R \equiv (3, 1, -\frac{2}{3})$,
and
$L = \begin{pmatrix} \nu_L \\ e_L \end{pmatrix} \equiv (1, 2, -1)$, $e_R \equiv (1, 1, -2)$.
In the standard model there are 12 gauge bosons and three family of fermions. The gauge fields of the standard model are the gauge bosons W^i_μ, B_μ and the gluons G^a_μ, where μ, ν are the Lorentz indices, $i = 1, 2, 3$ is the SU(2) gauge index and $a = 1, ..8$ is the SU(3) color index. The gauge field Lagrangian of the standard model is,

$$\mathcal{L} = -\frac{1}{4} \sum_{i=1,2,3} W^i_{\mu\nu} W^{i\mu\nu} - \frac{1}{4} B_{\mu\nu} B^{\mu\nu} - \frac{1}{4} \sum_{a=1,...8} G^a_{\mu\nu} G^{a\mu\nu}, \tag{1.1}$$

where the $\mathrm{SU(2)_L}$, $\mathrm{SU(3)_C}$ and $\mathrm{U(1)_Y}$ field strengths $W^i_{\mu\nu}$, $G^a_{\mu\nu}$ and $B_{\mu\nu}$ are respectively the following,

$$\begin{aligned} W^i_{\mu\nu} &= \partial_\mu W^i_\nu - \partial_\nu W^i_\mu + g\epsilon^{ijk} W^j_\mu W^k_\nu, \\ G^a_{\mu\nu} &= \partial_\mu G^a_\nu - \partial_\nu G^a_\mu + g_s f^{abc} G^b_\mu G^c_\nu, \\ B_{\mu\nu} &= \partial_\mu B_\nu - \partial_\nu B_\mu. \end{aligned} \tag{1.2}$$

In the above equations the $\mathrm{SU}(2)_L$ and the $\mathrm{SU}(3)_C$ gauge coupling constants are represented by g and g_s respectively. The gauge invariance of the standard model forbids us to write the bare mass term of the gauge bosons as,

$$\mathcal{L}_m = mF_\mu F^\mu \tag{1.3}$$

where F_μ generically represents the gauge fields W^i_μ, B_μ and G^a_μ. The term in Eq. (1.3) does not respect the gauge symmetry and hence is not allowed in the theory. Therefore, in the absence of any mass term of the gauge bosons, we should have twelve massless gauge bosons in the standard model. However, it is experimentally verified to a very large degree of accuracy through the experiments at LEP, CERN and Tevatron, Fermilab that in nature there are three massive gauge bosons $W^\pm$ and Z. In the standard model, the masses of the gauge bosons are generated by the novel Higgs mechanism via spontaneous symmetry breaking (SSB). For this purpose an $\mathrm{SU(2)_L}$ scalar doublet with hypercharge $Y = +1$ which is SU(3) gauge singlet has been included in the standard model. The Higgs spontaneously breaks the electroweak subgroup of the standard model gauge group to an $\mathrm{U(1)_{em}}$ subgroup, thereby generating three massive gauge bosons. We discuss the Higgs mechanism and fermion mass generation in the following subsection.

1.1.1 Higgs Mechanism and Fermion Mass

In the standard model the Higgs which is an $\mathrm{SU(2)_L}$ complex scalar doublet with hypercharge $Y = +1$ is denoted as,

$$H = \begin{pmatrix} H^+ \\ H^0 \end{pmatrix} \tag{1.4}$$

and transforms as $(1, 2, +1)$ under the standard model gauge group $\mathrm{SU(3)_C} \times \mathrm{SU(2)_L} \times \mathrm{U(1)_Y}$. The neutral component of Higgs takes vacuum expectation value (VEV) v, breaking the $\mathrm{SU(2)_L} \times \mathrm{U(1)_Y} \to \mathrm{U(1)_{em}}$ spontaneously. The spontaneous breaking of the continuous gauge symmetry generates three massive gauge bosons $W^\pm_\mu$ and Z_μ [3]. The photon A_μ and the gluon G^a_μ remain massless due to the $\mathrm{U(1)_{em}}$ symmetry and the unbroken $\mathrm{SU(3)_C}$ symmetry. The gauge-invariant Lagrangian of the scalar field is,

$$\mathcal{L} = (D^\mu H)^\dagger (D_\mu H) - V(H), \tag{1.5}$$

where the covariant derivative D^μ is

$$D_\mu H = (\partial_\mu - \frac{i}{2} g W^j_\mu . \tau^j - \frac{iY_H}{2} g' B_\mu) H. \tag{1.6}$$

In the above equation τ^j are the Pauli matrices, Y_H is the hypercharge of the Higgs field and g and g' are the $\mathrm{SU(2)_L}$ and $\mathrm{U(1)_Y}$ coupling constants. The potential of the Higgs field H is

$$V(H) = -\mu^2 H^\dagger H + \lambda (H^\dagger H)^2. \tag{1.7}$$

For positive μ^2 and λ, the Higgs field takes non-zero VEV v

$$\langle 0|H|0\rangle = \begin{pmatrix} 0 \\ v \end{pmatrix}; \quad v^2 = \frac{\mu^2}{2\lambda}. \tag{1.8}$$

The gauge boson masses are generated from the first term of Eq. (1.5) and are the following,

$$\mathcal{L} = M_W^2 W_\mu^+ W^{-\mu} + \frac{1}{2} M_Z^2 Z_\mu Z^\mu, \tag{1.9}$$

with

$$\begin{aligned} W_\mu^\pm &= \frac{W_\mu^1 \mp i W_\mu^2}{\sqrt{2}}, \\ M_W^2 &= \frac{g^2 v^2}{2}, \end{aligned} \tag{1.10}$$

and

$$\begin{aligned} Z_\mu &= \cos\theta_W W_\mu^3 - \sin\theta_W B_\mu, \\ \tan\theta_W &= \frac{g'}{g}; \quad M_Z^2 = \frac{v^2(g^2 + g'^2)}{2}. \end{aligned} \tag{1.11}$$

The angle of rotation θ_W is refereed as *Weinberg* angle and is related to the masses of the W and Z gauge bosons as,

$$\frac{M_W^2}{M_Z^2 \cos^2\theta_W} = 1. \tag{1.12}$$

The ratio $\frac{M_W^2}{M_Z^2 \cos^2\theta_W}$ is defined as the ρ parameter. Experimentally the measured value of the *Weinberg* angle is $\sin^2\theta_W = 0.23$ [4]. The other linear combination of W_μ^3 and B_μ is the photon A_μ

$$A_\mu = \cos\theta_W W_\mu^3 + \sin\theta_W B_\mu \tag{1.13}$$

which remain massless due to the $U(1)_{em}$ invariance. The vacuum expectation value v is $v \sim 174$ GeV in order to match the observed W and Z bosons masses, $M_W \sim 80.4$ GeV and $M_Z \sim 91.19$ GeV [4].

The Higgs gives masses not only to the gauge bosons, but also to the standard model fermions. Similar to the gauge bosons, one cannot write a bare mass term of the standard model fermions, because the bare mass term does not respect the gauge symmetry of the standard model. The fermion masses in the standard model are generated through the Yukawa Lagrangian which is

$$-\mathcal{L}_{Yuk} = Y^e \overline{L} H e_R + Y^u \overline{Q}_L \tilde{H} u_R + Y^d \overline{Q}_L H d_R + \text{h.c}, \tag{1.14}$$

where $\tilde{H} = i\tau_2 H^*$. The electron, up quark and down quark masses are generated from the above equation and are respectively the following,

$$m_e = Y^e v; \ m_u = Y^u v; \ m_d = Y^d v. \tag{1.15}$$

The neutrino has been considered massless in the standard model.

1.2 Problems of the Standard Model

Standard model gives a definite quantum description of the elementary particles. The model gives many successful predictions. For example, it predicts the existence of three massive gauge bosons which have experimentally been verified in LEP experiments at CERN, Geneva [5]. In addition, it predicts nine massless gauge bosons and the existence of massive quarks and leptons. Among its different successes one major success is the top quark discovery. Standard model predicted the existence of the top quark before it was discovered. The top quark was later observed at the Tevatron [6]. The electroweak properties of the standard model have been verified to a large degree of accuracy in experiments such as LEP and Tevatron [5, 6]. However,there are many issues which this theory does not explain or address. Here we list a few of them:

- A series of outstanding experiments like solar and atmospheric neutrino experiments, KamLAND, K2K, MINOS, CHOOZ provide information about the standard model neutrino mass splittings and its very peculiar mixing angles. Combined with cosmological bound specially from WMAP data, the sum of the light neutrino masses are bounded to 0.19 eV [7], while the observed solar and atmospheric mass splitting are $\Delta m^2_{21} \sim 10^{-5}$ eV^{2}and $\Delta m^2_{31} \sim 10^{-3}$ eV^2 respectively. This extremely small neutrino masses ($<$ eV) point towards a 10^{12} order mass hierarchy between the top quark and the neutrino. Other than the extremely small neutrino masses, the mixing in the leptonic sector is also a puzzle. Unlike the mixing in the quark sector, in the leptonic sector two of the mixing angles θ_{12} and θ_{23} are quite large ($\sin^2\theta_{12} \sim 0.32$, $\sin^2\theta_{23} \sim 0.46$) [8] while at present there is an upper bound on the third mixing angle θ_{13} as $\sin^2\theta_{13} < 0.05$ at 3σ Confidence Level (C.L) [8]. The observed mixing angles are in very close agreement with the tribimaximal mixing [9] pattern where the solar mixing angle is $\sin^2\theta_{12} = 0.33$, reactor mixing angle $\sin^2\theta_{13} = 0.0$ and the atmospheric mixing angle is maximal $\sin^2\theta_{23} = 0.5$. The maximal mixing angle θ_{23} and $\theta_{13} = 0$ points towards a possible $\mu - \tau$ symmetry [10] in the neutrino sector. The standard model of particle physics does not have any neutrino mass itself. In addition, the standard model does not shed any light if there is any fundamental principle governing this extremely small neutrino masses as well as the peculiar mixing. It is possible to extend the standard model by introducing gauge singlet neutrinos and to explain the observed neutrino mass as a consequence of the Dirac type of Yukawa interaction between this gauge singlet neutrinos, lepton doublet and the Higgs. However to explain the eV-neutrino mass one eventually will need a Yukawa which is $\mathcal{O}(10^{12})$ order of magnitude suppressed as compared to the top Yukawa, thereby leading to a fine-tuning problem. If the neutrino is a Majorana particle, then there is a very natural explanation to the smallness of the neutrino mass, which is the novel seesaw mechanism. The neutrino mass in this mechanism is generated from a dimension-5 operator and naturally suppressed by the mass scale of the new physics. The origin of such a higher dimensional operator requires some more ingredient than the standard model physics. We discuss in detail about the neutrino oscillation and mass generation in the next chapter.

- The fermion mass hierarchy is a puzzle in nature. In the standard model, all the fermion masses are generated identically, from a gauge invariant Yukawa Lagrangian. Still we have a $\mathcal{O}(10^6)$ order of magnitude mass hierarchy between top quark and electron masses. With the evidence of non-zero neutrino masses which are eV order, the hierarchy increases to $\mathcal{O}(10^{12})$. The standard model does not provide any answer to the mass hierarchy puzzle. Apart from this, there are 19 free parameters in the standard model. These are three lepton masses, six quark masses, three CKM mixing angles, one CP violating phase δ_{CKM}, three gauge coupling constants g, g' and g_S, the QCD vacuum angle θ_{QCD}, the Higgs quadratic coupling μ and self interacting Higgs quartic coupling λ. Except for the couplings μ and λ, the numerical values of all other parameters were fixed by experimental observation. With the inclusion of the neutrino mass, the number of free parameters increases even further. But, the standard model does not give any theoretical predictions for these parameters.

- One of the major theoretical drawback of the standard model is the hierarchy or the naturalness problem. The Higgs particle which is an essential ingredient of the standard model is not stable under quantum corrections. In the standard model the Higgs mass is not protected by any symmetry and the one loop correction to the Higgs mass is quadratically divergent. The one loop correction to the Higgs mass goes as Λ_{UV}^2, where the Λ_{UV} is the cut-off scale beyond which new physics is expected. Considering the validity of the standard model upto the Planck scale, the Higgs mass gets a quantum correction $\mathcal{O}(10^{18})$ GeV [11, 12]. Beyond standard model physics such as supersymmetry [11–13] gives a very natural solution to the hierarchy problem. We will discuss in detail the hierarchy problem and the minimal supersymmetric standard model in the next section.

- Cosmological and astrophysical observation suggest [14, 15] that the total matter density of the universe is $\Omega_M h^2 \sim 0.13$, while the observed baryonic matter density is $\Omega_h h^2 \sim 0.02$. Taken together, these observations strongly lead us to the conclusion that 80-85% [16] of the matter in the universe is non-luminous and non-baryonic dark matter. The standard model can not explain this dark matter abundance. Beyond standard model physics, for example minimal supersymmetric standard model provide a natural dark matter candidate.

- The universe is made by matter and not by antimatter. The observed value of the baryon asymmetry from the WMAP data and primordial nuclear abundance gives evidence for the matter and antimatter asymmetry $\frac{n_B}{n_\gamma} = (6.1 \pm 0.3) \times 10^{-10}$ [17]. If the universe has been started with a matter-antimatter symmetric state, then this baryon asymmetry is indeed a puzzle which the standard model cannot explain. The explanation certainly needs beyond standard model physics. One of the novel mechanism which can explain the baryon asymmetry of the universe is leptogenesis [18], which is inherently linked with the Majorana neutrino mass generation scheme, *i.e* the novel seesaw mechanism. In leptogenesis the lepton asymmetry is generated in the decay of standard model gauge singlet states(also SU(2) triplet states [19, 20]) [21], which gets converted into baryon asymmetry due to the presence of non-purturvative sphalaron transitions [22]. The same gauge singlet or SU(2) triplet fields generate the dimension-5 operator from which Majorana neutrino mass is generated. The detail about leptogenesis can be found in [17, 23].

- From experiments we know there are three generations of fermions in the standard model. However, theoretically standard model does not shed any light on the fermion generations.

- Aesthetically, we would like to have unification of the fundamental forces of nature. In nature we have the gravitational interaction, electromagnetic interaction, weak and strong interaction. Standard model unifies electromagnetic and weak interaction. But it fails to unify the other forces with the electroweak one and also it does not give a quantum description of gravity.

These above mentioned problems motivate one to look for beyond standard model physics scenarios. In the next section we discuss the minimal supersymmetric standard model. In chapter 2 we discuss the neutrino oscillation and neutrino mass generation in detail.

1.3 Minimal Supersymmetric Standard Model

Supersymmetry is a symmetry that transforms a boson into a fermion and vice versa. The main phenomenological motivation to extend the standard model into the minimal supersymmetric standard model lies in the quadratic divergence of the Higgs mass. In the standard model the Higgs mass is not protected by any symmetry and the one loop correction of the Higgs mass is quadratically divergent. The fermions which have Yukawa interaction with the Higgs as $\lambda_f H\overline{f}f$, contributes to the one loop correction to the Higgs mass as [11, 12]

$$\delta m_H^2 = -\frac{|\lambda_f|^2}{8\pi^2}\Lambda_{UV}^2 + ..., \tag{1.16}$$

where Λ_{UV} is the cut-off scale beyond which the new physics is expected. Considering the validity of the standard model upto the Planck scale, the Higgs mass gets a quantum correction $\mathcal{O}(10^{18})$. Cancellation of this divergences with the bare mass parameter would require fine-tuning of order one part in 10^{-18}, rendering the theory unnatural [11, 12]. This huge quantum correction due to fermionic contribution is cancelled by the scalar contribution, if we introduce scalar particle $\tilde{f}$ with the quartic interaction $\lambda_{\tilde{f}}|H|^2|\tilde{f}|^2$ and with the property $\lambda_{\tilde{f}} = |\lambda_f|^2$. Supersymmetry is the desired symmetry which naturally introduces a scalar particle $\tilde{f}$ for the fermionic field f with the same mass and the necessary criteria between the couplings $\lambda_{\tilde{f}} = |\lambda_f|^2$. The contribution of the $\tilde{f}$ scalar to the one loop correction of the Higgs mass is the following,

$$\delta m_H^2 = \frac{(\lambda_{\tilde{f}})}{8\pi^2}\Lambda_{UV}^2. \tag{1.17}$$

The total contribution to quadratic divergence of the Higgs mass in this case would be,

$$\delta m_H^2 = \frac{(\lambda_{\tilde{f}} - |\lambda_f|^2)}{8\pi^2}\Lambda_{UV}^2, \tag{1.18}$$

and hence will naturally vanish for $\lambda_{\tilde{f}} = |\lambda_f|^2$.

The operator Q that generates a supersymmetric transformation is an anticommuting spinor, with

$$Q|Boson\rangle = |Fermion\rangle, \tag{1.19}$$

and

$$Q|Fermion\rangle = |Boson\rangle \tag{1.20}$$

The hermitian conjugate of Q i.e $Q^\dagger$ is also a supersymmetry generator. Supersymmetry is a space-time symmetry and the possible form of supersymmetry is restricted by Haag-Lopuszanski-Sohnius extension of the Coleman-Mandula theorem [24]. For realistic theories like standard model, the theorem implies these following anticommutation and commutation relations between the different generators,

$$\begin{aligned} \{Q, Q^\dagger\} &= P^\mu \\ \{Q, Q\} &= \{Q^\dagger, Q^\dagger\} = 0 \\ [P^\mu, Q] &= [P^\mu, Q^\dagger] = 0, \end{aligned} \tag{1.21}$$

where P^μ is the four-momentum generator of spacetime translation.

The single particle state of supersymmetric theory fall into irreducible representations of the supersymmetric algebra, called supermultiplets. Each supermultiplet contains both fermionic and bosonic states, which are commonly known as superpartners of each other. Each supermultiplet or superfield contains equal number of bosonic and fermionic degrees of freedom with their masses to be equal. The supermultiplet which contains chiral fermions and gauge bosons are denoted as chiral superfield and vector superfield, respectively. In supersymmetry, a chiral superfield contains a Weyl fermion, a scalar and an auxiliary scalar field component denoted as F, whereas the vector superfield consists of the vector boson, its fermionic superpartner and an auxiliary scalar field D. Each MSSM chiral superfield is represented as,

$$\hat{\Phi} = \phi + \sqrt{2}\theta\tilde{\phi} + \theta\theta F_\phi, \tag{1.22}$$

where ϕ, $\tilde{\phi}$ are the scalar and fermionic fields and F_ϕ is the auxiliary field. The standard model is extended to the minimal supersymmetric standard model by introducing scalar and fermionic superpartners to each of the fermions and scalar of the standard model, respectively. The matter chiral superfield content of the MSSM and their $\mathrm{SU(3)_C \times SU(2)_L \times U(1)_Y}$ property are as follows,

$$\hat{Q}_i = \begin{pmatrix} \hat{U}_i \\ \hat{D}_i \end{pmatrix} \sim \begin{pmatrix} \tilde{u}_{L_i} & u_{L_i} \\ \tilde{d}_{L_i} & d_{L_i} \end{pmatrix} \equiv (3, 2, \tfrac{1}{3}), \quad \hat{L}_i = \begin{pmatrix} \hat{\nu}_i \\ \hat{E}_i \end{pmatrix} \equiv \begin{pmatrix} \tilde{\nu}_{L_i} & \nu_{L_i} \\ \tilde{e}_{L_i} & e_{L_i} \end{pmatrix} \equiv (1, 2, -1),$$

$$\hat{U}^c_i \equiv (\,\tilde{u}^c_i \quad u^c_i\,) \equiv (\bar{3}, 1, -\tfrac{4}{3}), \ \hat{D}^c_i \sim (\,\tilde{d}^c_i \quad d^c_i\,) \equiv (\bar{3}, 1, \tfrac{2}{3}) \text{ and } \hat{E}^c_i \sim (\,\tilde{e}^c_i \quad e^c_i\,) \equiv (1, 1, +2).$$

The Higgs chiral supermultiplets of the MSSM are,

$$\hat{H}_u = \begin{pmatrix} \hat{H}^+_u \\ \hat{H}^0_u \end{pmatrix} \equiv \begin{pmatrix} h^+_u & \tilde{h}^+_u \\ h^0_u & \tilde{h}^0_u \end{pmatrix} \sim (1, 2, +1), \quad \hat{H}_d = \begin{pmatrix} \hat{H}^0_d \\ \hat{H}^-_d \end{pmatrix} \sim \begin{pmatrix} h^0_d & \tilde{h}^0_d \\ h^-_d & \tilde{h}^-_d \end{pmatrix} \equiv (1, 2, -1).$$

The gauge multiplet of the MSSM corresponds to,

$$V^A_S \sim (\,g^A \quad \tilde{g}^A\,) \equiv (8, 1, 0), \quad V^i_W \sim (\,W^i \quad \tilde{W}^i\,) \equiv (1, 3, 0), \quad V_Y \sim (\,B \quad \tilde{B}\,) \equiv (1, 1, 0).$$

The Lagrangian of the MSSM is

$$\mathcal{L} = \int d^2\theta\, W + \int d^2\overline{\theta}\, \overline{W} + \int d^2\theta d^2\overline{\theta}\, \mathcal{K} + \int d^2\theta\, WW + \int d^2\overline{\theta}\, \overline{W}\,\overline{W}, \tag{1.23}$$

where $\mathcal{K}$ and W are the gauge invariant Kähler potential and superpotential respectively. The form of the gauge invariant Kähler potential is as the following

$$\mathcal{K} = \hat{\Phi}^\dagger e^{2gV}\hat{\Phi}, \tag{1.24}$$

where $\hat{\Phi}$ is the MSSM chiral superfield which transforms non-trivially under the gauge group with gauge coupling constant g. With all these particle contents the MSSM superpotential is given by,

$$W = W_{MSSM} + W_{\not{R}_p-MSSM}, \tag{1.25}$$

where W_{MSSM} and $W_{\not{R}_p-MSSM}$ are respectively the following,

$$W_{MSSM} = Y_e\hat{H}_d\hat{L}\hat{E}^c + Y_d\hat{H}_d\hat{Q}\hat{D}^c - Y_u\hat{H}_u\hat{Q}\hat{U}^c + \mu\hat{H}_u\hat{H}_d, \tag{1.26}$$

and

$$W_{\not{R}_p-MSSM} = -\epsilon\hat{H}_u\hat{L} + \lambda\hat{L}\hat{L}\hat{E}^c + \lambda'\hat{L}\hat{Q}\hat{D}^c + \lambda''\hat{U}^c\hat{D}^c\hat{D}^c. \tag{1.27}$$

The superpotential $W_{\not{R}_p-MSSM}$ violates a discrete symmetry known as R-parity or matter parity. The R-parity or matter parity is defined as $(-1)^{3(B-L)+2S}$, where B, L are the baryon, lepton number of the particle and S is the spin. Each of the standard model particle is R-parity even and their superpartners are odd under R-parity. In other words, the matter chiral superfield has R-parity -1 and the Higgs chiral superfield has R-parity $+1$.

Since, supersymmetry predicts equality between the masses of the particles and their superpartners and till date no superpartners of the standard model particles have been observed, hence supersymmetry must be broken. In the minimal supersymmetric standard model the supersymmetry is broken explicitly and softly to avoid any dimensionless quartic scalar coupling in the explicitly supersymmetry breaking Lagrangian. The soft supersymmetry breaking Lagrangian of MSSM is,

$$\begin{aligned} -\mathcal{L}^{\text{soft}}_{\text{MSSM}} &= (m^2_{\tilde{Q}})^{ij}\tilde{Q}^\dagger_i\tilde{Q}_j + (m^2_{\tilde{u}^c})^{ij}\tilde{u}^{c^*}_i\tilde{u}^c_j + (m^2_{\tilde{d}^c})^{ij}\tilde{d}^{c^*}_i\tilde{d}^c_j + (m^2_{\tilde{L}})^{ij}\tilde{L}^\dagger_i\tilde{L}_j \\ &+ (m^2_{\tilde{e}^c})^{ij}\tilde{e}^{c^*}_i\tilde{e}^c_j + m^2_{H_d}H^\dagger_d H_d + m^2_{H_u}H^\dagger_u H_u + (bH_uH_d + \text{h.c.}) \\ &+ \left[-A^{ij}_u H_u\tilde{Q}_i\tilde{u}^c_j + A^{ij}_d H_d\tilde{Q}_i\tilde{d}^c_j + A^{ij}_e H_d\tilde{L}_i\tilde{e}^c_j + \text{h.c.}\right] \\ &+ \frac{1}{2}\left(M^3\tilde{g}\tilde{g} + M^2\tilde{\lambda}^i\tilde{\lambda}^i + M^1\tilde{\lambda}^0\tilde{\lambda}^0 + \text{h.c.}\right). \end{aligned} \tag{1.28}$$

where i and j are generation indices, $m^2_{\tilde{Q}}$, $m^2_{\tilde{L}}$ and other terms in the first two lines of the above equation represent the mass-square of different squarks, slepton, sneutrino and Higgs fields. In the third line the trilinear interaction terms have been written down and in the fourth line M^3, M^2 and M^1 are respectively the masses of the gluinos $\tilde{g}$, winos $\tilde{\lambda}^{1,2,3}$ and bino $\tilde{\lambda}^0$.

Bibliography

[1] S. Weinberg, Phys. Rev. Lett **19**, 1264 (1967) ; Phys. Rev. D **5** 1412 (1972) ; A. Salam, in *Elementary Particle Theory: Relativistic Groups and Analyticity (Nobel Symposium No. 8*, ed. N. Svartholm (Almqvist and Wiksell, Stockholm, 1968); S. Glashow, Nucl. Phys. B **22**, 579 (1961) .

[2] For some original work and reviews see, D.J. Gross and F. Wilczek Phys. Rev. **8**, 3633 1973 ; Phys. Rev. D **9**, 908 (1974)

[3] S. R. Coleman and E. J. Weinberg, Phys. Rev. D **7**, 1888 (1973).

[4] Particle Data Group, http://pdg.lbl.gov

[5] The LEP Collaboration (ALEPH, DELPHI, L3 AND OPAL), the LEP Electroweak Working Group and the SLD Heavy Flavour Group, hep-ex/0412015; http://lepewwg.web.cern.ch/LEPEWWG.

[6] F. Abe *et al.* [CDF Collaboration], Phys. Rev. Lett. **74**, 2626 (1995) [arXiv:hep-ex/9503002]; S. Abachi *et al.* [D0 Collaboration], Phys. Rev. Lett. **74**, 2632 (1995) [arXiv:hep-ex/9503003].

[7] G. L. Fogli *et al.*, Phys. Rev. D **78**, 033010 (2008) [arXiv:0805.2517 [hep-ph]].

[8] M. C. Gonzalez-Garcia, M. Maltoni and J. Salvado, JHEP **1004**, 056 (2010) [arXiv:1001.4524 [hep-ph]].

[9] P. F. Harrison, D. H. Perkins and W. G. Scott, Phys. Lett. B **458**, 79 (1999); P. F. Harrison, D. H. Perkins and W. G. Scott, Phys. Lett. B **530** (2002) 167; P. F. Harrison and W. G. Scott, arXiv:hep-ph/0402006.

[10] T. Fukuyama and H. Nishiura, hep-ph/9702253; R. N. Mohapatra and S. Nussinov, Phys. Rev. D **60**, 013002 (1999); E. Ma and M. Raidal, Phys. Rev. Lett. **87**, 011802 (2001); C. S. Lam, Phys. Lett. B **507**, 214 (2001); P.F. Harrison and W. G. Scott, Phys. Lett. B **547**, 219 (2002); W. Grimus and L. Lavoura, Phys. Lett. B **572**, 189 (2003); J. Phys. G **30**, 73 (2004); Y. Koide, Phys. Rev. D **69**, 093001

(2004); A. Ghosal, hep-ph/0304090; W. Grimus *et al.*, Nucl. Phys. B **713**, 151 (2005); R. N. Mohapatra, JHEP **0410**, 027 (2004); R. N. Mohapatra and S. Nasri, Phys. Rev. D **71**, 033001 (2005); R. N. Mohapatra, S. Nasri and H. B. Yu, Phys. Lett. B **615**, 231 (2005); Phys. Rev. D **72**, 033007 (2005); B. Brahmachari and S. Choubey, Phys. Lett. B **642**, 495 (2006); F. Feruglio,Y. Lin, hep-ph/0712.1528.

[11] M. Drees, arXiv:hep-ph/9611409.

[12] S. P. Martin, arXiv:hep-ph/9709356.

[13] J. Wess and B. Zumino, Nucl. Phys. B **70**, 39 (1974); P. Fayet, Phys. Lett. B **64**, 159 (1976); P. Fayet, Phys. Lett. B **69**, 489 (1977); G. R. Farrar and P. Fayet, Phys. Lett. B **76**, 575 (1978).

[14] A. Borriello and P. Salucci, Mon. Not. Roy. Astron. Soc. **323**, 285 (2001) [arXiv:astro-ph/0001082].

[15] G. Hinshaw *et al.* [WMAP Collaboration], Astrophys. J. Suppl. **180**, 225 (2009) [arXiv:0803.0732 [astro-ph]].

[16] D. Hooper, arXiv:0901.4090 [hep-ph].

[17] M. C. Chen, arXiv:hep-ph/0703087.

[18] M. Fukugita and T. Yanagida, Phys. Lett. B **174**, 45 (1986).

[19] T. Hambye and G. Senjanovic, Phys. Lett. B **582**, 73 (2004) [arXiv:hep-ph/0307237]; T. Hambye, Y. Lin, A. Notari, M. Papucci and A. Strumia, Nucl. Phys. B **695**, 169 (2004) [arXiv:hep-ph/0312203].

[20] S. Antusch and S. F. King, JHEP **0601**, 117 (2006) [arXiv:hep-ph/0507333].

[21] X. d. Ji, Y. c. Li, R. N. Mohapatra, S. Nasri and Y. Zhang, Phys. Lett. B **651**, 195 (2007) [arXiv:hep-ph/0605088]; R. N. Mohapatra, S. Nasri and H. B. Yu, Phys. Lett. B **615**, 231 (2005) [arXiv:hep-ph/0502026].

[22] V. A. Rubakov and M. E. Shaposhnikov, Usp. Fiz. Nauk **166**, 493 (1996) [Phys. Usp. **39**, 461 (1996)] [arXiv:hep-ph/9603208].

[23] W. Buchmuller, P. Di Bari and M. Plumacher, Annals Phys. **315**, 305 (2005) [arXiv:hep-ph/0401240]; W. Buchmuller, P. Di Bari and M. Plumacher, New J. Phys. **6**, 105 (2004) [arXiv:hep-ph/0406014].

[24] S. R. Coleman and J. Mandula, Phys. Rev. **159**, 1251 (1967); R. Haag, J. T. Lopuszanski and M. Sohnius, Nucl. Phys. B **88**, 257 (1975).

Chapter 2

Neutrino Mass and Mixing

From many decades, the existence of neutrino is very well-known. In 1930 Pauli [1] postulated the existence of a very light neutral particle neutrino to rescue the principle of energy-momentum conservation in nuclear β-decay. After the discovery of the neutron by James Chadwick, it was speculated that the particle which Pauli postulated could be neutron. However, soon it was realized that the particle which Pauli proposed should be much lighter than neutron. In 1956, Clyde Cowan and Frederick Reines [2] observed antineutrinos, emitted by a nuclear reactor. The observed neutrino was later determined as a partner of the electron. In 1962, muon neutrinos were observed [3]. Finally, tau neutrinos were discovered in 2000 by the experiment DONUT at Fermilab [4], and so the tau neutrino became the last observed particle of the standard model. Hence, with the discovery of the tau-neutrino we have three flavors of neutrinos electron, muon and tau neutrinos ν_e, ν_μ and ν_τ in the standard model.

In the standard model the three flavors of neutrinos belong to three different doublet representations of the gauge group $\mathrm{SU(2)_L}$ and they have hypercharge $Y = -1$. There is no right handed neutrino in the standard model and hence theoretically with the particle contents of the standard model it is not possible to generate the neutrino masses. Given the experimental possibilities in the 60's, when the SM was being built, no evidence of neutrino masses were observed. Therefore the standard model with only left-handed neutrinos was compatible with data. However, the standard model, from 60 onwards faced two major problems, the solar and atmospheric neutrino anomalies. In 1968, Ray Davis detected the solar neutrinos coming from the Sun with a chlorine based detector in the Homestake mine, USA [5]. The flux measured in this experiment was reported to be only 1/3 of the expected one. The discrepancy originated the long-lasting "solar neutrino problem". Similar discrepancy has also been observed in the flux of the muon neutrinos coming from the Earth's atmosphere [6]. The discrepancies in the solar as well as in the atmospheric neutrino fluxes are possible to explain in terms of the phenomenon referred to "neutrino oscillation" [7], the transformation of one flavor of neutrino into another active flavor. In recent years, several outstanding experiments have confirmed the neutrino oscillation. In 1998 the Super-Kamiokande [8] experiment confirmed the neutrino oscillation in the atmospheric neutrino ν_μ. Later, in 2002 the solar neutrino experiment SNO [9] confirmed the solar neutrino oscillation and thus resolved the long-lasting solar neutrino puzzle. The reactor neutrino experiment KamLAND [10] also confirmed the neutrino oscillation observing the disappearance of antineutrino $\bar{\nu_e}$. The other long-baseline and reactor neutrino experiments like K2K and MINOS [11] all support the oscillation hypothesis. The neutrino oscillation has an immediate consequence that neutrinos do possesses mass. Below we discuss the flavor mixing and neutrino oscillation in detail.

2.1 Flavor Mixing and Neutrino Oscillation

Neutrino Mixing in the 3 Flavor Scheme

A neutrino involved in EW interaction is in the flavor eigenstate. For a massive neutrino the flavor eigenstate and the mass eigenstate are two different basis. We denote the mass eigenstate basis by ν_i, $i = 1, 2, 3$ and the flavor eigenstate by ν_α, $\alpha = e, \mu, \tau$. The two basis are related through a unitary transformation:

$$|\nu_\alpha\rangle = \sum_{i=1}^{3} U_{\alpha i} |\nu_i\rangle \tag{2.1}$$

The matrix U, known as the Pontecorvo-Maki-Nakagawa-Sakata *i.e* PMNS [12] mixing matrix in the name of Pontecorvo, Maki, Nakagawa and Sakata, is a 3×3 unitary matrix. The PMNS mixing matrix has 3 real mixing angles and 6 CP phases. However, all of these phases are not physical and can be rotated away by a redefinition of the fields. For a general $n \times n$ unitary matrix there are $n(n-1)/2$ mixing angles and $(n-1)(n-2)/2$ physical phases if the neutrino is a pure Dirac spinor, while $n(n-1)/2$ mixing angles and $n(n-1)/2$ phases remain if neutrino is Majorana spinor. Hence, if neutrinos are Dirac spinor, the PMNS mixing matrix will have one CP phase while for Majorana spinor the PMNS mixing matrix will have three physical phases. The PMNS mixing matrix is represented as,

$$U = \begin{pmatrix} c_{12}\, c_{13} & s_{12}\, c_{13} & s_{13}\, e^{-i\delta} \\ -c_{23}\, s_{12} - s_{23}\, s_{13}\, c_{12}\, e^{i\delta} & c_{23}\, c_{12} - s_{23}\, s_{13}\, s_{12}\, e^{i\delta} & s_{23}\, c_{13} \\ s_{23}\, s_{12} - c_{23}\, s_{13}\, c_{12}\, e^{i\delta} & -s_{23}\, c_{12} - c_{23}\, s_{13}\, s_{12}\, e^{i\delta} & c_{23}\, c_{13} \end{pmatrix} \begin{pmatrix} e^{i\alpha_1} & 0 & 0 \\ 0 & e^{i\alpha_2} & 0 \\ 0 & 0 & 1 \end{pmatrix} \tag{2.2}$$

where $c_{ij} = \cos\theta_{ij}$ and $s_{ij} = \sin\theta_{ij}$. θ_{ij} are mixing angles and δ the "Dirac" CP phase. If neutrinos are Majorana fields, there are two additional phases α_1, α_2, the "Majorana" CP phases.

$\Delta m^2_{21}(10^{-5}\ \mathrm{eV}^2\ )$	$7.59\ \pm 0.20\ \binom{+0.61}{-0.69}$
$\Delta m^2_{31}\ (10^{-3}\ \mathrm{eV}^2\ )$	$-2.36 \pm 0.07\ (\pm 0.36)$
$\Delta m^2_{31}\ (10^{-3}\ \mathrm{eV}^2\ )$	$+2.47 \pm 0.12\ (\pm 0.37)$
θ_{12}	$34.4 \pm 1.0 \begin{pmatrix} +3.2 \\ -2.9 \end{pmatrix}^0$
θ_{23}	$42.9^{+4.1}_{-2.8} \begin{pmatrix} +11.1 \\ -7.2 \end{pmatrix}^0$
θ_{13}	$7.3\,^{+2.1}_{-3.2}\ (\leq 13.3)^{\circ}$
δ_{CP}	$\in [0,\ 360]$

Table 2.1: The 1σ and 3σ allowed ranges of the neutrino oscillation parameters and the mass square differences.

The probability for a neutrino that propagates in vacuum with a energy E to oscillate from a flavor α to a flavor β, after having travelled a distance L, is given by

$$\begin{aligned} P(\nu_\alpha \to \nu_\beta) &= \Big| \sum_j U_{\alpha j} U^*_{\beta j}\, e^{-i\frac{m_j^2 L}{2E_j}} \Big|^2 \\ = \delta_{\alpha\beta} &- 4\sum_{i>j} \mathrm{Re}\left(\mathrm{U}_{\alpha\,\mathrm{i}}\, \mathrm{U}^*_{\alpha\,\mathrm{j}}\, \mathrm{U}^*_{\beta\,\mathrm{i}}\, \mathrm{U}_{\beta\,\mathrm{j}}\right) \times \sin^2\left(\frac{\Delta \mathrm{m}^2_{\mathrm{ij}}\,\mathrm{L}}{4\,\mathrm{E}}\right) \\ &+ 2\sum_{i>j} \mathrm{Im}\left(\mathrm{U}_{\alpha\,\mathrm{i}}\, \mathrm{U}^*_{\alpha\,\mathrm{j}}\, \mathrm{U}^*_{\beta\,\mathrm{i}}\, \mathrm{U}_{\beta\,\mathrm{j}}\right) \times \sin\left(\frac{\Delta \mathrm{m}^2_{\mathrm{ij}}\,\mathrm{L}}{4\,\mathrm{E}}\right), \end{aligned} \tag{2.3}$$

where $\Delta m^2_{i\,j} = m_i^2 - m_j^2$. To get a non-zero probability of the standard model neutrinos to oscillate from a flavor α to a flavor β, they should have masses and also nonzero mass-square difference Δm^2_{ij}. By measuring neutrino fluxes coming from different sources, the mass-square differences and the mixing parameters can be determined. Observation of the disappearance of the atmospheric ν_μ flux constrains the mixing angle θ_{23} and the mass-square difference $|\Delta m_{23}|^2$. Likewise observation of oscillations of solar neutrinos to other active flavors constrains the mixing angle θ_{12} and the solar mass-square difference Δm^2_{21}. In addition, the CHOOZ reactor experiment [13] constrains the 3rd mixing angle θ_{13}. In Table. 2.1 we present the recent 1σ and 3σ allowed ranges of the neutrino mass square differences and oscillation parameters [14]. From the neutrino oscillation experiments we know that the solar mass square difference $\Delta m^2_{21} > 0$, while at present we do not yet have any information whether the atmospheric mass square difference Δm^2_{31} is positive or negative, characterizing the normal and inverted mass ordering respectively [15]. We present an illustration of the two types of neutrino mass hierarchies in Fig. 2.1.

The oscillation experiments however, do not shed any light on the absolute neutrino mass $m_t = \sum_{i=1,2,3} m_i$. The absolute neutrino mass is constrained from the cosmological

Figure 2.1: The possible neutrino spectra: (a) normal mass hierarchy (b) inverted mass hierarchy.

observation. Measurement of WMAP 5 year analysis [16] give this following bound on the sum of the neutrino masses

$$\sum m_i \leq 0.19\text{eV} \tag{2.4}$$

There are other direct tests on neutrino mass, such as beta decay, neutrinoless double beta decay.

Beta Decay

In the beta decay experiments measuring the distortion in the end point spectrum, neutrino masses can be directly tested. In the following decay

$$d \to u + e^- + \bar{\nu}_e\,, \tag{2.5}$$

the energy of the electron is $E_e = Q - E_\nu$, which is maximal for $E_e = Q - m_{\nu_e}$, where m_{ν_e} is $m_{\nu_e} = m_1|U_{e1}|^2 + m_2|U_{e2}|^2 + m_3|U_{e3}|^2$. Here Q represents the energy released in the β decay. The energy spectrum of the electron is $\propto \sqrt{(Q-E_e)^2 - m_{\nu_e}^2}$, and so $m_{\nu_e} \neq 0$ will imply a deviation from the line $Q - E_e$. So far, the best constraint comes from MAINZ [17] and TROITSK [18] experiments:

$$m_{\nu_e} \leq 2.2\text{eV}. \tag{2.6}$$

The future beta decay experiment, Katrin [19], which is scheduled to begin data taking on 2010, is expected to reach a sensivity of 0.2eV to neutrino masses.

Neutrinoless Double-Beta Decay

Neutrinoless double-beta decay [20] experiment ($0\nu\,\beta\beta$) is very important for neutrino physics. The observation of such a process would imply that neutrinos are Majorana particles. In Fig.2.2, the Feynman diagram for this process has been shown. The neutrinoless

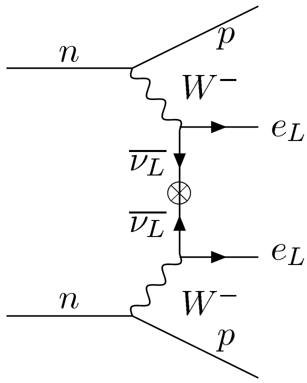

Figure 2.2: Feynman diagram of neutrinoless double beta decay

double-beta decay process is,

$$(A, Z) \to (A, Z+2) + 2\,e^-\,, \tag{2.7}$$

which violates lepton number by two units. The decay rate for this process is,

$$\Gamma_{0_\nu\,\beta\,\beta} \propto |\mathcal{M}|^2\,|m_{ee}|^2\,, \tag{2.8}$$

where $\mathcal{M}$ is the amplitude and m_{ee} which is the ee entry of the neutrino mass matrix

$$\begin{aligned} m_{ee} &= \sum_i U_{ei}^2\,m_i \\ &= \cos^2\theta_{13}(\mathrm{m_1 e^{2i\alpha_1}}\cos^2\theta_{12} + \mathrm{m_2 e^{2i\alpha_2}}\sin^2\theta_{12}) + \mathrm{m_3}\sin^2\theta_{13}. \end{aligned} \tag{2.9}$$

Hence this process depends on the Majorana CP violating phases $\alpha_{1,2}$.

2.2 Neutrino Mass

As we have seen in the previous section, the oscillation experiments indeed support a non-zero neutrino mass which can be either Dirac or Majorana. The Dirac and Majorana mass terms of a standard model neutrino will respectively be the following,

$$\begin{aligned} \mathcal{L}_{Dirac} &= \overline{N_R}\,m_\nu\,\nu_L + \mathrm{h.c}, \\ \mathcal{L}_{Majorana} &= \overline{\nu_L^C}\,m_\nu\,\nu_L + \mathrm{h.c.} \end{aligned} \tag{2.10}$$

To generate Dirac mass term one will require another spinor field N_R. Like the mass terms of all other standard model fermions, this Dirac or Majorana mass term of the standard model neutrino should also be generated from a gauge invariant Yukawa Lagrangian. The Dirac mass term of the standard model neutrino conserves lepton number while the

Majorana mass term breaks lepton number by two units. In the standard model with only left-handed neutrino fields and lepton number conservation, Dirac or Majorana any kind of neutrino mass is not possible to generate. Hence to explain the non-zero neutrino mass, we must look for beyond standard model physics. In addition to the experimental evidences of non-zero neutrino mass, the experiments also indicatate very tiny masses of the standard model neutrino, which is at most $\mathcal{O}($ eV$)$. This extremely tiny mass points towards a $\mathcal{O}(10^{12})$ order of magnitude mass hierarchy between the top quark and neutrino. The very elegant mechanism to explain the tiny Majorana neutrino mass is the novel seesaw mechanism. Below we describe the mass generation mechanism of a Dirac as well as of a Majorana neutrino.

2.2.1 Dirac Mass

The standard model can be extended by adding gauge singlet right handed neutrino N_R. The neutrino masses can be generated from the gauge invariant Yukawa Lagrangian. The Yukawa Lagrangian which incorporates the right handed neutrino state is,

$$-\mathcal{L}_{yuk} = Y_\nu \bar{N}_R \tilde{H}^\dagger L + \text{h.c} \tag{2.11}$$

The standard model Higgs H takes vacuum expectation value v and generate the following Dirac neutrino mass matrix,

$$m_\nu = Y_\nu v. \tag{2.12}$$

For $v \sim 174$ GeV, eV neutrino mass m_ν constraints the Yukawa $Y_\nu \sim 10^{-12}$, which is extremely tiny and leads to fine tuning problem into the theory.

2.2.2 Majorana Mass and Seesaw

The standard model neutrinos can be Majorana particles. The Majorana mass term of the standard model neutrinos has been given in Eq. (2.10), which violates lepton number by two units. The most elegant mechanism to explain the Majorana neutrino masses is the seesaw mechanism [21]. The Lepton number violating Majorana mass term can be from the dimension-5 *Weinberg* operator [22] $\hat{O} = \frac{\kappa_{ij}}{2}(\overline{L_i^C}\tilde{H}^*)(\tilde{H}^\dagger L_j)$, where i, j denote the generation indices and κ is the coupling-coefficient. After the electroweak symmetry breaking and Higgs takes a vacuum expectation value v, this dimension-5 operator generates the following Majorana mass term of the standard model neutrinos,

$$\frac{\kappa_{ij}}{2}(\overline{L_i^C}\tilde{H}^*)(\tilde{H}^\dagger L_j) \longrightarrow \frac{\kappa_{ij}}{2} v^2 \overline{\nu_{L_i}^C} \nu_{L_j} \tag{2.13}$$

Considering the standard model as an effective low energy theory, the dimension-5 operator $\hat{O} = \frac{LLHH}{M}$ [22,23] can be generated by integrating out some heavy modes of the full theory. The fields which get integrated out can be either a gauge singlet neutrino field N_R, or the SU(2) triplet field Δ with hypercharge $Y = +2$, or an SU(2) triplet field Σ_R with hypercharge $Y = 0$. Accordingly, the seesaw is characterized as type-I, type-II and type-III seesaw respectively. In Fig. 2.3 we present the Feynman diagram of the four point function $LLHH$. For the type-I seesaw, the coupling κ_{ij} is $\frac{Y_{\nu_i}^T Y_{\nu_j}}{M}$ while for type-III and type-II seesaw the coupling κ_{ij} is $\frac{Y_{\Sigma_i}^T Y_{\Sigma_j}}{M}$ and $\frac{Y_\Delta \mu_\Delta}{M_\Delta^2}$ respectively, where Y_ν, Y_Σ and Y_Δ are the Yukawa couplings and μ_Δ is the coupling between Higgs triplet Δ and the standard model Higgs doublet H. Below, we discuss in detail the different seesaw mechanisms.

Type-I Seesaw

The standard model is extended by adding the gauge singlet right handed neutrino N_R. The Majorana neutrino in this case is $N = N_R + N_R^C$. The right handed neutrino being a gauge singlet, interacts only with the standard model lepton doublet L and the Higgs H via the Yukawa interaction,

$$-\mathcal{L}_Y = Y_\nu \bar{N}_R \tilde{H}^\dagger L + \frac{1}{2} M \bar{N}_R N_R^C + \text{h.c}, \tag{2.14}$$

where $\tilde{H} = i\sigma_2 H^*$ and M is the lepton number violating mass term of the right handed neutrino N_R. After the Higgs H takes vacuum expectation value v, the following neutrino mass matrix will be generated from Eq. (2.14),

$$\mathcal{L}_m = \frac{1}{2} \begin{pmatrix} \overline{\nu_L^C} & \overline{N_R} \end{pmatrix} \begin{pmatrix} 0 & vY_\nu^T \\ vY_\nu & M \end{pmatrix} \begin{pmatrix} \nu_L \\ N_R^C \end{pmatrix} + \text{h.c.} \tag{2.15}$$

Assuming $M \gg vY_\nu$, the diagonalization of the mass matrix gives two eigenvalues M and $m_\nu \sim m_D^T M^{-1} m_D$, where we have defined $m_D = vY_\nu$. One can identify the eigenvalue M as the mass matrix of the heavy right handed neutrino and the later one m_ν is the mass matrix of the standard model neutrinos.

Type-II Seesaw

Standard model neutrino masses can be generated by adding the SU(2) triplet Higgs to the standard model field contents [24]. The Higgs triplet Δ has $U(1)_Y$ hypercharge $Y = +2$ and has the following Yukawa interaction,

$$-\mathcal{L}_Y = Y_\Delta L^T C i\sigma_2 \Delta L + \text{h.c} \tag{2.16}$$

where the Higgs triplet Δ is,

$$\Delta = \begin{pmatrix} \Delta^+/\sqrt{2} & \Delta^{++} \\ \Delta^0 & -\Delta^+/\sqrt{2} \end{pmatrix}. \tag{2.17}$$

The kinetic term of the Higgs triplet is,

$$\mathcal{L}_k \;=\; \mathrm{Tr}(D_\mu\Delta)^\dagger(D^\mu\Delta), \tag{2.18}$$

and the scalar interaction

$$\begin{aligned} V(H,\Delta) \;=\; & -m_H^2 H^\dagger H + \frac{\lambda}{4}(H^\dagger H)^2 \;+\; M_\Delta^2\; Tr\Delta^\dagger\Delta \;+\; \left(\mu_\Delta H^T\; i\sigma_2\Delta^\dagger H + \text{ h.c}\right) \;+ \\ & + \;\; \lambda_1(H^\dagger H)Tr\Delta^\dagger\Delta \;+\; \lambda_2\;\left(Tr\Delta^\dagger\Delta\right)^2 \;+\; \lambda_3\; Tr\left(\Delta^\dagger\Delta\right)^2 \;+ \\ & + \;\; \lambda_4\; H^\dagger\Delta\Delta^\dagger H. \end{aligned} \tag{2.19}$$

The mass of the neutrino originated from Eq. (2.16) is,

$$\mathcal{L}_m = Y_\Delta v_\Delta \overline{\nu_L^C}\nu_L + \text{h.c}, \tag{2.20}$$

where the vacuum expectation value of the triplet Higgs is $\langle\Delta\rangle = v_\Delta = \frac{\mu_\Delta v^2}{M_\Delta^2}$.

Type-III Seesaw

Other than type-I and type-II seesaw, the SU(2) triplet fermion Σ with hypercharge $Y = 0$ can also contribute in the neutrino mass generation [25]. The triplet fermion denoted as Σ is,

$$\Sigma = \frac{1}{\sqrt{2}}\sum_j \Sigma^j \cdot \sigma_j, \tag{2.21}$$

where σ_j are the Pauli matrices. The right-handed component of this multiplet in the 2×2 notation is then given by,

$$\Sigma_R = \begin{pmatrix} \Sigma_R^0/\sqrt{2} & \Sigma_R^+ \\ \Sigma_R^- & -\Sigma_R^0/\sqrt{2} \end{pmatrix}. \tag{2.22}$$

The corresponding charge-conjugated multiplet will then be,

$$\Sigma_R{}^C = C\overline{\Sigma_R}^T = \begin{pmatrix} \Sigma_R^0{}^C/\sqrt{2} & \Sigma_R^+{}^C \\ \Sigma_R^-{}^C & -\Sigma_R^0{}^C/\sqrt{2} \end{pmatrix}. \tag{2.23}$$

The object which transforms as the left-handed component of the Σ multiplet can be written as,

$$\tilde{\Sigma}_R^C = i\sigma_2\,\Sigma_R{}^C\, i\sigma_2 = \begin{pmatrix} \Sigma_R^0{}^C/\sqrt{2} & \Sigma_R^-{}^C \\ \Sigma_R^+{}^C & -\Sigma_R^0{}^C/\sqrt{2} \end{pmatrix}, \tag{2.24}$$

such that $\Sigma_i = \Sigma_{R_i} + \tilde{\Sigma}_{R_i}^C$. The Yukawa interaction of the triplet fermion fields is,

$$-\mathcal{L}_Y = \left[Y_l \bar{l}_R H^\dagger L + Y_\Sigma \tilde{H}^\dagger \overline{\Sigma}_R L + h.c.\right] + \frac{1}{2}M\;\mathrm{Tr}\left[\overline{\Sigma}_R\tilde{\Sigma}_R^C + h.c.\right], \tag{2.25}$$

The neutrino mass in this case is generated in the same way as for type-I seesaw. The low energy neutrino mass matrix is $M_\nu \sim m_D^T M^{-1} m_D$ where $m_D = \frac{Y_\Sigma v}{\sqrt{2}}$.

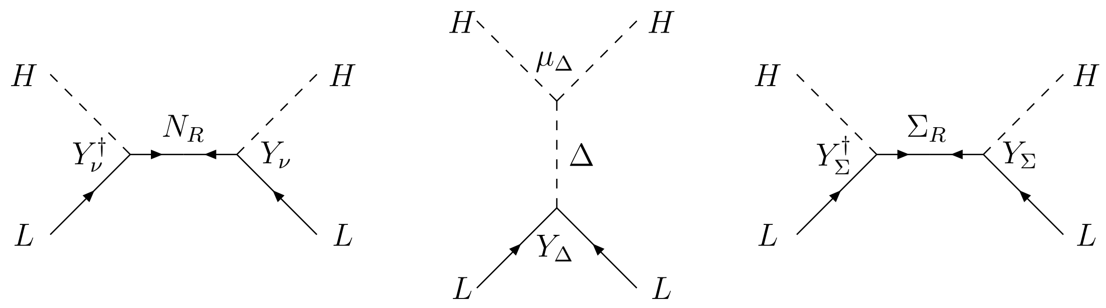

Figure 2.3: The three generic realizations of the Seesaw mechanism, depending on the nature of the heavy fields exchanged: SM singlet fermions (type I Seesaw) on the left, SM triplet scalars (type II Seesaw) and SM triplet fermions (type III Seesaw) on the right.

2.2.3 Supersymmetric Seesaw

In the non-supersymmetric seesaw, the Majorana fermion N contributes to the Higgs mass divergence which is cured by embedding the seesaw into a supersymmetry framework. In supersymmetric seesaw we denote the two component Weyl spinor by N, which will be accompanied by its scalar superpartner $\tilde{N}$ and the auxiliary field F_N. The superpotential which is identical to the Yukawa Lagrangian in the non-supersymmetric seesaw is the following,

$$W = Y_\nu \hat{L}\hat{H}_u\hat{N} + \frac{1}{2}M\hat{N}\hat{N}. \tag{2.26}$$

The fermion bilinear mass terms from the above superpotential will be,

$$\mathcal{L}_m = Y_\nu v_u \nu_L N + MNN, \tag{2.27}$$

which resembles Eq. (2.15).

2.2.4 Seesaw and Grand Unified Theory

In this section we discuss very briefly the GUT embedding of seesaw. We show how the type-I, type-II and type-III Yukawa interactions could come from a Lagrangian of a unified gauge group. Aesthetically we would like to have a unification of the strong and electroweak forces of nature. The standard model gauge group is a subgroup of the groups such as SU(5) and SO(10), and hence can be embedded within these groups. The generation of the higher dimensional *Weinberg* operator $\hat{O} = \frac{LLHH}{M}$ requires some more ingredients than that of the standard model field contents, which we have discussed in the previous section. The necessary extra particles which are required to generate the dimension-5 operator very naturally fit into a grand unified framework, for example the unified gauge group SU(5) or SO(10). All the standard model fermions as well as the right handed neutrino N_R can be exactly fitted to the spinorial 16_F representation of SO(10) [26]. The direct product of two 16_F field gives [27]

$$16 \times 16 = 10 + 120 + 126 \tag{2.28}$$

The Pati-Salam gauge group $\mathrm{SU}(4)_\mathrm{C} \times \mathrm{SU}(2)_\mathrm{L} \times \mathrm{SU}(2)_\mathrm{R}$ is a subgroup of the gauge group SO(10). The left-right symmetric gauge group $\mathrm{SU}(3)_\mathrm{C} \times \mathrm{SU}(2)_\mathrm{L} \times \mathrm{SU}(2)_\mathrm{R} \times \mathrm{U}(1)_\mathrm{B-L}$ is a subgroup of the Pati-Salam gauge group and hence is also a subgroup of the SO(10). One can understand the interactions between different representations of the SO(10) in terms of the Pati-Salam of left-right decomposition [28, 29]. The 16, 10, 120 and 126 fields of the SO(10) have these following decompositions under the Pati-Salam subgroup $\mathrm{SU}(4)_\mathrm{C} \times \mathrm{SU}(2)_\mathrm{L} \times \mathrm{SU}(2)_\mathrm{R}$

$$10 = (1, 2, 2) + (6, 1, 1)$$

$$16 = (4, 2, 1) + (\bar{4}, 1, 2)$$

$$120 = (1, 2, 2) + (10, 1, 1) + (\overline{10}, 1, 1) + (6, 3, 1) + (6, 1, 3) + (15, 2, 2)$$

and

$$\overline{126} = (6, 1, 1) + (10, 3, 1) + (\overline{10}, 1, 3) + (15, 2, 2)$$

The $\mathrm{SU}(3)_\mathrm{C} \times \mathrm{U}(1)_\mathrm{B-L}$ is a subgroup of $\mathrm{SU}(4)_\mathrm{C}$. The representations $\bar{4}$, 6, 10 and 15 hence can be further subdivided under the $\mathrm{SU}(3)_\mathrm{C} \times \mathrm{U}(1)_\mathrm{B-L}$ gauge group [28, 29]. With 16_F, 10, 126 field contents of SO(10), one could realize type-I and type-II seesaw as follows,

- The Dirac mass term $\overline{N}_R \tilde{H}^\dagger L$ of Eq. (2.14) is generated from the interaction $16_F 16_F 10_H$. The 10_H has a bi-doublet $\Phi_H = (1, 2, 2, 0)$. The lepton doublet $L = \begin{pmatrix} \nu_L \\ e_L \end{pmatrix}$ and $L_R = \begin{pmatrix} N_R \\ e_R \end{pmatrix}$ are components of 16_F fields and transforms as (1,2,1,-1) and (1,1,2,-1) under the left-right symmetry gauge group. The interaction of the bi-doublet Φ_H field with the SU(2) doublets $L = \begin{pmatrix} \nu_L \\ e_L \end{pmatrix}$ and $L_R = \begin{pmatrix} N_R \\ e_R \end{pmatrix}$ generates the Dirac mass term, after the electroweak symmetry is broken.

- The Majorana mass term $M \bar{N}_R N_R^C$ of Eq: (2.14) is generated from the Yukawa interaction $Y_{126} 16_F 16_F \overline{126}_H$ of SO(10). The $\overline{126}$ in the above contains a Higgs field Δ_R which transforms as a triplet under the $\mathrm{SU}(2)_\mathrm{R}$ gauge group and is singlet under $\mathrm{SU}(2)_\mathrm{L}$. The direct product of the multiplet L_R of 16_F with the Higgs triplet Δ_R of $\overline{126}$ generates the Majorana mass term of the right handed neutrino after the Higgs triplet Δ_R gets vacuum expectation value [30, 31]. Hence, the Majorana mass term of the right handed neutrino is $M \sim Y_{126} \langle \Delta_R \rangle$.

- The $LL\Delta$ term in Eq. (2.16) is generated from the interaction $16_F 16_F \overline{126}_H$. The SU(2) Higgs triplet field Δ is a component of the $\overline{126}$ representation of SO(10) and transforms as the $(1,3,1,2)$ representation under the left right symmetry gauge group $\mathrm{SU(3)_C} \times \mathrm{SU(2)_L} \times \mathrm{SU(2)_R} \times \mathrm{U(1)_{B-L}}$.

Another very well-explored unified gauge group is the SU(5), originally proposed by Georgi-Glashow [32]. For the type-III seesaw [33] one requires SU(2) triplet $Y = 0$ fermion field Σ_R, which can be part of a fermionic 24_F representation under the gauge group SU(5) [34]. The 24_F adjoint representation of SU(5) has the following decomposition under the standard model gauge group,

$$24_F = (1,3,0) \oplus (8,1,0) \oplus (3,2,-5/6) \oplus (\overline{3},2,5/6) \oplus (1,1,0) \tag{2.29}$$

Apart from the $(1,3,0)$ field component, the 24_F field also contains the $(1,1,0)$ field component. Hence, adding 24_F field to the basic SU(5) field contents $\overline{5}_F$, 10_F, 5_H, 24_H and 24_V one will obtain both type-I as well as type-III seesaw.

2.3 Flavor Symmetry

While the extremely small neutrino masses can be explained by the seesaw mechanism, the non-trivial mixing in the leptonic sector still remains a puzzle. The aesthetic believe of unification suggests that the standard model should be embedded in a higher ranked gauge group, for example SU(5) or SO(10). Although the quarks and leptons in a higher ranked gauge group belong to same representation, however the mixing in the leptonic sector is drastically different than the mixings in the quark sector. Unlike the quark mixing matrix V_{CKM}, the PMNS mixing matrix in the lepton sector contains two large mixing angles θ_{12} and θ_{23} and one small mixing angle θ_{13}. These particular mixings have been a puzzle to the physicists and without any symmetry it is difficult to understand the origin of these mixings. The flavor symmetry [35,36] gives natural explanation in favor of two large mixing angles and one small mixing angles. There are many symmetry groups like A_4, S_3, S_4, T' which can give explanation for the PMNS mixings as well as the mass hierarchy in the leptonic sector. Below, we discuss the group theoretical properties of two discrete symmetry groups A_4 and S_3 which have been extensively used in the literature in justifying the mass and mixing of the leptons. Details of the different flavor symmetry groups and its implication in the leptonic as well as in the quark sector can be found in [35,36].

2.3.1 The Flavor Symmetry Group A_4

Alternating group A_n is a group of even permutations of n objects. It is a subgroup of the permutation group S_n and has $\frac{n!}{2}$ elements. The non-Abelian group A_4 is the first alternating group which is not a direct product of cyclic groups, and is isomorphic to the tetrahedral group T_d. The group A_4 has 12 elements, which can be written in terms of the generators of the group S and T. The generators [35, 36] of A_4 satisfy the relation

$$S^2 = (ST)^3 = (T)^3 = 1 \tag{2.30}$$

There are three one-dimensional irreducible representations of the group A_4 denoted as

$$\begin{aligned} 1 \quad S = 1 \quad T = 1 \qquad (2.31)\\ 1' \quad S = 1 \quad T = \omega^2 \qquad (2.32)\\ 1'' \quad S = 1 \quad T = \omega \qquad (2.33) \end{aligned}$$

It is easy to check that there is no two-dimensional irreducible representation of this group. The three-dimensional unitary representations of T and S are

$$T = \begin{pmatrix} 1 & 0 & 0 \\ 0 & \omega^2 & 0 \\ 0 & 0 & \omega \end{pmatrix}, \qquad S = \frac{1}{3}\begin{pmatrix} -1 & 2 & 2 \\ 2 & -1 & 2 \\ 2 & 2 & -1 \end{pmatrix} . \tag{2.34}$$

where T has been chosen to be diagonal. The multiplication rules for the singlet and triplet representations are as follows

$$1 \times 1 = 1, \quad 1' \times 1'' = 1 \quad 3 \times 3 = 3 + 3_A + 1 + 1' + 1'' \quad . \tag{2.35}$$

For two triplets

$$a = (a_1, a_2, a_3), \qquad b = (b_1, b_2, b_3) \tag{2.36}$$

one can write

$$\begin{aligned} 1 \equiv (ab) &= (a_1 b_1 + a_2 b_3 + a_3 b_2) \qquad (2.37)\\ 1' \equiv (ab)' &= (a_3 b_3 + a_1 b_2 + a_2 b_1) \qquad (2.38)\\ 1'' \equiv (ab)'' &= (a_2 b_2 + a_1 b_3 + a_3 b_1) . \qquad (2.39) \end{aligned}$$

Note that while 1 remains invariant under the exchange of the second and third elements of a and b, $1'$ is symmetric under the exchange of the first and second elements while $1''$ is symmetric under the exchange of the first and third elements.

$$\begin{aligned} 3 \equiv (ab)_S &= \frac{1}{3}\Big(2a_1 b_1 - a_2 b_3 - a_3 b_2, 2a_3 b_3 - a_1 b_2 - a_2 b_1, 2a_2 b_2 - a_1 b_3 - a_3 b_1\Big) \qquad (2.40)\\ 3_A \equiv (ab)_A &= \frac{1}{3}\Big(a_2 b_3 - a_3 b_2, a_1 b_2 - a_2 b_1, a_1 b_3 - a_3 b_1\Big) . \qquad (2.41) \end{aligned}$$

The representation 3 has been considered in the literature [35] to generate the neutrino mass matrix. We can see that the first element here has 2-3 exchange symmetry,the second element has 1-2 exchange symmetry, while the third element has 1-3 exchange symmetry.

Conjugacy Class	Elements	1	$1'$	2
C_1	e	1	1	2
C_2	$(1\,2),(2\,3),(1\,3)$	1	-1	0
C_3	$(1\,2\,3),(3\,2\,1)$	1	1	-1

Table 2.2: Character table of S_3. The first column gives the classes, the second gives the elements in each class, and last three columns give the character corresponding to the three irreducible representations 1, $1'$ and 2.

2.3.2 The Flavor Symmetry Group S_3

The group S_3 is the permutation group of three distinct objects, and is the smallest non-abelian symmetry group. It consists of a set of rotations which leave an equilateral triangle invariant in three dimensions. The group has six elements divided into three conjugacy classes. The generators of the group are S and T which satisfy

$$S^2 = T^3 = (ST)^2 = 1 \ . \tag{2.42}$$

The elements are given by the permutations

$$G \equiv \Big\{ e, (1\,2), (1\,3), (2\,3), (1\,2\,3), (3\,2\,1) \Big\} \ , \tag{2.43}$$

which can be written in terms of the generators as

$$G \equiv \Big\{ e, ST, S, TS, T^2, T \Big\} \ . \tag{2.44}$$

One can see that the S_3 group contains two kinds of subgroups. It can be easily checked that the subgroup of elements

$$G_{Z_3} \equiv \Big\{ e, T, T^2 \Big\} \ , \tag{2.45}$$

form a group under Z_3. In addition, there are three S_2 permutation subgroups[1]

$$G_{S_{12}} \equiv \Big\{ e, (1\,2) \Big\} \ , \quad G_{S_{13}} \equiv \Big\{ e, (1\,3) \Big\} \ , \quad G_{S_{23}} \equiv \Big\{ e, (2\,3) \Big\} \ . \tag{2.46}$$

[1]The group S_2 is isomorphic to Z_2.

The group contains two one-dimensional and one two-dimensional irreducible representations. The one-dimensional representations are given by [37]

$$1: \quad S = 1, \quad T = 1 \tag{2.47}$$
$$1': \quad S = -1, \quad T = 1 \ . \tag{2.48}$$

The two-dimensional representation is given by

$$2: \quad S = \begin{pmatrix} 0 & 1 \\ 1 & 0 \end{pmatrix}, \quad T = \begin{pmatrix} \omega & 0 \\ 0 & \omega^2 \end{pmatrix} \ . \tag{2.49}$$

The character table is given in Table 2.2. Using the Table we can write down the rules for the tensor products. For the one-dimensional irreducible representations we have

$$1 \times 1 = 1, \quad 1 \times 1' = 1', \quad 1' \times 1' = 1 \ . \tag{2.50}$$

Tensor products between two doublets $\psi = (\psi_1, \psi_2)^T$ and $\phi = (\phi_1, \phi_2)^T$ are given as

$$2 \times 2 = 1 + 1' + 2 \ , \tag{2.51}$$

where

$$1 \equiv \psi_1\phi_2 + \psi_2\phi_1 \ , \tag{2.52}$$
$$1' \equiv \psi_1\phi_2 - \psi_2\phi_1 \ , \tag{2.53}$$
$$2 \equiv \begin{pmatrix} \psi_2\phi_2 \\ \psi_1\phi_1 \end{pmatrix} \ . \tag{2.54}$$

The complex conjugate doublet $\psi^\star$ is given as $2^\star$ for which the generators are $S^\star$ and $T^\star$. One can easily check that $\psi^\star$ does not transform as doublet (2) of S_3 and therefore for this case a meaningful way of writing the tensor products for the conjugate fields is by defining

$$\psi' \equiv \sigma_1\psi^\star = \begin{pmatrix} \psi_2^\star \\ \psi_1^\star \end{pmatrix} \ . \tag{2.55}$$

Using the relations $\sigma_1 S^\star \sigma_1 = S$ and $\sigma_1 T^\star \sigma_1 = T$ one can show that ψ' transforms as a doublet. Then the tensor products $\psi' \times \phi$ are given by Eq. (2.51) where

$$1 \equiv \psi_1^\star\phi_1 + \psi_2^\star\phi_2 \ , \tag{2.56}$$
$$1' \equiv \psi_2^\star\phi_2 - \psi_1^\star\phi_1 \ , \tag{2.57}$$
$$2 \equiv \begin{pmatrix} \psi_1^\star\phi_2 \\ \psi_2^\star\phi_1 \end{pmatrix} \ . \tag{2.58}$$

Bibliography

[1] W. Pauli, "Dear radioactive ladies and gentlemen," Phys. Today **31N9** (1978) 27.

[2] F. Reines and C. L. Cowan, Phys. Rev. **113**(1959) 273.

[3] G. Danby, J. M. Gaillard, K. Goulianos, L. M. Lederman, N. B. Mistry, M. Schwartz and J. Steinberger, "Observation of high-energy neutrino reactions and the existence of two kinds of neutrinos," Phys. Rev. Lett. **9** (1962) 36.

[4] K. Kodama *et al.* [DONUT Collaboration], "Observation of tau-neutrino interactions," Phys. Lett. B **504** (2001) 218 [arXiv:hep-ex/0012035].

[5] R. J. Davis, D. S. Harmer and K. C. Hoffman, "Search for neutrinos from the sun," Phys. Rev. Lett. **20** (1968) 1205; B. T. Cleveland *et al.*, "Measurement of the solar electron neutrino flux with the Homestake chlorine detector," Astrophys. J. **496**, 505 (1998).

[6] K. S. Hirata *et al.* [Kamiokande-II Collaboration], "Observation of a small atmospheric ν_μ/ν_e ratio in Kamiokande," Phys. Lett. B **280** (1992) 146; R. Becker-Szendy *et al.*, "The Electron-neutrino and muon-neutrino content of the atmospheric flux," Phys. Rev. D **46** (1992) 3720.

[7] S. M. Bilenky and B. Pontecorvo, "Lepton Mixing And Neutrino Oscillations," Phys. Rept. **41** (1978) 225.

[8] Y. Fukuda. *et al.* [Super-Kamiokande Collaboration], Phys. Rev. Lett. **81**1562 (1998); Y. Ashie *et al.* [Super-Kamiokande Collaboration], Phys. Rev. D **71**, 112005 (2005).

[9] J. N. Abdurashitov *et al.* [SAGE Collaboration], "Measurement of the solar neutrino capture rate with gallium metal," Phys. Rev. C **60** (1999) 055801 [arXiv:astro-ph/9907113]; W. Hampel *et al.* [GALLEX Collaboration], Phys. Lett. B **447**, 127 (1999); M. Altmann *et al.* [GNO Collaboration], "GNO solar neutrino observations: Results for GNO I," Phys. Lett. B **490** (2000) 16 [arXiv:hep-ex/0006034]; Q. R. Ahmad *et al.* [SNO Collaboration], "Direct evidence for neutrino flavor transformation

from neutral-current interactions in the Sudbury Neutrino Observatory," Phys. Rev. Lett. **89** (2002) 011301 [arXiv:nucl-ex/0204008]; S. Fukuda *et al.* [Super-Kamiokande Collaboration], Phys. Lett. B **539**, 179 (2002); B. Aharmim *et al.* [SNO Collaboration], Phys. Rev. C **72**, 055502 (2005); B. Collaboration, arXiv:0708.2251 [astro-ph].

[10] K. Eguchi *et al.*, [KamLAND Collaboration], Phys. Rev. Lett. **90**, 021802(2003); T. Araki *et al.* [KamLAND Collaboration], "Measurement of neutrino oscillation with KamLAND: Evidence of spectral distortion," Phys. Rev. Lett. **94** (2005) 081801 [arXiv:hep-ex/0406035].

[11] E. Aliu *et al.* [K2K Collaboration], Phys. Rev. Lett. **94**, 081802 (2005); D. G. Michael *et al.*. [MINOS Collaboration], Phys. Rev. Lett. **97**, 191801 (2006);

[12] B. Pontecorvo, "Mesonium and antimesonium," Sov. Phys. JETP **6** (1957) 429 [Zh. Eksp. Teor. Fiz. **33** (1957) 549]; Z. Maki, M. Nakagawa and S. Sakata, "Remarks on the unified model of elementary particles," Prog. Theor. Phys. **28** (1962) 870.

[13] Y. Declais *et al.* [Bugey Collaboration], "Search for neutrino oscillations at 15-meters, 40-meters, and 95-meters from a nuclear power reactor at Bugey," Nucl. Phys. B **434** (1995) 503; M. Apollonio *et al.* [CHOOZ Collaboration], "Limits on neutrino oscillations from the CHOOZ experiment," Phys. Lett. B **466** (1999) 415 [arXiv:hep-ex/9907037].

[14] M. C. Gonzalez-Garcia, M. Maltoni and J. Salvado, JHEP **1004**, 056 (2010) [arXiv:1001.4524 [hep-ph]].

[15] R. Gandhi, P. Ghoshal, S. Goswami, P. Mehta, S. U. Sankar and S. Shalgar, Phys. Rev. D **76**, 073012 (2007) [arXiv:0707.1723 [hep-ph]]; R. Gandhi, P. Ghoshal, S. Goswami and S. U. Sankar, Mod. Phys. Lett. A **25**, 2255 (2010) [arXiv:0905.2382 [hep-ph]]; A. Dighe, S. Goswami and S. Ray, arXiv:1009.1093 [hep-ph].

[16] E. Komatsu *et al.* [WMAP Collaboration], "Five-Year Wilkinson Microwave Anisotropy Probe Observations:Cosmological Interpretation," arXiv:0803.0547 [astro-ph]; G. L. Fogli *et al.*, Phys. Rev. D **78**, 033010 (2008) [arXiv:0805.2517 [hep-ph]].

[17] C. Kraus *et al.*, "Final results from phase II of the Mainz neutrino mass search in tritium beta decay," Eur. Phys. J. C **40** (2005) 447 [arXiv:hep-ex/0412056].

[18] A. I. Belesev *et al.*, "Results of the Troitsk experiment on the search for the electron anti-neutrino rest mass in tritium beta decay," Phys. Lett. B **350** (1995) 263.

[19] R. G. H. Robertson [KATRIN Collaboration], "KATRIN: an experiment to measure the neutrino mass," arXiv:0712.3893 [nucl-ex].

[20] H. V. Klapdor-Kleingrothaus *et al.* [Heidelberg-Moscow Collaboration], "Latest results from the Heidelberg-Moscow double-beta-decay experiment," Eur. Phys. J. A **12** (2001) 147 [arXiv:hep-ph/0103062]; R. Arnold *et al.* [NEMO Collaboration], "First results of the search of neutrinoless double beta decay with the NEMO 3 detector," Phys. Rev. Lett. **95** (2005) 182302 [arXiv:hep-ex/0507083]; S. Pascoli and S. T. Petcov, "Majorana Neutrinos, Neutrino Mass Spectrum and the $|\langle m \rangle| \sim 0.001$ eV Frontier in Neutrinoless Double Beta Decay," arXiv:0711.4993 [hep-ph].

[21] P. Minkowski, "Mu $\to$ E Gamma At A Rate Of One Out Of 1-Billion Muon Decays?," Phys. Lett. B **67** (1977) 421; M. Gell-Mann, P. Ramond and R. Slansky, "Complex Spinors And Unified Theories," in *Supergravity*, edited by P. van Nieuwenhuizen and D. Freedman, (North-Holland, 1979), p. 315; T. Yanagida, in *Proceedings of the Workshop on the Unified Theory and the Baryon Number in the Universe*, edited by O. Sawada and A. Sugamoto (KEK Report No. 79-18, Tsukuba, 1979), p. 95; R. N. Mohapatra and G. Senjanovic, "Neutrino mass and spontaneous parity nonconservation," Phys. Rev. Lett. **44** (1980) 912.

[22] S. Weinberg, "Baryon And Lepton Nonconserving Processes," Phys. Rev. Lett. **43** (1979) 1566.

[23] K. S. Babu, C. N. Leung and J. T. Pantaleone, Phys. Lett. B **319**, 191 (1993) [arXiv:hep-ph/9309223].

[24] M. Magg and C. Wetterich, "Neutrino Mass Problem And Gauge Hierarchy," Phys. Lett. B **94**, 61 (1980); G. Lazarides, Q. Shafi and C. Wetterich, "Proton Lifetime And Fermion Masses In An SO(10) Model," Nucl. Phys. B **181** (1981) 287; R. N. Mohapatra and G. Senjanovic, "Neutrino Masses And Mixings In Gauge Models With Spontaneous Parity Violation," Phys. Rev. D **23** (1981) 165; C. Wetterich, "Neutrino Masses And The Scale Of B-L Violation," Nucl. Phys. B **187** (1981) 343.

[25] R. Foot, H. Lew, X. G. He and G. C. Joshi, "Seesaw neutrino masses induced by a triplet of leptons," Z. Phys. C **44** (1989) 441; E. Ma, "Pathways to naturally small neutrino masses," Phys. Rev. Lett. **81** (1998) 1171 [arXiv:hep-ph/9805219].

[26] F. Wilczek and A. Zee, Phys. Rev. D **25**, 553 (1982); R. N. Mohapatra and B. Sakita, Phys. Rev. D **21**, 1062 (1980).

[27] R. Slansky, Phys. Rept. **79**, 1 (1981).

[28] R. N. Mohapatra and J. C. Pati, Phys. Rev. D **11**, 2558 (1975).

[29] G. Senjanovic and R. N. Mohapatra, Phys. Rev. D **12**, 1502 (1975).

[30] R. N. Mohapatra and G. Senjanovic, Phys. Rev. Lett. **44**, 912 (1980); R. N. Mohapatra and G. Senjanovic, Phys. Rev. D **23**, 165 (1981).

[31] K. S. Babu and R. N. Mohapatra, Phys. Rev. Lett. **70**, 2845 (1993) [arXiv:hep-ph/9209215].

[32] H. Georgi and S. L. Glashow, Phys. Rev. Lett. **32**, 438 (1974).

[33] J. Chakrabortty, A. Dighe, S. Goswami and S. Ray, Nucl. Phys. B **820**, 116 (2009) [arXiv:0812.2776 [hep-ph]].

[34] E. Ma, Phys. Rev. Lett. **81**, 1171 (1998) [arXiv:hep-ph/9805219]; B. Bajc and G. Senjanovic, JHEP **0708**, 014 (2007) [arXiv:hep-ph/0612029]; B. Bajc, M. Nemevsek and G. Senjanovic, Phys. Rev. D **76**, 055011 (2007) [arXiv:hep-ph/0703080]; R. N. Mohapatra, N. Okada and H. B. Yu, Phys. Rev. D **78**, 075011 (2008) [arXiv:0807.4524 [hep-ph]].

[35] G. Altarelli and F. Feruglio, New J. Phys. **6**, 106 (2004) [arXiv:hep-ph/0405048]; G. Altarelli and F. Feruglio, arXiv:1002.0211 [hep-ph].

[36] E. Ma and G. Rajasekaran, Phys. Rev. D **64**, 113012 (2001) [arXiv:hep-ph/0106291]; K. S. Babu, E. Ma and J. W. F. Valle, Phys. Lett. B **552**, 207 (2003) [arXiv:hep-ph/0206292]; G. Altarelli and F. Feruglio, Nucl. Phys. B **741**, 215 (2006) [arXiv:hep-ph/0512103]; C. Hagedorn, M. Lindner and R. N. Mohapatra, JHEP **0606**, 042 (2006) [arXiv:hep-ph/0602244]. A. Dighe and N. Sahu, arXiv:0812.0695 [hep-ph]; S. F. King, AIP Conf. Proc. **1200**, 103 (2010) [arXiv:0909.2969 [hep-ph]];

[37] F. Feruglio and Y. Lin, Nucl. Phys. B **800**, 77 (2008) [arXiv:0712.1528 [hep-ph]].

Chapter 3

Two Higgs Doublet Type-III Seesaw

3.1 Introduction

In the previous chapter we have discussed the different possibilities to generate the dimension-5 [1] operator $\hat{\mathcal{O}}(\frac{LLHH}{M})$, which give rise to the Majorana neutrino masses after the electroweak symmetry breaking. In this scheme which is the novel seesaw mechanism [2], the neutrino masses turn out to be naturally small as they are suppressed by the heavy mass scale M of the integrated-out heavy modes. We have also discussed the different seesaw mechanisms which are referred in the literature as type-I, type-II [3] and type-III [4–12]. Distinct from the type-I, the type-III seesaw has the following crucial feature. Since the additional heavy fermions belong to the adjoint representation of SU(2), they have gauge interactions. This makes it easier to produce them in collider experiments. With the LHC all set to take data, it is pertinent to check the viability of testing the seesaw models at colliders. The implications of the type-III seesaw at LHC was first studied in [13] and [14] in the context of a SU(5) GUT model. In the SU(5) model it is possible to naturally have the adjoint fermions in the 100 GeV to 1 TeV mass range, opening up the possibility of observing them at LHC. The authors of these papers identified the dilepton channel with 4 jets as the signature of the triplet fermions. Subsequently, a lot of work has followed on testing type-III seesaw at LHC [15–17].

In the usual type-III (and also type-I) version of the seesaw model with one Higgs doublet, the neutrino mass matrix is,

$$m_\nu = -v^2 Y_\Sigma^T \frac{1}{M} Y_\Sigma. \tag{3.1}$$

where v is the vacuum expectation value of the Higgs field, M is the mass matrix of the triplet fermions and Y_Σ is the Yukawa couplings of the triplet fermions with the standard model lepton doublets and Higgs. To predict neutrino masses ~ 0.1 eV without fine tuning the Yukawas, one requires that $M \sim 10^{14}$ GeV. On the other hand, an essential requisite of producing the heavy fermion triplet signatures at the LHC, is that they should not be heavier than a few hundred GeV. One can immediately see that if $M \sim 300$ GeV, then $m_\nu \sim 0.1$ eV demands that the Yukawa coupling $Y_\Sigma \sim 10^{-6}$. This in a way tentamounts to fine tuning of the Yukawas, and smothers out the very motivation for the seesaw mechanism, which was to explain the smallness of the neutrino mass without unnaturally reducing the Yukawa couplings.

In this work, we propose a seesaw model with few hundred GeV triplet fermions, without any drastic reduction of the Yukawa couplings. We do that by introducing an additional Higgs doublet and imposing a Z_2 symmetry in our model, which ensures that this extra Higgs doublet couples to only the exotic triplet fermions, while the standard Higgs couples to all other standard model particles [18]. As a result the smallness of the neutrino masses can be explained from the the smallness of the VEV of the second Higgs doublet, while all standard model fermions get their masses from the VEV of the standard Higgs. These large Yukawas result in extremely fast decay rates for the heavy fermions in our model and hence have observational consequences for the heavy fermion phenomenology at LHC. This fast decay of the triplet fermions distinguishes the two Higgs doublet type-III seesaw model from the usual one Higgs doublet models.

The presence of two Higgs doublets in our model also enhances the richness of the phenomenology at LHC. We have in our model two neutral physical scalar and one neutral physical pseudoscalar and a pair of charged scalars. Due to constraints on the vacuum expectation value from smallness of neutrino mass, our Higgs mixing angle is very small [19–23]. We study this crucial link between neutrino and Higgs physics in our model and its implications for LHC in detail.

Another feature associated with neutrinos which has puzzled model builders is its unique mixing pattern. While all mixing angles are tiny in the quark sector, for the leptons we have observed two large (θ_{12} and $\theta_{23} \sim \frac{\pi}{4}$) and one small mixing angle $\theta_{13} \sim 0$. The most simple way of generating this is by imposing a μ-τ exchange symmetry on the low energy neutrino mass matrix [24]. In our work we assume a μ-τ symmetry in the Yukawa couplings and in the heavy fermion mass matrix. This leads to μ-τ symmetry in the light neutrino mass matrix and hence the correct predictions for the neutrino oscillation data. Due to the μ-τ symmetry, the mixing matrices of the heavy fermions turn out to be non-trivial. This affects the flavor structure of the heavy fermion decays at colliders, which can be used to test μ-τ symmetry at LHC. We study in detail the collider phenomenology of this μ-τ symmetric model with three heavy SU(2) triplet fermions and two Higgs SU(2) doublets and give predictions for LHC.

We proceed as follows. In section 3.2, we present the lepton Yukawa part of the model within a general framework and give expressions for the masses and mixings of the charged and neutral components of both light as well as heavy leptons. In section 3.3, we present our μ-τ symmetric model and give specific forms for the mass and mixing parameters. We show that the mixing for heavy fermions is highly non-trivial as an artifact of the imposed μ-τ symmetry. In section 3.4, we study the cross-section for the heavy fermion production at LHC, as a function of the fermion mass. In section 3.5, we study the decay rates of these heavy fermions into the standard model leptons, Higgs and gauge bosons. We compare and contrast our model against the usual type-III seesaw models with only one Higgs. We also show the consequences of non-trivial mixing of the heavy fermions on the flavor structure of their decays. In section 3.6, we discuss the decay rates and branching ratios of the Higgs decays. We probe issues on Higgs decays, which are specific and unique to our model. Section 3.7 is devoted to the discussion of displaced decay vertices as a result of the very long living h^0 in our model. In section 3.8, we list the different possible final state particles and their corresponding collider signature channels which could be used to test our model. We calculate the effective cross-sections for these channels at LHC. We highlight some of the channels with very large effective cross-sections and discuss qualitatively the standard model backgrounds. Finally, in section 3.9 we present our conclusions. Discussion of the scalar potential, the Higgs mass spectrum and the constraints from neutrino data on the Higgs sector is discussed in detail in Appendix A. The lepton-Higgs coupling vertices are listed in Appendix B.1, the lepton-gauge coupling vertices are listed in Appendix B.2, and the quark-Higgs coupling vertices are listed in Appendix B.3.

3.2 Yukawa Couplings and Lepton Masses and Mixing

In this section we describe the model. We add three SU(2) triplet fermions to the standard model particle content. These fermions belong to the adjoint representation of SU(2). They are assigned hypercharge $Y = 0$ and are self-conjugate. In the Cartesian basis the triplet is

$$\Psi_i = \begin{pmatrix} \Sigma_i^1 \\ \Sigma_i^2 \\ \Sigma_i^3 \end{pmatrix}, \tag{3.2}$$

where $i = 1, 2, 3$ and $\Psi_i = {\Psi_i}^C$. In the compact 2×2 notation they will be represented in our convention as

$$\Sigma_i = \frac{1}{\sqrt{2}} \sum_j \Sigma_i^j \cdot \sigma_j, \tag{3.3}$$

where σ_j are the Pauli matrices. The right-handed component of this multiplet in the 2×2 notation is then given by

$$\Sigma_{Ri} = \begin{pmatrix} \Sigma_{Ri}^0/\sqrt{2} & \Sigma_{Ri}^+ \\ \Sigma_{Ri}^- & -\Sigma_{Ri}^0/\sqrt{2} \end{pmatrix}, \tag{3.4}$$

where

$$\Sigma^{\pm}_{Ri} = \frac{\Sigma^1_{Ri} \mp i\Sigma^2_{Ri}}{\sqrt{2}} \quad \text{and} \quad \Sigma^0_{Ri} = \Sigma^3_{Ri} \tag{3.5}$$

are the components of the triplet in the charge eigenbasis. The corresponding charge-conjugated multiplet will then be

$$\Sigma_{R_i}{}^C = C\overline{\Sigma_R}^T = \begin{pmatrix} \Sigma^{0\ C}_{Ri}/\sqrt{2} & \Sigma^{+\ C}_{Ri} \\ \Sigma^{-\ C}_{Ri} & -\Sigma^{0\ C}_{Ri}/\sqrt{2} \end{pmatrix}. \tag{3.6}$$

The object which transforms as the left-handed component of the Σ multiplet can then be written as

$$\tilde{\Sigma}^C_{R_i} = i\sigma_2\, \Sigma_{R_i}{}^C\, i\sigma_2 = \begin{pmatrix} \Sigma^{0\ C}_{Ri}/\sqrt{2} & \Sigma^{-\ C}_{Ri} \\ \Sigma^{+\ C}_{Ri} & -\Sigma^{0\ C}_{Ri}/\sqrt{2} \end{pmatrix}, \tag{3.7}$$

such that $\Sigma_i = \Sigma_{R_i} + \tilde{\Sigma}^C_{R_i}$, where

$$\Sigma = \begin{pmatrix} \Sigma^0/\sqrt{2} & \Sigma^+ \\ \Sigma^- & -\Sigma^0/\sqrt{2} \end{pmatrix}. \tag{3.8}$$

For notational convenience, in this chapter we have changed our notations and we denote the standard model Higgs as Φ_1. In addition to the usual standard model doublet Φ_1, in our model we include a new SU(2) scalar doublet Φ_2. This new doublet couples only to the triplet fermions introduced above. The triplet fermions on the other hand are restricted to couple with only the new Φ_2 doublet and not with Φ_1. This can be ensured very easily by giving Z_2 charge of -1 to the triplet fermions Σ_i and the scalar doublet Φ_2, and Z_2 charge $+1$ to all standard model particles. In this model we work with a mildly broken Z_2 symmetry. We will break this Z_2 symmetry mildly in the scalar potential. We discuss the phenomenological consequences of this Z_2 symmetry and its breaking when we introduce the scalar potential and present the Higgs mass spectrum in Appendix A. The part of the Lagrangian responsible for the lepton masses which respects the Z_2 symmetry can be written as

$$-\mathcal{L}_Y = \left[Y_{l_{ij}}\bar{l}_{R_i}\Phi_1^\dagger L_j + Y_{\Sigma_{ij}}\tilde{\Phi}_2^\dagger\overline{\Sigma}_{R_i}L_j + \text{h.c.}\right] + \frac{1}{2}M_{ij}\,\text{Tr}\left[\overline{\Sigma}_{R_i}\tilde{\Sigma}^C_{R_j} + \text{h.c.}\right], \tag{3.9}$$

where L and l_R are the usual left-handed lepton doublet and right-handed charged leptons respectively, Y_l and Y_Σ are the 3×3 Yukawa coupling matrices, and $\tilde{\Phi}_2 = i\sigma_2\Phi_2^*$. Once the Higgs doublets Φ_1 and Φ_2 take Vacuum Expectation Value (VEV)

$$\langle\Phi_1\rangle = \begin{pmatrix} 0 \\ v \end{pmatrix}, \quad \langle\Phi_2\rangle = \begin{pmatrix} 0 \\ v' \end{pmatrix}, \tag{3.10}$$

we generate the following neutrino mass matrix

$$\mathcal{L}_\nu = \frac{1}{2}\begin{pmatrix}\overline{\nu^C_{L_i}} & \overline{\Sigma^0_{R_i}}\end{pmatrix}\begin{pmatrix}0 & \frac{v'}{\sqrt{2}}Y^T_{\Sigma_{ij}} \\ \frac{v'}{\sqrt{2}}Y_{\Sigma_{ij}} & M_{ij}\end{pmatrix}\begin{pmatrix}\nu_{L_j} \\ \Sigma^{0\,C}_{R_j}\end{pmatrix} + \text{h.c.}, \tag{3.11}$$

and the following charged lepton mass matrix

$$\begin{aligned}\mathcal{L}_l &= \begin{pmatrix}\overline{l_{R_i}} & \overline{\Sigma^-_{R_i}}\end{pmatrix}\begin{pmatrix}vY_{l_{ij}} & 0 \\ v'Y_{\Sigma_{ij}} & M_{ij}\end{pmatrix}\begin{pmatrix}l_{L_j} \\ \Sigma^{+\,C}_{R_j}\end{pmatrix} + \text{h.c.}, && (3.12)\\ &= \begin{pmatrix}\overline{l_{R_i}} & \overline{\Sigma^-_{R_i}}\end{pmatrix} M_l \begin{pmatrix}l_{L_j} \\ \Sigma^{+\,C}_{R_j}\end{pmatrix} + \text{h.c.}, && (3.13)\end{aligned}$$

Due to the imposed Z_2 symmetry neutrino mass matrix in Eq. 3.11 depend *only* on the new Higgs VEV v' while in the charged lepton mass matrix both the VEV's enter. The value of v' is determined by the scale of the standard model neutrino masses and is independent of the mass scale of all other fermions. Therefore, the neutrino masses can be naturally light, without having to fine tune the Yukawa couplings Y_Σ to unnaturally small values.

Since we have 3 generation of triplet fermions, the mass matrix in Eq. 3.11 is 6×6. The symmetric 6×6 neutrino matrix can be diagonalized by a unitary transformation to yield 3 light and 3 heavy Majorana neutrinos. The 6×6 unitary matrix U which accomplishes this satisfies the following equations,

$$U^T \begin{pmatrix}0 & m_D^T \\ m_D & M\end{pmatrix} U = \begin{pmatrix}D_m & 0 \\ 0 & D_M\end{pmatrix}, \quad \text{and} \quad \begin{pmatrix}\nu_L \\ \Sigma^{0\,C}_R\end{pmatrix} = U \begin{pmatrix}\nu'_L \\ \Sigma'^{0\,C}_R\end{pmatrix}, \tag{3.14}$$

where $m_D = v'Y_\Sigma/\sqrt{2}$, and

$$D_m = \begin{pmatrix}m_1 & 0 & 0 \\ 0 & m_2 & 0 \\ 0 & 0 & m_3\end{pmatrix}, \qquad D_M = \begin{pmatrix}M_{\Sigma_1} & 0 & 0 \\ 0 & M_{\Sigma_2} & 0 \\ 0 & 0 & M_{\Sigma_3}\end{pmatrix}. \tag{3.15}$$

Here m_i and M_{Σ_i} $(i = 1, 2, 3)$ are the low and high energy mass eigenvalues of the Majorana neutrinos respectively. In the above, the primed basis represents the fields in their mass basis. The mixing matrix U can be parameterized as a product of two matrices

$$U = W_\nu U_\nu \tag{3.16}$$

where W_ν is the matrix which brings the 6×6 neutrino matrix given by Eq. (3.11) in its block diagonal form as

$$W_\nu^T \begin{pmatrix}0 & m_D^T \\ m_D & M\end{pmatrix} W_\nu = \begin{pmatrix}m_\nu & 0 \\ 0 & \tilde{M}\end{pmatrix}, \tag{3.17}$$

while U_ν diagonalizes m_ν and $\tilde{M}$ as

$$U_\nu^T \begin{pmatrix} m_\nu & 0 \\ 0 & \tilde{M} \end{pmatrix} U_\nu \;=\; \begin{pmatrix} D_m & 0 \\ 0 & D_M \end{pmatrix}. \tag{3.18}$$

The above parameterization therefore enables us to analytically estimate the mass eigenvalues and the mixing matrix U in terms of W_ν and U_ν by a two step process, by first calculating W_ν and then U_ν. This matrix W_ν can be parameterized as [25]

$$W_\nu = \begin{pmatrix} \sqrt{1-BB^\dagger} & B \\ -B^\dagger & \sqrt{1-B^\dagger B} \end{pmatrix}, \tag{3.19}$$

where $B = B_1 + B_2 + B_3 + ...$ and $B_j \sim (1/M)^j$, where M is the mass scale of the heavy Majorana fermions. Using an expansion in $1/M$ and keeping only terms second order in $1/M$, we get

$$W_\nu \simeq \begin{pmatrix} 1 - \frac{1}{2} m_D^\dagger (M^{-1})^* M^{-1} m_D & m_D^\dagger (M^{-1})^* \\ -M^{-1} m_D & 1 - \frac{1}{2} M^{-1} m_D m_D^\dagger (M^{-1})^* \end{pmatrix}. \tag{3.20}$$

The light and heavy neutrino mass matrices obtained at this block diagonal stage are given by (upto second order in $1/M$)

$$m_\nu \;=\; -m_D^T M^{-1} m_D, \tag{3.21}$$

$$\tilde{M} \;=\; M + \frac{1}{2}\left(m_D m_D^\dagger (M^{-1})^* + (M^{-1})^* m_D^* m_D^T\right). \tag{3.22}$$

While Eq. (3.21) is the standard seesaw formula for the light neutrino mass matrix, Eq. (3.22) gives the heavy neutrino mass matrix. These can be diagonalized by two 3×3 unitary matrices U_0 and U_Σ, respectively. In our parametrization

$$U_\nu = \begin{pmatrix} U_0 & 0 \\ 0 & U_\Sigma \end{pmatrix}, \tag{3.23}$$

where U_0 and U_Σ satisfy the following equations,

$$\begin{aligned} U_0^T m_\nu U_0 &= D_m \\ U_\Sigma^T \tilde{M} U_\Sigma &= D_M. \end{aligned} \tag{3.24}$$

For the charged leptons we follow an identical method for determining the mass eigenvalues and the mixing matrices. However, since the charged lepton mass matrix M_l given by Eq. (3.13) is a Dirac mass matrix, one has to diagonalize it using a bi-unitary transformation

$$T^\dagger \begin{pmatrix} m_l & 0 \\ \sqrt{2} m_D & M \end{pmatrix} S = \begin{pmatrix} D_l & 0 \\ 0 & D_H \end{pmatrix} = M_{l_d}, \tag{3.25}$$

where $m_l = vY_l$, while D_l and D_H are diagonal matrices containing the light and heavy charged lepton mass eigenvalues. With the above definition for the diagonalization, the right-handed and left-handed weak and mass eigenbasis for the charged leptons are related respectively as,

$$\begin{pmatrix} l_L \\ \Sigma_R^{+C} \end{pmatrix} = S \begin{pmatrix} l'_L \\ \Sigma'^{+C}_R \end{pmatrix}, \quad \text{and} \quad \begin{pmatrix} l_R \\ \Sigma_R^{-} \end{pmatrix} = T \begin{pmatrix} l'_R \\ \Sigma'^{-}_R \end{pmatrix}. \tag{3.26}$$

We denote the four component mass eigenstates of the standard model leptons and the fermion triplet by $l_m^{\pm} = l'^{\pm}_R + l'^{\pm}_L$, $\nu_m = \nu'_L + \nu'^{C}_L$, $\Sigma^0_m = \Sigma'^0_R + \Sigma'^{0\,C}_R$ and $\Sigma^{\pm}_m = \Sigma'^{\pm}_R + \Sigma'^{\mp C}_R$. Instead of using Eq. (3.25) directly for the diagonalization, we will work with the matrices

$$M_l^\dagger M_l = S\, M_{l_d}^\dagger M_{l_d}\, S^\dagger, \quad \text{and} \quad M_l M_l^\dagger = T\, M_{l_d} M_{l_d}^\dagger\, T^\dagger, \tag{3.27}$$

to obtain S and T respectively. As for the neutrinos, we parameterize

$$S = W_L U_L, \quad \text{and} \quad T = W_R U_R, \tag{3.28}$$

where W_L and W_R are the unitary matrices which bring $M_l^\dagger M_l$ and $M_l M_l^\dagger$ to their block diagonal forms, respectively,

$$W_L^\dagger\, M_l^\dagger M_l\, W_L = \begin{pmatrix} \tilde{m}_l{}^\dagger \tilde{m}_l & 0 \\ 0 & \tilde{M}_H^\dagger \tilde{M}_H \end{pmatrix}, \quad \text{and} \quad W_R^\dagger\, M_l M_l^\dagger\, W_R = \begin{pmatrix} \tilde{m}_l \tilde{m}_l{}^\dagger & 0 \\ 0 & \tilde{M}_H \tilde{M}_H^\dagger \end{pmatrix} \tag{3.29}$$

Using arguments similar to that used for the neutrino sector, and keeping terms up to second order in $1/M$, we obtain

$$W_L = \begin{pmatrix} 1 - m_D^\dagger (M^{-1})^* M^{-1} m_D & \sqrt{2} m_D^\dagger (M^{-1})^* \\ -\sqrt{2} M^{-1} m_D & 1 - M^{-1} m_D m_D^\dagger (M^{-1})^* \end{pmatrix}, \tag{3.30}$$

$$W_R = \begin{pmatrix} 1 & \sqrt{2} m_l m_D^\dagger (M^{-1})^* M^{-1} \\ -\sqrt{2} (M^{-1})^* M^{-1} m_D m_l^\dagger & 1 \end{pmatrix}, \tag{3.31}$$

The square of the mass matrices for the light and heavy charged leptons in the flavor basis obtained after block diagonalization by W_R and W_L are given by

$$\tilde{m}_l \tilde{m}_l^\dagger = m_l m_l^\dagger - 2 m_l m_D^\dagger (M^{-1})^* M^{-1} m_D m_l^\dagger, \tag{3.32}$$

$$\begin{aligned} \tilde{M}_H \tilde{M}_H^\dagger &= M M^\dagger + 2 m_D m_D^\dagger + (M^{-1})^* M^{-1} m_D m_l^\dagger m_l m_D^\dagger \\ &+ m_D m_l^\dagger m_l m_D^\dagger (M^{-1})^* M^{-1}, \end{aligned} \tag{3.33}$$

and

$$\tilde{m}_l^\dagger \tilde{m}_l = m_l^\dagger m_l - [m_D^\dagger M^{*-1} M^{-1} m_D m_l^\dagger m_l + \text{h.c}] \tag{3.34}$$

$$\begin{aligned} \tilde{M}_H^\dagger \tilde{M}_H &= M^\dagger M + M^{-1} m_D m_D^\dagger M + M^\dagger m_D m_D^\dagger (M^{-1})^* + M^{-1} (m_D m_D^\dagger)^2 (M^{-1})^* \\ &+ [M^{-1} (M^{-1})^* M^{-1} m_D (m_l^\dagger m_l) m_D^\dagger M - \frac{1}{2} M^{-1} m_D m_D^\dagger M^{*-1} M^{-1} m_D m_D^\dagger M + \\ &\text{h.c}] \end{aligned} \tag{3.35}$$

It is evident that the masses of the heavy charged leptons obtained from Eqs. (3.33) and (3.35) are approximately the same as that obtained for the neutral heavy fermion using Eq. (3.22). Indeed a comparison of these equations show that at tree level, the difference between the neutral and charged heavy fermions are of the order of the neutrino mass and can be hence neglected. One-loop effects bring a small splitting between the masses of the heavy charged and neutral fermions, which is of the order of hundred MeV. This allows the decay channel $\Sigma^{\pm} = \Sigma^{0} + \pi^{\pm}$ at colliders, as discussed in detail in [14, 15]. In this work we neglect this tiny difference and assume that the masses of all heavy fermions are the same.

The matrices $\tilde{m}_l^{\dagger}\tilde{m}_l$ and $\tilde{M}_H^{\dagger}\tilde{M}_H$ are diagonalized by U_l and U_h^L giving,

$$U_L = \begin{pmatrix} U_l & 0 \\ 0 & U_h^L \end{pmatrix}. \tag{3.36}$$

Similarly the $\tilde{m}_l\tilde{m}_l^{\dagger}$ and $\tilde{M}_H\tilde{M}_H^{\dagger}$ matrices are diagonalized by U_r and U_h^R and hence give,

$$U_R = \begin{pmatrix} U_r & 0 \\ 0 & U_h^R \end{pmatrix}. \tag{3.37}$$

Finally, the low energy observed neutrino mass matrix is given by

$$U_{PMNS} = U_l^{\dagger}U_0. \tag{3.38}$$

Here both U_l and U_0 are unitary matrices and hence U_{PMNS} is unitary.

3.3 A μ-τ Symmetric Model

As discussed in the introduction we wish to impose μ-τ symmetry on our model in order to comply with the neutrino data so that $\theta_{13} = 0$ and $\theta_{23} = \pi/4$. Henceforth, we impose the μ-τ exchange symmetry on both the neutrino Yukawa matrix Y_Σ and the Majorana mass matrix for the heavy fermions M. Therefore, the neutrino Yukawa matrix takes the form

$$Y_\Sigma = \begin{pmatrix} a_4 & a_{11} & a_{11} \\ a'_{11} & a_6 & a_8 \\ a'_{11} & a_8 & a_6 \end{pmatrix}, \tag{3.39}$$

In addition to the μ-τ symmetry, we also assume (for simplicity) that $a'_{11} = a_{11}$, which reduces the number of parameters in the theory. For simplicity, we also assume all entries of Y_Σ to be real. The heavy Majorana mass matrix is given by

$$M = \begin{pmatrix} M_1 & 0 & 0 \\ 0 & M_2 & 0 \\ 0 & 0 & M_2 \end{pmatrix}, \tag{3.40}$$

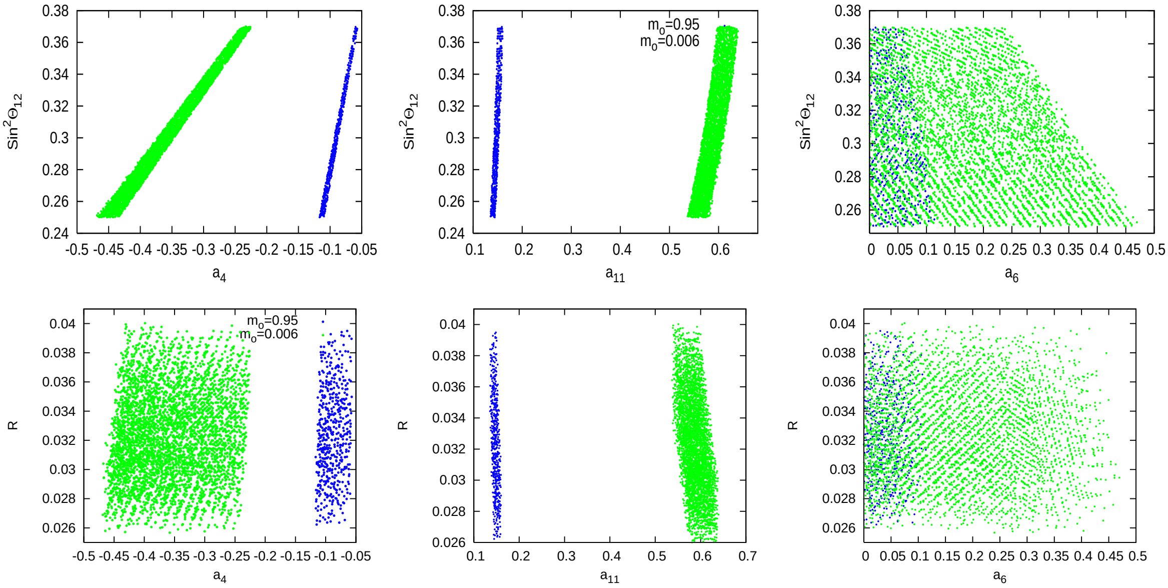

Figure 3.1: Scatter plots showing variation of $\sin^2\theta_{12}$ (upper panels) and $R = \Delta m^2_{21}/|\Delta m^2_{31}|$ (lower panels) as a function of a_4, a_{11} and a_6. All Yukawa couplings apart from the one plotted on the x-axis, are allowed to vary freely. Only points which predict oscillation parameters within their current 3σ values are shown. Blue points are for $m_0 = v'^2/(2M_1) = 0.95$ eV while the green points are for $m_0 = 0.006$ eV.

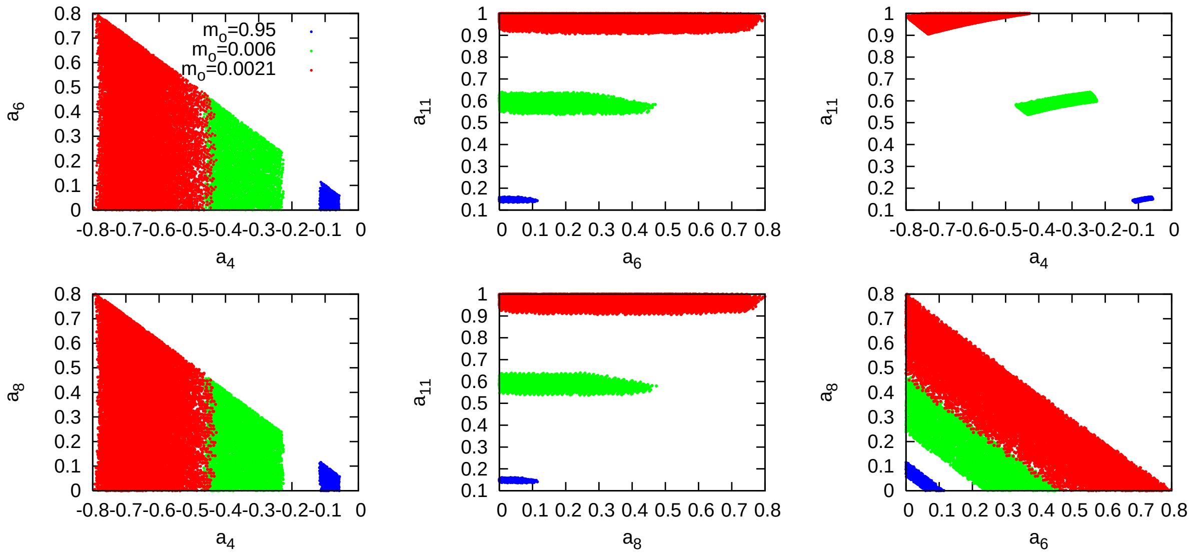

Figure 3.2: Scatter plot showing the values of the Yukawa couplings which give all oscillation parameters within their current 3σ allowed ranges. Allowed points are shown for $m_0 = 0.96$ eV (blue), 0.006 eV (green) and 0.0021 eV (red). All Yukawa couplings apart from the ones plotted in the x-axis and y-axis are allowed to vary freely, in each panel.

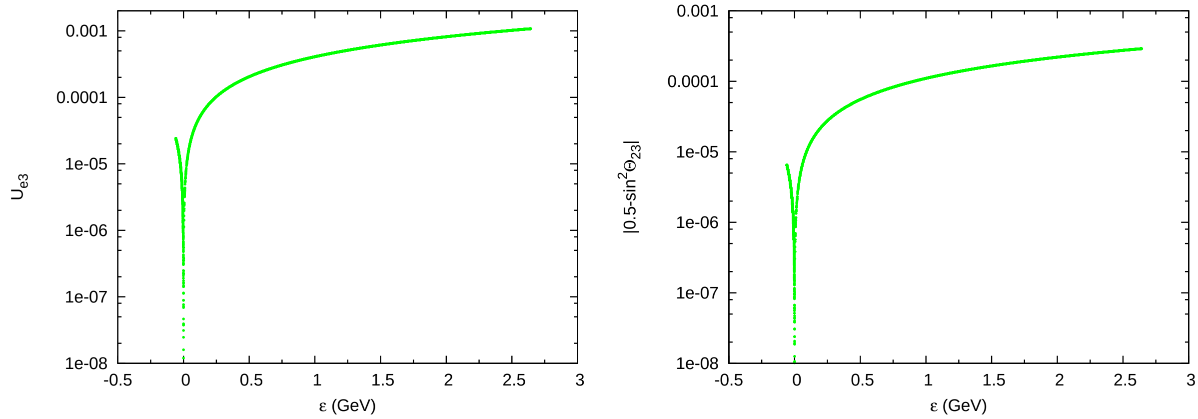

Figure 3.3: Non-zero values of U_{e3} and $|0.5 - \sin^2\theta_{23}|$ predicted when μ-τ symmetry is broken. Shown are the oscillation parameters against the μ-τ symmetry breaking parameter $\epsilon = M_3 - M_2$. Only points which reproduce the current neutrino observations within their 3σ C.L. are shown. The plot is generated at a fixed set of Yukawa couplings and heavy neutrino masses.

where without loosing generality we have chosen to work in a basis where M is real and diagonal. Here the condition $M_3 = M_2$ is imposed due to the $\mu - \tau$ symmetry.

The above choice of Yukawa and heavy fermion mass matrix lead to the following form of the light neutrino mass matrix

$$m_\nu \simeq \frac{v'^2}{2}\begin{pmatrix} \frac{a_4^2}{M_1}+\frac{2a_{11}^2}{M_2} & a_{11}\left(\frac{a_4}{M_1}+\frac{a_6+a_8}{M_2}\right) & a_{11}\left(\frac{a_4}{M_1}+\frac{a_6+a_8}{M_2}\right) \\ a_{11}\left(\frac{a_4}{M_1}+\frac{a_6+a_8}{M_2}\right) & \frac{a_{11}^2}{M_1}+\frac{a_6^2+a_8^2}{M_2} & \frac{a_{11}^2}{M_1}+\frac{2a_6a_8}{M_2} \\ a_{11}\left(\frac{a_4}{M_1}+\frac{a_6+a_8}{M_2}\right) & \frac{a_{11}^2}{M_1}+\frac{2a_6a_8}{M_2} & \frac{a_{11}^2}{M_1}+\frac{a_6^2+a_8^2}{M_2} \end{pmatrix}, \tag{3.41}$$

where we have used the seesaw formula given by Eq. (3.21). It is evident from the above mass matrix that the scale of the neutrino masses emerges as $\sim v'^2a^2/(2\,M)$, where a is a typical value of the Yukawa coupling in Eq. (3.39) and M the scale of heavy fermion masses. In this work, we restrict the heavy fermion masses to be less than 1 TeV in order that they can be produced at the LHC. Therefore in principle, neutrino masses of ~ 0.1 eV could have been obtained with just the standard model Higgs doublet by reducing the Yukawa couplings to values $\sim 10^{-6}$. However with the addition of an extra Higgs doublet, it is possible to generate neutrino mass even with relatively large Yukawa coupling. We introduced a different Higgs doublet Φ_2 in our model, which couples only to the exotic fermions. On the other hand, Yukawa coupling of the standard Higgs Φ_1 with the exotic fermions was forbidden in our model by the Z_2 symmetry. Hence, only the VEV of this new Higgs doublet appears in Eq. (3.41). Since this Higgs Φ_2 is not coupled to any standard model particle, it could have a VEV which could be different. Therefore, we demand that $v' \sim 10^5$ eV in order to generate neutrino masses of ~ 0.1 eV keeping the Yukawa couplings ~ 1.

We next turn to predictions of this model for the mass squared differences and the mixing angles. Since the neutrino mass matrix we obtained in Eq. (3.41) has μ-τ symmetry it follows that

$$\theta_{13} = 0 \quad \text{and} \quad \theta_{23} = \pi/4. \tag{3.42}$$

To find the mixing angle θ_{12} and the mass squared differences Δm^2_{21} and Δm^2_{31} [1], one needs to diagonalize the mass matrix m_ν given in Eq. (3.41). In fact, the form of m_ν in Eq. (3.41) is the standard form of the neutrino mass matrix with μ-τ symmetry, and hence the expression of mixing angle θ_{12} as well Δm^2_{21} and Δm^2_{31} can be found in the literature (see for *e.g.* [26]). We show in Fig. 3.1 the variation of $\sin^2\theta_{12}$ (upper panels) and $R = \Delta m^2_{21}/|\Delta m^2_{31}|$ (lower panels) with the Yukawa couplings a_4, a_{11} and a_6. We do not show the corresponding dependence on a_8 since it looks almost identical to the panel corresponding to a_6. The figure is produced assuming inverted mass hierarchy for the neutrino, *i.e.*, $\Delta m^2_{31} < 0$. The neutrino mass matrix given by Eq. (3.41) could very easily yield $\Delta m^2_{31} > 0$ and hence the normal mass hierarchy (see for *e.g.* [26]). However, for the sake of illustration, we will show results for only the inverted hierarchy. In every panel of Fig. 3.1, all Yukawa couplings apart from the one plotted on the x-axis, are allowed to vary freely. The points show the predicted values of $\sin^2\theta_{12}$ (upper panels) and R (lower panels) as a function of the Yukawa couplings for which all oscillation parameters are within the 3σ values given in [27], For this figure we take $M_1 = M_2$ for simplicity and define $m_0 = v'^2/(2M_1)$. The blue points are for $m = 0.95$ eV while the green points are for $m_0 = 0.006$ eV.

Fig. 3.2 is a scatter plot showing the values of the Yukawa couplings which give all oscillation parameters within their 3σ allowed ranges given in [27]. Again as in the previous plot we assume $M_1 = M_2$, define $m_0 = v'^2/(2\,M_1)$ and show the allowed points for $m_0 = 0.96$ eV (blue), 0.006 eV (green) and 0.0021 eV (red). All Yukawa couplings apart from the ones shown in the x-axis and y-axis are allowed to vary freely, in each panel.

Since the μ and τ charged lepton masses are different, we phenomenologically choose to not impose the μ-τ symmetry on the charged lepton mass matrix[2]. Hence, without loosing generality, the charged lepton Yukawa matrix can be taken as

$$Y_l = \begin{pmatrix} Y_e & 0 & 0 \\ 0 & Y_\mu & 0 \\ 0 & 0 & Y_\tau \end{pmatrix}, \; . \tag{3.43}$$

The masses of the light charged leptons can then be obtained from Eqs. (3.32) and/or (3.34). For our choice of Y_Σ and M, it turns out that $m_e \approx vY_e$, $m_\mu \approx vY_\mu$, and $m_\tau \approx vY_\tau$,

[1]We define $\Delta m^2_{ij} = m^2_i - m^2_j$.

[2]Our choice of the lepton masses and mixing are dictated solely by observations.

if we neglect terms proportional to v'^2. The mixing matrices U_l and U_r which diagonalize $\tilde{m}_l^\dagger \tilde{m}_l$ (cf. Eq. (3.34)) and $\tilde{m}_l \tilde{m}_l^\dagger$ (cf. Eq. (3.32)) respectively, turn out to be unit matrices at leading order.

$$U_l \simeq \begin{pmatrix} 1 & 0 & 0 \\ 0 & 1 & 0 \\ 0 & 0 & 1 \end{pmatrix}, \qquad U_r \simeq \begin{pmatrix} 1 & 0 & 0 \\ 0 & 1 & 0 \\ 0 & 0 & 1 \end{pmatrix}, \tag{3.44}$$

Finally, we show in Fig. 3.3 the impact of μ-τ symmetry breaking on the low energy neutrino parameters. For the sake of illustration we choose a particular form for this breaking, by taking $M_3 \neq M_2$. Departure from μ-τ symmetry results in departure of U_{e3} from zero and $\sin^2\theta_{23}$ from 0.5. We show in Fig. 3.3 the U_{e3} (left hand panel) and $|0.5 - \sin^2\theta_{23}|$ generated as a function of the symmetry breaking parameter $\epsilon = M_3 - M_2$. The figure is generated for $a_4 = -0.066$, $a_{11} = 0.171$, $a_6 = 0.064$, $a_8 = 0.0037$ and $m_0 = 0.745$ eV. We have fixed $M_1 = M_2 = 299$ GeV in this plot. For $\epsilon = 0$, μ-τ symmetry is restored and both U_{e3} and $0.5 - \sin^2\theta_{23}$ go to zero. We show only points in this figure for which the current data can be explained within 3σ. We note that for $\epsilon > 0$ the curve extends to about $M_3 = M_2 + 2.6$ GeV, for this set of model parameters. For $\epsilon < 0$, the allowed range for ϵ is far more restricted.

We next turn our attention to the predictions of this model for the heavy fermion sector. The 6×6 mixing matrices, which govern the mixing of the heavy leptons with light ones, can also be obtained as discussed before. We will see in the next section that all the four 3×3 blocks of the matrices U, S and T are extremely important for phenomenology at the LHC. We denote these 3×3 blocks as

$$U = \begin{pmatrix} U_{11} & U_{12} \\ U_{21} & U_{22} \end{pmatrix} = \begin{pmatrix} (W_\nu)_{11} U_0 & (W_\nu)_{12} U_\Sigma \\ (W_\nu)_{21} U_0 & (W_\nu)_{22} U_\Sigma \end{pmatrix}, \tag{3.45}$$

$$S = \begin{pmatrix} S_{11} & S_{12} \\ S_{21} & S_{22} \end{pmatrix} = \begin{pmatrix} (W_L)_{11} U_l & (W_L)_{12} U_h^L \\ (W_L)_{21} U_l & (W_L)_{22} U_h^L \end{pmatrix}, \tag{3.46}$$

$$T = \begin{pmatrix} T_{11} & T_{12} \\ T_{21} & T_{22} \end{pmatrix} = \begin{pmatrix} (W_R)_{11} U_r & (W_R)_{12} U_h^R \\ (W_R)_{21} U_r & (W_R)_{22} U_h^R \end{pmatrix}, \tag{3.47}$$

The matrices W_ν, W_L and W_R have been given in Eqs. (3.20), (3.30) and (3.31) respectively. Hence, the 3×3 blocks in S, T and in U can be estimated for our choice of m_D, M and m_l. In particular, we note that S_{11} and T_{11} are close to 1, while U_{11} is given almost by U_{PMNS}. The off-diagonal blocks U_{12}, U_{21}, S_{12} and S_{21}, are suppressed by $\sim m_D/M$, while T_{12} and T_{21} are suppressed by $\sim m_D m_l/M^2$. Finally, the matrices $U_{22} = (W_\nu)_{22} U_\Sigma$, $S_{22} = (W_L)_{22} U_h^L$, and while $T_{22} = (W_R)_{22} U_h^R \simeq U_h^R$. To estimate these we need to evaluate first the matrices which diagonalize the heavy fermion mass matrices $\tilde{M}$, $\tilde{M}_H^\dagger \tilde{M}_H$, and $\tilde{M}_H \tilde{M}_H^\dagger$ respectively. For M and m_D with μ-τ symmetry and with the parameters given in Table 3.1, it turns out that

$$U_\Sigma \simeq U_h^L \simeq U_h^R \simeq \begin{pmatrix} 1 & 0 & 0 \\ 0 & \frac{1}{\sqrt{2}} & -\frac{1}{\sqrt{2}} \\ 0 & \frac{1}{\sqrt{2}} & \frac{1}{\sqrt{2}} \end{pmatrix}, \tag{3.48}$$

thereby yielding

$$U_{22} \simeq \begin{pmatrix} 1 & 0 & 0 \\ 0 & \frac{1}{\sqrt{2}} & -\frac{1}{\sqrt{2}} \\ 0 & \frac{1}{\sqrt{2}} & \frac{1}{\sqrt{2}} \end{pmatrix}. \tag{3.49}$$

$$S_{22} \simeq \begin{pmatrix} 1 & 0 & 0 \\ 0 & \frac{1}{\sqrt{2}} & -\frac{1}{\sqrt{2}} \\ 0 & \frac{1}{\sqrt{2}} & \frac{1}{\sqrt{2}} \end{pmatrix}. \tag{3.50}$$

$$T_{22} \simeq \begin{pmatrix} 1 & 0 & 0 \\ 0 & \frac{1}{\sqrt{2}} & -\frac{1}{\sqrt{2}} \\ 0 & \frac{1}{\sqrt{2}} & \frac{1}{\sqrt{2}} \end{pmatrix}. \tag{3.51}$$

To be more precise, the structure of the 3rd column of U_Σ, U_h^L and U_h^R (and hence of U_{22}, S_{22} and T_{22}), is an immediate consequence of the μ-τ symmetry in M and m_D. The matrices U_Σ, U_h^L and U_h^R will be almost unit matrices, only if $M_1 \ll M_2 \ll M_3$. Breaking of the μ-τ symmetry either in m_D or in M, will destroy this non-trivial form for U_Σ, U_h^R and U_h^L. But having μ-τ symmetry in *both* Y_Σ and M is both theoretically as well as phenomenologically well motivated. We will see later that this non-trivial form of the matrices U_Σ, U_h^L and U_h^R will lead to certain distinctive signatures at LHC.

Among the different mixing matrices, while U_Σ, U_h^L and U_h^R have the form given by Eq. (3.48), U_l and $U_r \simeq I$, though both M and Y_l were taken as real and diagonal. The main reason for this drastic difference is the following. While we take exact μ-τ symmetry for M, for Y_l we take a large difference between Y_μ and Y_τ values. This choice was dictated by the observed charged lepton masses.

We comment very briefly regarding the extent of deviation from unitarity. From the discussion of the previous section and Eq. (3.20), it is evident that the deviation from unitarity of the light neutrino mixing matrix is $\propto m_D^2/M_\Sigma^2 \simeq m_\nu/M_\Sigma$, where m_ν and M_Σ are the light neutrino and heavy lepton mass scales respectively. Therefore, an important difference between our model with TeV scale triplet fermion and the usual GUT seesaw models (for example type-I) is that the extent of non-unitarity for our model is much larger. This will result in comparatively larger lepton flavor violating decays. Detailed calculations for lepton flavor violating radiative as well as tree level decays of a generic type-III seesaw model have been published in [28, 29]. The authors of these papers have also worked out the current constraints on the deviation from unitarity. Even for 100 GeV mass range heavy leptons, the predicted non-unitarity and lepton flavor violating decay rates should be below the current experimental bounds.

3.4 Heavy Fermion Production at LHC

Here we discuss the heavy fermion production at LHC. The triplet fermions couple to the standard model particles through the Yukawa couplings as well as gauge couplings. We give in Appendix B, the detailed Yukawa and gauge couplings of the neutral and charged heavy fermions with the standard model leptons, vector bosons, and Higgs particles. We have kept the masses of the heavy fermions in the 100 GeV to 1 TeV range. Therefore, it should be possible to produce these fermions at LHC. In this section, we will study in depth the production and detection possibilities of the heavy leptons in our type-III seesaw model. Compared to the usual type-III seesaw model, there are two distinctly new aspects in our analysis – (i) presence of two Higgs doublet instead of one, leading to a rich collider phenomenology, (ii) presence of μ-τ symmetry in our model.

The heavy triplet fermion production at LHC has been discussed by many earlier papers At LHC we will be looking at the following production channels

$$pp \to \Sigma^{\pm}_m\Sigma^{\mp}_m, \Sigma^{\pm}_{\rm m}\Sigma^{0}_{\rm m}, \Sigma^{0}_{\rm m}\Sigma^{0}_{\rm m}.$$

To remind once more, the subscript "m" denote 4 component fields in their mass basis. The exotic fermions have both Yukawa couplings to Higgs as well as gauge couplings to vector bosons. Therefore, they could be in principle produced through either gauge mediated partonic processes (left diagram) or through Higgs mediated partonic processes (right diagram)

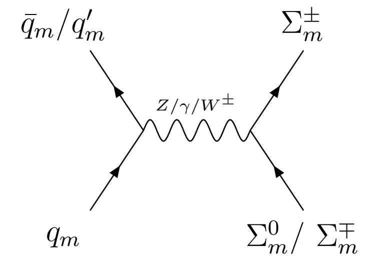

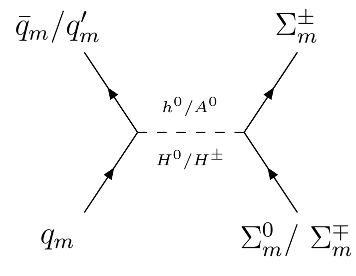

However, it turns out that the vertex factors for the couplings of heavy fermions to gauge bosons which are relevant for the formers production, *viz.*, $\Sigma^+_m\Sigma^-_m Z/\gamma$ and $\Sigma^0_m\Sigma^{\pm}_m W^{\mp}$, are much larger than those involving the Higgs, *viz.*, $\Sigma^+_m\Sigma^-_m H^0/h^0/A^0$ and $\Sigma^0_m\Sigma^{\pm}_m H^{\mp}$. To illustrate this with a specific example, we compare the $\Sigma^+_m\Sigma^-_m Z$ coupling

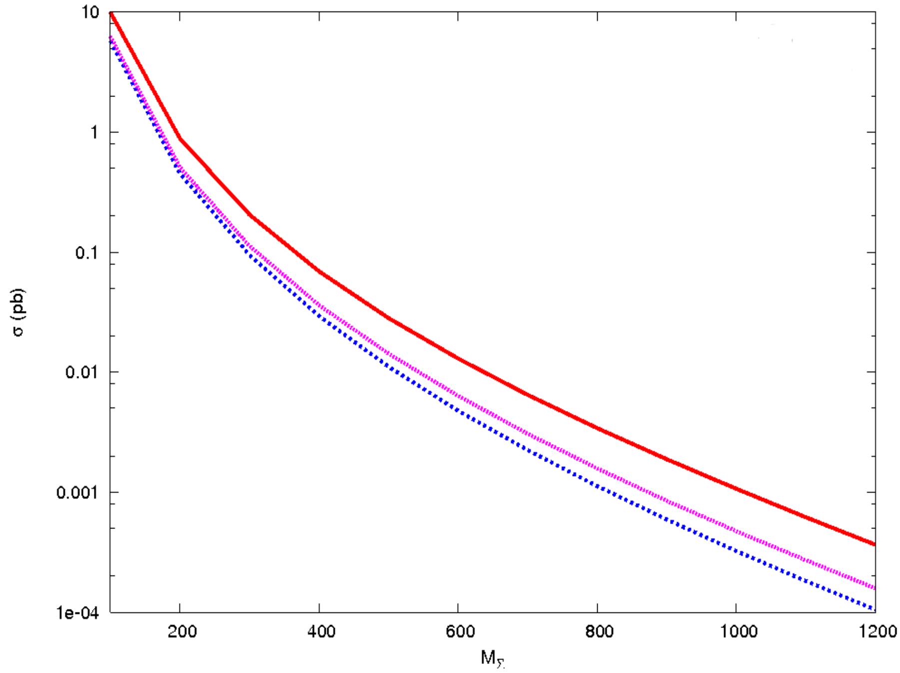

Figure 3.4: Variation of production cross section of $\Sigma_m^\pm$, Σ_m^0 with the mass of exotic leptons. The blue, red and pink lines correspond to $\Sigma_m^-\Sigma_m^0$, $\Sigma_m^+\Sigma_m^0$ and $\Sigma_m^-\Sigma_m^+$ production respectively.

given in Eqs. (B16) and (B17) with the $\Sigma_m^+\Sigma_m^- h^0$ coupling given in Table 3.13. It is easy to see that the $\Sigma_m^+\Sigma_m^- Z/\gamma$ coupling has terms proportional to $T_{22}^\dagger T_{22}$ and $S_{22}^\dagger S_{22}$, while the $\Sigma_m^+\Sigma_m^- h^0$ coupling depends on terms which have an off-diagonal mixing matrix block. Since the off-diagonal mixing matrix blocks are much smaller than the diagonal ones (as discussed before), it is not surprising that the couplings of two exotic fermions to the Higgs particles are much smaller than to the gauge bosons. Hence the heavy exotic fermions will be produced predominantly via the gauge boson mediated processes. We calculate the cross-sections using the Calchep package [30].

In Fig. 3.4 we show the production cross-section for $\Sigma_m^-\Sigma_m^0$ (bold dotted line), $\Sigma_m^+\Sigma_m^0$ (solid line), and $\Sigma_m^+\Sigma_m^-$ (fine dotted line), at LHC as a function of the corresponding heavy fermion mass. It is straightforward to see that the $\Sigma_m^0\Sigma_m^0 Z$ (and $\Sigma_m^0\Sigma_m^0 W^\pm$) couplings are absent. A very small $\Sigma_m^0\Sigma_m^0 Z$ is generated through mixing from the $\nu^0\nu^0 Z$ coupling. However, this is extremely small. Hence, $\Sigma_m^0\Sigma_m^0$ production through gauge interactions is heavily suppressed and is not shown in Fig. 3.4. The production cross-sections of the heavy fermions fall sharply with their mass. More precisely, $\sigma(\Sigma_m^\pm\Sigma_m^\mp) = 112$ fb, $\sigma(\Sigma_m^+\Sigma_m^0) = 206$ fb and $\sigma(\Sigma_m^-\Sigma_m^0) = 95$ fb, for $M_{\Sigma_i} \simeq 300$ GeV. However, for $M_{\Sigma_i} \simeq 600$ GeV this quickly falls to $\sigma(\Sigma_m^\pm\Sigma_m^\mp) = 6$ fb, $\sigma(\Sigma_m^+\Sigma_m^0) = 13$ fb, and $\sigma(\Sigma_m^-\Sigma_m^0) = 4$

fb. Therefore, it is obvious that the lightest amongst the three generation of heavy fermions will be predominantly produced at the collider, and will hence dominate the phenomenology. The production cross-sections that we get is identical to that obtained in earlier papers [15, 16]. This is not unexpected since our model is different from all the earlier models in the Higgs sector. However as discussed above, it is the gauge interactions which predominantly produce the exotic leptons. The gauge-lepton couplings in our model is same as in the earlier works. Since the heavy fermion production comes mostly from the gauge mediated sub-processes, we get the same production cross-sections as the other literatures.

3.5 Heavy Fermion Decays

Once produced at LHC, the heavy fermions will decay to different lighter states due to its interaction with different standard model particles. In particular, they could decay into light leptons and Higgs due to their Yukawa couplings, or to light leptons and vector bosons due to their gauge interactions. The light leptons could be either the charged leptons or the neutrinos. The Higgs could be either the neutral Higgs h^0, H^0, A^0, or the charged Higgs $H^\pm$. The gauge bosons could be either $W^\pm$ or Z. The Higgs and gauge bosons would eventually give the final state particles in the detector, which will be tagged at the experiment. This will be studied in detail in the following sections. Here we concentrate on only the two body tree level decay rates and branching ratios of the exotic leptons $\Sigma_m^\pm$ and Σ_m^0. All possible vertices and the corresponding vertex factors for the Yukawa interactions of $\Sigma_m^\pm$ and Σ_m^0 are given in Tables 3.13, 3.14, 3.15. The vertices and vertex factors for the charged and neutral current gauge interactions can be found in Appendix B.2. Presence of two Higgs doublets and μ-τ symmetry in Y_Σ and M will have direct implications in the partial decay widths for different decay processes.

3.5.1 Decay to Light Leptons and Higgs

In this subsection, we perform a detailed study of all two-body decays of these fermions into a lepton and a Higgs. Since we have two Higgs doublets in our model, we have a pair of charged Higgs $H^\pm$, and three neutral Higgs – h^0 and H^0 are CP even, while A^0 is CP odd. The Higgs mass spectrum and mixing is given in Appendix A. The decay width Γ for $\Sigma_{m_i} \to l_{m_j} X$ is given by

$$\Gamma = \frac{M_{\Sigma_i}}{32\pi}\Big[1 - \frac{(M_X - m_{l_j})^2}{{M_{\Sigma_i}}^2}\Big]^{\frac{1}{2}} \times \Big[1 - \frac{(M_X + m_{l_j})^2}{{M_{\Sigma_i}}^2}\Big]^{\frac{1}{2}} \times A_{ji}, \tag{3.52}$$

where M_{Σ_i}, M_X and m_{l_j} are the masses of $\Sigma^0_{m_i}/\Sigma^\pm_{m_i}$, X and l_{m_j}, respectively, where X is the relevant Higgs involved. The l_{m_j} could be either a charged lepton $l_m^\pm$ or a neutrino

ν_m . Accordingly m_{l_j} will represent the charged lepton or light neutrino masses D_l or D_m respectively. For the charged Higgs $H^\pm$ mode, and the neutral Higgs h^0 and H^0 mode, the factor A_{ji} is given as

$$\begin{aligned} A_{ji} &= \Big(|(C_{l\Sigma}^{X,L})_{ji}|^2 + |(C_{l\Sigma}^{X,R})_{ji}|^2\Big)\Big(1 - \frac{(M_X^2 - m_{l_j}^2)}{M_{\Sigma_i}^2}\Big) \\ &+ \Big((C_{l\Sigma}^{X,L})^*_{ji}(C_{l\Sigma}^{X,R})_{ji} + (C_{l\Sigma}^{X,R})^*_{ji}(C_{l\Sigma}^{X,L})_{ji}\Big)\frac{m_{l_j}}{M_{\Sigma_i}}, \end{aligned} \tag{3.53}$$

while for the CP-odd neutral Higgs A^0 the factor is

$$\begin{aligned} A_{ji} &= \Big(|(C_{l\Sigma}^{X,L})_{ji}|^2 + |(C_{l\Sigma}^{X,R})_{ji}|^2\Big)\Big(1 - \frac{(M_X^2 - m_{l_j}^2)}{M_{\Sigma_i}^2}\Big) \\ &- \Big((C_{l\Sigma}^{X,L})^*_{ji}(C_{l\Sigma}^{X,R})_{ji} + (C_{l\Sigma}^{X,R})^*_{ji}(C_{l\Sigma}^{X,L})_{ji}\Big)\frac{m_{l_j}}{M_{\Sigma_i}}. \end{aligned} \tag{3.54}$$

In the above equations $(C_{l\Sigma}^{X,L})/(C_{l\Sigma}^{X,R})$ are the relevant vertex factors given in Table 3.13, 3.14 and 3.15, and i, j represents the generation. In all numerical results that follow we will fix the model parameters (Yukawa couplings and entries of M mass matrix) to their values given in Table 3.1. This set of model parameters yield $\Delta m_{21}^2 = 7.67 \times 10^{-5}$ eV^2, $\Delta m_{31}^2 = -2.435 \times 10^{-3}$ eV^2 and $\sin^2\theta_{12} = 0.33$. Of course $\theta_{13} = 0$ and $\theta_{23} = \pi/4$. In this work, we take the value of $M_{h^0} = 40$ GeV, $M_{H^0} = 150$ GeV, $M_{A^0} = 140$ GeV and $M_{H^\pm} = 170$ GeV. We also present the heavy fermion decay branching ratios for the case where we have taken the light Higgs mass $m_{h^0} = 70$ GeV. Also, for all cases where we present results for fixed values of the heavy fermion masses, we take $M_{\Sigma_1} = 300$ GeV and $M_{\Sigma_2} = M_{\Sigma_3} = 600$ GeV.

a_4	a_6	a_8	a_{11}	m_o/eV	$\frac{M_2}{M_1}$	$\frac{M_3}{M_1}$
0.145	0.097	0.109	4×10^{-4}	2.356	2.0	2.0

Table 3.1: Model parameters used for all numerical results in section 5 and 6. This set of model parameters yield $\Delta m_{21}^2 = 7.67 \times 10^{-5}$ eV^2, $\Delta m_{31}^2 = -2.435 \times 10^{-3}$ eV^2 and $\sin^2\theta_{12} = 0.33$. Of course $\theta_{13} = 0$ and $\theta_{23} = \pi/4$. Parameter $m_0 = v'^2/(2M_1)$.

$\Sigma_m^\pm \to l_m^\pm h^0/H^0/A^0$

Let us begin with the decay of heavy charged leptons into light charged leptons and neutral Higgs. The Higgs concerned in this case could be h^0, H^0, or A^0. We start by probing the decay rate $\Sigma_{m_i}^\pm \to l_{m_j}^\pm h^0$. From Eq. (3.52) we see that the decay rate is governed by the factor A_{ji}, which in turn depends on the vertex factors given in Table 3.13. The vertex

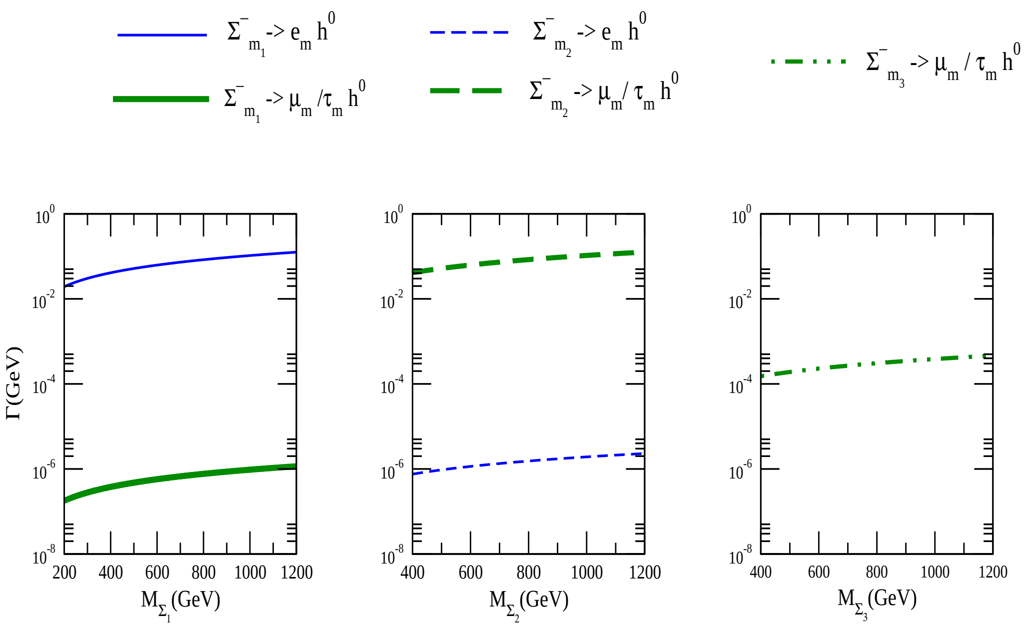

Figure 3.5: Variation of $\Gamma(\Sigma^-_{m_i} \to l^-_{m_j} h^0)$ with M_{Σ_i}

factors are given in terms of the 3×3 block matrices S_{ab} and T_{ab}, where $a, b = 1, 2$. We have seen in the earlier sections that S_{12}, T_{12} and T_{21} are heavily suppressed – the first one by $\mathcal{O}(m_D/M)$ and T_{12} and T_{21} by $\mathcal{O}((m_l m_D)/M^2)$. The vertex factors also depend on the Higgs mixing angle α. In Appendix A, we have shown how the neutrino mass constrains the neutral Higgs mixing such that $\sin\alpha \sim 10^{-6}$ and $\cos\alpha \sim 1$. Therefore, for the $\Sigma^\pm_{m_i} \to l^\pm_m h^0$ decay the dominating vertex factor is

$$C^{h^0,R}_{l^\pm\Sigma^\pm} \simeq \frac{1}{\sqrt{2}} S^\dagger_{11} Y^\dagger_\Sigma T_{22} \cos\alpha. \tag{3.55}$$

We have seen in Eq. (3.46) that $S_{11} \simeq 1$ if we neglect terms of the order of $\mathcal{O}(m_D^2/M^2)$. Therefore,

$$C^{h^0,R}_{l^\pm\Sigma^\pm} \simeq \begin{pmatrix} a_4 & \sqrt{2}a_{11} & 0 \\ a_{11} & \frac{1}{\sqrt{2}}(a_6 + a_8) & \frac{1}{\sqrt{2}}(a_8 - a_6) \\ a_{11} & \frac{1}{\sqrt{2}}(a_6 + a_8) & \frac{1}{\sqrt{2}}(a_6 - a_8) \end{pmatrix}. \tag{3.56}$$

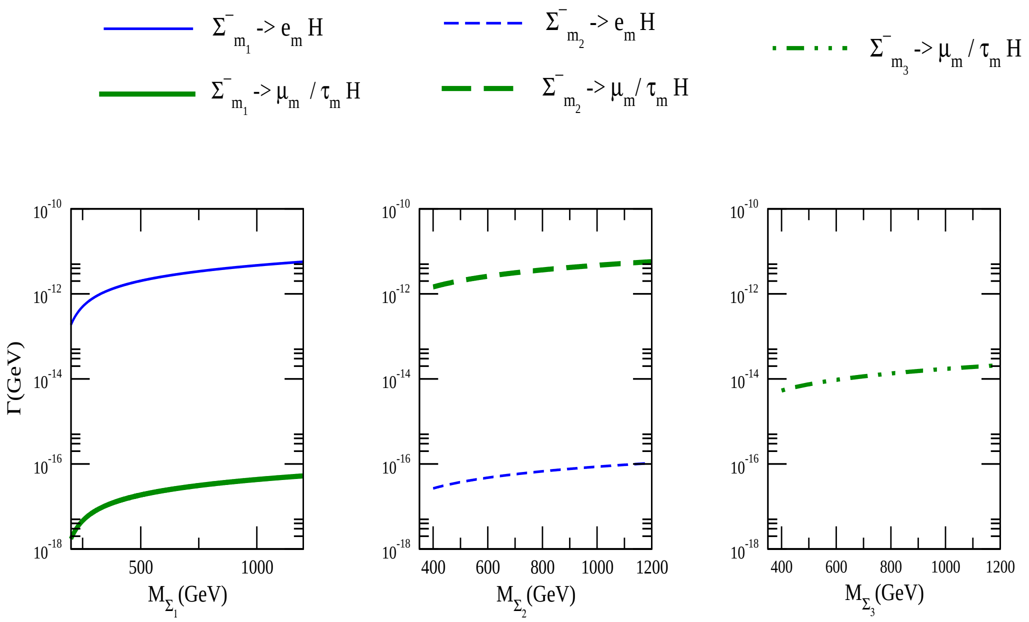

Figure 3.6: Variation of $\Gamma(\Sigma^-_{m_i} \to l_{m_j} H)$ with M_{Σ_i}

From Eq. (3.56) we can see that $(C^{h^0,R}_{l^\pm\Sigma^\pm})_{13} \simeq 0$. In fact one can check that this happens because T_{22} given by Eq. (3.51) has a specific form, which is due to μ-τ symmetry. The consequence of this is that decay of $\Sigma^-_{m3} \to e^-_m h^0$ will be forbidden to leading order. For 300 and 600 GeV triplet fermions, the effect of the lepton masses m_{l_j} on the decay width is negligible. Hence using Eq. (3.52) and Eq. (3.56) the decay rate of all heavy charged fermions into $\mu^\pm_m$ is predicted to be equal to their decay rate into $\tau^\pm_m$. This is also an obvious consequence of the μ-τ symmetry.

The partial decay widths for $\Sigma^-_{m_i} \to l^-_{m_j} h^0$ from an exact numerical calculation in shown in Fig. 3.5, as a function of the heavy charged fermion mass. The thin blue lines are decay into e^-_m, while the thick green lines are for decay into μ^-_m/τ^-_m. As expected, we notice the following two consequences of μ-τ symmetry

- Decay rate of $\Sigma^-_{m3} \to e^-_m h^0$ is zero, hence not shown in this plot.
- The decay rate of the heavy fermions into μ^-_m is equal to that into τ^-_m.

We can also see that for $\Sigma^-_{m_1}$ decay, the decay rate into e^-_m is about 5 orders of magnitude larger than into μ^-_m/τ^-_m. The trend is opposite for $\Sigma^-_{m_2}$ decay, where the decay is predominantly into μ^-_m/τ^-_m. Both of these features can be understood from Eq. (3.56) and the values of the Yukawa couplings taken (cf. Table 3.1). $\Sigma^-_{m_1}$ decay into e^-_m and μ^-_m/τ^-_m is proportional to a_4^2 and a_{11}^2, respectively. The ratio of the decay widths seen in the figure matches the ratio $a_4^2/(a_{11}^2) \sim 10^5$. Similarly, one can check that for $\Sigma^-_{m_2}$ decay, the corresponding ratio is $4a_{11}^2/(a_6+a_8)^2$, which agrees with the middle panel of Fig. 3.5. Finally, the fact that the decay rate of $\Sigma^-_{m_3} \to \mu^-_m h^0$ is less than that of $\Sigma^-_{m_2} \to \mu^-_m h^0$ can also be understood in terms of Eq. (3.56) and the Yukawa coupling values taken for the calculation.

We next turn to the decay width for $\Sigma^\pm_{m_i} \to l^\pm_{m_j} H^0$. Expression for the decay rate is same as that given by Eq. (3.52) except that now M_{h^0} is replaced by the H^0 mass M_{H^0}. For this decay channel the A_{ji} factor is dominantly given by

$$C^{H^0,R}_{l^\pm\Sigma^\pm} \simeq \frac{1}{\sqrt{2}} S^\dagger_{11} Y^\dagger_\Sigma T_{22} \sin\alpha. \tag{3.57}$$

Note that compared to the effective vertex factor for $\Sigma^\pm_{m_i} \to l^\pm_{m_j} h^0$ given in Eq. (3.55), the effective vertex factor given above for $\Sigma^\pm_{m_i} \to l^\pm_{m_j} H^0$ is suppressed by $\sin\alpha$. Since $\sin\alpha \sim 10^{-6}$, the decay rate of $\Sigma^\pm_{m_i}$ into H^0 are heavily suppressed. We show in Fig. 3.6 this decay rate calculated from exact numerical results. Comparing Fig. 3.5 with Fig. 3.6, we see that decays into H^0 are suppressed by a factor of about $\sim 10^{11}$, as expected from the order of magnitude estimate. Therefore, we can neglect $\Sigma^\pm_{m_i} \to l^\pm_{m_j} H^0$ for all practical purposes.

From Table 3.13 it is easy to see that the decay rate $\Sigma^\pm_{m_i} \to l^\pm_{m_j} A^0$ will be almost identical to that that predicted for $\Sigma^\pm_{m_i} \to l^\pm_{m_j} h^0$. The dominant vertex factors for the two process are the same and hence the only difference could come from the difference between the Higgs masses. However, it is easy to see from Eq. (3.52) that the effect of the Higgs mass on the decay rate is not very significant, especially for relatively heavy fermions.

$\Sigma^0_m \to l^\mp_m H^\pm$

The decay rate for this channel is also given by Eq. (3.52), and is governed primarily by the vertex factor

$$C^{H^\pm,R}_{l^\pm\Sigma^0} \simeq \frac{1}{\sqrt{2}} S^\dagger_{11} Y^\dagger_\Sigma U^*_{22} \cos\beta. \tag{3.58}$$

As discussed in detail in the Appendix, the factor $\cos\beta \sim 1$. The matrix U_{22} displays features similar to the matrix T_{22}. Therefore, the form of dominant vertex factor for this case is similar to that given in Eq. (3.56). The corresponding decay rates are shown in Fig.

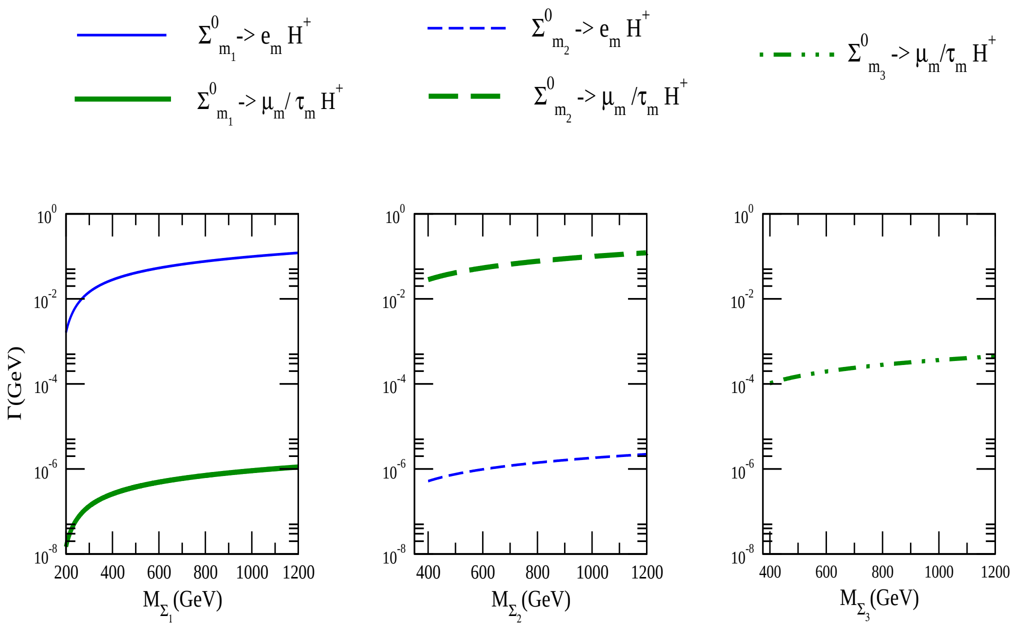

Figure 3.7: Variation of $\Gamma(\Sigma^0_{m_i} \to l_{m_j} H^+)$ with M_{Σ_i}

3.7. All features seen for $\Sigma^-_{m_i} \to l_{m_j} h^0$ is also seen here. Decay channel $\Sigma^0_{m3} \to e^{\mp}_{m_j} H^{\pm}$ is forbidden. Decay rates to $\mu^{\mp}_m$ is equal to decay rate to $\tau^{\mp}_m$. The huge hierarchy in the decay rates of $\Sigma^0_{m_1}$ and $\Sigma^0_{m_2}$ into e_m and μ_m/τ_m are also present due to same reason as given for $\Sigma^-_m \to l^-_m h^0$ decays. The decay rate and flavor structure for the final state charged leptons is therefore seen to be same here as for the decay of charged heavy fermions into charged light leptons and h^0. However, in this case we have a charged Higgs in the final state and it should be easy to tag this and differentiate the two processes in the detector at LHC.

$\Sigma^0_m \to \nu_m\, h^0/H^0/A^0$

We next turn to the decay channels with a light neutrino in the final state. This will give missing energy in the final state. Decay of the neutral Σ^0_m will create a neutrino and a neutral Higgs. As in the case of decay of $\Sigma^{\pm}_m$ to charged leptons and neutral Higgs, one can check from Table 3.14 that the decay to the Higgs H^0 is heavily suppressed due to the $\sin\alpha$ term. However, decay to h^0 is driven by the vertex factor

$$C^{h^0,R}_{\nu\Sigma^0} = \frac{1}{2} U^\dagger_{11} Y^\dagger_\Sigma U^*_{22} \cos\alpha. \tag{3.59}$$

For the decay $\Sigma^0_{m_i} \to \nu_{m_j} A^0$ we find from Table 3.14 that the dominant vertex factor is

$$C^{A^0,R}_{\nu\Sigma^0} = -\frac{i}{2} U^\dagger_{11} Y^\dagger_\Sigma U^*_{22} \cos\beta. \tag{3.60}$$

Since $\cos\beta \simeq \cos\alpha$, the decay rate and flavor structure for this channel will be similar to what we found for the $\Sigma^0_{m_i} \to \nu_{m_j} h^0$ channel. The main difference comes in the difference between the masses of the h^0 and A^0 Higgs.
For the $\Sigma^0_{m_i} \to \nu_{m_j} H^0$ decay, one can see from Table 3.14 that the vertex factors for both P_L as well as P_R vertices, are suppressed by $\sin\alpha$. Therefore, this decay rate can be neglected.

$\Sigma^\pm_m \to \nu_m\, H^\pm$

From Table 3.15 the vertex factor for this decay will be

$$C^{H^\pm,L}_{\nu\Sigma^\mp} \simeq U^T_{11} Y^T_\Sigma S_{22} \cos\beta. \tag{3.61}$$

As we have seen in section 3.3, the structure of S_{22} is very similar to that of U_{22}. Hence, a comparison of the vertex factor for this process with the one from $\Sigma^0_{m_i} \to \nu_{m_j} h^0$ and $\Sigma^0_{m_i} \to \nu_{m_j} A^0$ shows that all three will have decay rates of comparable magnitude, modulo the difference in the masses of the scalars h^0, A^0 and $H^\pm$.

3.5.2 Decay to Light Leptons and Vector Bosons

The exotic heavy leptons have gauge interactions. Therefore, it is expected that they will also decay into final state particles with vector bosons, $W^\pm$ and Z. The decay width Γ for $\Sigma^\pm_{m_i} \to l^\pm_{m_j}/\nu_{m_j} V$ and $\Sigma^0_{m_i} \to l^\pm_{m_j}/\nu_{m_j} V$ in the $m_{l_j} = 0$ limit is given by

$$\Gamma = \frac{M_{\Sigma_i}}{32\pi}\left[1 - \frac{{M_V}^2}{{M_\Sigma}^2}\right]^2 \left[2 + \frac{{M_\Sigma}^2}{{M_V}^2}\right]\Big(|(C^{V,L}_{l^\pm\Sigma})_{ji}|^2 + |(C^{V,R}_{l^\pm\Sigma})_{ji}|^2\Big), \tag{3.62}$$

where $C^{V,L}_{l^\pm\Sigma}$ and $C^{V,R}_{l^\pm\Sigma}$ are the relevant vertex factors given in Appendix B.2, and M_V is the mass of the vector boson involved. The dominant vertex factor relevant for $\Sigma^\pm_m \to l^\pm_m Z$ and $\Sigma^0_m \to l^\pm_m W^\mp$ in terms of Y_Σ, M, v' and the mixing matrices are given respectively by

$$C^{Z,L}_{l^\pm\Sigma^\pm} \simeq \frac{v'}{2}\frac{g}{c_w}\, {U_l}^\dagger Y^\dagger_\Sigma M^{-1} U^L_h, \quad \text{and} \quad C^{W^\mp,L}_{l^\pm\Sigma^0} \simeq -\frac{v'}{2}\, g\, {U_l}^\dagger Y^\dagger_\Sigma M^{-1} U_\Sigma. \tag{3.63}$$

For the other two channels $\Sigma_m^0 \to \nu_m Z$ and $\Sigma_m^\pm \to \nu_m W^\pm$, they are given respectively by

$$\begin{aligned} C^{Z,L}_{\nu\Sigma^0} &\simeq \frac{v'}{2\sqrt{2}}(gc_w + g's_w)U^\dagger_{PMNS}Y^\dagger_\Sigma M^{-1}U_\Sigma, \\ C^{W^\mp,R}_{\nu\Sigma^\pm} &\simeq -\frac{v'}{\sqrt{2}}\, g\, U^T_{PMNS}Y^T_\Sigma M^{-1}U^R_h. \end{aligned} \tag{3.64}$$

The gauge interaction part of our model is identical to that for the one Higgs doublet type-III seesaw considered earlier. Some of these vertex factors can therefore can be seen to agree with that given in [29]. The only difference is that we include the matrices U_l, U_h^R and U_Σ in our general expressions, while these were taken as unit matrices in [29].

3.5.3 Comparing $\Sigma_m^{\pm/0}$ Decays to Higgs and Gauge Bosons

In Fig. 3.8 we show the decay rates $\Sigma_{m_1}^- \to \nu_{m_1} W^-$ (long-dashed blue line), $\Sigma_{m_1}^- \to e_m^- Z$ (dot-dashed green line), $\Sigma_{m_1}^0 \to \nu_{m_1} Z$ (dot-dashed magenta line), $\Sigma_{m_1}^0 \to e_m^- W^+$ (thin solid red line), $\Sigma_{m_1}^- \to e_m^- H^0$ (dotted maroon line), $\Sigma_{m_1}^- \to \nu_{m_1} H^-$ (dashed violet line), and $\Sigma_{m_1}^- \to e_m^- h^0$ (thick solid dark green line). To clarify the notation once more, ν_{m_j} corresponds to the charged lepton $l_{m_j}^\pm$, where $l_{m_j}^\pm$ represent $e_m^\pm$, $\mu_m^\pm$ and $\tau_m^\pm$ for $j = 1, 2, 3$ respectively. One can see that all decays to gauge bosons are suppressed with respect to decays to h^0 (and A^0) and $H^\pm$ by a factor of more than 10^{10}. The reason for this can be seen by comparing the vertex factors involved in decays to Higgs h^0, A^0 and $H^\pm$ (cf. Eqs. (3.55), (3.58), (3.59), (3.60), (3.61)), with decays to gauge bosons (cf. Eqs. (3.63) and (3.64)). It is clear that while the former vertex factors do not have any suppression factor, the latter are all suppressed by v'/M. Another important difference between the decay rates to Higgs given in Eq. (3.52), and gauge bosons given in Eq. (3.62), is in the kinematic factors. Comparison of the two equations reveals that (for $m_{l_j} = 0$), there is an additional factor of $(2 + M_\Sigma^2/M_V^2)$ for the gauge boson decays. This factor folded with the factor $\frac{g^2 v'^2}{M^2}$ which comes from the couplings, gives a suppression $\frac{g^2 v'^2}{M^2}$ and $\frac{g^2 v'^2}{M_V^2}$. Since we have taken $v' \sim 10^{-3}$-10^{-4} GeV, $M = 300, 600$ GeV and the gauge boson masses are $M_V \sim 80, 90$ GeV, the decays to gauge bosons are suppressed by a factor of $\sim 10^{10}$-10^{12} compared to the decays to Higgs. Therefore, branching ratios of the heavy fermion decay to $W^\pm$ and Z can be neglected in our model and we concentrate on only decays to h^0, A^0 and $H^\pm$ in our next section. Note that the decay to H^0 is also suppressed by a factor of 10^{10}-10^{12}, as was also pointed out earlier. We had seen that this suppression is due to $\sin^2\alpha$ coming from the vertex factor for this process. Since $\sin^2\alpha \sim 10^{-12}$, we find that the decay rate for this case is of the same order of magnitude as the decays to the gauge bosons. Hence, this is also neglected henceforth.

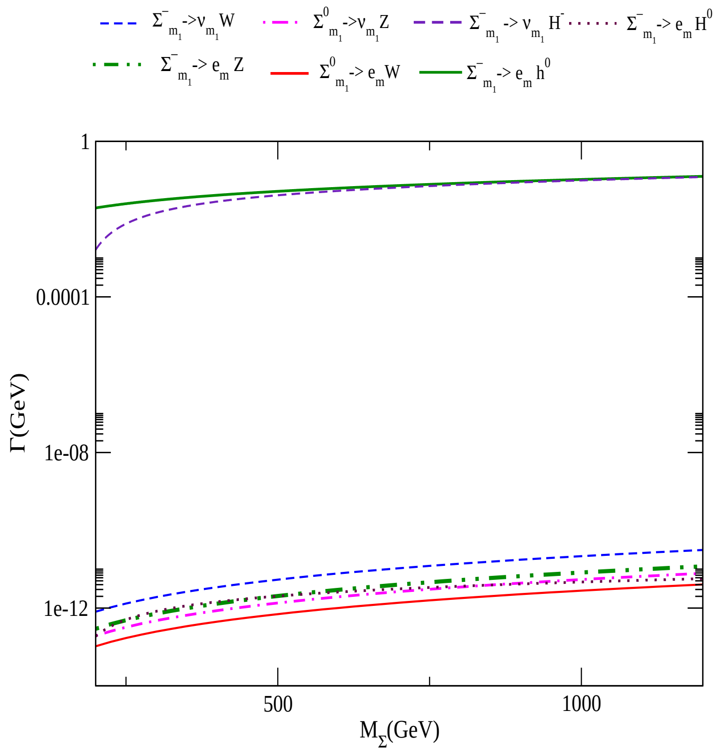

Figure 3.8: Comparison of the decay rate of the heavy fermion into (i) Higgs and (ii) vector bosons, in our two Higgs doublet model.

3.5.4 Comparison Between One and Two Higgs Doublet Models

It is pertinent to compare the two-body decays of the heavy fermions in our two Higgs doublet model with the usual type-III seesaw models considered earlier which have one Higgs doublet. The expressions for heavy fermion decays to Higgs and gauge bosons in the one Higgs doublet models have been given before in the literature [14–17], and we give them here for the sake of comparison. The decay rates to gauge bosons in the one Higgs doublet model is given as (for $m_{l_j} = 0$)

$$\Gamma^{1HDM}(\Sigma^0_m \to \nu_m Z) \simeq \frac{\lambda^2 M_\Sigma}{64\pi}(1 - \frac{M_Z^2}{{M_\Sigma}^2})^2(1 + 2\frac{M_Z^2}{{M_\Sigma}^2}), \tag{3.65}$$

$$\Gamma^{1HDM}(\Sigma^0_m \to l^\mp_m W^\pm) \simeq \frac{\lambda^2 M_\Sigma}{32\pi}(1 - \frac{M_W^2}{{M_\Sigma}^2})^2(1 + 2\frac{M_W^2}{{M_\Sigma}^2}), \tag{3.66}$$

$$\Gamma^{1HDM}(\Sigma^\pm_m \to l^\pm_m Z) \simeq \frac{\lambda^2 M_\Sigma}{32\pi}(1-\frac{M_Z^2}{{M_\Sigma}^2})^2(1+2\frac{M_Z^2}{{M_\Sigma}^2}), \quad (3.67)$$
$$\Gamma^{1HDM}(\Sigma^\pm_m \to \nu_m W^\pm) \simeq \frac{\lambda^2 M_\Sigma}{16\pi}(1-\frac{M_Z^2}{{M_\Sigma}^2})^2(1+2\frac{M_Z^2}{{M_\Sigma}^2}). \quad (3.68)$$

where λ is the triplet fermion – lepton doublet – Higgs doublet Yukawa coupling in the one Higgs doublet model, and all mixing terms are neglected. This should be compared with the corresponding expression given in Eq. (3.62), which on neglecting all mixing and hence flavor effects reduces to (for $m_{l_j}=0$)

$$\Gamma^{2HDM}(\Sigma^0_m \to \nu_m Z) \simeq \frac{Y_\Sigma^2 M_\Sigma}{64\pi}\frac{v'^2}{V^2}(1-\frac{M_Z^2}{{M_\Sigma}^2})^2(1+2\frac{M_Z^2}{{M_\Sigma}^2}), \quad (3.69)$$
$$\Gamma^{2HDM}(\Sigma^0_m \to l^\mp_m W^\pm) \simeq \frac{Y_\Sigma^2 M_\Sigma}{32\pi}\frac{v'^2}{V^2}(1-\frac{M_W^2}{{M_\Sigma}^2})^2(1+2\frac{M_W^2}{{M_\Sigma}^2}), \quad (3.70)$$
$$\Gamma^{2HDM}(\Sigma^\pm_m \to l^\pm_m Z) \simeq \frac{Y_\Sigma^2 M_\Sigma}{32\pi}\frac{v'^2}{V^2}(1-\frac{M_Z^2}{{M_\Sigma}^2})^2(1+2\frac{M_Z^2}{{M_\Sigma}^2}), \quad (3.71)$$
$$\Gamma^{2HDM}(\Sigma^\pm_m \to \nu_m W^\pm) \simeq \frac{Y_\Sigma^2 M_\Sigma}{16\pi}\frac{v'^2}{V^2}(1-\frac{M_Z^2}{{M_\Sigma}^2})^2(1+2\frac{M_Z^2}{{M_\Sigma}^2}). \quad (3.72)$$

where $V^2 = v^2 + v'^2$ is the electroweak breaking scale. The scale of the Yukawa coupling constants and VEVs are fixed by the neutrino mass $m_\nu \sim \lambda^2 V^2/M_\Sigma$ for the one Higgs doublet model and $m_\nu \sim Y_\Sigma^2 v'^2/M_\Sigma$. If one replaces λ^2 and $Y_\Sigma^2 v'^2/V^2$ with $m_\nu M_\Sigma/V^2$ in both set of expressions, one can see that the the decay rates of heavy fermions into gauge bosons are identical for both models.

The rates for decay into Higgs for the one Higgs doublet model neglecting flavor effects, is given by (for $m_{l_j}=0$)

$$\Gamma^{1HDM}(\Sigma^0_m \to \nu_m H^0) \simeq \frac{\lambda^2 M_\Sigma}{64\pi}(1-\frac{M_H^2}{{M_\Sigma}^2})^2, \quad (3.73)$$
$$\Gamma^{1HDM}(\Sigma^\pm_m \to l^\pm_m H^0) \simeq \frac{\lambda^2 M_\Sigma}{32\pi}(1-\frac{M_H^2}{{M_\Sigma}^2})^2. \quad (3.74)$$

For the two Higgs doublet model, the corresponding decay rates are given by Eq. (3.52), which on neglecting all flavor effects reduces to (for $m_{l_j}=0$)

$$\Gamma^{2HDM}(\Sigma^0_m \to \nu_m h^0/A^0) \simeq \frac{Y_\Sigma^2 \cos^2\alpha\, M_\Sigma}{64\pi}(1-\frac{M_{h/A}^2}{{M_\Sigma}^2})^2, \quad (3.75)$$
$$\Gamma^{2HDM}(\Sigma^\pm_m \to l^\pm_m h^0/A^0) \simeq \frac{Y_\Sigma^2 \cos^2\alpha\, M_\Sigma}{32\pi}(1-\frac{M_{h/A}^2}{{M_\Sigma}^2})^2, \quad (3.76)$$

$$\Gamma^{2HDM}(\Sigma_m^0 \to \nu_m H^0) \simeq \frac{Y_\Sigma^2 \sin^2\alpha \, M_\Sigma}{64\pi}(1 - \frac{M_H^2}{{M_\Sigma}^2})^2, \quad (3.77)$$

$$\Gamma^{2HDM}(\Sigma_m^\pm \to l_m^\pm H^0) \simeq \frac{Y_\Sigma^2 \sin^2\alpha \, M_\Sigma}{32\pi}(1 - \frac{M_H^2}{{M_\Sigma}^2})^2, \quad (3.78)$$

where the first two expressions are for decays to h^0 or A^0 and the last two for decays to H^0. Again, for the same value of $M_\Sigma \sim 100$ GeV in both models, one requires $\lambda \sim 10^{-5}$-10^{-6} for the one Higgs doublet model in order to produce $m_\nu \sim 0.1$ eV, while $Y_\Sigma \sim 1$ for our two Higgs doublet model. Therefore, clearly

$$\Gamma^{2HDM}(\Sigma_m^0 \to \nu_m h^0/A^0) \sim 10^{11} \times \Gamma^{1HDM}(\Sigma_m^0 \to \nu_m H^0),$$

$$\Gamma^{2HDM}(\Sigma_m^\pm \to l_m^\pm h^0/A^0) \sim 10^{11} \times \Gamma^{1HDM}(\Sigma_m^\pm \to l_m^\pm H^0).$$

Hence, the the exotic fermions decay about 10^{11} times faster in our model compared to the one Higgs doublet model. This could lead to observational consequences at LHC. In particular, authors of [15] talk about using "displaced vertices" as a signature of the type-III seesaw mechanism. In our model the lifetime of the exotic fermions is a factor of 10^{11} shorter and so will be the gap between their primary production vertex and the decay vertex. This model therefore predicts no displaced vertex for the heavy fermion decays. The other decay modes such as $\Sigma_m^0 \to \nu_m H^0$ and $\Sigma_m^\pm \to l_m^\pm H^0$ are suppressed by the $\sin^2\alpha \sim 10^{-12}$ factor and hence turn out to be comparable to the decay rates in the one Higgs doublet model. As a result, the branching ratio to this mode is negligible and can be neglected. In our model, decay of triplet fermions into h^0, A^0 and $H^\pm$ are predominant. We discuss the decay modes of the different Higgs fields h^0,H^0, A^0 and $H^\pm$ in section 3.6. Among the different Higgs fields, the h^0 decay predominantly into $b\bar{b}$ pairs, but with a very long lifetime, as we will discuss in section 3.6.

3.5.5 Flavor Structure and the Decay Branching Ratios

In this section we present the branching fractions of the heavy fermion decays. Table 3.2 shows the branching fractions for the $\Sigma_m^\pm$, while Table 3.3 gives the branching fraction for Σ_m^0 decays. For the channels with neutrino in the final state, we give the sum of the branching fraction into all the three generations, as observationally it will be impossible to see the neutrino generations at LHC. We do not show decays to gauge bosons and H^0 as they are suppressed by a factor of 10^{11} with respect to the decays into h^0, A^0 and $H^\pm$. As a result of the inherent μ-τ symmetry in the model, $\Sigma_{m_3}^{\pm/0}$ decays to electrons is strictly forbidden and branching ratios of their decay into μ_m and τ_m leptons are equal. We find that due to the form of U_{22}, S_{22} and T_{22} given in Eqs. (3.49), (3.50) and (3.51), the probability of $\Sigma_{m_2}^{\pm/0}$ to decay into μ_m and τ_m leptons is equal. We also find that the branching fractions of $\Sigma_{m_2}^\pm$ is almost equal to the branching fractions of $\Sigma_{m_3}^\pm$, and similarly for the neutral heavy fermions. The difference between the branching fraction to h^0, A^0

Decay modes	$\Sigma^{\pm}_{m_1}$	$\Sigma^{\pm}_{m_2}$	$\Sigma^{\pm}_{m_3}$
$\nu_m\, H^{\pm}$	0.363	0.473	0.473
$e^{\pm}_m\, A^0$	0.247	2.28×10^{-6}	0.0
$\mu^{\pm}_m\, A^0$	2.3×10^{-6}	0.125	0.125
$\tau^{\pm}_m\, A^0$	2.3×10^{-6}	0.125	0.125
$e^{\pm}_m\, h^0$	0.389	2.5×10^{-6}	0.0
$\mu^{\pm}_m\, h^0$	3.6×10^{-6}	0.139	0.139
$\tau^{\pm}_m\, h^0$	3.6×10^{-6}	0.139	0.139

Table 3.2: Decay branching fractions of $\Sigma^{\pm}_{m_1}$, $\Sigma^{\pm}_{m_2}$ and $\Sigma^{\pm}_{m_3}$ for M_{h^0}=40, M_{H^0}=150, $M_{H^{\pm}} =$ 170 GeV and $M_{A^0} =$ 140 GeV. We have taken model parameters $M_1 =$ 300 GeV and $M_2 = M_3 =$ 600 GeV.

Decay modes	$\Sigma^{0}_{m_1}$	$\Sigma^{0}_{m_2}$	$\Sigma^{0}_{m_3}$
$e^{\mp}_m\, H^{\pm}$	0.368	4.3×10^{-6}	0.0
$\mu^{\mp}_m\, H^{\pm}$	3.4×10^{-6}	0.236	0.236
$\tau^{\mp}_m\, H^{\pm}$	3.4×10^{-6}	0.236	0.236
$\nu_m\, A^0$	0.243	0.250	0.250
$\nu_m\, h^0$	0.386	0.277	0.277

Table 3.3: Decay branching fractions of $\Sigma^{0}_{m_1}$, $\Sigma^{0}_{m_2}$ and $\Sigma^{0}_{m_3}$ for M_{h^0}=40, M_{H^0}=150, $M_{H^{\pm}} =$ 170 GeV and $M_A =$ 140 GeV. We have taken model parameters $M_1 =$ 300 GeV and $M_2 = M_3 =$ 600 GeV.

and $H^{\pm}$ is mainly driven by the difference in the masses which we have chosen for these Higgses. In Table. 3.2 and Table. 3.3 we have taken the light Higgs mass $M_{h^0} = 40$ GeV. We also present the branching fractions of the heavy triplet fermions for the light Higgs mass $M_{h^0} = 70$ GeV in Table. 3.4 and in Table. 3.5.

3.6 Higgs Decay

In the previous section we have seen that the heavy fermions $\Sigma^{\pm}_m$, Σ^0_m will decay predominantly into h^0, A^0 or $H^{\pm}$ associated with a lepton. In this section we discuss the possible decay modes of the Higgs h^0, A^0 and $H^{\pm}$. We tabulate those few which have significant branching ratios. The branching ratios of the different Higgs decay modes depend on the choice for the Higgs masses as well as our choice of the mixing angles α and β, which appear in the coupling. The part of the Lagrangian containing the interaction terms of

Decay modes	$\Sigma^{\pm}_{m_1}$	$\Sigma^{\pm}_{m_2}$	$\Sigma^{\pm}_{m_3}$
$\nu_m\, H^{\pm}$	0.381	0.475	0.475
$e^{\pm}_m\, A^0$	0.251	2.30×10^{-6}	0.0
$\mu^{\pm}_m\, A^0$	2.31×10^{-6}	0.126	0.126
$\tau^{\pm}_m\, A^0$	2.31×10^{-6}	0.126	0.126
$e^{\pm}_m\, h^0$	0.37	2.51×10^{-6}	0.0
$\mu^{\pm}_m\, h^0$	3.39×10^{-6}	0.137	0.137
$\tau^{\pm}_m\, h^0$	3.39×10^{-6}	0.137	0.137

Table 3.4: Decay branching fractions of $\Sigma^{\pm}_{m_1}$, $\Sigma^{\pm}_{m_2}$ and $\Sigma^{\pm}_{m_3}$ for M_{h^0}=70, M_{H^0}=150, $M_{H^{\pm}} =$ 170 GeV and $M_{A^0} = 140$ GeV. We have taken model parameters $M_1 = 300$ GeV and $M_2 = M_3 = 600$ GeV.

Decay modes	$\Sigma^{0}_{m_1}$	$\Sigma^{0}_{m_2}$	$\Sigma^{0}_{m_3}$
$e^{\mp}_m\, H^{\pm}$	0.381	4.35×10^{-6}	0.0
$\mu^{\mp}_m\, H^{\pm}$	3.51×10^{-6}	0.238	0.238
$\tau^{\mp}_m\, H^{\pm}$	3.51×10^{-6}	0.238	0.238
$\nu_m\, A^0$	0.251	0.252	0.252
$\nu_m\, h^0$	0.368	0.272	0.272

Table 3.5: Decay branching fractions of $\Sigma^{0}_{m_1}$, $\Sigma^{0}_{m_2}$ and $\Sigma^{0}_{m_3}$ for M_{h^0}=70, M_{H^0}=150, $M_{H^{\pm}} =$ 170 GeV and $M_A = 140$ GeV. We have taken model parameters $M_1 = 300$ GeV and $M_2 = M_3 = 600$ GeV.

the Higgs with the leptons and quarks are given in Appendix B. The interaction of Higgs fields with the gauge fields comes from the Higgs kinetic terms and is the same as the general two Higgs doublet model. Possible decay channels for the charged Higgs involve the $W^{\pm}$ and the neutral CP even Higgs. In the two Higgs doublet model, the $W^{\pm} - H^{\mp} - H^0$ coupling is proportional to $\sin(\beta - \alpha)$, whereas $W^{\pm} - H^{\mp} - h^0$ coupling is proportional to $\cos(\beta - \alpha)$ [19]. In Appendix A, we have shown how constraint from neutrino mass drives $\sin\alpha \sim \sin\beta \sim 10^{-6}$. Therefore, in our model $H^{\pm} \to W^{\pm}H^0$ is always suppressed, irrespective of the Higgs mass. In fact, the only decay channel possible for the charged Higgs in our model is $H^{\pm} \to W^{\pm}h^0$, for which the decay branching fraction

$$BR(H^{\pm} \to W^{\pm}h^0) = 1.0. \tag{3.79}$$

The $W^{\pm}$ next decay into either $q_m q'_m$ pairs or $l^{\pm}_m \nu_m$ pairs. The branching fractions of the neutral Higgs h^0, H^0 and A^0 are given in Table. 3.6 and also in Table. 3.7. Though H^0 is almost never produced through heavy fermion decays in our model, we have included

Decay modes	h^0	H^0	A^0
$b_m\bar{b}_m$	0.89	0.87	0.87
$\tau_m\bar{\tau}_m$	0.07	0.09	0.09
$c_m\bar{c}_m$	0.04	0.04	0.04

Table 3.6: Decay branching fractions of h^0, H^0 and A^0 for $M_{h^0} = 40$ GeV, $M_{H^0} = 150$ GeV, and $M_{A^0} = 140$ GeV.

Decay modes	h^0
$b_m\bar{b}_m$	0.88
$\tau_m\bar{\tau}_m$	0.08
$c_m\bar{c}_m$	0.04

Table 3.7: Decay branching fractions of h^0, H^0 and A^0 for $M_{h^0} = 70$ GeV.

them in the table for completeness. We find that the neutral Higgs decay to $b_m\bar{b}_m$ pairs almost 88-89% of the times for $M_{h^0} = 70, 40$ GeV respectively. The decays to $\tau_m\bar{\tau}_m$ and $c_m\bar{c}_m$ happen less than few percent of the times. In our following sections where we look for collider signatures, we will consider h^0 decays to only $b_m\bar{b}_m$ and $\tau_m\bar{\tau}_m$ pairs.

Finally, a short discussion on direct production of h^0, without involving the heavy fermion decays, is in order. In this work we have considered one of the cases where the lightest Higgs mass as low as 40 GeV. This might appear to be a cause of concern, given that such a Higgs was not observed at LEP. However, it is easy to see that this Higgs mass is not excluded by the direct Higgs searches at LEP-2. This is because the coupling corresponding to $Z - Z - h^0$ vertex is given by $(gM_Z/\cos\theta_w)\sin(\beta-\alpha)$. Since in our model $\sin(\beta-\alpha)$ is almost zero, the LEP-2 bound on Higgs mass does not pose any serious threat to our model, irrespective of the mass of h^0.

3.7 Displaced h^0 Decay Vertex

Amongst the most significant difference of our model with the usual type-III seesaw model are the decay lifetimes of the heavy fermions and h^0. The total decay rate for 300 GeV Σ_m^0 is about 10^{-2} GeV. This gives the corresponding rest frame lifetime as 10^{-13} cm. The lifetime for $\Sigma_m^\pm$ is similar. One can check that for the usual one Higgs doublet models, the rest frame lifetime for the heavy fermions is $\simeq 0.5$ cm [15] for $m_\nu = 0.1$ eV and $M_\Sigma \sim 100$ GeV, which is rather large. The authors of [15] therefore proposed that the displaced decay vertex of heavy fermion could be a typical signature of the one Higgs type-

III seesaw model. Clearly, for our model with two Higgs doublets, the decay lifetime is almost 10^{13} times smaller and hence we predict no displaced vertex for the heavy fermion decay. This can be used as a distinguishing signature between the two models.

Another very important and unique feature of our model is the very long lifetime of our neutral Higgs h^0, which comes due to the smallness of $\sin\alpha$. In fact, since $\sin\alpha \sim 10^{-6}$, the lifetime for h^0 in our model is 10^{12} times larger compared to the standard model Higgs. In particular, the h^0 total decay rate is around 10^{-15} GeV. This gives h^0 a rest frame lifetime of 4.97 cm. For a h^0 with hundred GeV of energy, the lifetime in the lab frame is should be few 10s of cm. Therefore, we expect a big gap between the decay vertices of the heavy fermion and the h^0. This displaced h^0 decay vertex should be detectable at the LHC detectors ATLAS and CMS.

We would like to make just a few qualitative remarks about the prospects of detecting the displaced h^0 vertex. The h^0 decay predominantly into $b_m\bar{b}_m$ pairs. While b-tagging is a very important and standard tool for collider experiments, and while both ATLAS [31] and CMS [32] have been developing algorithms for tagging the b, there is an additional complication with b-tagging in our model which should be pointed out here. Since the h^0 lifetime is a few 10s of cm in the lab frame, it is expected to decay inside the silicon tracker of ATLAS and CMS. In particular, the pixel tracker of CMS and ATLAS which are only few cm from the center of the beam pipe, will miss the h^0 decay vertex. However, the silicon strip trackers would be useful in observing the b-jets. The tracks from the primary and secondary vertices of the b-hadron should be seen. In addition, one could use the two other standard tools for tagging the b-jets. Firstly, one could the tag the lepton in the jet coming from the semi-leptonic decays of the b-hadron. These leptons are expected to have smaller p_T compared to the ones coming from $W^\pm$ and Z decays, and hence this is called soft-lepton tagging [31, 32]. More importantly, one could construct the invariant mass distribution of the 2 b-jets. This should give us a sharp peak corresponding to the h^0. We therefore expect that ATLAS and CMS should be able to detect the displaced h^0 decay vertex. This would give a characteristic and unambiguous signal of our model.

3.8 Model Signatures at the LHC

For notational simplicity, we change our convention in this section. Here, we do not use the subscript “m” any further to denote the fields in their mass basis. All the triplet fermions, standard model leptons and quarks fields written in this section are in the mass basis and we denote them simply by the notations $\Sigma^{\pm,0}$, $l^\pm$, ν , b and so on. In the previous sections we have discussed in details the production and subsequent decays of the exotic fermions, as well as the decay branching fractions of the intermediate Higgs into final state particles. In this section we describe the signatures of the two Higgs doublet type-III seesaw model at the LHC. We will present a comprehensive list of final state particles and their corresponding collider signatures.

The most important characteristics of our model are the following:

1. Presence of μ-τ symmetry in Y_Σ and M. This is expected to show-up in the flavor of the final state lepton coming directly from the $\Sigma^{\pm/0}$ decay vertex.

2. Presence of two CP even neutral Higgses (h^0 and H^0), one CP odd neutral Higgs (A^0), and a pair of charged Higgs ($H^\pm$).

3. Predominant decay of the heavy fermions into light leptons, and h^0, A^0 or $H^\pm$. Decays into H^0 and gauge bosons almost never happen.

4. Very short lifetime for the heavy fermion due to the very large Yukawa couplings.

5. Predominant decay of h^0 and A^0 into $b\bar{b}$ pairs 88-89% and 87% of the time, respectively. They decay also into $\tau\bar{\tau}$ 7-9% of the time.

6. Very large lifetime of h^0.

7. The Higgs $H^\pm$ decays into $W^\pm h^0$ and almost never into $W^\pm H^0$.

In what follows, we will use these model characteristics to identify the different final state channels at the collider. We identify the possible channels in the collider for our model and calculate the respective effective cross-sections. The results are given in Tables 3.8, 3.9 and 3.10. We will also discuss some of the most important channels and the characteristic backgrounds, if any, associated with them. In this section we have only given results for effective cross-sections for the decay of $\Sigma_1^{\pm/0}$ with $M_{\Sigma_1} = 300$ GeV. Results for the other heavy fermion generations can be similarly obtained. We have considered the light Higgs mass $M_{h^0} = 40$ GeV, while calculating the effective cross sections given in Table 3.8, Table 3.9 and Table 3.10. For the other choice M_{h^0}=70 GeV, the effective cross section does not change significantly. However, as an example we have also calculated the effective cross section for few of the significant channels which have large cross section and tabulate them in Table 3.12 for the case $M_{h^0} = 70$ GeV.

3.8.1 Signatures from $\Sigma^+\Sigma^-$ decays

We give in Table 3.8 the possible collider signatures coming from the decay of $\Sigma^+\Sigma^-$ pairs, for our two Higgs doublet type-III seesaw model. In the last column we also give the corresponding effective cross-sections for these channels in units of fb. The final cross-sections can be obtained only after putting in the various cuts and efficiency factors. These efficiency factors will have to be folded with the cross-sections given in Table 3.8 to get the final effective cross-sections for the various channels. We have not addressed these issues in this present work. Few clarifications on our notation is in order. Light charged leptons could be released in the final state through two ways: (i) from the decay of the

Sl no	Channels	Effective cross-section (in fb)
1	$\Sigma^+\Sigma^- \to l^+l^-h^0h^0 \to 4b + OSD$	35.84
2	$\Sigma^+\Sigma^- \to l^+l^-h^0h^0 \to 2b + OSD + 2\tau$	3.67
3	$\Sigma^+\Sigma^- \to l^+l^-h^0h^0 \to OSD + 4\tau$	0.37
4	$\Sigma^+\Sigma^- \to l^+h^0H^-\nu \to 4b + l + 2j + \not{p}_T$	26.88
5	$\Sigma^+\Sigma^- \to l^+h^0H^-\nu \to 4b + OSD(l+l') + \not{p}_T$	8.92
6	$\Sigma^+\Sigma^- \to l^+h^0H^-\nu \to 4b + l + \tau + \not{p}_T$	4.48
7	$\Sigma^+\Sigma^- \to l^+h^0H^-\nu \to 2b + l + 2\tau + 2j + \not{p}_T$	2.69
8	$\Sigma^+\Sigma^- \to l^+h^0H^-\nu \to 2b + l + 3\tau + \not{p}_T$	0.45
9	$\Sigma^+\Sigma^- \to l^+h^0H^-\nu \to 2b + OSD(l+l') + 2\tau + \not{p}_T$	0.9
10	$\Sigma^+\Sigma^- \to l^+h^0H^-\nu \to l + 4\tau + 2j + \not{p}_T$	0.28
11	$\Sigma^+\Sigma^- \to l^+h^0H^-\nu \to OSD(l+l') + 4\tau + \not{p}_T$	0.04
12	$\Sigma^+\Sigma^- \to l^+h^0H^-\nu \to l + 5\tau + \not{p}_T$	0.02
13	$\Sigma^+\Sigma^- \to H^+\nu H^-\nu \to 4b + 4j + \not{p}_T$	15.68
14	$\Sigma^+\Sigma^- \to H^+\nu H^-\nu \to 4b + 2j + l' + \not{p}_T$	10.52
15	$\Sigma^+\Sigma^- \to H^+\nu H^-\nu \to 4b + 2j + \tau + \not{p}_T$	5.26
16	$\Sigma^+\Sigma^- \to H^+\nu H^-\nu \to 4b + OSD' + \not{p}_T$	0.86
17	$\Sigma^+\Sigma^- \to H^+\nu H^-\nu \to 4b + 2\tau + \not{p}_T$	0.43
18	$\Sigma^+\Sigma^- \to H^+\nu H^-\nu \to 4b + 1\tau + 1l' + \not{p}_T$	0.53
19	$\Sigma^+\Sigma^- \to H^+\nu H^-\nu \to 2b + 2\tau + 4j + \not{p}_T$	3.25
20	$\Sigma^+\Sigma^- \to H^+\nu H^-\nu \to 2b + 2\tau + 2j + l' + \not{p}_T$	2.12
21	$\Sigma^+\Sigma^- \to H^+\nu H^-\nu \to 2b + 3\tau + 2j + \not{p}_T$	1.06
22	$\Sigma^+\Sigma^- \to H^+\nu H^-\nu \to 2b + 2\tau + OSD' + \not{p}_T$	0.32
23	$\Sigma^+\Sigma^- \to H^+\nu H^-\nu \to 2b + 4\tau + \not{p}_T$	0.08
24	$\Sigma^+\Sigma^- \to H^+\nu H^-\nu \to 2b + 3\tau + l' + \not{p}_T$	0.02
25	$\Sigma^+\Sigma^- \to H^+\nu H^-\nu \to 4\tau + 4j + \not{p}_T$	0.15
26	$\Sigma^+\Sigma^- \to H^+\nu H^-\nu \to 4\tau + 2j + l' + \not{p}_T$	0.10
27	$\Sigma^+\Sigma^- \to H^+\nu H^-\nu \to 5\tau + 2j + \not{p}_T$	0.05
28	$\Sigma^+\Sigma^- \to H^+\nu H^-\nu \to 5\tau + l' + \not{p}_T$	0.006
29	$\Sigma^+\Sigma^- \to H^+\nu H^-\nu \to 4\tau + OSD' + \not{p}_T$	0.02
30	$\Sigma^+\Sigma^- \to H^+\nu H^-\nu \to 6\tau + \not{p}_T$	0.005

Table 3.8: Effective cross-sections (in fb) for different $\Sigma^+\Sigma^-$ decay channels for $M_{\Sigma_1} = 300$ GeV.

heavy fermions $\Sigma^{\pm} \to l^{\pm} h^0$ and $\Sigma^0 \to l^{\pm} H^{\mp}$, (ii) from the decays of $W \to l\bar{\nu}$. The charged leptons released from the $\Sigma^{\pm/0}$ decays are different from those from $W^{\pm}$ in two respects. Firstly, the former carry the information on the flavor structure of the model as discussed in the previous sections, while the latter do not. Secondly, since they come from decays of the heavier $\Sigma^{\pm/0}$, they are expected to be harder than the ones from $W^{\pm}$ decays. We refer to the charged leptons from the $\Sigma^{\pm/0}$ decays as l and the ones from $W^{\pm}$ decays as l'. The notation OSD stands for opposite sign dileptons from $\Sigma^{\pm/0}$ decays, while OSD' stands for opposite sign dileptons from $W^{\pm}$ decays. When we have one charged lepton from $\Sigma^{\pm/0}$ decay and an opposite sign charged lepton from $W^{\pm}$ decay, then it is denoted as $OSD(l + l')$ and so on.

While we provide an exhaustive list of channels for the $\Sigma^+\Sigma^-$ decay mode in Table 3.8, not all of them can be effectively used at the LHC. We will highlight below a few of these channels which appear to be particularly interesting.

- One of the main decay channels of $\Sigma^{\pm}$ is $\Sigma^{\pm} \to l^{\pm}\, h^0$. The h^0 with mass of 40/70 GeV, then decays subsequently to $b\bar{b}$ pairs giving rise to a final state signal of a pair of opposite sign dileptons (OSD) + 4 b-jets.

  $$\Sigma^+\Sigma^- \to l^+l^-h^0h^0 \to l^+l^-b\bar{b}b\bar{b} \to 4b + OSD.$$

  We have seen from Table 3.2 that the branching ratio for $\Sigma^{\pm} \to l^{\pm}\, A^0$ is also comparable. This will also produce the same collider signature of $4b + OSD$ for 140 GeV A^0 mass . The only observable difference will be that the b-jets produced from the A^0 decay will be harder as A^0 is much more massive than h^0. Here and everywhere else in this section, we will ignore the information on the hardness of the b-jets and present the sum of the cross-sections with h^0 and A^0 in the intermediate state. We should also stress that while we write only h^0 explicitly in the intermediate channels in the Tables, the cross-sections given in the final column always also include A^0 as well as h^0. One finds that the effective cross-section for this channel is 35.84 fb for 40 GeV M_{h^0}, which is rather high. For M_{h^0}=70 GeV, the cross section differs very small, as can be seen from Table 3.12. The OSD released are expected to be hard, as they come from the decay of the massive fermions.

  Instead of decaying into $b\bar{b}$ pair, the h^0s could decay into $\tau\bar{\tau}$. If one of the h^0 decays into $b\bar{b}$ and the other into $\tau\bar{\tau}$, we will get

  $$\Sigma^+\Sigma^- \to l^+l^-h^0h^0 \to l^+l^-b\bar{b}\tau\bar{\tau} \to 2b + OSD + 2\tau.$$

  This has an effective cross-section of 3.67 fb. A third possibility exists where both the h^0 decay into $\tau\bar{\tau}$ pairs. The effective cross-section for this channel is small as can be seen from the Table 3.8, and will get smaller once the τ detection efficiencies are folded.

- The other dominant decay channel for $\Sigma^\pm$ decay is $\Sigma^\pm \to \nu H^\pm$. The neutrino will give missing energy while $H^\pm$ will decay into $H^\pm \to W^\pm h^0$. The $W^\pm$ could decay hadronically giving 2 jets or leptonically giving either a τ-jet + missing energy or e/μ lepton + missing energy. Since the lepton released in the $\Sigma^\pm \to l^\pm h^0$ is important both for understanding the flavor structure of the mixing matrix as well as for tagging the channel in order to reduce the background, we consider first the case where one of heavy charged fermion decays into a hard charged lepton and h^0 and the other into a neutrino and $H^\pm$. The most interesting channels in this case turn out to be:

$$\Sigma^+\Sigma^- \to l^+h^0H^-\nu \to l^+h^0h^0W^-\nu \to 4b + l + 2j + \not{p}_T,$$

$$\Sigma^+\Sigma^- \to l^+h^0H^-\nu \to l^+h^0h^0W^-\nu \to 4b + l + \tau + \not{p}_T,$$

  where for the former, the two h^0 (one from the Σ^+ decay and another from H^- decay) produce 4 b-jets, and the W^- decays produce two hadronic jets. In the latter channel, the W^- decays into $\tau\nu_\tau$, producing a τ-jet. The effective cross-section for the former channel is 26.88 fb, while that for the latter is 4.48 fb. The effective cross-sections for the other channels with $l^+h^0h^0W^-\nu$ in the intermediate states are given in Table 3.8. However, their cross-sections are smaller.

- Finally, both the charged heavy fermions could decay through the $H^\pm\nu$ mode. In this case we have the following leading order possibilities:

$$\Sigma^+\Sigma^- \to H^+\nu H^-\nu \to h^0h^0W^+W^-\nu\nu \to 4b + 4j + \not{p}_T,$$

$$\Sigma^+\Sigma^- \to H^+\nu H^-\nu \to h^0h^0W^+W^-\nu\nu \to 4b + 2j + l' + \not{p}_T,$$

$$\Sigma^+\Sigma^- \to H^+\nu H^-\nu \to h^0h^0W^+W^-\nu\nu \to 4b + 2j + \tau + \not{p}_T.$$

  The mode $\Sigma^+\Sigma^- \to 4b + OSD' + \not{p}_T$, appearing at serial number 16 in Table 3.8 could have been easy to tag as it contains $4b$-jets and pair of opposite sign dileptons coming from $W^\pm$ decay, and missing energy. However, the effective cross-section for this channel is relatively low. Note that none of the channels with $H^+\nu H^-\nu$ in their intermediate state have l in their final state. For these channels therefore, it is impossible to say anything about the flavor structure of the model.

3.8.2 $\Sigma^\pm\Sigma^0$ decay

We give in Tables 3.9 and 3.10, the possible decay channels, final state configurations of particles, and their corresponding effective cross-sections for the $\Sigma^\pm\Sigma^0$ production and decays. For the leptons we follow the same convention for our notation as done for the previous section.

Sl no	Channels	Effective cross-section (in fb)
1	$\Sigma^{\pm}\Sigma^{0} \to l^{\pm}h^{0}h^{0}\nu \to 4b + l + \not{p}_T$	96.3
2	$\Sigma^{\pm}\Sigma^{0} \to l^{\pm}h^{0}h^{0}\nu \to 2b + l + 2\tau + \not{p}_T$	19.7
3	$\Sigma^{\pm}\Sigma^{0} \to l^{\pm}h^{0}h^{0}\nu \to l + 2\tau + \not{p}_T$	0.99
4	$\Sigma^{\pm}\Sigma^{0} \to H^{\pm}\nu h^{0}\nu \to 4b + 1l' + \not{p}_T$	107.4
5	$\Sigma^{\pm}\Sigma^{0} \to H^{\pm}\nu h^{0}\nu \to 4b + \tau + \not{p}_T$	53.7
6	$\Sigma^{\pm}\Sigma^{0} \to H^{\pm}\nu h^{0}\nu \to 4b + 2j + \not{p}_T$	35.98
7	$\Sigma^{\pm}\Sigma^{0} \to H^{\pm}\nu h^{0}\nu \to 2b + 2\tau + 2j + \not{p}_T$	7.36
8	$\Sigma^{\pm}\Sigma^{0} \to H^{\pm}\nu h^{0}\nu \to 2b + 2\tau + l' + \not{p}_T$	2.42
9	$\Sigma^{\pm}\Sigma^{0} \to H^{\pm}\nu h^{0}\nu \to 2b + 3\tau + \not{p}_T$	1.21
10	$\Sigma^{\pm}\Sigma^{0} \to H^{\pm}\nu h^{0}\nu \to 4\tau + 2j + \not{p}_T$	0.38
11	$\Sigma^{\pm}\Sigma^{0} \to H^{\pm}\nu h^{0}\nu \to l' + 4\tau + \not{p}_T$	0.12
12	$\Sigma^{\pm}\Sigma^{0} \to H^{\pm}\nu h^{0}\nu \to 5\tau + \not{p}_T$	0.06
13	$\Sigma^{\pm}\Sigma^{0} \to l^{\pm}H^{\mp}l^{\pm}h^{0} \to 4b + 2l + 2j$	36.12
14	$\Sigma^{\pm}\Sigma^{0} \to l^{\pm}H^{\mp}l^{\pm}h^{0} \to 4b + 3l(2l + l') + \not{p}_T$	12.04
15	$\Sigma^{\pm}\Sigma^{0} \to l^{\pm}H^{\mp}l^{\pm}h^{0} \to 4b + 2l + 1\tau + \not{p}_T$	6.02
16	$\Sigma^{\pm}\Sigma^{0} \to l^{\pm}H^{\mp}l^{\pm}h^{0} \to 2b + 2l + 2\tau + 2j$	7.4
17	$\Sigma^{\pm}\Sigma^{0} \to l^{\pm}H^{\mp}l^{\pm}h^{0} \to 2b + 3l(2l + l') + 2\tau + \not{p}_T$	2.4
18	$\Sigma^{\pm}\Sigma^{0} \to l^{\pm}H^{\mp}l^{\pm}h^{0} \to 2b + 2l + 3\tau + \not{p}_T$	1.20
19	$\Sigma^{\pm}\Sigma^{0} \to l^{\pm}H^{\mp}l^{\pm}h^{0} \to 2l + 4\tau + 2j$	0.36
20	$\Sigma^{\pm}\Sigma^{0} \to l^{\pm}H^{\mp}l^{\pm}h^{0} \to 3l(2l + l') + 4\tau + \not{p}_T$	0.12
21	$\Sigma^{\pm}\Sigma^{0} \to l^{\pm}H^{\mp}l^{\pm}h^{0} \to 2l + 5\tau + \not{p}_T$	0.06

Table 3.9: Effective cross-sections (in fb) of different $\Sigma^{\pm}\Sigma^{0}$ decay channels for $M_{\Sigma_1} = 300$ GeV.

Sl no	Channels	Effective cross-section (in fb)
1	$\Sigma^\pm\Sigma^0 \to H^\pm\nu H^\pm l^\mp \to 4b + l + 4j + \not{p}_T$	13.36
2	$\Sigma^\pm\Sigma^0 \to H^\pm\nu H^\pm l^\mp \to 4b + l + \tau + 2j + \not{p}_T$	4.38
3	$\Sigma^\pm\Sigma^0 \to H^\pm\nu H^\pm l^\mp \to 4b + OSD(l + l') + 2j + \not{p}_T$	6.57
4	$\Sigma^\pm\Sigma^0 \to H^\pm\nu H^\pm l^\mp \to 4b + LSD(l + l') + 2j + \not{p}_T$	2.19
5	$\Sigma^\pm\Sigma^0 \to H^\pm\nu H^\pm l^\mp \to 4b + OSD(l + l') + \tau + \not{p}_T$	1.09
6	$\Sigma^\pm\Sigma^0 \to H^\pm\nu H^\pm l^\mp \to 4b + LSD(l + l') + \tau + \not{p}_T$	0.37
7	$\Sigma^\pm\Sigma^0 \to H^\pm\nu H^\pm l^\mp \to 2b + OSD(l + l') + 2\tau + 2j + \not{p}_T$	1.35
8	$\Sigma^\pm\Sigma^0 \to H^\pm\nu H^\pm l^\mp \to 2b + LSD(l + l') + 2\tau + 2j + \not{p}_T$	0.45
9	$\Sigma^\pm\Sigma^0 \to H^\pm\nu H^\pm l^\mp \to 2b + OSD(l + l') + 3\tau + \not{p}_T$	0.23
10	$\Sigma^\pm\Sigma^0 \to H^\pm\nu H^\pm l^\mp \to 2b + LSD(l + l') + 3\tau + \not{p}_T$	0.08
11	$\Sigma^\pm\Sigma^0 \to H^\pm\nu H^\pm l^\mp \to OSD(l + l') + 4\tau + 2j + \not{p}_T$	0.06
12	$\Sigma^\pm\Sigma^0 \to H^\pm\nu H^\pm l^\mp \to LSD(l + l') + 4\tau + 2j + \not{p}_T$	0.02
13	$\Sigma^\pm\Sigma^0 \to H^\pm\nu H^\pm l^\mp \to 2b + l + 2\tau + 4j + \not{p}_T$	2.78
14	$\Sigma^\pm\Sigma^0 \to H^\pm\nu H^\pm l^\mp \to l + 4\tau + 4j + \not{p}_T$	0.14
15	$\Sigma^\pm\Sigma^0 \to H^\pm\nu H^\pm l^\mp \to 4b + 3l(l + 2l') + \not{p}_T$	1.68
16	$\Sigma^\pm\Sigma^0 \to H^\pm\nu H^\pm l^\mp \to 2b + 3l(l + 2l') + 2\tau + \not{p}_T$	0.32
15	$\Sigma^\pm\Sigma^0 \to H^\pm\nu H^\pm l^\mp \to 3l(l + 2l') + 4\tau + \not{p}_T$	0.02
16	$\Sigma^\pm\Sigma^0 \to H^\pm\nu H^\pm l^\mp \to 4b + l + 2\tau + \not{p}_T$	0.42
17	$\Sigma^\pm\Sigma^0 \to H^\pm\nu H^\pm l^\mp \to 2b + l + 4\tau + \not{p}_T$	0.08
18	$\Sigma^\pm\Sigma^0 \to H^\pm\nu H^\pm l^\mp \to l + 5\tau + 2j + \not{p}_T$	0.04
19	$\Sigma^\pm\Sigma^0 \to H^\pm\nu H^\pm l^\mp \to l + 6\tau + \not{p}_T$	0.004
20	$\Sigma^\pm\Sigma^0 \to H^\pm\nu H^\pm l^\mp \to l + l' + 5\tau + \not{p}_T$	0.008

Table 3.10: Effective cross-sections (in fb) of different $\Sigma^\pm\Sigma^0$ decay channels for $M_{\Sigma_1} = 300$ GeV.

Sl no	Channels	Effective cross-section in fb
1	4b +OSD	35.84
2	$4b + l + \not{p}_T$	96.3
3	$4b + l' + \not{p}_T$	107.4
4	$4b + \tau + \not{p}_T$	53.7
5	$4b + l + 2j + \not{p}_T$	26.88
6	$4b + 2l + 2j$	36.12
7	$4b + 3l(2l + l') + \not{p}_T$	12.04

Table 3.11: Effective cross-sections in fb for $M_{\Sigma_1} = 300$ GeV, for the most important channels for our model.

- We begin by looking at the $\Sigma^\pm\Sigma^0$ decays where $\Sigma^\pm \to l^\pm h^0$ and $\Sigma^0 \to \nu h^0$. This would lead to the following final state configuration

$$\Sigma^\pm\Sigma^0 \to l^\pm h^0 h^0 \nu \to 4b + l + \not{p}_T,$$

with a very large effective cross-section of 96.3 fb. This channel should be easy to tag. The 4 b-jets come from the displaced h^0 vertices, and the lepton released is hard. This lepton will also carry information on the μ-τ symmetric flavor structure of the model. For the choice of Higgs mass $M_{h^0} = 70$ GeV, the effective cross section reduces to 89.6. Another unambiguous channel with significant effective cross-section coming from the $l^\pm h^0 h^0 \nu$ intermediate state is

$$\Sigma^\pm\Sigma^0 \to l^\pm h^0 h^0 \nu \to 2b + l + 2\tau + \not{p}_T,$$

where one of the h^0 decays into $\tau\bar{\tau}$.

- The other intermediate state which has very large effective cross-sections is $\Sigma^\pm\Sigma^0 \to \nu H^\pm \, \nu h^0$. The $H^\pm$ would decay into $W^\pm h^0$, and $W^\pm$ into a lepton l' finally giving

$$\Sigma^\pm\Sigma^0 \to H^\pm \nu h^0 \nu \to 4b + l' + \not{p}_T,$$

with an effective cross-section of 107.4 fb. Alternatively, the W^- could instead decay into $\tau\bar{\nu}_\tau$ giving

$$\Sigma^\pm\Sigma^0 \to H^\pm \nu h^0 \nu \to 4b + \tau + \not{p}_T,$$

Sl no	Channels	Effective cross-section in fb
1	4b +OSD	33.45
2	$4b + l +\not{p}_T$	89.60
3	$4b + l + 2j +\not{p}_T$	26.4
4	$4b + 2l + 2j$	36.1
5	$4b + 3l(2l + l') +\not{p}_T$	12.04

Table 3.12: Effective cross-sections in fb for $M_{\Sigma_1} = 300$ GeV and $M_{h^0} = 70$ GeV for the important channels for our model.

with effective cross-section of 53.7 fb, or decay into qq' giving

$$\Sigma^{\pm}\Sigma^0 \to H^{\pm}\nu h^0\nu \to 4b + 2j +\not{p}_T,$$

with an effective cross-section of 35.98 fb.

- Large effective cross-section in the $\Sigma^{\pm}\Sigma^0$ channel is also expected from the following decay chain

$$\Sigma^{\pm}\Sigma^0 \to l^{\pm}h^0 l^{\pm}H^{\mp} \to 4b + 2l + 2j,$$

with effective cross-section of 36.12 fb. Both the leptons in this channel come from the heavy fermion decay vertices and carry the flavor information of the model. Choice of a 70 GeV M_{h^0} does not alter the cross section as can be seen from Table. 3.12.

- $\Sigma^{\pm}\Sigma^0$ could also decay through the intermediate states $H^{\pm}\nu H^{\pm}l^{\mp}$. This leads to 20 possible final state particles and collider signatures. These are listed in Table 3.10. However, the only one which has sizable effective cross-section is

$$\Sigma^{\pm}\Sigma^0 \to H^{\pm}\nu H^{\pm}l^{\mp} \to 4b + l + 4j +\not{p}_T.$$

However, this channel has 4 light quark jets, which is always prone to problems with backgrounds.

In Table. 3.12, we have shown the effective cross section for few of the channels considering the Higgs mass $M_{h^0} = 70$ GeV, while in the other tables the Higgs mass has been taken as 40 GeV. The choice of the Higgs mass as 70 GeV does not make any significant change in the effective cross sections. Hence we do not repeat the calculation of the effective cross section for all the possible channels for the case of $M_{h^0} = 70$ GeV.

3.8.3 Backgrounds

In Tables 3.8, 3.9 and 3.10 we provided a comprehensive list of collider signature channels for the heavy fermions, and their corresponding effective cross-sections. In the previous subsection we had also discussed some of the most important channels with large effective cross-sections. In Table 3.11 and in Table 3.12 we give a subset of those highlighted in sections 3.8.1 and 3.8.2. These are expected to be the most unambiguous channels, with smallest backgrounds and the largest signal cross-sections. In almost all channels listed in Table 3.11 and in Table 3.12, the final collider signature contains 4 b-jets and a hard lepton coming from the primary heavy fermion decay vertex. In addition, the 4 b-jets come from the h^0 decay vertex which is significantly displaced with respect to the heavy fermion decay vertex. The main source of standard model background for the channels with 4 b-jets and a lepton are the $t\bar{t}b\bar{b}$ modes, which can give multiple b-jets, leptons and missing energy. However, as mentioned many before, the b-jets come from h^0 displaced vertex and should not have any standard model background. Having the hard lepton in the final state further cuts down the background. Therefore, each of these collider channels are expected to have very little to no backgrounds. For a detailed signal to background analysis one requires a detailed simulation for the final state topology, which is outside the scope of this work. Nevertheless we add a few lines discussing qualitatively the possibility of backgrounds for some of the listed channels in Table 3.11.

- 4b +OSD: Here the two opposite sign dileptons come from the $\Sigma^+\Sigma^-$ decays. Since the $\Sigma^\pm$ are heavy with $M_{\Sigma^\pm} = 300$ GeV, the leptons will be very hard and we can put a cut of $p_T \gtrsim 100$ GeV. The displaced h^0 vertex should remove all backgrounds.

- $4b + l + \not{p}_T$: Here $t\bar{t}b\bar{b}$ does not directly give any background, unless one of the leptons from the final state is missed. However, the p_T cut on the hard lepton and the displaced h^0 vertices should effectively remove any residual background.

- $4b + l' + \not{p}_T$: Here the p_T cut on the lepton cannot be imposed as the lepton here comes from $W^\pm$ decay. However, the 4 b-jets still come from the displaced h^0 vertices and that should anyway take care of killing all backgrounds to a large extent.

- $4b + l + 2jet + \not{p}_T$: The main background could again come from standard model $t\bar{t}b\bar{b}$ channels. This can also be removed by the displaced h^0 vertex and a cut of $p_T \gtrsim 100$ GeV for the lepton.

- $4b + 2l + 2j$: Similar to the first case, but with 2 extra jets.

- $4b + 3l(2l + l') + \not{p}_T$: Out of the 3 leptons in this channel, two are hard and one is relatively soft. In addition we have the h^0 displaced vertex. Therefore, this channel is expected to be absolutely background free.

3.9 Conclusions

The seesaw mechanism has remained the most elegant scheme to explain the smallness of the neutrino masses without having to unnaturally fine tune the Yukawa couplings to arbitrary small values. In the so-called type-III seesaw, three hypercharge $Y = 0$, SU(2) triplet fermions are added to the standard model particle contents. These exotic fermions are color singlets and belong to the adjoint representation of SU(2). These exotic fermions have Yukawa couplings with the standard model lepton doublet and the Higgs doublet. Once these heavy leptons are integrated out from the theory, the dimension-5 *Weinberg* operator is generated. After electroweak symmetry breaking Majorana neutrino masses are generated from this operator. In this novel seesaw mechanism, the smallness of the neutrino mass is explained by the largeness of the heavy fermion mass and without having to fine tune the Yukawa couplings to very small values. To generate neutrino masses $m_\nu \sim 0.1$ eV, one requires that the heavy fermion mass should be $\sim 10^{14}$ GeV with $Y_\Sigma \sim 1$. Being in the adjoint representation of SU(2), one of the most interesting feature of these exotic fermions is that they have gauge couplings, and therefore can be produced at collider experiments. The only constraint for the production of these particles at LHC is that their mass should be in a few 100 GeV range. However, in order to produce neutrino masses $m_\nu \sim 0.1$ eV, one would then have to tune the Yukawa couplings to be $\sim 10^{-6}$.

In this work we propose an extended type-III seesaw model with two SU(2) Higgs doublets along with the three adjoint SU(2) fermion triplets. The addition of the 2nd Higgs doublet opens up the possibility to avoid very small Yukawa coupling. We impose an additional Z_2 symmetry such that one of the Higgs doublets, called Φ_1, has positive charge while the other, called Φ_2, has negative charge under this symmetry. In addition, we demand that all standard model particles have positive charge with respect to Z_2 while the three new exotic fermion triplets are negatively charged. Therefore, Φ_1 behaves like the standard model Higgs, while Φ_2 is coupled *only* to the exotic fermion triplets. As a result, the neutrino mass term coming from the seesaw formula depends on the VEV of Φ_2 (v'), while all other fermion masses are dependent on the VEV of Φ_1 (v). We can therefore choose a value for v' such that $m_\nu \sim 0.1$ eV for exotic fermion masses ~ 100 GeV, without having to fine tune the Yukawa couplings to very small values.

Another typical feature about neutrinos concern their peculiar mixing pattern which should be explained by the underlying theory. The current neutrino oscillation data indicates an inherent μ-τ symmetry in the low energy neutrino mass matrix. It is therefore expected that this μ-τ symmetry should also exist at the high scale, either on its own or as a sub-group of a bigger flavor group. We imposed an exact μ-τ symmetry on both the Yukawa coupling of the triplet fermions Y_Σ as well as on their Majorana mass matrix M. Therefore the low energy neutrino matrix m_ν obtained after the seesaw had an in-built μ-τ symmetry. As a result our model predicts $\theta_{23} = \pi/4$ and $\theta_{13} = 0$. The oscillation parameters depend on the model parameters in Y_Σ and M.

A very important and new aspect which emerged from our study concerns the mixing in the heavy fermion sector. We showed that for the case where M was μ-τ symmetric, the matrices U_Σ, U_h^L and U_h^R were highly non-trivial, and in particular had the last column as $(0, -1/\sqrt{2}, 1/\sqrt{2})$. We showed that flavor structure of our model was reflected in the pattern of heavy fermion decays into light charged leptons. The state $\Sigma_{m_3}^{\pm/0}$ decayed equally into muons and taus and almost never decayed into electrons. This feature exists not only for our model, but for any model with an underlying flavor symmetry group that imposes μ-τ symmetry on the heavy Majorana mass matrix M, for example the model given in [33].

Next, we turned to the production and detection of heavy fermions at LHC. We discussed quantitatively and in details the cross-section for the heavy fermion production at LHC and their decay rates. While the production cross-sections for our model turned out to be same as that in all earlier calculations done in the context of the one Higgs doublet model, the decay pattern for the heavy fermions in our case was found to be different. The μ-τ permutation symmetry showed up in the flavor pattern of the heavy fermion decays through the matrices U_Σ, U_h^L and U_h^R. The decay rate of the heavy fermions in this model is more than 10^{11} times larger than that found for the one Higgs doublet model and is $\sim 10^{-2}$ GeV for 300 GeV heavy fermions. Therefore, while for the one Higgs doublet case one could attempt to look for displaced heavy fermion decay vertices, in our case they will decay almost instantaneously. We found that this tremendous decay rate came from the very fast decays of $\Sigma_m^{\pm/0}$ into light leptons and Higgs h^0, A^0 or $H^\pm$ which stem from the very large Yukawa couplings in our model. As the Yukawa couplings are a factor of $10^5 - 10^6$ larger in our model, the decay rates which depend on the square of the Yukawa couplings are a factor 10^{10}-10^{12} higher.

The other distinctive feature of our model appeared in the pattern of the Higgs decays. The smallness of the neutrino masses constrained the neutral Higgs mixing angle α to be very small. This resulted in a very small decay rate for the h^0 Higgs. For a mass of $M_{h^0} = 40$ GeV, the h^0 lifetime in the Higgs rest frame comes out to be about 5 cm. This will give a displaced decay vertex in the LHC detectors, ATLAS and CMS. Finally, we discussed in detail the expected collider signatures for the two Higgs doublet type-III seesaw model with μ-τ symmetry. We have presented the effective cross section of the different channels and qualitatively discussed about the background. The channels with b-jets and hard leptons are the most significant one as our model signature.

Appendix

A: The Scalar Potential and Higgs Spectrum

Our model has two SU(2) complex Higgs doublets Φ_1 and Φ_2, with hypercharge $Y = 1$. The scalar potential can then be written as

$$\begin{aligned} V &= \lambda_1 \left(\Phi_1^\dagger \Phi_1 - v^2\right)^2 + \lambda_2 \left(\Phi_2^\dagger \Phi_2 - v'^2\right)^2 + \lambda_3 \left((\Phi_1^\dagger \Phi_1 - v^2) + (\Phi_2^\dagger \Phi_2 - v'^2)\right)^2 \\ &\quad + \lambda_4 \left((\Phi_1^\dagger \Phi_1)(\Phi_2^\dagger \Phi_2) - (\Phi_1^\dagger \Phi_2)(\Phi_2^\dagger \Phi_1)\right) + \lambda_5 \left(\mathrm{Re}(\Phi_1^\dagger \Phi_2) - v v' \cos\xi\right)^2 \\ &\quad + \lambda_6 \left(\mathrm{Im}(\Phi_1^\dagger \Phi_2) - v v' \sin\xi\right)^2, \end{aligned} \tag{A1}$$

where

$$\langle \Phi_1 \rangle = \begin{pmatrix} 0 \\ v \end{pmatrix}, \quad \langle \Phi_2 \rangle = \begin{pmatrix} 0 \\ v' e^{i\xi} \end{pmatrix}, \quad \text{and} \quad \tan\beta = \frac{v'}{v}. \tag{A2}$$

According to our Z_2 charge assignment, Φ_1 carries charge $+1$, while Φ_2 has -1 charge. Therefore, the λ_5 term is zero when the symmetry is exact. We will discuss the phenomenological consequences of this and argue in favor of a mild breaking of this Z_2 symmetry. With the scalar potential Eq. (A1) it is straightforward to obtain the Higgs mass matrix and obtain the corresponding mass spectrum. The physical degrees of freedoms contain the charged Higgs $H^\pm$ and the neutral Higgs H^0, h^0, and A^0. While H^0 and h^0 are CP even, A^0 is CP odd. If we work in a simplified scenario where ξ is taken as zero, then it is is quite straightforward to derive the mass of the charged Higgs $H^\pm$ and the CP-odd Higgs A^0. The masses are given as

$$M^2_{H^\pm} = \lambda_4 (v^2 + v'^2), \quad \text{and} \quad M^2_{A^0} = \lambda_6 (v^2 + v'^2), \tag{A3}$$

respectively. The mass matrix for the neutral CP-even Higgs is

$$M' = \begin{pmatrix} 4v^2(\lambda_1 + \lambda_3) + v'^2 \lambda_5 & (4\lambda_3 + \lambda_5) v v' \\ (4\lambda_3 + \lambda_5) v v' & 4v'^2(\lambda_2 + \lambda_3) + v^2 \lambda_5 \end{pmatrix}. \tag{A4}$$

The mixing angle, obtained from diagonalizing the above matrix is given by

$$\tan 2\alpha = \frac{2\, M_{12}}{M_{11} - M_{22}}, \tag{A5}$$

and the corresponding masses are

$$M^2_{H^0,h^0} = \frac{1}{2}\{M_{11} + M_{22} \pm \sqrt{(M_{11} - M_{22})^2 + 4M_{12}^2}. \tag{A6}$$

The physical Higgs are given in terms of components of Φ_1 and Φ_2 as follows. The neutral Higgs are given as

$$\begin{aligned} H^0 &= \sqrt{2}\left((\mathrm{Re}\Phi_1^0 - v)\cos\alpha + (\mathrm{Re}\Phi_2^0 - v')\sin\alpha\right), && \text{(A7)} \\ h^0 &= \sqrt{2}\left(-(\mathrm{Re}\Phi_1^0 - v)\sin\alpha + (\mathrm{Re}\Phi_2^0 - v')\cos\alpha\right), && \text{(A8)} \\ A^0 &= \sqrt{2}(-\mathrm{Im}\Phi_1^0\sin\beta + \mathrm{Im}\Phi_2^0\cos\beta), && \text{(A9)} \end{aligned}$$

while the charged Higgs are

$$H^\pm = -\Phi_1^\pm\sin\beta + \Phi_2^\pm\cos\beta. \tag{A10}$$

The Goldstones turn out to be

$$\begin{aligned} G^\pm &= \Phi_1^\pm\cos\beta + \Phi_2^\pm\sin\beta && \text{(A11)} \\ G^0 &= \sqrt{2}(\mathrm{Im}\Phi_1^0\cos\beta + \mathrm{Im}\Phi_2^0\sin\beta). && \text{(A12)} \end{aligned}$$

The requirement from small neutrino masses $m_\nu \sim 0.1$ eV constrains $v' \sim 10^{-4}$ GeV. Therefore, for our model we get from Eqs. (A2) and (A5)

$$\tan\beta \sim 10^{-6}, \quad \text{and} \quad \tan 2\alpha \sim \tan\beta \sim 10^{-6}. \tag{A13}$$

One can estimate from Eq. (A6), that in the limit $v' \ll v$,

$$M_{H^0}^2 \simeq (\lambda_1 + \lambda_3)v^2, \quad \text{and} \quad M_{h^0}^2 \simeq \lambda_5 v^2. \tag{A14}$$

We should point out here that in the limit of exact Z_2 symmetry, $\lambda_5 = 0$ exactly, and in that case $M_{h^0}^2 \propto v'^2$. Since $v' \sim 10^{-4}$ GeV, this would give a very tiny mass for the neutral Higgs h^0. To prevent that, we introduce a mild explicit breaking of the Z_2 symmetry, by taking $\lambda_5 \neq 0$ in the scalar potential. This not only alleviates the problem of an extremely light Higgs boson, it also circumvents spontaneous breaking of Z_2, when the Higgs develop vacuum expectation value. This saves the model from complications such as creation of domain walls, due to the spontaneous breaking of a discrete symmetry. The extent of breaking of Z_2 is determined by the strength of λ_5. Since we wish to impose only a mild breaking, we take $\lambda_5 \sim 0.05$. This gives us a light neutral Higgs mass of $M_h^0 \simeq 40$ GeV from Eq. (A14). For 70 GeV light Higgs mass, the coupling λ_5 increases to 0.16. Since all other $\lambda_i \sim 1$, the mass of the other CP even neutral Higgs, the CP odd neutral Higgs and the charged Higgs are all seen to be $\sim v$ GeV from Eqs. (A3) and (A14). We will work with $M_H^0 = 150$ GeV, and $M_H^\pm = 170$ GeV. We take M_A^0 as 140 GeV.

We also require the couplings of our Higgs with the gauge bosons. This is needed in order to understand the Higgs decay and the subsequent collider signatures of our model. These are standard expressions and are well documented (see for instance [19]). One can check that certain couplings depend on $\sin\alpha$ and $\sin(\beta - \alpha)$. From Eq. (A13) we can see that these couplings are almost zero. Others depend on $\cos\alpha$ and $\cos(\beta-\alpha)$ and therefore large. We refer to [19] for a detailed discussion on the general form for the couplings.

B: The Interaction Lagrangian

B.1: Lepton-Higgs Coupling

The lepton Yukawa part of the Lagrangian for our two Higgs doublet model was given in Eq. (3.9) as,

$$-\mathcal{L}_Y = \left[Y_{l_{ij}} \bar{l}_{R_i} \Phi_1^\dagger L_j + Y_{\Sigma_{ij}} \tilde{\Phi}_2^\dagger \overline{\Sigma}_{R_i} L_j + \text{h.c.} \right] + \frac{1}{2} M_{ij} \, \text{Tr} \left[\overline{\Sigma}_{R_i} \tilde{\Sigma}_{R_j}^C + \text{h.c.} \right]. \tag{B1}$$

From this the individual Yukawa coupling vertex factors between two fermions and a Higgs can be extracted. We have three generations of heavy and light neutral leptons and three generations of heavy and light charged leptons. In addition, we have three neutral and a pair of charged Higgs. The Yukawa interaction between any pair of fermions and a corresponding physical Higgs field can be extracted from Eq. (B1). We list below all Yukawa possible interactions *in the mass basis* of the particles. The vertex factors are denoted as $C_{FI}^{X,L/R}$, where I and F are the initial and final state fermions respectively, X is the physical Higgs involved and L/R are for either the vertex with P_L or P_R respectively, where P_L and P_R are the left and right chiral projection operators respectively. Note that we have suppressed the generation indices for clarity of the expressions. But the generation indices are implicitly there and the vertex factors are all 3×3 matrices.

$$\begin{aligned} -\mathcal{L}_{l,\Sigma^-}^{H^0} &= H^0 \{ \bar{l}_m (C_{ll}^{H^0,L} P_L + C_{ll}^{H^0,R} P_R) l_m + \{ \bar{l}_m (C_{l\Sigma^-}^{H^0,L} P_L + C_{l\Sigma^-}^{H^0,R} P_R) \Sigma_m^- + \text{h.c} \} \\ &\quad + \overline{\Sigma_m^-} (C_{\Sigma^-\Sigma^-}^{H^0,L} P_L + C_{\Sigma^-\Sigma^-}^{H^0,R} P_R) \Sigma_m^- \} \end{aligned} \tag{B2}$$

$$\begin{aligned} -\mathcal{L}_{l,\Sigma^-}^{h^0} &= h^0 \{ \bar{l}_m (C_{ll}^{h^0,L} P_L + C_{ll}^{h^0,R} P_R) l_m + \{ \bar{l}_m (C_{l\Sigma^-}^{h^0,L} P_L + C_{l\Sigma^-}^{h^0,R} P_R) \Sigma_m^- + \text{h.c} \} \\ &\quad + \overline{\Sigma_m^-} (C_{\Sigma^-\Sigma^-}^{h^0,L} P_L + C_{\Sigma^-\Sigma^-}^{h^0,R} P_R) \Sigma_m^- \} \end{aligned} \tag{B3}$$

$$\begin{aligned} -\mathcal{L}_{l,\Sigma^-}^{A^0} &= A^0 \{ \bar{l}_m (C_{ll}^{A^0,L} P_L + C_{ll}^{A^0,R} P_R) l_m + \{ \bar{l}_m (C_{l\Sigma^-}^{A^0,L} P_L + C_{l\Sigma^-}^{A^0,R} P_R) \Sigma_m^- + \text{h.c} \} \\ &\quad + \overline{\Sigma_m^-} (C_{\Sigma^-\Sigma^-}^{A^0,L} P_L + C_{\Sigma^-\Sigma^-}^{A^0,R} P_R) \Sigma_m^- \} \end{aligned} \tag{B4}$$

$$\begin{aligned} -\mathcal{L}_{l,\Sigma^-}^{G^0} &= G^0 \{ \bar{l}_m (C_{ll}^{G^0,L} P_L + C_{ll}^{G^0,R} P_R) l_m + \{ \bar{l}_m (C_{l\Sigma^-}^{G^0,L} P_L + C_{l\Sigma^-}^{G^0,R} P_R) \Sigma_m^- + \text{h.c} \} \\ &\quad + \overline{\Sigma_m^-} (C_{\Sigma^-\Sigma^-}^{G^0,L} P_L + C_{\Sigma^-\Sigma^-}^{G^0,R} P_R) \Sigma_m^- \} \end{aligned} \tag{B5}$$

$$-\mathcal{L}^{H^0}_{\nu,\Sigma^0} = H^0\{\overline{\nu_m}(C^{H^0,L}_{\nu\nu}P_L + C^{H^0,R}_{\nu\nu}P_R)\nu_m + \{\overline{\nu}_m(C^{H^0,L}_{\nu\Sigma^0}P_L + C^{H^0,R}_{\nu\Sigma^0}P_R)\Sigma^0_m + \mathrm{h.c}\}$$
$$+\overline{\Sigma^0_m}(C^{H^0,L}_{\Sigma^0\Sigma^0}P_L + C^{H^0,R}_{\Sigma^0\Sigma^0}P_R)\Sigma^0_m\} \tag{B6}$$

$$-\mathcal{L}^{h^0}_{\nu,\Sigma^0} = h^0\{\overline{\nu}_m(C^{h^0,L}_{\nu\nu}P_L + C^{h^0,R}_{\nu\nu}P_R)\nu_m + \{\overline{\nu}_m(C^{h^0,L}_{\nu\Sigma^0}P_L + C^{h^0,R}_{\nu\Sigma^0}P_R)\Sigma^0_m + \mathrm{h.c}\}$$
$$+\overline{\Sigma^0_m}(C^{h^0,L}_{\Sigma^0\Sigma^0}P_L + C^{h^0,R}_{\Sigma^0\Sigma^0}P_R)\Sigma^0_m\} \tag{B7}$$

$$-\mathcal{L}^{A^0}_{\nu,\Sigma^0} = A^0\{\overline{\nu}_m(C^{A^0,L}_{\nu\nu}P_L + C^{A^0,R}_{\nu\nu}P_R)\nu_m + \{\overline{\nu}_m(C^{A^0,L}_{\nu\Sigma^0}P_L + C^{A^0,R}_{\nu\Sigma^0}P_R)\Sigma^0_m + \mathrm{h.c}\}$$
$$+\overline{\Sigma^0_m}(C^{A^0,L}_{\Sigma^0\Sigma^0}P_L + C^{A^0,R}_{\Sigma^0\Sigma^0}P_R)\Sigma^0_m\} \tag{B8}$$

$$-\mathcal{L}^{G^0}_{\nu,\Sigma^0} = G^0\{\overline{\nu}_m(C^{G^0,L}_{\nu\nu}P_L + C^{A^0,R}_{\nu\nu}P_R)\nu_m + \{\overline{\nu}_m(C^{G^0,L}_{\nu\Sigma^0}P_L + C^{G^0,R}_{\nu\Sigma^0}P_R)\Sigma^0_m + \mathrm{h.c}\}$$
$$+\overline{\Sigma^0_m}(C^{G^0,L}_{\Sigma^0\Sigma^0}P_L + C^{G^0,R}_{\Sigma^0\Sigma^0}P_R)\Sigma^0_m\} \tag{B9}$$

$$-\mathcal{L}^{H^\pm}_{l,\Sigma^0,\nu,\Sigma^-} = H^-\{\bar{l}_m(C^{H^-,L}_{l\nu}P_L + C^{H^-,R}_{l\nu}P_R)\nu_m + \bar{l}_m(C^{H^-,L}_{l\Sigma^0}P_L + C^{H^-,R}_{l\Sigma^0}P_R)\Sigma^0_m$$
$$+\overline{\Sigma^-_m}(C^{H^-,L}_{\Sigma^-\Sigma^0}P_L + C^{H^-,R}_{\Sigma^-\Sigma^0}P_R)\Sigma^0_m\} + H^+\{\bar{\nu}_m(C^{H^+,L}_{\nu\Sigma^-}P_L + C^{H^+,R}_{\nu\Sigma^-}P_R)\Sigma^-_m\}$$
$$+\mathrm{h.c} \tag{B10}$$

$$-\mathcal{L}^{G^\pm}_{l,\Sigma^0,\nu,\Sigma^-} = G^-\{\bar{l}_m(C^{G^-,L}_{l\nu}P_L + C^{G^-,R}_{l\nu}P_R)\nu_m + \bar{l}_m(C^{G^-,L}_{l\Sigma^0}P_L + C^{G^-,R}_{l\Sigma^0}P_R)\Sigma^0_m$$
$$+\overline{\Sigma^-_m}(C^{G^-,L}_{\Sigma^-\Sigma^0}P_L + C^{G^-,R}_{\Sigma^-\Sigma^0}P_R)\Sigma^0_m\} + G^+\{\bar{\nu}_m(C^{G^+,L}_{\nu\Sigma^-}P_L + C^{G^+,R}_{\nu\Sigma^-}P_R)\Sigma^-_m\}$$
$$+\mathrm{h.c} \tag{B11}$$

The exact vertex factors $C^{X,L/R}_{FI}$ for our two Higgs doublet type-III seesaw model are listed in Tables 3.13, 3.14, 3.15.

B.2: Lepton-Gauge coupling

The lepton-gauge couplings come from the kinetic energy terms for the Σ fields in the Lagrangian. The kinetic energy terms are given as

$$-\mathcal{L}_k = \overline{\Sigma_R}i\gamma^\mu D_\mu \Sigma_R + L^{SM}_k, \tag{B12}$$

$C^{H^0,L}_{ll}$	$\frac{1}{\sqrt{2}}(T^\dagger_{11}Y_lS_{11}\cos\alpha + T^\dagger_{21}Y_\Sigma S_{11}\sin\alpha)$	$C^{H^0,R}_{ll}$	$\frac{1}{\sqrt{2}}(S^\dagger_{11}Y_l^\dagger T_{11}\cos\alpha + S^\dagger_{11}Y_\Sigma^\dagger T_{21}\sin\alpha)$
$C^{H^0,L}_{l\Sigma^-}$	$\frac{1}{\sqrt{2}}(T^\dagger_{11}Y_lS_{12}\cos\alpha + T^\dagger_{21}Y_\Sigma S_{12}\sin\alpha)$	$C^{H^0,R}_{l\Sigma^-}$	$\frac{1}{\sqrt{2}}(S^\dagger_{11}Y_l^\dagger T_{12}\cos\alpha + S^\dagger_{11}Y_\Sigma^\dagger T_{22}\sin\alpha)$
$C^{H^0,L}_{\Sigma^-\Sigma^-}$	$\frac{1}{\sqrt{2}}(T^\dagger_{12}Y_lS_{12}\cos\alpha + T^\dagger_{22}Y_\Sigma S_{12}\sin\alpha)$	$C^{H^0,R}_{\Sigma^-\Sigma^-}$	$\frac{1}{\sqrt{2}}(S^\dagger_{12}Y_l^\dagger T_{12}\cos\alpha + S^\dagger_{12}Y_\Sigma^\dagger T_{22}\sin\alpha)$
$C^{h^0,L}_{ll}$	$\frac{-1}{\sqrt{2}}(T^\dagger_{11}Y_lS_{11}\sin\alpha - T^\dagger_{21}Y_\Sigma S_{11}\cos\alpha)$	$C^{h^0,R}_{ll}$	$\frac{-1}{\sqrt{2}}(S^\dagger_{11}Y_l^\dagger T_{11}\sin\alpha - S^\dagger_{11}Y_\Sigma^\dagger T_{21}\cos\alpha)$
$C^{h^0,L}_{l\Sigma^-}$	$\frac{-1}{\sqrt{2}}(T^\dagger_{11}Y_lS_{12}\sin\alpha - T^\dagger_{21}Y_\Sigma S_{12}\cos\alpha)$	$C^{h^0,R}_{l\Sigma^-}$	$\frac{-1}{\sqrt{2}}(S^\dagger_{11}Y_l^\dagger T_{12}\sin\alpha - S^\dagger_{11}Y_\Sigma^\dagger T_{22}\cos\alpha)$
$C^{h^0,L}_{\Sigma^-\Sigma^-}$	$\frac{-1}{\sqrt{2}}(T^\dagger_{12}Y_lS_{12}\sin\alpha - T^\dagger_{22}Y_\Sigma S_{12}\cos\alpha)$	$C^{h^0,R}_{\Sigma^-\Sigma^-}$	$\frac{-1}{\sqrt{2}}(S^\dagger_{12}Y_l^\dagger T_{12}\sin\alpha - S^\dagger_{12}Y_\Sigma^\dagger T_{22}\cos\alpha)$
$C^{A^0,L}_{ll}$	$\frac{i}{\sqrt{2}}(T^\dagger_{11}Y_lS_{11}\sin\beta + T^\dagger_{21}Y_\Sigma S_{11}\cos\beta)$	$C^{A^0,R}_{ll}$	$\frac{-i}{\sqrt{2}}(S^\dagger_{11}Y_l^\dagger T_{11}\sin\beta + S^\dagger_{11}Y_\Sigma^\dagger T_{21}\cos\beta)$
$C^{A^0,L}_{l\Sigma^-}$	$\frac{i}{\sqrt{2}}(T^\dagger_{11}Y_lS_{12}\sin\beta + T^\dagger_{21}Y_\Sigma S_{12}\cos\beta)$	$C^{A^0,R}_{l\Sigma^-}$	$\frac{-i}{\sqrt{2}}((S^\dagger_{11}Y_l^\dagger T_{12}\sin\beta + S^\dagger_{11}Y_\Sigma^\dagger T_{22}\cos\beta)$
$C^{A^0,L}_{\Sigma^-\Sigma^-}$	$\frac{i}{\sqrt{2}}(T^\dagger_{12}Y_lS_{12}\sin\beta + T^\dagger_{22}Y_\Sigma S_{12}\cos\beta)$	$C^{A^0,R}_{\Sigma^-\Sigma^-}$	$\frac{-i}{\sqrt{2}}(S^\dagger_{12}Y_l^\dagger T_{12}\sin\beta + S^\dagger_{12}Y_\Sigma^\dagger T_{22}\cos\beta)$
$C^{G^0,L}_{ll}$	$\frac{-i}{\sqrt{2}}(T^\dagger_{11}Y_lS_{11}\cos\beta - T^\dagger_{21}Y_\Sigma S_{11}\sin\beta)$	$C^{G^0,R}_{ll}$	$\frac{i}{\sqrt{2}}(S^\dagger_{11}Y_l^\dagger T_{11}\cos\beta - S^\dagger_{11}Y_\Sigma^\dagger T_{21}\sin\beta)$
$C^{G^0,L}_{l\Sigma^-}$	$\frac{-i}{\sqrt{2}}(T^\dagger_{11}Y_lS_{12}\cos\beta - T^\dagger_{21}Y_\Sigma S_{12}\sin\beta)$	$C^{G^0,R}_{l\Sigma^-}$	$\frac{i}{\sqrt{2}}(S^\dagger_{11}Y_l^\dagger T_{12}\cos\beta - S^\dagger_{11}Y_\Sigma^\dagger T_{22}\sin\beta)$
$C^{G^0,L}_{\Sigma^-\Sigma^-}$	$\frac{-i}{\sqrt{2}}(T^\dagger_{12}Y_lS_{12}\cos\beta - T^\dagger_{22}Y_\Sigma S_{12}\sin\beta)$	$C^{G^0,R}_{\Sigma^-\Sigma^-}$	$\frac{i}{\sqrt{2}}(S^\dagger_{12}Y_l^\dagger T_{12}\cos\beta - S^\dagger_{12}Y_\Sigma^\dagger T_{22}\sin\beta)$

Table 3.13: The vertex factors for P_L (P_R) and their corresponding exact expression in terms of the Yukawa couplings and mixing matrices are given in the first (third) and second (forth) column respectively. The vertex factors listed here are for Yukawa interactions of the charged leptons with neutral Higgs.

$C^{H^0,L}_{\nu\nu}$	$\frac{\sin\alpha}{2}(U^T_{21}Y_\Sigma U_{11})$	$C^{H^0,R}_{\nu\nu}$	$\frac{\sin\alpha}{2}(U^\dagger_{11}Y^\dagger_\Sigma U^*_{21})$
$C^{H^0,L}_{\nu\Sigma^0}$	$\frac{\sin\alpha}{2}(U^T_{21}Y_\Sigma U_{12})$	$C^{H^0,R}_{\nu\Sigma^0}$	$\frac{\sin\alpha}{2}(U^\dagger_{11}Y^\dagger_\Sigma U^*_{22})$
$C^{H^0,L}_{\Sigma^0\Sigma^0}$	$\frac{\sin\alpha}{2}(U^T_{22}Y_\Sigma U_{12})$	$C^{H^0,R}_{\Sigma^0\Sigma^0}$	$\frac{\sin\alpha}{2}(U^\dagger_{12}Y^\dagger_\Sigma U^*_{22})$
$C^{h^0,L}_{\nu\nu}$	$\frac{\cos\alpha}{2}(U^T_{21}Y_\Sigma U_{11})$	$C^{h^0,R}_{\nu\nu}$	$\frac{\cos\alpha}{2}(U^\dagger_{11}Y^\dagger_\Sigma U^*_{21})$
$C^{h^0,L}_{\nu\Sigma^0}$	$\frac{\cos\alpha}{2}(U^T_{21}Y_\Sigma U_{12})$	$C^{h^0,R}_{\nu\Sigma^0}$	$\frac{\cos\alpha}{2}(U^\dagger_{11}Y^\dagger_\Sigma U^*_{22})$
$C^{h^0,L}_{\Sigma^0\Sigma^0}$	$\frac{\cos\alpha}{2}(U^T_{22}Y_\Sigma U_{12})$	$C^{h^0,R}_{\Sigma^0\Sigma^0}$	$\frac{\cos\alpha}{2}(U^\dagger_{12}Y^\dagger_\Sigma U^*_{22})$
$C^{A^0,L}_{\nu\nu}$	$\frac{i\cos\beta}{2}(U^T_{21}Y_\Sigma U_{11})$	$C^{A^0,R}_{\nu\nu}$	$-\frac{i\cos\beta}{2}(U^\dagger_{11}Y^\dagger_\Sigma U^*_{21})$
$C^{A^0,L}_{\nu\Sigma^0}$	$\frac{i\cos\beta}{2}(U^T_{21}Y_\Sigma U_{12})$	$C^{A^0,R}_{\nu\Sigma^0}$	$-\frac{i\cos\beta}{2}(U^\dagger_{11}Y^\dagger_\Sigma U^*_{22})$
$C^{A^0,L}_{\Sigma^0\Sigma^0}$	$\frac{i\cos\beta}{2}(U^T_{22}Y_\Sigma U_{12})$	$C^{A^0,R}_{\Sigma^0\Sigma^0}$	$-\frac{i\cos\beta}{2}(U^\dagger_{12}Y^\dagger_\Sigma U^*_{22})$
$C^{G^0,L}_{\nu\nu}$	$\frac{i\sin\beta}{2}(U^T_{21}Y_\Sigma U_{11})$	$C^{G^0,R}_{\nu\nu}$	$-\frac{i\sin\beta}{2}(U^\dagger_{11}Y^\dagger_\Sigma U^*_{21})$
$C^{G^0,L}_{\nu\Sigma^0}$	$\frac{i\sin\beta}{2}(U^T_{21}Y_\Sigma U_{12})$	$C^{G^0,R}_{\nu\Sigma^0}$	$-\frac{i\sin\beta}{2}(U^\dagger_{11}Y^\dagger_\Sigma U^*_{22})$
$C^{G^0,L}_{\Sigma^0\Sigma^0}$	$\frac{i\sin\beta}{2}(U^T_{22}Y_\Sigma U_{12})$	$C^{G^0,R}_{\Sigma^0\Sigma^0}$	$-\frac{i\sin\beta}{2}(U^\dagger_{12}Y^\dagger_\Sigma U^*_{22})$

Table 3.14: The vertex factors for P_L (P_R) and their corresponding exact expression in terms of the Yukawa couplings and mixing matrices are given in the first (third) and second (forth) column respectively. The vertex factors listed here are for Yukawa interactions of the neutral leptons with neutral Higgs.

$C_{l\nu}^{H^-,L}$	$-T_{11}^{\dagger}Y_l U_{11}\sin\beta$	$C_{l\nu}^{H^-,R}$	$(\frac{1}{\sqrt{2}}S_{11}^{\dagger}Y_{\Sigma}^{\dagger}U_{21}{}^* - S_{21}^{\dagger}Y_{\Sigma}{}^*U_{11}{}^*)\cos\beta$
$C_{l\Sigma^0}^{H^-,L}$	$-T_{11}^{\dagger}Y_l U_{12}\sin\beta$	$C_{l\Sigma^0}^{H^-,R}$	$(\frac{1}{\sqrt{2}}S_{11}^{\dagger}Y_{\Sigma}^{\dagger}U_{22}{}^* - S_{21}^{\dagger}Y_{\Sigma}{}^*U_{12}{}^*)\cos\beta$
$C_{\nu\Sigma^-}^{H^+,L}$	$(\frac{1}{\sqrt{2}}U_{21}^T Y_{\Sigma}S_{12} - U_{11}^T {Y_{\Sigma}}^T S_{22})\cos\beta$	$C_{\nu\Sigma^-}^{H^+,R}$	$-U_{11}^{\dagger}{Y_l}^{\dagger}T_{12}\sin\beta$
$C_{\Sigma^-\Sigma^0}^{H^-,L}$	$-T_{12}^{\dagger}Y_l U_{12}\sin\beta$	$C_{\Sigma^-\Sigma^0}^{H^-,R}$	$(\frac{1}{\sqrt{2}}S_{12}^{\dagger}Y_{\Sigma}^{\dagger}U_{22}{}^* - S_{22}^{\dagger}Y_{\Sigma}{}^*U_{12}{}^*)\cos\beta$
$C_{l\nu}^{G^-,L}$	$T_{11}^{\dagger}Y_l U_{11}\cos\beta$	$C_{l\nu}^{G^-,R}$	$(\frac{1}{\sqrt{2}}S_{11}^{\dagger}Y_{\Sigma}^{\dagger}U_{21}{}^* - S_{21}^{\dagger}Y_{\Sigma}{}^*U_{11}{}^*)\sin\beta$
$C_{l\Sigma^0}^{G^-,L}$	$T_{11}^{\dagger}Y_l U_{12}\cos\beta$	$C_{l\Sigma^0}^{G^-,R}$	$(\frac{1}{\sqrt{2}}S_{11}^{\dagger}Y_{\Sigma}^{\dagger}U_{22}{}^* - S_{21}^{\dagger}Y_{\Sigma}{}^*U_{12}{}^*)\sin\beta$
$C_{\nu\Sigma^-}^{G^+,L}$	$(\frac{1}{\sqrt{2}}U_{21}^T Y_{\Sigma}S_{12} - U_{11}^T {Y_{\Sigma}}^T S_{22})\sin\beta$	$C_{\nu\Sigma^-}^{G^+,R}$	$U_{11}^{\dagger}{Y_l}^{\dagger}T_{12}\cos\beta$
$C_{\Sigma^-\Sigma^0}^{G^-,L}$	$T_{12}^{\dagger}Y_l U_{12}\cos\beta$	$C_{\Sigma^-\Sigma^0}^{G^-,R}$	$(\frac{1}{\sqrt{2}}S_{12}^{\dagger}Y_{\Sigma}^{\dagger}U_{22}{}^* - S_{22}^{\dagger}Y_{\Sigma}{}^*U_{12}{}^*)\sin\beta$

Table 3.15: The vertex factors for P_L (P_R) and their corresponding exact expression in terms of the Yukawa couplings and mixing matrices are given in the first (third) and second (forth) column respectively. The vertex factors listed here are for Yukawa interactions of the charged as well as neutral leptons with charged Higgs.

where the first term is for heavy triplet fermion field and the second term contains the corresponding contributions from all standard model fields. The covariant derivative is defined as

$$D_\mu = \partial_\mu + ig[W_\mu, \Sigma]. \tag{B13}$$

Inserting the covariant derivative in Eq. (B12) one obtains the following interaction terms between leptons and gauge fields

$$\mathcal{L}_{int} = \mathcal{L}_{NC}^{l,\Sigma^-} + \mathcal{L}_{NC}^{\nu,\Sigma^0} + \mathcal{L}_{CC}, \tag{B14}$$

where the first two terms contain the neutral current interactions between $l^\pm$ and $\Sigma^\pm$ (first term) and between ν and Σ^0 (second term) respectively. The last term gives the charged current interaction between the leptons. The neutral current interaction Lagrangian involving l and Σ^- is given by

$$\begin{aligned} \mathcal{L}_{NC}^{l,\Sigma^-} &= \bar{l}_m\gamma^\mu\{c_{ll}^{Z,R}P_R + c_{ll}^{Z,L}P_L\}l_m\,Z_\mu + \{\bar{l}_m\gamma^\mu\{c_{l\Sigma^-}^{Z,R}P_R + c_{l\Sigma^-}^{Z,L}P_L\}\Sigma_m^-\,Z_\mu + \text{h.c}\} \\ &+\overline{\Sigma_m^-}\gamma^\mu\{c_{\Sigma^-\Sigma^-}^{Z,R}P_R + c_{\Sigma^-\Sigma^-}^{Z,L}P_L\}\Sigma_m^-\,Z_\mu, \end{aligned} \tag{B15}$$

where

$$\begin{aligned} c_{ll}^{Z,R} &= \frac{g}{c_w}s_w^2(T_{11}^{\dagger}T_{11}) - c_w g(T_{21}^{\dagger}T_{21}), \\ c_{l\Sigma^-}^{Z,R} &= \frac{g}{c_w}s_w^2(T_{11}^{\dagger}T_{12}) - c_w g(T_{21}^{\dagger}T_{22}), \\ c_{\Sigma^-\Sigma^-}^{Z,R} &= \frac{g}{c_w}s_w^2(T_{12}^{\dagger}T_{12}) - c_w g(T_{22}^{\dagger}T_{22}), \end{aligned} \tag{B16}$$

$$\begin{aligned}
c_{ll}^{Z,L} &= \frac{g}{c_w}(-\frac{1}{2}+s_w^2)(S_{11}^\dagger S_{11}) - c_w g(S_{21}^\dagger S_{21}),\\
c_{l\Sigma^-}^{Z,L} &= \frac{g}{c_w}(-\frac{1}{2}+s_w^2)(S_{11}^\dagger S_{12}) - c_w g(S_{21}^\dagger S_{22}),\\
c_{\Sigma^-\Sigma^-}^{Z,L} &= \frac{g}{c_w}(-\frac{1}{2}+s_w^2)(S_{12}^\dagger S_{12}) - c_w g(S_{22}^\dagger S_{22}). \qquad \text{(B17)}
\end{aligned}$$

The neutral current interaction Lagrangian involving the neutral leptons is given by

$$\begin{aligned}
\mathcal{L}_{NC}^{\nu,\Sigma^0} &= (gc_w+g's_w)\frac{1}{2}\overline{\nu}\gamma^\mu\{(U_{11}^\dagger U_{11})P_L\}\nu Z_\mu\\
&+(gc_w+g's_w)\frac{1}{2}\overline{\Sigma^0}\gamma^\mu\{(U_{12}^\dagger U_{12})P_L\}\Sigma^0 Z_\mu\\
&+\{(gc_w+g's_w)\frac{1}{2}\overline{\nu}\gamma^\mu\{(U_{11}^\dagger U_{12})P_L\}\Sigma^0 Z_\mu + \text{h.c}\}. \qquad \text{(B18)}
\end{aligned}$$

The charged current interaction Lagrangian is given by

$$\begin{aligned}
\mathcal{L}_{CC} &= g\overline{\nu}\gamma^\mu\{\{(U_{21}^\dagger S_{21}) + \frac{1}{\sqrt{2}}(U_{11}^\dagger S_{11})\}P_L + (U_{21}^T T_{21})P_R\}lW_\mu^+ \qquad \text{(B19)}\\
&+g\overline{\nu}\gamma^\mu\{\{(U_{21}^\dagger S_{22}) + \frac{1}{\sqrt{2}}(U_{11}^\dagger S_{12})\}P_L + (U_{21}^T T_{22})P_R\}\Sigma^- W_\mu^+\\
&+g\overline{\Sigma^0}\gamma^\mu\{\{(U_{22}^\dagger S_{21}) + \frac{1}{\sqrt{2}}(U_{12}^\dagger S_{11})\}P_L + (U_{22}^T T_{21})P_R\}lW_\mu^+\\
&+g\overline{\Sigma^0}\gamma^\mu\{\{(U_{22}^\dagger S_{22}) + \frac{1}{\sqrt{2}}(U_{12}^\dagger S_{12})\}P_L + (U_{22}^T T_{22})P_R\}\Sigma^- W_\mu^+ + \text{h.c}
\end{aligned}$$

B.3: Quark-Higgs coupling

The the Yukawa Lagrangian for quark sector is given by

$$-\mathcal{L}_Q = Y_{U_{ij}}\overline{u_{R_i}}\tilde{\Phi}_1^\dagger Q_j + Y_{D_{ij}}\overline{d_{R_i}}\Phi_1^\dagger Q_j + \text{h.c}, \qquad \text{(B20)}$$

where Q is the left-handed quark doublet and u_R and d_R are the right-handed "up" and "down" types of quark fields. Again, primes denote the flavor bases. After the electroweak spontaneous symmetry breaking the up and down quark mass matrices are obtained as

$$\begin{aligned}
M_U &= Y_U v \qquad \text{(B21)}\\
M_D &= Y_D v
\end{aligned}$$

Note that only Φ_1 couples to both the up and down quark fields due to the imposed Z_2 symmetry, while the Yukawa couplings of Φ_2 to quarks is forbidden[3]. However, due to the

[3]This is a major difference between our model and other two Higgs doublet models where the Higgs which couples to the neutrinos also couples to the up type quarks, while the one which couples to the charged leptons couples to the down type quarks.

mixing between Higgs fields as discussed in Appendix A, all the physical Higgs particles would couple to the quark fields. Here we list all the interaction vertices between quarks and Higgs fields, which are specific to our model. The fields represents the fields in the mass basis.

$$-\mathcal{L}^{H^0}_{u,d} = \frac{1}{\sqrt{2}}\frac{cos\alpha}{v}\overline{u}_m M_u u_m H^0 + \frac{1}{\sqrt{2}}\frac{cos\alpha}{v}\overline{d}_m M_d d_m H^0 \tag{B22}$$

$$-\mathcal{L}^{h^0}_{u,d} = -\frac{1}{\sqrt{2}}\frac{sin\alpha}{v}\overline{u}_m M_u u_m h^0 - \frac{1}{\sqrt{2}}\frac{sin\alpha}{v}\overline{d}_m M_d d_m h^0 \tag{B23}$$

$$-\mathcal{L}^{A^0}_{u,d} = i\frac{1}{\sqrt{2}}\frac{sin\beta}{v}\overline{u}_m \gamma^5 M_u u_m A^0 - i\frac{1}{\sqrt{2}}\frac{sin\beta}{v}\overline{d}_m \gamma^5 M_d d_m A^0 \tag{B24}$$

$$-\mathcal{L}^{G^0}_{u,d} = -i\frac{1}{\sqrt{2}}\frac{cos\beta}{v}\overline{u}_m \gamma^5 M_u u_m G^0 + i\frac{1}{\sqrt{2}}\frac{cos\beta}{v}\overline{d}_m \gamma^5 M_d d_m G^0 \tag{B25}$$

$$-\mathcal{L}^{G^\pm}_{u,d} = \frac{cos\beta}{v}\overline{u}_m (V_{CKM} M_d P_R - M_u V_{CKM} P_L) d_m G^+ + \text{h.c} \tag{B26}$$

$$-\mathcal{L}^{H^\pm}_{u,d} = -\frac{sin\beta}{v}\overline{u}_m (V_{CKM} M_d P_R - M_u V_{CKM} P_L) d_m H^+ + \text{h.c} \tag{B27}$$

Bibliography

[1] S. Weinberg, Phys. Rev. Lett. **43**, 1566 (1979).

[2] P. Minkowski, Phys. Lett. B **67**, 421 (1977); M. Gell-Mann, P. Ramond, and R. Slansky, *Supergravity* (P. van Nieuwenhuizen et al. eds.), North Holland, Amsterdam, 1980, p. 315; T. Yanagida, in *Proceedings of the Workshop on the Unified Theory and the Baryon Number in the Universe* (O. Sawada and A. Sugamoto, eds.), KEK, Tsukuba, Japan, 1979, p. 95; S. L. Glashow, *The future of elementary particle physics*, in *Proceedings of the 1979 Cargèse Summer Institute on Quarks and Leptons* (M. Lévy et al. eds.), Plenum Press, New York, 1980, pp. 687; R. N. Mohapatra and G. Senjanović, Phys. Rev. Lett. **44**, 912 (1980).

[3] M. Magg and C. Wetterich, Phys. Lett. B **94**, 61 (1980); J. Schechter and J. W. F. Valle, Phys. Rev. D **22**, 2227 (1980); C. Wetterich, Nucl. Phys. B **187**, 343 (1981); G. Lazarides, Q. Shafi and C. Wetterich, Nucl. Phys. B **181**, 287 (1981); R. N. Mohapatra and G. Senjanovic, Phys. Rev. D **23**, 165 (1981).

[4] R. Foot, H. Lew, X. G. He and G. C. Joshi, Z. Phys. C **44**, 441 (1989).

[5] E. Ma, Phys. Rev. Lett. **81**, 1171 (1998) [arXiv:hep-ph/9805219].

[6] E. Ma and D. P. Roy, Nucl. Phys. B **644**, 290 (2002) [arXiv:hep-ph/0206150]; R. Adhikari, J. Erler and E. Ma, Phys. Lett. B **672**, 136 (2009) [arXiv:0810.5547 [hep-ph]].

[7] T. Hambye, Y. Lin, A. Notari, M. Papucci and A. Strumia, Nucl. Phys. B **695**, 169 (2004) [arXiv:hep-ph/0312203].

[8] P. Fileviez Perez, Phys. Lett. B **654**, 189 (2007) [arXiv:hep-ph/0702287]; P. Fileviez Perez, Phys. Rev. D **76**, 071701 (2007) [arXiv:0705.3589 [hep-ph]].

[9] R. N. Mohapatra, N. Okada and H. B. Yu, Phys. Rev. D **78**, 075011 (2008) [arXiv:0807.4524 [hep-ph]].

[10] P. Fileviez Perez, JHEP **0903**, 142 (2009) [arXiv:0809.1202 [hep-ph]].

[11] I. Gogoladze, N. Okada and Q. Shafi, Phys. Lett. B **668**, 121 (2008) [arXiv:0805.2129 [hep-ph]].

[12] J. Chakrabortty, A. Dighe, S. Goswami and S. Ray, arXiv:0812.2776 [hep-ph].

[13] B. Bajc and G. Senjanovic, JHEP **0708**, 014 (2007) [arXiv:hep-ph/0612029].

[14] B. Bajc, M. Nemevsek and G. Senjanovic, Phys. Rev. D **76**, 055011 (2007) [arXiv:hep-ph/0703080].

[15] R. Franceschini, T. Hambye and A. Strumia, Phys. Rev. D **78**, 033002 (2008) [arXiv:0805.1613 [hep-ph]].

[16] F. del Aguila and J. A. Aguilar-Saavedra, Nucl. Phys. B **813**, 22 (2009) [arXiv:0808.2468 [hep-ph]].

[17] A. Arhrib, B. Bajc, D. K. Ghosh, T. Han, G. Y. Huang, I. Puljak and G. Senjanovic, arXiv:0904.2390 [hep-ph].

[18] S. Gabriel and S. Nandi, Phys. Lett. B **655**, 141 (2007) [arXiv:hep-ph/0610253].

[19] *"THE HIGGS HUNTER'S GUIDE"*, J. F. Gunion, H. E. Haber, G. L. Kane and S. Dawson, Perseus Publishings, Massachusetts.

[20] D. Atwood, S. Bar-Shalom and A. Soni, Phys. Lett. B **635**, 112 (2006) [arXiv:hep-ph/0502234].

[21] S. Antusch, M. Drees, J. Kersten, M. Lindner and M. Ratz, Phys. Lett. B **525**, 130 (2002) [arXiv:hep-ph/0110366].

[22] K. Matsuda, Y. Koide, T. Fukuyama and H. Nishiura, Phys. Rev. D **65**, 033008 (2002) [Erratum-ibid. D **65**, 079904 (2002)] [arXiv:hep-ph/0108202].

[23] M. Aoki, S. Kanemura and O. Seto, arXiv:0904.3829 [hep-ph].

[24] T. Fukuyama and H. Nishiura, hep-ph/9702253; R. N. Mohapatra and S. Nussinov, Phys. Rev. D **60**, 013002 (1999); E. Ma and M. Raidal, Phys. Rev. Lett. **87**, 011802 (2001); C. S. Lam, Phys. Lett. B **507**, 214 (2001); P.F. Harrison and W. G. Scott, Phys. Lett. B **547**, 219 (2002); T. Kitabayashi and M. Yasue, Phys. Rev. D **67**, 015006 (2003); W. Grimus and L. Lavoura, Phys. Lett. B **572**, 189 (2003); J. Phys. G **30**, 73 (2004); Y. Koide, Phys. Rev. D **69**, 093001 (2004); A. Ghosal, hep-ph/0304090; W. Grimus *et al.*, Nucl. Phys. B **713**, 151 (2005); R. N. Mohapatra, JHEP **0410**, 027 (2004); A. de Gouvea, Phys. Rev. D **69**, 093007 (2004); R. N. Mohapatra and W. Rodejohann, Phys. Rev. D **72**, 053001 (2005); R. N. Mohapatra and S. Nasri, Phys. Rev. D **71**, 033001 (2005); R. N. Mohapatra, S. Nasri and H. B. Yu, Phys.

Lett. B **615**, 231 (2005); Phys. Rev. D **72**, 033007 (2005); Y. H. Ahn*et al.*, Phys. Rev. D **73**, 093005 (2006); B. Brahmachari and S. Choubey, Phys. Lett. B **642**, 495 (2006); K. Fuki, M. Yasue, hep-ph/0608042. S. Choubey and W. Rodejohann, Eur. Phys. J. C **40**, 259 (2005).

[25] W. Grimus and L. Lavoura, JHEP **0011**, 042 (2000) [arXiv:hep-ph/0008179].

[26] M. Mitra and S. Choubey, Phys. Rev. D **78**, 115014 (2008) [arXiv:0806.3254 [hep-ph]].

[27] M. Maltoni, T. Schwetz, M. A. Tortola and J. W. F. Valle, New J. Phys. **6**, 122 (2004), hep-ph/0405172 v6; A. Bandyopadhyay, S. Choubey, S. Goswami, S. T. Petcov and D. P. Roy, arXiv:0804.4857 [hep-ph]. G. L. Fogli *et al.*, Phys. Rev. D **78**, 033010 (2008) [arXiv:0805.2517 [hep-ph]].

[28] A. Abada, C. Biggio, F. Bonnet, M. B. Gavela and T. Hambye, JHEP **0712**, 061 (2007) [arXiv:0707.4058 [hep-ph]].

[29] A. Abada, C. Biggio, F. Bonnet, M. B. Gavela and T. Hambye, Phys. Rev. D **78**, 033007 (2008) [arXiv:0803.0481 [hep-ph]].

[30] See *"http://hep.pa.msu.edu/people/belyaev/public/calchep/index.html"* .

[31] G. Aad *et al.* [The ATLAS Collaboration], arXiv:0901.0512 [hep-ex].

[32] See the CMS Physics Technical Design Report (Volume I and II) at *http://cms.web.cern.ch/cms/Physics/index.html*

[33] G. Altarelli and F. Feruglio, Nucl. Phys. B **741**, 215 (2006); G. Altarelli , F. Feruglio and Y. Lin, Nucl. Phys. B **775**, 31 (2007).

Chapter 4

R Parity Violation and Neutrino Mass

4.1 Introduction

We have discussed the minimal supersymmetric standard model in chapter 1. The superpotential of the minimal supersymmetric standard model, which conserves a discrete Z_2 symmetry R-parity is

$$W_{MSSM} = Y_e \hat{H}_d \hat{L} \hat{E}^c + Y_d \hat{H}_d \hat{Q} \hat{D}^c - Y_u \hat{H}_u \hat{Q} \hat{U}^c + \mu \hat{H}_u \hat{H}_d. \tag{4.1}$$

R-parity or matter parity is defined as $R_p = (-1)^{3(B-L)+2S}$. For the standard model particles the charge is $+1$ and for the superpartners of the standard model particle it is -1. Apart from the above superpotential of the R-parity conserving minimal supersymmetric standard model, the $\mathrm{SU(3)_C \times SU(2)_L \times U(1)_Y}$ gauge invariance also allows the following R-parity violating superpotential

$$W_{\not{R}_p-MSSM} = -\epsilon \hat{H}_u \hat{L} + \lambda \hat{L} \hat{L} \hat{E}^c + \lambda' \hat{L} \hat{Q} \hat{D}^c + \lambda'' \hat{U}^c \hat{D}^c \hat{D}^c. \tag{4.2}$$

The 1st, 2nd and 3rd term of the above superpotential violate lepton number whereas the 4th term breaks baryon number conservation. The Majorana masses of the standard model neutrinos can be explained by the effective dimension-5 operator $\frac{LLHH}{M}$, which violate lepton number by two-units. Hence, the lepton number violation in the superpotential $W_{\not{R}_p-MSSM}$ opens up the possibility to generate non-zero neutrino mass [1–10]. This can be done through one loop [4,5] and two loop [6] diagrams generated via the lepton number breaking trilinear couplings λ and λ' (see Eq. (4.2)). Small neutrino masses can also be generated by the R-parity violating bilinear coupling $\hat{H}_u \hat{L}$ [1, 2], through the neutrino-higgsino $\nu - \tilde{h}_u^0$ mixing. However these lepton and baryon number violating couplings of the superpotential $W_{\not{R}_p-MSSM}$ are severely constrained by non-observation of proton decay and data on heavy flavor physics from Belle and Babar [11]. In particular, the simultaneous presence of the lepton number violating λ, λ' couplings and the baryon number violating λ'' coupling are constrained as $\lambda'_{11k}\lambda''_{11k} \leq 10^{-24}(m_{\tilde{k}}/100\text{GeV})$. For other λ' and λ'' couplings the bound is $\lambda'_{ijk}\lambda''_{lmn} \leq 10^{-9}$ [11]. Comparable bound exist on the product of λ and λ'' couplings [12]. Once R-parity conservation is implemented, all the terms of $W_{\not R_p-MSSM}$ are forbidden and hence the minimal supersymmetric standard model does not suffer any proton decay constraint. However, only the absence of λ'' term is sufficient and minimalistic choice to avoid the proton decay constraint. Sticking to a renormalizable perturbation theory if R-parity is violated spontaneously, one can easily justify the absence of the baryon number violating λ'' operator in the superpotential $W_{\not R_p-MSSM}$, while at the same time the bilinear R-parity violating operator and trilinear R-parity violating operators are possible to generate. In this scenario R-parity is conserved in the superpotential. Once the sneutrino fields acquire vacuum expectation values, R-parity breaking terms are generated spontaneously [9, 10, 13–17]. In presence of additional singlet or triplet matter chiral fields, this provides a natural explanation for the origin of the R-parity and lepton number violating bilinear term[1] ϵ, without generating the baryon number violating λ'' term in the superpotential. Therefore, one can generate neutrino masses without running into problems with proton decay in this class of supersymmetric models.

There have been earlier attempts to construct spontaneous R-parity violating models within the MSSM gauge group [9, 10, 13, 14] and with the MSSM particle contents. In all these models the R-parity is broken spontaneously when the sneutrino acquires a VEV. This automatically breaks lepton number spontaneously. If lepton number is a global symmetry, this will give rise to a massless Goldstone called the Majoron [18]. All models which predict presence of Majoron are severely constrained. The phenomenology of the models with singlet Majoron has been studied in detail in [10, 14].

A possible way of avoiding the Majoron is by gauging the U(1) symmetry associated with lepton number such that the spontaneous R-parity and lepton number violation comes with the new gauge symmetry breaking. This gives rise to an additional neutral gauge boson and the phenomenology of these models have also been studied extensively in the literature [15, 16]. This idea has been used in a series of recent papers [17].

In this work we study spontaneous R-parity violation in the presence of a $\mathrm{SU(2)_L}$ triplet $Y = 0$ matter chiral superfield, where we stick to the gauge group of the minimal supersymmetric standard model. Lepton number is broken explicitly in our model by the Majorana mass term of the heavy fermionic triplet, thereby circumventing the problem of the Majoron. We break R-parity spontaneously by giving vacuum expectation values to the 3 MSSM sneutrinos and the one additional sneutrino associated with the triplet which leads to the lepton-higgsino and lepton-gaugino mixing in addition to the conventional Yukawa driven neutrino-triplet neutrino mixing. This opens up the possibility of generating neutrino mass from a combination of the conventional type-III seesaw and the

[1]It is possible to realize the other terms λ and λ' from the R-parity conserving MSSM superpotential only after redefinition of basis [1].

gaugino seesaw. We restrict ourself to just one additional $\mathrm{SU(2)_L}$ triplet $Y = 0$ matter chiral superfield, and explore the possibility of getting viable neutrino mass splitting and the mixing angles at tree level. With one generation of heavy triplet we get two massive neutrinos while the third state remains massless. Like the neutralino sector we also have R-parity conserving mixing between the standard model charged leptons and the heavy triplet charged lepton states. The spontaneous R-parity breaking brings about mixing between the charginos and the charged leptons, and hence modifies the chargino mass spectrum. In addition to the usual charged leptons, our model contains a pair of heavy charged fermions coming from the fermionic component of the triplet superfield. Another novel feature of our model comes from the fact that the additional triplet fermions and sfermions have direct gauge interactions. Hence they offer a much richer collider phenomenology. We discuss in brief about the possibility of detecting our model at colliders and the predicted R-parity violating signatures.

The main aspects of our spontaneous R-parity violating model are the following:

- We introduce one chiral superfield containing the triplets of $\mathrm{SU(2)_L}$ and with $Y = 0$.
- We have an explicit breaking of the lepton number due to the presence of the mass term of this chiral superfield in the superpotential. Therefore unlike as in [9, 10, 13, 14], the spontaneous breaking of R-parity does not create any Majoron in our model. Since we do not have any additional gauge symmetry, we also do not have any additional neutral gauge boson as in [15–17].
- Since we have only one additional triplet chiral superfield we have two massive neutrinos, with the lightest one remaining massless. One of the neutrinos get mass due to type-III seesaw and another due to gaugino seesaw. Combination of both gives rise to a neutrino mass matrix which is consistent with the current data.
- The triplet chiral superfield in our model modifies not only the neutrino-neutralino mass matrix, but also the charged lepton – chargino mass matrix. Being a triplet, it contains one neutral Majorana fermion Σ^0, two charged fermions $\Sigma^\pm$, one sneutrino $\tilde{\Sigma}^0$, and two charged sfermions $\tilde{\Sigma}^\pm$. Therefore, our neutral fermion mass matrix is a 8×8 matrix, giving mixing between the gauginos, higgsinos as well as the new TeV-scale neutral fermion Σ^0. Likewise, the new charged fermions $\Sigma^\pm$ will mix with the charginos and the charged leptons.
- There are thus new TeV-mass neutral and charged leptons and charged scalars in our model, which will have mixing with other MSSM particles. These could be probed at future colliders and could lead to a rich phenomenology. We give a very brief outline of the collider signatures in this work.

The chapter is organized as follows. In section 4.2 we describe the model and in section 4.3 we present the symmetry breaking analysis. In section 4.4, we discuss the neutralino-neutrino mass matrix and in section 4. 5 we discuss the chargino-charged lepton mass matrix. We concentrate on the neutrino phenomenology in section 4.6 and discuss the possibility of getting correct mass splittings and mixings even with one generation of $\mathrm{SU(2)_L}$ triplet matter chiral supermultiplet. In section 4.7 we discuss about detecting our model in colliders and finally in section 4.8 we present our conclusion. Discussion on soft-supersymmetry breaking terms, gaugino-lepton-slepton mixing and the analytic expression of the low energy neutrino mass matrix have been presented in Appendix A, Appendix B and in Appendix C, respectively. In Appendix C we also analyze the constraints on the different sneutrino vacuum expectation values coming from the neutrino mass scale.

4.2 The Model

In this section, we discuss about our model. The superpotential of the supersymmetric standard model has given in Eq. (4.1) and in Eq. (4.2). In this work we will explore spontaneous R-parity violation in the presence of $\mathrm{SU(2)_L}$ triplet $Y = 0$ matter chiral superfield. The matter chiral supermultiplets of the model are:

$\hat{Q} = \begin{pmatrix} \hat{U} \\ \hat{D} \end{pmatrix}$, $\hat{L} = \begin{pmatrix} \hat{\nu} \\ \hat{E} \end{pmatrix}$, $\hat{U}^c$, $\hat{D}^c$ and $\hat{E}^c$

and the Higgs chiral supermultiplets are :

$\hat{H}_u = \begin{pmatrix} \hat{H}_u^+ \\ \hat{H}_u^0 \end{pmatrix}$, $\hat{H}_d = \begin{pmatrix} \hat{H}_d^0 \\ \hat{H}_d^- \end{pmatrix}$.

In addition to the standard supermultiplet contents of the MSSM we introduce one $\mathrm{SU(2)_L}$ triplet matter chiral supermultiplet $\hat{\Sigma}_R^c$ with $U(1)_Y$ hypercharge $Y = 0$. We represent $\hat{\Sigma}_R^c$ as

$$\hat{\Sigma}_R^c = \frac{1}{\sqrt{2}} \begin{pmatrix} \hat{\Sigma}_R^{0c} & \sqrt{2}\hat{\Sigma}_R^{-c} \\ \sqrt{2}\hat{\Sigma}_R^{+c} & -\hat{\Sigma}_R^{0c} \end{pmatrix}. \tag{4.3}$$

The three different chiral superfields in this multiplet are

$$\hat{\Sigma}_R^{+c} = \tilde{\Sigma}_R^{+c} + \sqrt{2}\theta\Sigma_R^{+c} + \theta\theta F_{\Sigma_R^{+c}}, \tag{4.4}$$

$$\hat{\Sigma}_R^{-c} = \tilde{\Sigma}_R^{-c} + \sqrt{2}\theta\Sigma_R^{-c} + \theta\theta F_{\Sigma_R^{-c}}, \tag{4.5}$$

$$\hat{\Sigma}_R^{0c} = \tilde{\Sigma}_R^{0c} + \sqrt{2}\theta\Sigma_R^{0c} + \theta\theta F_{\Sigma_R^{0c}}. \tag{4.6}$$

The SU(2) triplet fermions are Σ_R^{+c}, Σ_R^{-c} and Σ_R^{0c} and their scalar superpartners are represented as $\tilde{\Sigma}_R^{+c}$, $\tilde{\Sigma}_R^{-c}$ and $\tilde{\Sigma}_R^{0c}$ respectively. $F_{\Sigma_R^{+c},\Sigma_R^{-c},\Sigma_R^{0c}}$ represent the different auxiliary fields of the above mentioned multiplet. R-parity of $\hat{\Sigma}_R^c$ is -1 where componentwise the fermions Σ_R^{+c}, Σ_R^{-c} and Σ_R^{0c} have R-parity $+1$ and their scalar superpartners have R-parity -1. With these field contents, the R-parity conserving superpotential W of our model will be

$$W = W_{MSSM} + W_\Sigma, \tag{4.7}$$

where W_{MSSM} has already been written in Eq. (4.1) and W_Σ is given by

$$W_\Sigma = -Y_{\Sigma_i} \hat{H}_u{}^T (i\sigma_2) \hat{\Sigma}_R^c \hat{L}_i + \frac{M}{2} Tr[\hat{\Sigma}_R^c \hat{\Sigma}_R^c]. \tag{4.8}$$

W_Σ is clearly R-parity conserving. The scalar fields $\tilde{\Sigma}_R^{0c}$ and $\tilde{\nu}_{L_i}$ are odd under R-parity. Hence in this model, R-parity would be spontaneously broken by the vacuum expectation values of these sneutrino fields. We will analyze the potential and spontaneous R-parity violation in the next section. On writing explicitly, one will get these following few terms from the above superpotential W_Σ,

$$\begin{aligned} W_\Sigma \;\; = \;\; & \frac{Y_{\Sigma_i}}{\sqrt{2}} \hat{H}_u^0 \hat{\Sigma}_R^{0c} \hat{\nu}_{L_i} + Y_{\Sigma_i} \hat{H}_u^0 \hat{\Sigma}_R^{-c} \hat{l}_i^{\,-} + \frac{Y_{\Sigma_i}}{\sqrt{2}} \hat{H}_u^+ \hat{\Sigma}_R^{0c} \hat{l}_i^{\,-} - Y_{\Sigma_i} \hat{H}_u^+ \hat{\Sigma}_R^{+c} \hat{\nu}_{L_i} \\ & + \frac{M}{2} \hat{\Sigma}_R^{0c} \hat{\Sigma}_R^{0c} + M \hat{\Sigma}_R^{+c} \hat{\Sigma}_R^{-c}. \end{aligned} \tag{4.9}$$

The kinetic terms of the $\hat{\Sigma}_R^c$ field is

$$L_\Sigma^k = \int d^4\theta Tr[\hat{\Sigma_R^c}^\dagger e^{2gV} \hat{\Sigma_R^c}]. \tag{4.10}$$

The soft supersymmetry breaking Lagrangian of this model is

$$L^{\rm soft} = L^{\rm soft}_{\rm MSSM} + L^{\rm soft}_\Sigma. \tag{4.11}$$

For completeness we write the $L^{\rm soft}_{\rm MSSM}$ Lagrangian in the Appendix A. $L^{\rm soft}_\Sigma$ contains the supersymmetry breaking terms corresponding to scalar $\tilde{\Sigma}_R^c$ fields and is given by

$$L^{\rm soft}_\Sigma = -m_\Sigma^2 {\rm Tr}[\tilde{\Sigma}_{\rm R}^{\rm c\dagger} \tilde{\Sigma}_{\rm R}^{\rm c}] - (\tilde{\rm m}^2 {\rm Tr}[\tilde{\Sigma}_{\rm R}^{\rm c} \tilde{\Sigma}_{\rm R}^{\rm c}] + {\rm h.c}) - ({\rm A}_{\Sigma_{\rm i}} H_u^T {\rm i}\sigma_2 \tilde{\Sigma}_{\rm R}^{\rm c} \tilde{\rm L}_{\rm i} + {\rm h.c}), \tag{4.12}$$

where

$$\tilde{\Sigma}_R^c = \frac{1}{\sqrt{2}} \begin{pmatrix} \tilde{\Sigma}_R^{0c} & \sqrt{2}\tilde{\Sigma}_R^{-c} \\ \sqrt{2}\tilde{\Sigma}_R^{+c} & -\tilde{\Sigma}_R^{0c} \end{pmatrix}. \tag{4.13}$$

We explicitly show in the Appendix A all the possible trilinear terms which will be generated from Eq. (4.9) and the interaction terms between gauginos and SU(2) triplet fermion and sfermion coming from Eq. (4.10). In the next section we analyze the neutral component of the potential and discuss spontaneous R-parity violation through $\tilde{\Sigma}_R^{0c}$ and $\tilde{\nu}_{L_i}$ vacuum expectation values.

4.3 Symmetry Breaking

In this section we write down the scalar potential which will be relevant to analyze the symmetry breaking of the Lagrangian. The potential is

$$V = V_F + V_D + V_{soft}, \tag{4.14}$$

where V_F and V_D, the contributions from different auxiliary components of the chiral superfield and different vector supermultiplets are given by

$$V_F = \sum_k F_k^* F_k \tag{4.15}$$

$$V_D = \frac{1}{2}\sum_a D^a D^a \tag{4.16}$$

respectively. Here the index k denotes all possible auxiliary components of the matter chiral superfields whereas the index a is the gauge index. The contribution from the soft supersymmetry breaking Lagrangian is given by V_{soft}. Below we write down the neutral component of the potential which would be relevant for our symmetry breaking analysis. The neutral component of the potential is given by

$$V_{neutral} = V_F^n + V_D^n + V_{soft}^n, \tag{4.17}$$

where

$$V_F^n = |F_{H_u^0}|^2 + |F_{H_d^0}|^2 + |F_{\tilde{\nu}_{L_i}}|^2 + |F_{\tilde{\Sigma}_R^{0c}}|^2. \tag{4.18}$$

The different F_k are given by

$$F^*_{H_u^0} = \mu H_d^0 - \sum_i \frac{Y_{\Sigma_i}}{\sqrt{2}} \tilde{\Sigma}_R^{0c} \tilde{\nu}_{L_i} + ..., \tag{4.19}$$

$$F^*_{H_d^0} = \mu H_u^0 + ..., \tag{4.20}$$

$$F^*_{\tilde{\Sigma}_R^{0c}} = -\sum_i \frac{Y_{\Sigma_i}}{\sqrt{2}} H_u^0 \tilde{\nu}_{L_i} - M\tilde{\Sigma}_R^{0c} + ..., \tag{4.21}$$

$$F^*_{\tilde{\nu}_{L_i}} = -\frac{Y_{\Sigma_i}}{\sqrt{2}} H_u^0 \tilde{\Sigma}_R^{0c} + ... \tag{4.22}$$

In the above equations ... represents other terms which will not contribute to the neutral component of the potential. With all these F_k's, V_F^n is given by

$$V_F^n = |\mu H_d^0|^2 + |\mu H_u^0|^2 + \frac{1}{2}|\sum_i Y_{\Sigma_i}\tilde{\Sigma}_R^{0c}\tilde{\nu}_{L_i}|^2 + \frac{1}{2}\sum_i |Y_{\Sigma_i} H_u^0 \tilde{\Sigma}_R^{0c}|^2 + \frac{1}{2}|\sum_i Y_{\Sigma_i} H_u^0 \tilde{\nu}_{L_i}|^2 \quad (4.23)$$

$$-[\mu H_d^0 (\sum_i \frac{Y_{\Sigma_i}}{\sqrt{2}}\tilde{\Sigma}_R^{0c}\tilde{\nu}_{L_i})^* + c.c] + |M|^2 \tilde{\Sigma}_R^{0c^*}\tilde{\Sigma}_R^{0c} + [\sum_i \frac{Y_{\Sigma_i}}{\sqrt{2}} H_u^0 \tilde{\nu}_{L_i} (M\tilde{\Sigma}_R^{0c})^* + c.c] \quad (4.24)$$

As we have three generation of leptons hence the generation index i runs as i=1,2,3. The D term contribution of $V_{neutral}$ is given as

$$V_D^n = \frac{1}{8}(g^2 + g'^2)(|H_d^0|^2 - |H_u^0|^2 + \sum_i |\tilde{\nu}_{L_i}|^2)^2. \quad (4.25)$$

The component $\tilde{\Sigma}_R^{0c}$ which has $Y = 0$ and the third component of the isospin $T_3 = 0$ does not contributes to V_D^n. The soft supersymmetry breaking contributions to the neutral part of the potential is given by V_{soft}^n where

$$\begin{aligned} V_{soft}^n &= -(bH_u^0 H_d^0 + c.c) + m_{H_u}^2 |H_u^0|^2 + m_{H_d}^2 |H_d^0|^2 \\ &\quad + m_\Sigma^2 \tilde{\Sigma}_R^{0c^*}\tilde{\Sigma}_R^{0c} + [\tilde{m}^2 \tilde{\Sigma}_R^{0c}\tilde{\Sigma}_R^{0c} + c.c] \\ &\quad + \sum_i m_{\tilde{\nu}_i}^2 \tilde{\nu}_{L_i}^* \tilde{\nu}_{L_i} + [\sum_i \frac{A_{\Sigma_i}}{\sqrt{2}} H_u^0 \tilde{\Sigma}_R^{0c}\tilde{\nu}_{L_i} + c.c]. \end{aligned} \quad (4.26)$$

We represent the vacuum expectation values of H_u^0, H_d^0, $\tilde{\nu}_{L_i}$ and $\tilde{\Sigma}_R^{0c}$ as $\langle H_u^0 \rangle = v_2$, $\langle H_d^0 \rangle = v_1$, $\langle \tilde{\nu}_{L_i} \rangle = u_i$ and $\langle \tilde{\Sigma}_R^{0c} \rangle = \tilde{u}$. We have considered a diagonal $m_{\tilde{\nu}}^2$ matrix. In terms of these vacuum expectation values the neutral component of the potential is

$$\begin{aligned} \langle V_{neutral} \rangle &= (|\mu|^2 + m_{H_u}^2)|v_2|^2 + (|\mu|^2 + m_{H_d}^2)|v_1|^2 - (bv_1 v_2 + c.c) \\ &\quad + \frac{1}{8}(g^2 + g'^2)(|v_1|^2 - |v_2|^2 + \sum_i |u_i|^2)^2 + (|M|^2 + m_\Sigma^2)|\tilde{u}|^2 \\ &\quad + \sum_i m_{\tilde{\nu}_i}^2 |u_i|^2 + [\tilde{m}^2 \tilde{u}^2 + c.c] + \frac{1}{2}|\sum_i Y_{\Sigma_i}\tilde{u}u_i|^2 + \frac{1}{2}\sum_i |Y_{\Sigma_i}|^2 |\tilde{u}v_2|^2 \\ &\quad + \frac{1}{2}|\sum_i Y_{\Sigma_i} u_i v_2|^2 + (\sum_i \frac{A_{\Sigma_i}}{\sqrt{2}} v_2 u_i \tilde{u} + c.c) - (\mu v_1 (\sum_i \frac{Y_{\Sigma_i}}{\sqrt{2}}\tilde{u}u_i)^* + c.c) \\ &\quad + [\sum_i \frac{Y_{\Sigma_i}}{\sqrt{2}} v_2 u_i (M\tilde{u})^* + c.c]. \end{aligned} \quad (4.27)$$

For simplicity we assume all the vacuum expectation values and all the parameters are real. Hence $\langle V_{neutral} \rangle$ simplifies to

$$\langle V_{neutral} \rangle = (\mu^2 + m_{H_u}^2)v_2^2 + (\mu^2 + m_{H_d}^2)v_1^2 - 2bv_1 v_2 + \frac{1}{8}(g^2 + g'^2)(v_1^2 - v_2^2 + \sum_i u_i^2)^2$$

$$+(M^2+m_\Sigma^2)\tilde{u}^2+\sum_i m_{\tilde{\nu}_i}^2 u_i^2+2\tilde{m}^2\tilde{u}^2+\frac{1}{2}(\sum_i Y_{\Sigma_i}u_i)^2\tilde{u}^2+\frac{1}{2}\sum_i (Y_{\Sigma_i})^2\tilde{u}^2 v_2^2$$
$$+\frac{1}{2}(\sum_i Y_{\Sigma_i}u_i)^2 v_2^2+\sqrt{2}\sum_i(A_{\Sigma_i}v_2u_i\tilde{u}-\mu v_1 Y_{\Sigma_i}\tilde{u}u_i+Y_{\Sigma_i}Mv_2u_i\tilde{u}). \quad (4.28)$$

Minimizing $\langle V_{neutral}\rangle$ with respect to v_1, v_2, $\tilde{u}$ and u_i we get the following four equations,

$$2(\mu^2+m_{H_d}^2)v_1-2bv_2+\frac{v_1}{2}(g^2+g'^2)(v_1^2-v_2^2+\Sigma_i u_i^2)-\sqrt{2}\mu\tilde{u}\sum_i Y_{\Sigma_i}u_i=0, \quad (4.29)$$

$$2(\mu^2+m_{H_u}^2)v_2-2bv_1-\frac{v_2}{2}(g^2+g'^2)(v_1^2-v_2^2+\sum_i {u_i}^2)+v_2((\sum_i Y_{\Sigma_i}u_i)^2$$
$$+\sum_i (Y_{\Sigma_i})^2\tilde{u}^2)+\sqrt{2}\sum_i (A_{\Sigma_i}+Y_{\Sigma_i}M)u_i\tilde{u}=0, \quad (4.30)$$

$$2(m_\Sigma^2+2M^2+2\tilde{m}^2)\tilde{u}+(\sum_i Y_{\Sigma_i}u_i)^2\tilde{u}+\sqrt{2}\sum_i (A_{\Sigma_i}v_2u_i-\mu Y_{\Sigma_i}v_1u_i+Y_{\Sigma_i}Mv_2u_i)$$
$$+\sum_i (Y_{\Sigma_i})^2\tilde{u}v_2^2=0, \quad (4.31)$$

$$\frac{u_i}{2}(g^2+g'^2)(v_1^2-v_2^2+\sum_j u_j^2)+(v_2^2+\tilde{u}^2)[{Y_{\Sigma_i}}^2u_i+Y_{\Sigma_i}\sum_{j\neq i}Y_{\Sigma_j}u_j]+\sqrt{2}A_{\Sigma_i}v_2\tilde{u}$$
$$+\sqrt{2}[Y_{\Sigma_i}Mv_2\tilde{u}-\mu Y_{\Sigma_i}v_1\tilde{u}]+2m_{\tilde{\nu}_i}^2u_i=0. \quad (4.32)$$

respectively. In the last equation the index i is *not summed over*. As mentioned before, since $\tilde{\nu}_{L_i}$ and $\tilde{\Sigma}_R^{0c}$ have nontrivial R-parity, hence R-parity is spontaneously broken when $\tilde{\nu}_{L_i}$ and $\tilde{\Sigma}_R^{0c}$ take vacuum expectation values. As a result of this spontaneous R-parity violation, the bilinear term LH_u which will contribute to the neutrino mass matrix is generated. We will discuss in detail about the neutralino-neutrino and chargino-charged lepton mass matrix in the next section.

The minimization conditions given in Eqs. (4.29)-(4.32) can be used to give constraints on the vacuum expectation values u_i and $\tilde{u}$. In order to get such relations we drop the generation indices for the moment and consider $u_i=u$ for simplicity. In this case Y_Σ, A_Σ and $m_{\tilde{\nu}_i}^2$ contain no generation index and would be just three numbers. From the simplified version of the last two equations Eq. (4.31) and Eq. (4.32) it can then be shown that in the limit that u is small, the two R-parity breaking vacuum expectation values u and $\tilde{u}$ are proportional to each other. Combining these two equations one gets

$$\tilde{u}^2=\frac{u^2}{{Y_\Sigma}^2v_2^2+2(m_\Sigma^2+2\tilde{m}^2+2M^2)}[\frac{1}{2}(g^2+g'^2)(v_1^2-v_2^2+u^2)+2m_{\tilde{\nu}}^2+{Y_\Sigma}^2v_2^2]. \quad (4.33)$$

Hence for small u which is demanded from the smallness of neutrino mass (discussed in the next section and in Appendix C), $\tilde{u}$ will also be of the same order as u unless there is a cancellation between the terms in the denominator. In this work we will stick to the possibility of small u and $\tilde{u}$. We will show in the next section that one needs $u \sim 10^{-3}$ GeV to explain the neutrino data. Hence $\tilde{u}$ will also have to be 10^{-3} GeV. In the $u = 0$ limit, $\tilde{u}$ would also be 0 and this is our usual R-parity conserving scenario.

4.4 Neutralino-Neutrino Mass Matrix

In this section we discuss the consequence of R-parity violation through the neutralino-neutrino mixing. It is well known [19] that R-parity violation results in mixing between the neutrino-neutralino states. In our model the neutrino sector is enlarged and includes both the standard model neutrino ν_{L_i}, as well as the heavier neutrino state Σ_R^{0c}, which is a component of SU(2) triplet superfield. Since R-parity is violated we get higgsino-neutrino mixing terms $\frac{Y_{\Sigma_i}}{\sqrt{2}}\tilde{u}\tilde{H}_u^0\nu_{L_i}$ and $\frac{Y_{\Sigma_i}}{\sqrt{2}}u\tilde{H}_u^0\Sigma_R^{0c}$, in addition to the conventional R-parity conserving Dirac mass term $\frac{Y_{\Sigma_i}}{\sqrt{2}}v_u\Sigma_R^{0c}\nu_{L_i}$. The R-parity breaking former two terms originated from the term $\frac{Y_{\Sigma_i}}{\sqrt{2}}\hat{H}_u^0\hat{\Sigma}_R^{0c}\hat{\nu}_{L_i}$ in Eq. (4.9), once the sneutrino fields $\tilde{\nu}_{L_i}$ and $\tilde{\Sigma}_R^{0c}$ get vacuum expectation values. The third term also has the same origin and it is the conventional Dirac mass term in type I or type-III seesaw. In addition to the higgsino-neutrino mixing terms generated from the superpotential W_Σ, there would also be gaugino-neutrino mixing terms generated from the Kähler potential of the $\hat{L}_i$ and $\hat{\Sigma}_R^c$. In the Appendix B we show explicitly the contributions coming from W_Σ and the neutrino-sneutrino-gaugino terms originating from the kinetic term of the triplet superfield $\hat{\Sigma}_R^c$ written down in Eq. (4.10). Here we write the color singlet neutral-fermion mass matrix of this model in the basis $\psi = (\tilde{\lambda}^0,\tilde{\lambda}^3,\tilde{\mathrm{H}}_\mathrm{d}^0,\tilde{\mathrm{H}}_\mathrm{u}^0,\Sigma_\mathrm{R}^{0c},\nu_{\mathrm{L}_1},\nu_{\mathrm{L}_2},\nu_{\mathrm{L}_3})^\mathrm{T}$ where with one generation of Σ_R^c, the neutral fermion mass matrix is a 8×8 matrix. The mass term is given by

$$L_n = -\frac{1}{2}\psi^T M_n \psi + h.c. \tag{4.34}$$

where

$$M_n = \frac{1}{\sqrt{2}}\begin{pmatrix} \sqrt{2}M^1 & 0 & -g'v_1 & g'v_2 & 0 & -g'u_1 & -g'u_2 & -g'u_3 \\ 0 & \sqrt{2}M^2 & gv_1 & -gv_2 & 0 & gu_1 & gu_2 & gu_3 \\ -g'v_1 & gv_1 & 0 & -\sqrt{2}\mu & 0 & 0 & 0 & 0 \\ g'v_2 & -gv_2 & -\sqrt{2}\mu & 0 & \sum_i Y_{\Sigma_i}u_i & Y_{\Sigma_1}\tilde{u} & Y_{\Sigma_2}\tilde{u} & Y_{\Sigma_3}\tilde{u} \\ 0 & 0 & 0 & \sum_i Y_{\Sigma_i}u_i & \sqrt{2}M & Y_{\Sigma_1}v_2 & Y_{\Sigma_2}v_2 & Y_{\Sigma_3}v_2 \\ -g'u_1 & gu_1 & 0 & Y_{\Sigma_1}\tilde{u} & Y_{\Sigma_1}v_2 & 0 & 0 & 0 \\ -g'u_2 & gu_2 & 0 & Y_{\Sigma_2}\tilde{u} & Y_{\Sigma_2}v_2 & 0 & 0 & 0 \\ -g'u_3 & gu_3 & 0 & Y_{\Sigma_3}\tilde{u} & Y_{\Sigma_3}v_2 & 0 & 0 & 0 \end{pmatrix} \tag{4.35}$$

Here $M^{1,2}$ are the soft supersymmetry breaking gaugino mass parameters (see Appendix B), whereas M corresponds to the triplet-fermion bilinear term. We define the 3×5 matrix m_D as

$$m_D^T = \frac{1}{\sqrt{2}} \begin{pmatrix} -g'u_1 & gu_1 & 0 & Y_{\Sigma_1}\tilde{u} & Y_{\Sigma_1}v_2 \\ -g'u_2 & gu_2 & 0 & Y_{\Sigma_2}\tilde{u} & Y_{\Sigma_2}v_2 \\ -g'u_3 & gu_3 & 0 & Y_{\Sigma_3}\tilde{u} & Y_{\Sigma_3}v_2 \end{pmatrix}. \tag{4.36}$$

Defined in this way, the 8×8 neutral fermion mass matrix can be written as

$$M_n = \begin{pmatrix} M' & m_D \\ m_D^T & 0 \end{pmatrix}, \tag{4.37}$$

where M' represents the 5×5 matrix

$$M' = \frac{1}{\sqrt{2}} \begin{pmatrix} \sqrt{2}M^1 & 0 & -g'v_1 & g'v_2 & 0 \\ 0 & \sqrt{2}M^2 & gv_1 & -gv_2 & 0 \\ -g'v_1 & gv_1 & 0 & -\sqrt{2}\mu & 0 \\ g'v_2 & -gv_2 & -\sqrt{2}\mu & 0 & \sum_i Y_{\Sigma_i}u_i \\ 0 & 0 & 0 & \sum_i Y_{\Sigma_i}u_i & \sqrt{2}M \end{pmatrix}. \tag{4.38}$$

The low energy neutrino mass would be generated once the neutralino and exotic triplet fermions get integrated out. Hence the low energy neutrino mass matrix m_ν is

$$m_\nu \sim -m_D^T M'^{-1} m_D. \tag{4.39}$$

For M' in the TeV range, $m_\nu \sim 1$ eV demands that m_D should be 10^{-3} GeV. If one takes $v_2 \sim 100$ GeV then this sets $Y_\Sigma \sim 10^{-5}$ and the scale of u to be 10^{-3} GeV. Since in our model for small value of u, the $\tilde{u}$ and u are proportional to each other, hence we naturally get $\tilde{u} \sim u \sim 10^{-3}$ GeV. We have discussed in more detail in Appendix C how the smallness of neutrino mass can restrict the vacuum expectation values u_i, $\tilde{u}$ and the Yukawas Y_{Σ_i}. One can clearly see from Eq. (4.35) that in the $u = 0$ and $\tilde{u} = 0$ limit, the gaugino-higgsino sector completely decouples from the standard model neutrino-exotic neutrino sector and the low energy neutrino mass would be governed via the usual type-III seesaw only. In the work presented in the previous chapter, we have taken a large Yukawa coupling $Y_\Sigma \sim 1$. In the present work since we do not extend the Higgs sector than the minimal supersymmetric standard model and in addition we choose a TeV scale triplet fermion mass parameter M, hence from the neutrino mass constraint the Yukawa is bounded to take such a small value $Y_\Sigma < 10^{-5}$. However, as of the two Higgs doublet type-III seesaw model presented in the previous chapter, one can further extend the Higgs sector of this model by two SU(2) doublet, so that one of the new Higgs contributes to the neutrino mass generation. In that case, one can choose a small VEV of the new Higgs doublet and take the large Yukawa.

4.5 Chargino-Charged Lepton Mass Matrix

Like the neutralino-neutrino mixing as discussed in the previous section, R-parity violation will also result in chargino-charged lepton mixing, which in our model is significantly different compared to the other existing models of spontaneous and explicit R-parity violation, because of the presence of extra heavy triplet charged fermionic states in our model. Like the enlarged neutrino sector (ν_{L_i},Σ_R^{0c}) we have also an extended charged lepton sector. With one generation of $\hat{\Sigma}_R^c$ we have two additional heavier triplet charged leptons Σ_R^{+c} and Σ_R^{-c} in our model, in addition to the standard model charged leptons. Hence we get mixing between the charginos and the standard model charged leptons as well as the heavier triplet charged leptons. The possible contributions to the different mixing terms would come from the superpotential as well as from the kinetic terms of the different superfields. Since we have written down explicitly the charginos-charged lepton-sneutrino interaction terms in Appendix, it is straightforward to see the contribution to the mass matrix coming from Eq. (B5), Eq. (B6) and Eq. (B8) once the $\tilde{\Sigma}_R^{0c}$ and $\tilde{\nu}_{L_i}$ states get vacuum expectation values. The chargino-charged lepton mass matrix in the basis $\psi_1^T = (\tilde{\lambda}^+,\tilde{\mathrm{H}}_\mathrm{u}^+,\mathrm{l}_1^\mathrm{c},\mathrm{l}_2^\mathrm{c},\mathrm{l}_3^\mathrm{c},\Sigma_\mathrm{R}^{-\mathrm{c}})^T$ and $\psi_2 = (\tilde{\lambda}^-,\tilde{\mathrm{H}}_\mathrm{d}^-,\mathrm{l}_1,\mathrm{l}_2,\mathrm{l}_3,\Sigma_\mathrm{R}^{+\mathrm{c}})^T$ is

$$L_c = -\psi_1^T M_c \psi_2 + h.c, \tag{4.40}$$

where

$$M_c = \frac{1}{\sqrt{2}} \begin{pmatrix} \sqrt{2}M^2 & \sqrt{2}gv_1 & \sqrt{2}gu_1 & \sqrt{2}gu_2 & \sqrt{2}gu_3 & g\tilde{u} \\ \sqrt{2}gv_2 & \sqrt{2}\mu & Y_{\Sigma_1}\tilde{u} & Y_{\Sigma_2}\tilde{u} & Y_{\Sigma_3}\tilde{u} & -\sum_i \sqrt{2}Y_{\Sigma i}u_i \\ 0 & -\sqrt{2}Y_{e_1}u_1 & \sqrt{2}Y_{e_1}v_1 & 0 & 0 & 0 \\ 0 & -\sqrt{2}Y_{e_2}u_2 & 0 & \sqrt{2}Y_{e_2}v_1 & 0 & 0 \\ 0 & -\sqrt{2}Y_{e_3}u_3 & 0 & 0 & \sqrt{2}Y_{e_3}v_1 & 0 \\ -g\tilde{u} & 0 & \sqrt{2}Y_{\Sigma_1}v_2 & \sqrt{2}Y_{\Sigma_2}v_2 & \sqrt{2}Y_{\Sigma_3}v_2 & \sqrt{2}M \end{pmatrix} \tag{4.41}$$

The chargino-charged lepton mass matrix would be diagonalized by bi-unitary transformation $M_c = TM_c^dS^\dagger$.

4.6 Neutrino Mass and Mixing

R-parity violation can contribute significantly to the 3×3 standard model light neutrino mass matrix. In this section we concentrate on determining the neutrino mass square differences and the appropriate mixings. With only one generation of singlet/triplet heavy Majorana neutrino it is not possible to get viable neutrino mass square differences and mixings in the R-parity conserving type-I or type-III seesaw scenario. Since R-parity is violated, we have neutrino-neutralino mixing apart from the conventional standard model neutrino-heavy neutrino mixing, which has significant effect in determining the low energy neutrino mass square differences and mixing angles of PMNS mixing matrix[2], through the gaugino and higgsino mass parameters $M^{1,2}$, μ and the R-parity violating sneutrino vacuum expectation values u_i and $\tilde{u}$. Below we write the approximate 3×3 standard model neutrino mass matrix. Since $Y_{\Sigma i}$, u_i and $\tilde{u}$ are very small, all the terms which are proportional to $Y^2_{\Sigma_i} u_i^2$ and the terms $Y^3_{\Sigma_i} u_i \tilde{u}$ are neglected and we write down only the leading order terms. The exact analytical expression of the low energy neutrino mass matrix for our model has been given in the Appendix C. The approximate light neutrino mass matrix has the following form,

$$m_\nu \sim \frac{v_2^2}{2M} A + \frac{\alpha\mu}{2} B + \frac{\alpha \tilde{u} v_1}{2\sqrt{2}} C, \tag{4.42}$$

where the matrix A, B and C respectively are,

$$A = \begin{pmatrix} Y^2_{\Sigma_1} & Y_{\Sigma_1} Y_{\Sigma_2} & Y_{\Sigma_1} Y_{\Sigma_3} \\ Y_{\Sigma_1} Y_{\Sigma_2} & Y^2_{\Sigma_2} & Y_{\Sigma_2} Y_{\Sigma_3} \\ Y_{\Sigma_1} Y_{\Sigma_3} & Y_{\Sigma_2} Y_{\Sigma_3} & Y^2_{\Sigma_3} \end{pmatrix}, \tag{4.43}$$

$$B = \begin{pmatrix} u_1^2 & u_1 u_2 & u_1 u_3 \\ u_1 u_2 & u_2^2 & u_2 u_3 \\ u_1 u_3 & u_2 u_3 & u_3^2 \end{pmatrix}, \tag{4.44}$$

$$C = \begin{pmatrix} 2u_1 Y_{\Sigma_1} & u_1 Y_{\Sigma_2} + u_2 Y_{\Sigma_1} & u_1 Y_{\Sigma_3} + u_3 Y_{\Sigma_1} \\ u_1 Y_{\Sigma_2} + u_2 Y_{\Sigma_1} & 2u_2 Y_{\Sigma_2} & u_2 Y_{\Sigma_3} + u_3 Y_{\Sigma_2} \\ u_1 Y_{\Sigma_3} + u_3 Y_{\Sigma_1} & u_2 Y_{\Sigma_3} + u_3 Y_{\Sigma_2} & 2u_3 Y_{\Sigma_3} \end{pmatrix}. \tag{4.45}$$

The parameter α depends on gaugino masses $M^{1,2}$, the higgsino mass parameter μ and two vacuum expectation values $v_{1,2}$ as follows

$$\alpha = \frac{(M_1 g^2 + M_2 g'^2)}{M_1 M_2 \mu - (M_1 g^2 + M_2 g'^2) v_1 v_2}. \tag{4.46}$$

The 1st term in Eq. (4.42) which depends only on the Yukawa couplings Y_{Σ_i}, triplet fermion mass parameter M and the vacuum expectation value v_2, is the conventional R-parity conserving type-I or type-III seesaw term. The 2nd and 3rd terms involve the gaugino mass parameters $M^{1,2}$, the higgsino mass parameter μ and R-parity violating vacuum expectation values u_i and $\tilde{u}$. Hence the appearance of these two terms are undoubtedly the artifact of R-parity violation.

[2]The standard charged lepton mass matrix which is obtained from Eq. (4.41) turns out to be almost diagonal and therefore the PMNS mixing comes almost entirely from M_ν.

We next discuss the neutrino oscillation parameters, the three angles in the U_{PMNS} mixing matrix and two mass square differences Δm^2_{21} and Δm^2_{31}. Note that with the mass matrix m_ν given in Eq. (4.43), i.e taking only the effect of triplet Yukawa contribution into account one would get the three following mass eigenvalues for the three light standard model neutrinos,

$$m_1 = 0, \quad m_2 = 0, \quad m_3 = \frac{v_2^2}{2M}(Y^2_{\Sigma_1} + Y^2_{\Sigma_2} + Y^2_{\Sigma_3}).$$

and the eigenvectors

$$\frac{1}{\sqrt{Y^2_{\Sigma_1} + Y^2_{\Sigma_3}}}\begin{pmatrix} -Y_{\Sigma_3} \\ 0 \\ Y_{\Sigma_1} \end{pmatrix}, \quad \frac{1}{\sqrt{Y^2_{\Sigma_1} + Y^2_{\Sigma_2}}}\begin{pmatrix} -Y_{\Sigma_2} \\ Y_{\Sigma_1} \\ 0 \end{pmatrix}, \quad \frac{1}{\sqrt{Y^2_{\Sigma_1} + Y^2_{\Sigma_2}}}\begin{pmatrix} Y_{\Sigma_1} \\ Y_{\Sigma_2} \\ Y_{\Sigma_3} \end{pmatrix}$$

respectively. Clearly, two of the light neutrinos emerge as massless while the third one gets mass, which is in conflict with the low energy neutrino data. Similarly if one has only matrix B which comes as a consequence of R-parity violation then one also would obtain only one light neutrino to be massive, in general determining only the largest atmospheric mass scale [20, 21] . However the simultaneous presence of the matrix A, B and C in Eq. (4.42) make a second eigenvalue non-zero, while the third one remains zero. With the choice $\tilde{u}$ as of the same order of u, the third term in Eq. (4.42) would be suppressed compared to the first two terms. Hence the simultaneous presence of the matrix A and B are very crucial to get both the solar and atmospheric mass splitting and the allowed oscillation parameters. Eigenvalues of the full M_ν given in Eq. (4.42) are

$$m_1 = 0, \quad m_{2,3} \sim \frac{1}{2}[W \mp \sqrt{W^2 - V}], \tag{4.47}$$

where

$$W = \frac{v_2^2}{2M}\sum_i Y^2_{\Sigma_i} + \frac{\mu\alpha}{2}\sum_i u_i^2 + \frac{\tilde{u}v_1\alpha}{\sqrt{2}}\sum_i u_i Y_{\Sigma_i}, \tag{4.48}$$

and

$$\begin{aligned} V \;=\; & 4(\frac{v_2^2\mu\alpha}{4M} - \frac{\tilde{u}^2 v_1^2\alpha^2}{8})[Y^2_{\Sigma_1}(u_2^2 + u_3^2) + Y^2_{\Sigma_2}(u_3^2 + u_1^2) + Y^2_{\Sigma_3}(u_1^2 + u_2^2) \\ & -2(u_1u_2Y_{\Sigma_1}Y_{\Sigma_2} + u_1u_3Y_{\Sigma_1}Y_{\Sigma_3} + u_2u_3Y_{\Sigma_2}Y_{\Sigma_3})]. \end{aligned} \tag{4.49}$$

Similarly we have obtained approximate analytic expressions for the mixing matrix, however the expressions obtained are too complicated and hence we do not present them here. Instead we show in Tables 4.1 and Table 4.2 an example set of model parameters

$(M^{1,2}, M, \mu, Y_{\Sigma_i}, v_{1,2}, \tilde{u}, u_i)$ which give the experimentally allowed mass-square differences Δm^2_{21} and Δm^2_{31} and mixing angles $\sin^2\theta_{12}$, $\sin^2\theta_{23}$ and $\sin^2\theta_{13}$, as well as the total neutrino mass m_t. The values obtained for these neutrino parameters for the model points given in Tables 4.1 and Table 4.2 is shown in Table 4.3. We have presented these results assuming $\Delta m^2_{31} > 0$ (normal hierarchy).

M^1 (GeV)	M^2 (GeV)	M (GeV)	μ (GeV)	Y_{Σ_1}	Y_{Σ_2}	Y_{Σ_3}
300	600	353.24	88.31	5.62×10^{-7}	8.72×10^{-7}	3.84×10^{-8}

Table 4.1: Sample point in the parameter space for the case of normal hierarchy. $M^{1,2}$ is the gaugino mass parameter, μ is higgsino mass parameter, M is triplet fermion mass parameter, Y_{Σ_1}, Y_{Σ_2} and Y_{Σ_3} correspond to the superpotential coupling between the standard model Lepton superfields $\hat{L}_i$, SU(2) triplet superfield $\hat{\Sigma}^{0c}_R$ and Higgs superfield $\hat{H}_u$.

v_1 (GeV)	v_2(GeV)	$\tilde{u}$(GeV)	u_1(GeV)	u_2 (GeV)	u_3(GeV)
10.0	100.0	5.74×10^{-3}	1.69×10^{-5}	9.55×10^{-5}	1.26×10^{-4}

Table 4.2: Sample point in the parameter space for the case of normal hierarchy. $v_{1,2}$ are the vacuum expectation values of $H^0_{d,u}$ fields respectively, $\langle \nu_{L_i} \rangle = u_i$ for i=1,2,3 and $\tilde{u}$ is the vacuum expectation value of triplet sneutrino state $\tilde{\Sigma}^{0c}_R$.

Δm^2_{21} (eV^2)	Δm^2_{31} (eV^2)	$\sin^2\theta_{12}$	$\sin^2\theta_{23}$	$\sin^2\theta_{13}$	m_t (eV)
7.44×10^{-5} eV^2	2.60×10^{-3} eV^2	0.33	0.507	4.34×10^{-2}	10^{-2}

Table 4.3: Values for neutrino oscillation parameters for the input parameters specified in Table 4.1 and in Table 4.2.

At this point we would like to comment on the possibility of radiatively-induced neutrino mass generation in our model. In a generic R-parity violating MSSM, both the lepton number and baryon number violating operators are present. Apart from the tree level bilinear term $\epsilon \hat{L}\hat{H}_u$ which mixes neutrino with higgsino, the trilinear lepton number violating operators $\lambda \hat{L}\hat{L}\hat{E}^c$, $\lambda' \hat{L}\hat{Q}\hat{D}^c$ and also the bilinear operator $\hat{L}\hat{H}_u$ contribute to the radiatively-induced neutrino mass generation [4–6]. In general there could be several loops governed by the $\lambda\lambda$, $\lambda'\lambda'$, BB, ϵB couplings. However in the spontaneous R-parity violating model, working in the weak basis we would only have $\hat{L}\hat{H}_u$ operator coming from $\hat{H}_u\hat{\Sigma}^c_R\hat{L}$ term in the superpotential, unless we do a basis redefinition. Similarly in the scalar potential we would obtain $H_u\tilde{L}$ coupling coming out from $H_u\tilde{\Sigma}^c_R\tilde{L}$ term in Eq. (4.12). Hence we can have loops governed by $A_\Sigma A_\Sigma$ couplings, like the BB

loop in Fig. 3 of [4]. For the sake of completeness we have presented the diagram in Fig. 4.1. The one loop corrected neutrino mass coming out from this diagram would be $m_\nu \sim \frac{g^2\tilde{u}^2}{64\pi^2 cos^2\beta}\frac{A_{\Sigma_i}A_{\Sigma_j}}{\tilde{m}^3}$. In general for moderate values of $\cos\beta$, if one chooses the average slepton mass $\tilde{m}$ to be in the TeV order and the soft supersymmetry breaking coupling $A_\Sigma \sim 10^2$ GeV, then because $\tilde{u} \sim 10^{-3}$ GeV, the contribution coming from this diagram would be roughly suppressed by a factor of 10^{-2} compared to the tree level neutrino mass. Similar conclusion can be drawn for the ϵA_Σ [4] loop induced neutrino mass, shown in Fig. 4.2. In our model the R-parity violating λ and λ' couplings do not get generated in the weak basis. However, from the R-parity conserving superpotential given in Eq. (4.1) it would be possible to generate λ and λ' couplings via mixings and only after transforming to a mass basis or after rotating away the bilinear R-parity violating term. Hence, in general for our model we would expect the contributions coming from the $\lambda\lambda$ and $\lambda'\lambda'$ loops to be suppressed compared to the tree level neutrino masses. Apart from these different bilinear and trilinear radiatively induced neutrino mass generation, there could be another source of radiative neutrino mass, namely the non-universality in the slepton mass matrices. In the R-parity conserving limit the analysis would be same as of [22], only triplet fermions in our model are generating the Majorana sneutrino masses $\tilde{\nu}_i\tilde{\nu}_j$. However, in this work we stick to the universality of the slepton masses, hence this kind of radiative neutrino mass generation will not play any non trivial role. Due to the RG running from the high scale to the low scale the universal soft supersymmetry breaking slepton masses could possibly get some off-diagonal contribution [23], which we do not address in this present work.

4.7 Collider Signature

In this section we discuss very briefly about the possibility of testing our model in collider experiments. Because R-parity is violated in our model there will be extra channels compared to the R-parity conserving minimal supersymmetric standard model, which carry the information about R-parity violation. As R-parity gets broken, the triplet neutral heavy lepton Σ_R^{0c} and standard model neutrino ν_{Li} mix with the neutral higgsino $\tilde{H}_u^0$ and $\tilde{H}_d^0$, with bino $\tilde{\lambda}^0$ and wino $\tilde{\lambda}^3$, in addition to the usual R-parity conserving Dirac mixing between them. Hence in the mass basis with one generation of heavy triplet fermion, there will be 5 neutralinos in our model. We adopt the convention where the neutralino state $\tilde{\chi}_i^0$ are arranged according to the descending order of their mass and $\tilde{\chi}_5^0$ is the lightest neutralino. If one adopts gravity mediated supersymmetry breaking as the origin of soft supersymmetry breaking Lagrangian, then the lightest neutralino is in general the lightest supersymmetric particle (LSP). But as R-parity is broken, in any case LSP will not be stable [20,24]. For MSSM, the production mechanism of neutralinos and sneutrinos in colliders have been extensively discussed in [25,26]. Depending on the parameters, the lightest neutralino can be gaugino dominated or higgsino dominated.

In our model in addition to the standard model neutrinos we also have a heavy triplet neutral fermion Σ_R^{0c}. Hence in this kind of model where heavy triplet fermions are present, the lightest neutralino can also be Σ_R^{0c} dominated. Here we present a very qualitative discussion on the possible neutralino, sneutrino, slepton and chargino decay modes.

- (A) Neutralino two body decay: As R-parity is violated, the lightest neutralino can decay through R-parity violating decay modes. It can decay via the two body decay mode $\tilde{\chi}_5^0 \to lW$ or $\tilde{\chi}_5^0 \to \nu Z$. Other heavier neutralinos can decay to the lighter neutralino state $\tilde{\chi}_i^0 \to \tilde{\chi}_j^0 Z$, or through the decay modes $\tilde{\chi}_i^0 \to l^\pm W^\mp/\nu Z$. The gauge boson can decay leptonically or hadronically producing

$$
\begin{aligned}
\tilde{\chi}_i^0 &\to l^\pm W^\mp \to l^\pm l^\mp + \not{E}_T, \\
\tilde{\chi}_i^0 &\to l^\pm W^\mp \to l^\pm + 2j, \\
\tilde{\chi}_i^0 &\to \nu Z \to l^\pm l^\mp + \not{E}_T, \\
\tilde{\chi}_i^0 &\to \nu Z \to 2b + \not{E}_T.
\end{aligned}
$$

- (B) Sneutrino and slepton decay: Because of R-parity violation the slepton can decay to a charged lepton and a neutrino [27] via $\tilde{l} \to \nu l$. The sneutrino can also have the possible decay $\tilde{\nu} \to l^+ l^-$. In the explicit R-parity violating scenario, this interaction term between $\tilde{\nu} l^\pm l^\mp$ and $\tilde{l} l \nu$ would have significant contribution from λLLE^C. Here $l^\pm$, ν and $\tilde{l}$ all are in mass basis. In the spontaneous R-parity violating scenario these interactions are possible only after basis redefinition. The different contributions to the above mentioned interaction terms will come from the MSSM R-parity conserving term $\hat{H}_d \hat{L} \hat{E}^c$ as well as from the kinetic terms of the different superfields after one goes to the mass basis.

- (C) Three body neutralino decay modes: The other possible decay modes for the neutralino are $\tilde{\chi}_i^0 \to \nu\tilde{\nu}$, $l^\pm \tilde{l}^\mp$, νh. If the lightest neutralino $\tilde{\chi}_5^0$ is the lightest supersymmetric particle, then the slepton or sneutrino would be virtual. The sneutrino or slepton can decay through the R-parity violating decay modes. Hence neutralino can have three body final states such as $\tilde{\chi}_i^0 \to \nu\tilde{\nu} \to \nu l^\pm l^\mp$, $\tilde{\chi}_i^0 \to l^\pm \tilde{l}^\mp \to l^\pm \nu l^\mp$.

Our special interest is in the case where the lightest neutralino state is significantly triplet fermion Σ^0 dominated. Besides the Yukawa interaction, the triplet fermion $\Sigma^\pm$,Σ^0 have gauge interactions. Hence they could be produced at a significant rate in a proton proton collider such as LHC through gauge interactions. The triplet fermions $\Sigma^\pm$ and Σ^0 could be produced via $pp \to W^\pm/Z \to \Sigma^\pm\Sigma^0/\Sigma^\mp$ [3] channels apart from the Higgs mediated channels. In fact the production cross section of these triplet fermions should be more compared to the production cross section of the singlet neutrino dominated

[3]By $\Sigma^\pm$,Σ^0 we mean chargino state $\tilde{\chi}^\pm$ or neutralino state $\tilde{\chi}^0$ significantly dominated by $\Sigma^\pm$ and Σ^0 respectively.

neutralino states [7], as for the former case the triplet fermions have direct interactions with the gauge bosons. The decay channels for these triplet neutral fermions are as $\Sigma^0 \to \nu Z$, $\Sigma^0 \to l^{\pm} W^{\mp}$, $\Sigma^0 \to \nu h$ and also $\Sigma^0 \to \nu\tilde{\nu}^*, l\tilde{l}^*$ followed by R-parity violating subsequent decays of the slepton/sneutrino.

Apart from the neutralino sector in our model, the charged higgsino and charged winos mix with standard model leptons and heavy charged leptons $\Sigma^{\pm}$. Hence, just like in the neutralino sector, there will also be R-parity violating chargino decay. The chargino $\tilde{\chi_i}^{\pm}$ can decay into the following states, $\tilde{\chi_i}^{\pm} \to l^{\pm}Z$, νW, $\nu h^{\pm}$ and also to $\tilde{\chi_i}^{\pm} \to l\tilde{\nu} \to ll^{\pm}l^{\mp}$, $\tilde{\chi_i}^{\pm} \to \nu\tilde{l} \to \nu\nu l$. Just like as for the neutralinos, depending on the parameters, in this kind of model with heavy extra triplet fermions the lightest chargino could be as well $\Sigma^{\pm}$ dominated. Moreover, because of R-parity violation, there will be mixing between the the slepton and charged Higgs and sneutrino and neutral Higgs. The sneutrino state $\tilde{\Sigma}^{\pm}$ can have the decays $\tilde{\Sigma}^{\pm} \to \nu l^{\pm}$, $\tilde{\nu}W^{\pm}$, $\tilde{l}^{\pm}Z$. Similarly, $\tilde{\Sigma}^0$ can decay into $\tilde{\Sigma}^0 \to l^+l^-$. Apart from these above mentioned decay channels, some other possible decay channels are, $\tilde{\Sigma}^+ \to \bar{d}u$, $\tilde{\Sigma}^0 \to u\bar{u}$, $\Sigma^+ \to \tilde{u}\bar{d}$. For the R-parity conserving seesaw scenario, these decay modes will be totally absent, as there is no mixing between the triplet/singlet fermion and the higgsino/gauginos and mixing between sfermions and Higgs bosons.

We would also like to comment about the possibility of lepton flavor violation in our model. For the non-supersymmetric type-III seesaw, the reader can find detailed study on lepton flavor violation in [28]. Embedding the triplet fermions in a supersymmetric framework opens up many new diagrams which can contribute to lepton flavor violation, for example $\mu \to e\gamma$. In general the sneutrino, triplet sneutrino, different sleptons and the charginos or neutralinos can flow within the loop [23, 29–31]. In our model the R-parity violating effect comes very selectively. The main contribution comes via the bilinear R-parity violating terms which get only generated spontaneously. Hence as discussed before, we ignore λ and λ' dominated diagrams [30] and we expect that the lepton flavor violating contribution would be mainly governed by the soft supersymmetry breaking off-diagonal slepton mass contribution. Since we stick to the universal soft supersymmetry breaking slepton masses, only RG running might generate the off diagonal supersymmetry breaking slepton masses [23]. In the R-parity conserving limit the soft supersymmetry breaking slepton masses get a contribution $m_L^2 \propto (3m_0^2 + A_0^2)(Y_\Sigma Y_\Sigma^T) log(\frac{M_X}{M_\Sigma})$ [4]. For m_0,A_0 $\sim$TeV and $Y_\Sigma \sim 10^{-6}$, $m_L^2 \sim 10^{-6}\ log(\frac{M_X}{M_\Sigma})\mathrm{GeV}^2$. The branching ratio would be roughly $\frac{\alpha^3}{G_F^2}\frac{|m_L^2|^2}{\tilde{m}^8} tan^2\beta$. However, because of extremely small Yukawa $Y_\Sigma \sim 10^{-6} - 10^{-8}$ our model would not violate the bound coming from $\mu \to e\gamma$.

[4]For simplicity we have taken Y_Σ to be real.

4.8 Conclusion

In this work we have explored the possibility of spontaneous R-parity violation in the context of basic MSSM gauge group and have explored its impact on the neutrino mass and mixing. Since the R-parity violating terms also break lepton number, spontaneous R-parity violation could potentially generate the massless mode Majoron. We avoid the problem of the Majoron by introducing explicit breaking of lepton number in the R-parity conserved part of the superpotential. We do this by adding a SU(2) triplet $Y = 0$ matter chiral superfield $\hat{\Sigma}_R^c$ in our model. The gauge invariant bilinear term in these triplet superfields provides explicit lepton number violation in our model. The superpartners of the standard model neutrino and the triplet heavy neutrino states acquire vacuum expectation values u and $\tilde{u}$, thereby breaking R-parity spontaneously.

From the minimization condition of the scalar potential, we showed that in our model, the vacuum expectation values of the superpartner of the triplet heavy neutrino and the standard model neutrinos turn out to be proportional to each other. For the supersymmetry breaking soft masses in the TeV range, smallness of neutrino mass ($\sim eV$) constraints the standard model sneutrino vacuum expectation value $u \sim 10^{-3}$ GeV. Since for small u the sneutrino vacuum expectation values u and $\tilde{u}$ are proportional, hence in the absence of any fine tuned cancellation between the different soft parameters, one can expect that $\tilde{u}$ will be of the same order as u, i.e 10^{-3} GeV. We have analyzed the neutralino-neutrino mass matrix and have shown that the R-parity violation can have significant effect in determining the correct neutrino mass and mixing. Since neutrino experiments demand at least two massive neutrinos, we restrict ourselves to only on one generation of $\hat{\Sigma}_R^c$ superfield. While in R-parity conserving type-III susy seesaw with only one generation of triplet neutrino state Σ_R^{0c}, two of the standard model neutrinos turn out to be massless. In addition, if one invokes R-Parity violation then one among the massless states can be made massive. Alongwith the neutralino-neutrino mixing, we have chargino-charged lepton mixing in our model.

Finally we discussed the neutralino, chargino , slepton and sneutrino decay decays and the possible collider signature of this model. Because of R-parity violation the neutralino and chargino can decay through a number of R-parity violating decay channels alongwith the possible R-parity violating decays of sneutrinos and sleptons. In the context of our model, we have listed few of these channels.

Appendix

A: Soft supersymmetry breaking lagrangian of MSSM

The soft supersymmetry breaking Lagrangian of this model is given by,

$$L^{\rm soft} = L^{\rm soft}_{\rm MSSM} + L^{\rm soft}_{\Sigma}, \tag{A1}$$

where $L^{\rm soft}_{\Sigma}$ has been written in Eq. (4.12) and the MSSM soft supersymmetry breaking lagrangian has the following form,

$$\begin{aligned}
-\mathcal{L}^{\rm soft}_{\rm MSSM} &= (m^2_{\tilde{Q}})^{ij}\tilde{Q}^{\dagger}_i\tilde{Q}_j + (m^2_{\tilde{u}^c})^{ij}\tilde{u}^{c^*}_i\tilde{u}^c_j + (m^2_{\tilde{d}^c})^{ij}\tilde{d}^{c^*}_i\tilde{d}^c_j + (m^2_{\tilde{L}})^{ij}\tilde{L}^{\dagger}_i\tilde{L}_j \\
&+ (m^2_{\tilde{e}^c})^{ij}\tilde{e}^{c^*}_i\tilde{e}^c_j + m^2_{H_d}H^{\dagger}_d H_d + m^2_{H_u}H^{\dagger}_u H_u + (bH_uH_d + \text{H.c.}) \\
&+ \left[-A^{ij}_u H_u\tilde{Q}_i\tilde{u}^c_j + A^{ij}_d H_d\tilde{Q}_i\tilde{d}^c_j + A^{ij}_e H_d\tilde{L}_i\tilde{e}^c_j + \text{H.c.}\right] \\
&+ \frac{1}{2}\left(M^3\tilde{g}\tilde{g} + M^2\tilde{\lambda}^i\tilde{\lambda}^i + M^1\tilde{\lambda}^0\tilde{\lambda}^0 + \text{H.c.}\right).
\end{aligned} \tag{A2}$$

where i and j are generation indices, $m^2_{\tilde{Q}}$, $m^2_{\tilde{L}}$ and other terms in the first two lines of the above equation represent the mass-square of different squarks, slepton, sneutrino[5] and Higgs fields. In the third line the trilinear interaction terms have been written down and in the fourth line M^3, M^2 and M^1 are respectively the masses of the gluinos $\tilde{g}$, winos $\tilde{\lambda}^{1,2,3}$ and bino $\tilde{\lambda}^0$.

B: Gaugino-lepton-slepton mixing

In this section we write down explicitly all the interaction terms generated from W_Σ, as well as the gaugino-triplet leptons-triplet sleptons interaction terms originating from L^k_Σ. As has already been discussed in section 2, W_Σ is given by

$$W_\Sigma = -Y_{\Sigma_i}\hat{H}^T_u(i\sigma_2)\hat{\Sigma}^c_R\hat{L}_i + \frac{M}{2}Tr[\hat{\Sigma}^c_R\hat{\Sigma}^c_R]. \tag{B1}$$

$$\begin{aligned}
W_\Sigma &= \frac{Y_{\Sigma_i}}{\sqrt{2}}\hat{H}^0_u\hat{\Sigma}^{0c}_R\hat{\nu}_{L_i} + Y_{\Sigma_i}\hat{H}^0_u\hat{\Sigma}^{-c}_R\hat{l}^{\,-}_i + \frac{Y_{\Sigma_i}}{\sqrt{2}}\hat{H}^+_u\hat{\Sigma}^{0c}_R\hat{l}^{\,-}_i - Y_{\Sigma_i}\hat{H}^+_u\hat{\Sigma}^{+c}_R\hat{\nu}_{L_i} \\
&+ \frac{M}{2}\hat{\Sigma}^{0c}_R\hat{\Sigma}^{0c}_R + M\hat{\Sigma}^{+c}_R\hat{\Sigma}^{-c}_R.
\end{aligned} \tag{B2}$$

In Table. 4.4 we show all the trilinear interaction terms generated from $Y_{\Sigma_i}\hat{H}_u\hat{\Sigma}^c_R\hat{L}_i$.

[5] $m^2_{\tilde{\nu}}$ represents the mass square of the superpartner of the standard model neutrino and $m^2_{\tilde{\nu}}$=$m^2_{\tilde{L}}$.

$\frac{Y_{\Sigma_i}}{\sqrt{2}}\hat{H}_u^0\hat{\Sigma}_R^{0c}\hat{\nu}_{L_i}$	$Y_{\Sigma_i}\hat{H}_u^0\hat{\Sigma}_R^{-c}\hat{l_i}^-$	$\frac{Y_{\Sigma_i}}{\sqrt{2}}\hat{H}_u^+\hat{\Sigma}_R^{0c}\hat{l_i}^-$	$-Y_{\Sigma_i}\hat{H}_u^+\hat{\Sigma}_R^{+c}\hat{\nu}_{L_i}$
$-\frac{Y_{\Sigma_i}}{\sqrt{2}}\tilde{H}_u^0\Sigma_R^{0c}\tilde{\nu}_{L_i}$ $-\frac{Y_{\Sigma_i}}{\sqrt{2}}\tilde{H}_u^0\nu_{L_i}\tilde{\Sigma}_R^{0c}$ $-\frac{Y_{\Sigma_i}}{\sqrt{2}}H_u^0\Sigma_R^{0c}\nu_{L_i}$	$-Y_{\Sigma_i}\tilde{H}_u^0\Sigma_R^{-c}\tilde{l_i^-}$ $-Y_{\Sigma_i}\tilde{H}_u^0\tilde{\Sigma}_R^{-c}l_i^-$ $-Y_{\Sigma_i}H_u^0\Sigma_R^{-c}l_i^-$	$-\frac{Y_{\Sigma_i}}{\sqrt{2}}H_u^+\Sigma_R^{0c}l_i^-$ $-\frac{Y_{\Sigma_i}}{\sqrt{2}}\tilde{H}_u^+\Sigma_R^{0c}\tilde{l_i}^-$ $-\frac{Y_{\Sigma_i}}{\sqrt{2}}\tilde{H}_u^+\tilde{\Sigma}_R^{0c}l_i^-$	$Y_{\Sigma_i}\tilde{H}_u^+\Sigma_R^{+c}\nu_{L_i}$ $Y_{\Sigma_i}\tilde{H}_u^+\tilde{\Sigma}_R^{+c}\nu_{L_i}$ $Y_{\Sigma_i}\tilde{H}_u^+\Sigma_R^{+c}\tilde{\nu}_{L_i}$

Table 4.4: Trilinear interaction terms between standard model leptons/sleptons, Higgs/higgsinos and the SU(2) triplet fermions/sfermions. These interaction terms originate from the superpotential W_Σ.

The Káhler potential of the $\hat{\Sigma}_R^c$ field is given by

$$L_\Sigma^k = \int d^4\theta Tr[\hat{\Sigma_R^c}^\dagger e^{2gV}\hat{\Sigma_R^c}]. \tag{B3}$$

where V represents the SU(2) vector supermultiplets. From the above kinetic term one will get the following gaugino-triplet fermion-triplet sfermion interactions

$$-L_{\Sigma-\tilde{\Sigma}-\tilde{\lambda}^3} = \frac{g}{\sqrt{2}}((\tilde{\Sigma}_R^{-c})^*\tilde{\lambda}^3\Sigma_R^{-c} - (\tilde{\Sigma}_R^{+c})^*\tilde{\lambda}^3\Sigma_R^{+c}) + h.c, \tag{B4}$$

$$-L_{\Sigma-\tilde{\Sigma}-\tilde{\lambda}^+} = \frac{g}{\sqrt{2}}((\tilde{\Sigma}_R^{0c})^*\tilde{\lambda}^+\Sigma_R^{+c} - (\tilde{\Sigma}_R^{-c})^*\tilde{\lambda}^+\Sigma_R^{0c}) + h.c, \tag{B5}$$

$$-L_{\Sigma-\tilde{\Sigma}-\tilde{\lambda}^-} = \frac{g}{\sqrt{2}}((\tilde{\Sigma}_R^{+c})^*\tilde{\lambda}^-\Sigma_R^{0c} - (\tilde{\Sigma}_R^{0c})^*\tilde{\lambda}^-\Sigma_R^{-c}) + \text{h.c.} \tag{B6}$$

Note that the mixing terms between the gauginos and triplet fermions $\tilde{\lambda}^+\Sigma_R^{+c}$ and $\tilde{\lambda}^-\Sigma_R^{-c}$ contribute to the color singlet charged fermion mass matrix Eq. (4.41) and these mixing terms are generated from Eq. (B5) and Eq. (B6) respectively, once $\tilde{\Sigma}_R^{0c}$ gets vacuum expectation value. In addition to these interaction terms between gauginos, triplet leptons and triplet sleptons, we also explicitly write down the gaugino-standard model lepton-slepton interaction terms which will be generated from the kinetic term of the $\hat{L}_i$ superfields

$$L_L^k = \int d^4\theta \hat{L}_i^\dagger e^{2gV+2g'V'}\hat{L}_i. \tag{B7}$$

$$\begin{aligned} L_L^k &= -\frac{g}{\sqrt{2}}\tilde{\nu}_{L_i}^*\tilde{\lambda}^3\nu_{L_i} - \frac{g}{\sqrt{2}}\tilde{l}_i^{\,*}\tilde{\lambda}^3 l_i^- - g\tilde{\nu}_{L_i}^*\tilde{\lambda}^+ l_i^- - g\tilde{l}_i^{\,*}\tilde{\lambda}^-\nu_{Li} \\ &\quad + \frac{g'}{\sqrt{2}}\tilde{\nu}_{L_i}^*\tilde{\lambda}^0\nu_{L_i} + \frac{g'}{\sqrt{2}}\tilde{l}_i^*\tilde{\lambda}^0 l_i^- + \text{h.c.} \end{aligned} \tag{B8}$$

Similar interaction terms would be generated from $\hat{E}^c$ kinetic term and kinetic terms of other superfields like the Higgs $\hat{H}_{u,d}$ and other quarks. Looking at Eq. (B8) it is clear that once the sneutrino fields $\tilde{\nu}_{L_i}$ get vacuum expectation values the first and fifth term of the above equation would contribute to gaugino-neutrino mixing while the third term would contribute in the chargino-charged lepton mixing, as have already been shown in Eq. (4.35) and in Eq. (4.41).

C: The Neutrino Mass, Y_Σ and u

In this section we discuss in detail how the smallness of neutrino mass restricts the order of magnitude of the Yukawa Y_Σ and the sneutrino vacuum expectation value u. Below we write the analytical expression of the low energy neutrino mass of our model. The 3×3 neutrino mass matrix is

$$m_\nu \sim -{m_D}^T {M'}^{-1} m_D, \tag{C1}$$

where m_D and M' have already been given in Eq. (4.36) and in Eq. (4.38) respectively. With the specified m_D and M', the 3×3 standard model neutrino mass matrix m_ν has the following form,

$$\begin{aligned} -m_\nu &= 2{v_2}^2\alpha_1 A + 2M\mu^2\alpha_t B + \sqrt{2}\alpha_t\tilde{u}v_1 M\mu C + M\alpha_t v_1^2\tilde{u}^2 A \\ &\quad -\sqrt{2}\alpha_t\tilde{u}v_1^2 v_2 \sum_{i=1,2,3} u_i Y_{\Sigma_i} A - \alpha_t v_1 v_2 \mu F. \end{aligned} \tag{C2}$$

The matrix A, B and C have already been presented in Eq. (4.43), Eq. (4.44) and Eq. (4.45). The matrix F has the following form,

$$F = \begin{pmatrix} F_{11} & F_{12} & F_{13} \\ F_{12} & F_{22} & F_{23} \\ F_{13} & F_{23} & F_{33} \end{pmatrix}, \tag{C3}$$

where the elements of F are

$$F_{ij}(i \neq j) = Y_{\Sigma_i}Y_{\Sigma_j}(u_i^2 + u_j^2) + u_i u_j (Y_{\Sigma_i}^2 + Y_{\Sigma_j}^2) + u_k Y_{\Sigma_k}(u_i Y_{\Sigma_j} + u_j Y_{\Sigma_i}), \tag{C4}$$

and

$$F_{ii} = 2Y_{\Sigma_i}^2 u_i^2 + 2u_i Y_{\Sigma_i} \sum_{k \neq i} Y_{\Sigma_k} u_k. \tag{C5}$$

The indices *i, j, k* in Eq. (C4) and the index i in Eq. (C5) are *not summed* over. α_t has this following expression,

$$\alpha_t = \frac{(M_1 g^2 + M_2 g'^2)}{4MM_1M_2\mu^2 - 4M\mu(M_1g^2 + M_2g'^2)v_1v_2 - (M_1g^2 + M_2g'^2)v_1^2(\Sigma_i u_i Y_{\Sigma_i})^2}, \tag{C6}$$

while the parameter α_1 is

$$\alpha_1 = \frac{M_1 M_2 \mu^2 - (M_1 g^2 + M_2 g'^2) v_1 v_2 \mu}{4MM_1 M_2 \mu^2 - 4M\mu(M_1 g^2 + M_2 g'^2) v_1 v_2 - (M_1 g^2 + M_2 g'^2) v_1^2 (\Sigma_i u_i Y_{\Sigma_i})^2}. \tag{C7}$$

Below we show how the choice of TeV scale gaugino masses and the triplet fermion mass M dictate the sneutrino vacuum expectation value u to be smaller than 10^{-3} GeV and the Yukawa $Y_\Sigma \leq 10^{-5}$ to have consistent small ($\leq eV$) standard model neutrino mass. We consider the following three cases and show that only Case (A) is viable.

Case (A): If one assumes $MM_1M_2\mu^2$ and $M\mu(M_1g^2 + M_2g'^2)v_1v_2 \gg (M_1g^2 + M_2g'^2)u_i^2 Y_{\Sigma_i}^2 v_1^2$, the first and second term dominate over the third one[6], in the denominator of Eq. (C6) and Eq. (C7). Then α_t and α_1 simplify to

$$\alpha_t \sim \frac{(M_1 g^2 + M_2 g'^2)}{4MM_1M_2\mu^2} + ..., \tag{C8}$$

and

$$\alpha_1 \sim \frac{1}{4M} + ... \tag{C9}$$

The neutrino mass matrix Eq. (C2) will have the following form,

$$\begin{aligned} m_\nu \sim\; & \frac{v_2^2 Y_\Sigma^2}{2M} + \frac{u^2(M_1g^2 + M_2g'^2)}{2M_1M_2} + \sqrt{2}\tilde{u}v_1uY_\Sigma \frac{(M_1g^2 + M_2g'^2)}{4M_1M_2\mu} + \frac{v_1^2\tilde{u}^2Y_\Sigma^2(M_1g^2 + M_2g'^2)}{4M_1M_2\mu^2} \\ & -\sqrt{2}\tilde{u}v_1^2v_2uY_\Sigma^3 \frac{(M_1g^2 + M_2g'^2)}{4MM_1M_2\mu^2} - v_1v_2\mu u^2 Y_\Sigma^2 \frac{(M_1g^2 + M_2g'^2)}{4MM_1M_2\mu^2}. \end{aligned} \tag{C10}$$

The order of Y_Σ and u would be determined from the first two terms of the above equation respectively. The fourth, fifth and sixth terms of Eq. (C10) cannot determine the order of Y_Σ and u. To show this with an example let us consider the contribution coming from the fourth term $\frac{(M_1g^2+M_2g'^2)v_1^2\tilde{u}^2Y_\Sigma^2}{M_1M_2\mu^2}$. Contribution of the order of 1 eV from this term demands $Y_\Sigma^2\tilde{u}^2 \sim 10^{-4}\mathrm{GeV}^2$ for $M^{1,2}$ in the TeV range, $\mu \sim 10^2$ GeV and v_1 in the GeV range[7]. But if one assumes that $Y_\Sigma \sim 1$ and $\tilde{u}^2 \sim 10^{-4}GeV^2$ then we get the contribution from the first term of Eq. (C10) $\frac{v_2^2Y_\Sigma^2}{M} \gg 1\mathrm{eV}$, for $M \sim$ TeV and $v_2 \sim 100$ GeV. The choice $Y_\Sigma^2 \sim 10^{-4}$ and $\tilde{u} \sim 1$ GeV also leads to $\frac{v_2^2Y_\Sigma^2}{M} \gg 1\mathrm{eV}$ for $v_2 \sim 10^2$ GeV. The other option is to have $Y_\Sigma^2 \sim 10^{-12}$ and $\tilde{u}^2 \sim 10^8\mathrm{GeV}^2$ so that $Y_\Sigma^2\tilde{u}^2 \sim 10^{-4}\mathrm{GeV}^2$. But to satisfy this choice one needs 10^7 order of magnitude hierarchy between the two vacuum expectation values $\tilde{u}$ and u [8]. This in turn demands acute hierarchy between the different soft supersymmetry

[6] Most likely between the first and second terms, the first term would have larger value for the choice of TeV scale gaugino mass.

[7] As an example $v_1 \sim 10$ GeV.

[8] As the scale of u is fixed from the second term of Eq. (C10) and $u < 10^{-3}$ GeV.

breaking mass terms in Eq. (4.33). Similarly, Y_Σ and u could also not be fixed from fifth and sixth terms of Eq. (C10). Hence, we fix Y_Σ and u from the first two terms only. The third term is larger than the fourth, fifth and sixth terms, but will still be subdominant compared to the first two terms [9] . The contribution from the first three terms to the low energy neutrino mass matrix is

$$m_\nu \sim \frac{v_2^2 Y_\Sigma^2}{2M} + \frac{u^2(M_1 g^2 + M_2 g'^2)}{2M_1 M_2} + \sqrt{2}\tilde{u} v_1 u Y_\Sigma \frac{(M_1 g^2 + M_2 g'^2)}{4 M_1 M_2 \mu}. \tag{C11}$$

It is straightforward to see from the first term of this approximate expression, that $m_\nu \leq 1eV$ demands $Y_\Sigma^2 \leq 10^{-10}$ for M in the TeV range and $v_2 \sim 100$ GeV. On the other hand for $M_{1,2}$ also in the TeV range, the bound on sneutrino vacuum expectation value u comes from the second term as $u^2 \leq 10^{-6}\ GeV^2$. For the choice of $\tilde{u} \sim u$, which is a natural consequence of the scalar potential minimization conditions, one can check that the third term in Eq. (C11) would be much smaller compared to the second term because of the presence of an additional suppression factor Y_Σ. Hence, neutrino masses demand that $Y_\Sigma \leq 10^{-5}$ and u and $\tilde{u} \leq 10^{-3}$ GeV. One can explicitly check that for this above mentioned Y_Σ, u and $\tilde{u}$ the contributions coming from 4th, 5th and 6th terms of Eq. (C10) are smaller compared to the 1st three terms.

Case (B): If one assumes $M M_1 M_2 \mu^2 \lll (M_1 g^2 + M_2 g'^2) u_i^2 Y_{\Sigma_i}^2 v_1^2$, which is possible to achieve only for large value of the vacuum expectation value u and Yukawa Y_Σ [10], so that in the denominator of Eq. (C7) the third term dominates over the first two. Then the last term in Eq. (C2) contributes as $\sim \frac{v_1 v_2 \mu Y_\Sigma^2 u^2}{v_1^2 u^2 Y_\Sigma^2} \sim \frac{\mu v_2}{v_1} \gg 1$eV for μ, v_2 and v_1 in the hundred GeV and GeV range. Therefore, this limit is not a viable option.

Case(C): We consider the last possibility $M M_1 M_2 \mu^2 \sim (M_1 g^2 + M_2 g'^2) u_i^2 Y_{\Sigma_i}^2 v_1^2$, which also demands large Yukawas and large vacuum expectation value u. If one considers $M^{1,2}$ and M in the TeV range and μ, v_2 in the hundred GeV range, then demanding that the first term in Eq. (C2) should be smaller than eV results in the bound $Y_\Sigma^2 \leq 10^{-10}$. Hence, in order to satisfy $M M_1 M_2 \mu^2 \sim (M_1 g^2 + M_2 g'^2) u_i^2 Y_{\Sigma_i}^2 v_1^2$, one needs $u \geq 10^9$ GeV for v_1 in the GeV range. For such large values of u, the second term in Eq. (C2) will give a very large contribution to the neutrino mass. This case is therefore also ruled out by the neutrino data.

Hence Case (B) and Case (C) which demand large u and Y_Σ are clearly inconsistent with the neutrino mass scale, and the only allowed possibility is Case (A). This case requires $u \leq 10^{-3}$ GeV and $Y_\Sigma \leq 10^{-5}$, for the gaugino and triplet fermion masses $M^{1,2}$ and M in the TeV range. As for small u, $\tilde{u}$ and u are proportional to each other, one obtains $\tilde{u} \sim 10^{-3}$ GeV as well.

[9] As the third term $\propto \tilde{u} u Y_\Sigma$ and from the 1st two terms Y_Σ and u will turn out to be small.

[10] To satisfy this condition, the combination of Y_Σ and u has to be such that $u_i^2 Y_{\Sigma_i}^2 \gg 10^8$GeV^2 for $M^{1,2}, M \sim TeV$, μ in hundred GeV and v_1 in GeV range.

Bibliography

[1] S. Roy and B. Mukhopadhyaya, Phys. Rev. D **55**, 7020 (1997) [arXiv:hep-ph/9612447].

[2] A. S. Joshipura and M. Nowakowski, Phys. Rev. D **51**, 2421 (1995) [arXiv:hep-ph/9408224]; C. Liu, Mod. Phys. Lett. A **12**, 329 (1997) [arXiv:hep-ph/9609410]; A. Datta, B. Mukhopadhyaya and S. Roy, Phys. Rev. D **61**, 055006 (2000) [arXiv:hep-ph/9905549]; A. S. Joshipura, R. D. Vaidya and S. K. Vempati, Nucl. Phys. B **639**, 290 (2002) [arXiv:hep-ph/0203182].

[3] A. S. Joshipura and S. K. Vempati, Phys. Rev. D **60**, 095009 (1999) [arXiv:hep-ph/9808232]; D. E. Kaplan and A. E. Nelson, JHEP **0001**, 033 (2000) [arXiv:hep-ph/9901254].

[4] Y. Grossman and S. Rakshit, Phys. Rev. D **69**, 093002 (2004) [arXiv:hep-ph/0311310]; S. Rakshit, Mod. Phys. Lett. A **19**, 2239 (2004) [arXiv:hep-ph/0406168].

[5] M. Drees, S. Pakvasa, X. Tata and T. ter Veldhuis, Phys. Rev. D **57**, 5335 (1998) [arXiv:hep-ph/9712392]; E. J. Chun, S. K. Kang, C. W. Kim and U. W. Lee, Nucl. Phys. B **544**, 89 (1999) [arXiv:hep-ph/9807327]; S. Rakshit, G. Bhattacharyya and A. Raychaudhuri, Phys. Rev. D **59**, 091701 (1999) [arXiv:hep-ph/9811500]; R. Adhikari and G. Omanovic, Phys. Rev. D **59**, 073003 (1999); M. Hirsch, M. A. Diaz, W. Porod, J. C. Romao and J. W. F. Valle, Phys. Rev. D **62**, 113008 (2000) [Erratum-ibid. D **65**, 119901 (2002)] [arXiv:hep-ph/0004115]; A. S. Joshipura, R. D. Vaidya and S. K. Vempati, Phys. Rev. D **65**, 053018 (2002) [arXiv:hep-ph/0107204]; S. Davidson and M. Losada, JHEP **0005**, 021 (2000) [arXiv:hep-ph/0005080]; A. Dedes, S. Rimmer and J. Rosiek, JHEP **0608**, 005 (2006) [arXiv:hep-ph/0603225].

[6] F. Borzumati and J. S. Lee, Phys. Rev. D **66**, 115012 (2002) [arXiv:hep-ph/0207184]; P. Dey, A. Kundu, B. Mukhopadhyaya and S. Nandi, JHEP **0812**, 100 (2008) [arXiv:0808.1523 [hep-ph]].

[7] D. E. Lopez-Fogliani and C. Munoz, Phys. Rev. Lett. **97**, 041801 (2006) [arXiv:hep-ph/0508297]; P. Ghosh and S. Roy, JHEP **0904**, 069 (2009) [arXiv:0812.0084 [hep-

ph]]; A. Bartl, M. Hirsch, A. Vicente, S. Liebler and W. Porod, JHEP **0905**, 120 (2009) [arXiv:0903.3596 [hep-ph]].

[8] A. Abada and G. Moreau, JHEP **0608**, 044 (2006) [arXiv:hep-ph/0604216]; B. Mukhopadhyaya and R. Srikanth, Phys. Rev. D **74**, 075001 (2006) [arXiv:hep-ph/0605109].

[9] A. Santamaria and J. W. F. Valle, Phys. Lett. B **195**, 423 (1987); A. Santamaria and J. W. F. Valle, Phys. Rev. Lett. **60**, 397 (1988); A. Santamaria and J. W. F. Valle, Phys. Rev. D **39**, 1780 (1989).

[10] A. Masiero and J. W. F. Valle, Phys. Lett. B **251**, 273 (1990).

[11] I. Hinchliffe and T. Kaeding, Phys. Rev. D **47**, 279 (1993); A. Y. Smirnov and F. Vissani, Phys. Lett. B **380**, 317 (1996) [arXiv:hep-ph/9601387]; H. K. Dreiner, arXiv:hep-ph/9707435; J. H. Jang, Y. G. Kim and J. S. Lee, Phys. Rev. D **58**, 035006 (1998) [arXiv:hep-ph/9711504]. G. Bhattacharyya and A. Raychaudhuri, Phys. Rev. D **57**, 3837 (1998) [arXiv:hep-ph/9712245]; P. Nath and P. Fileviez Perez, Phys. Rept. **441**, 191 (2007) [arXiv:hep-ph/0601023]; M. Artuso *et al.*, Eur. Phys. J. C **57**, 309 (2008) [arXiv:0801.1833 [hep-ph]].

[12] G. Bhattacharyya and P. B. Pal, Phys. Rev. D **59**, 097701 (1999) [arXiv:hep-ph/9809493].

[13] P. Fayet, Phys. Lett. B **69**, 489 (1977); C. S. Aulakh and R. N. Mohapatra, Phys. Lett. B **119**, 136 (1982); J. R. Ellis, G. Gelmini, C. Jarlskog, G. G. Ross and J. W. F. Valle, Phys. Lett. B **150**, 142 (1985); G. G. Ross and J. W. F. Valle, Phys. Lett. B **151**, 375 (1985).

[14] P. Nogueira, J. C. Romao and J. W. F. Valle, Phys. Lett. B **251**, 142 (1990); J. C. Romao, N. Rius and J. W. F. Valle, Nucl. Phys. B **363**, 369 (1991); J. C. Romao and J. W. F. Valle, Phys. Lett. B **272**, 436 (1991); J. C. Romao and J. W. F. Valle, Nucl. Phys. B **381**, 87 (1992); J. C. Romao, F. de Campos and J. W. F. Valle, Phys. Lett. B **292**, 329 (1992) [arXiv:hep-ph/9207269]; J. C. Romao, C. A. Santos and J. W. F. Valle, Phys. Lett. B **288**, 311 (1992); M. Shiraishi, I. Umemura and K. Yamamoto, Phys. Lett. B **313**, 89 (1993); G. F. Giudice, A. Masiero, M. Pietroni and A. Riotto, Nucl. Phys. B **396**, 243 (1993) [arXiv:hep-ph/9209296]; I. Umemura and K. Yamamoto, Nucl. Phys. B **423**, 405 (1994); J. C. Romao, J. Rosiek and J. W. F. Valle, Phys. Lett. B **351**, 497 (1995) [arXiv:hep-ph/9502211]; J. C. Romao, F. de Campos, M. A. Garcia-Jareno, M. B. Magro and J. W. F. Valle, Nucl. Phys. B **482**, 3 (1996) [arXiv:hep-ph/9604244]. A. Bartl, W. Porod, F. de Campos, M. A. Garcia-Jareno, M. B. Magro, J. W. F. Valle and W. Majerotto, Nucl. Phys. B **502**, 19 (1997) [arXiv:hep-ph/9612436];

[15] M. C. Gonzalez-Garcia and J. W. F. Valle, Nucl. Phys. B **355**, 330 (1991).

[16] J. W. F. Valle, Phys. Lett. B **196**, 157 (1987).

[17] P. Fileviez Perez and S. Spinner, Phys. Lett. B **673**, 251 (2009) [arXiv:0811.3424 [hep-ph]]; V. Barger, P. Fileviez Perez and S. Spinner, Phys. Rev. Lett. **102**, 181802 (2009) [arXiv:0812.3661 [hep-ph]]; P. Fileviez Perez and S. Spinner, Phys. Rev. D **80**, 015004 (2009) [arXiv:0904.2213 [hep-ph]]; L. L. Everett, P. Fileviez Perez and S. Spinner, Phys. Rev. D **80**, 055007 (2009) [arXiv:0906.4095 [hep-ph]]; P. Fileviez Perez and S. Spinner, arXiv:0909.1841 [hep-ph].

[18] Y. Chikashige, R. N. Mohapatra and R. D. Peccei, Phys. Rev. Lett. **45**, 1926 (1980); Y. Chikashige, R. N. Mohapatra and R. D. Peccei, Phys. Lett. B **98**, 265 (1981); G. B. Gelmini and M. Roncadelli, Phys. Lett. B **99**, 411 (1981).

[19] R. Barbieri, D. E. Brahm, L. J. Hall and S. D. H. Hsu, Phys. Lett. B **238**, 86 (1990); F. Takayama and M. Yamaguchi, Phys. Lett. B **476**, 116 (2000) [arXiv:hep-ph/9910320]; S. Y. Choi, D. J. . Miller and P. M. Zerwas, Nucl. Phys. B **711**, 83 (2005) [arXiv:hep-ph/0407209]; S. Y. Choi, H. E. Haber, J. Kalinowski and P. M. Zerwas, Nucl. Phys. B **778**, 85 (2007) [arXiv:hep-ph/0612218]; M. Hirsch, A. Vicente and W. Porod, Phys. Rev. D **77**, 075005 (2008) [arXiv:0802.2896 [hep-ph]].

[20] B. Mukhopadhyaya, S. Roy and F. Vissani, Phys. Lett. B **443**, 191 (1998) [arXiv:hep-ph/9808265].

[21] E. J. Chun, D. W. Jung and J. D. Park, Phys. Lett. B **557**, 233 (2003) [arXiv:hep-ph/0211310].

[22] S. Davidson and S. F. King, Phys. Lett. B **445**, 191 (1998) [arXiv:hep-ph/9808296].

[23] J. A. Casas and A. Ibarra, Nucl. Phys. B **618**, 171 (2001) [arXiv:hep-ph/0103065].

[24] E. A. Baltz and P. Gondolo, Phys. Rev. D **57**, 2969 (1998) [arXiv:hep-ph/9709445]; M. Chemtob, Prog. Part. Nucl. Phys. **54**, 71 (2005) [arXiv:hep-ph/0406029]; J. P. Hall and S. F. King, JHEP **0908**, 088 (2009) [arXiv:0905.2696 [hep-ph]].

[25] For a review see *e.g.*, R. Barbier *et al.*, Phys. Rept. **420**, 1 (2005) [arXiv:hep-ph/0406039]; M. Chemtob, Prog. Part. Nucl. Phys. **54**, 71 (2005) [arXiv:hep-ph/0406029]; S. P. Martin, Phys. Rev. D **46**, 2769 (1992) [arXiv:hep-ph/9207218].

[26] H. Baer, C. h. Chen, F. Paige and X. Tata, Phys. Rev. D **50**, 4508 (1994) [arXiv:hep-ph/9404212]; A. Bartl, W. Porod, D. Restrepo, J. Romao and J. W. F. Valle, Nucl. Phys. B **600**, 39 (2001) [arXiv:hep-ph/0007157].

[27] A. Bartl, M. Hirsch, T. Kernreiter, W. Porod and J. W. F. Valle, JHEP **0311**, 005 (2003) [arXiv:hep-ph/0306071].

[28] A. Abada, C. Biggio, F. Bonnet, M. B. Gavela and T. Hambye, Phys. Rev. D **78**, 033007 (2008) [arXiv:0803.0481 [hep-ph]].

[29] F. Borzumati and A. Masiero, Phys. Rev. Lett. **57**, 961 (1986); A. Masiero, S. K. Vempati and O. Vives, Nucl. Phys. B **649**, 189 (2003) [arXiv:hep-ph/0209303].

[30] B. de Carlos and P. L. White, Phys. Rev. D **54**, 3427 (1996) [arXiv:hep-ph/9602381].

[31] B. C. Allanach, A. Dedes and H. K. Dreiner, Phys. Rev. D **60**, 056002 (1999) [arXiv:hep-ph/9902251]; D. F. Carvalho, M. E. Gomez and J. C. Romao, Phys. Rev. D **65**, 093013 (2002) [arXiv:hep-ph/0202054]; B. C. Allanach, A. Dedes and H. K. Dreiner, Phys. Rev. D **69**, 115002 (2004) [Erratum-ibid. D **72**, 079902 (2005)] [arXiv:hep-ph/0309196]; S. Rimmer, arXiv:hep-ph/0610406.

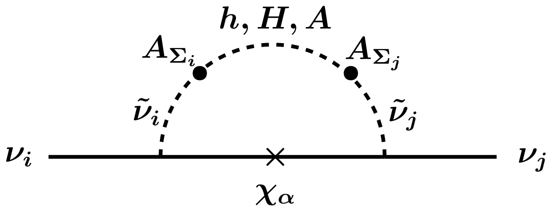

Figure 4.1: The $A_\Sigma A_\Sigma$ loop-generated neutrino mass. The cross on the internal solid line represents the majorana mass for the neutralino and the blob on the dashed line represents the mixing between sneutrino and the neutral Higgs.

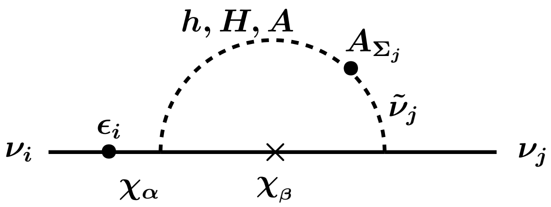

Figure 4.2: Neutrino Majorana mass generated by ϵA_Σ loop.

Chapter 5

A_4 Flavor Symmetry and Neutrino Phenomenology

5.1 Introduction

We have discussed in chapter 2 about neutrino oscillation and mass generation mechanism of the standard model neutrino. Other than small neutrino masses, the PMNS mixing shows a very drastic difference as compared to the Cabibo mixing angles in the quark sector. Recent analysis of neutrino oscillation data [1–6] suggest that the solar mixing angle is $\theta_{12} \sim 34.4^0$, while the atmospheric mixing angle is $\theta_{23} \sim 42.9^0$. We have given the present 1σ and 3σ range of the oscillation parameters in chapter 2. At present there is an upper bound on the CHOOZ mixing angle θ_{13} [1,7] as $\theta_{13} \leq 13.3^0$. The neutrino oscillation data suggest that unlike in the quark sector, in the leptonic sector two of the oscillation angles are large while the third one is small. The aesthetic belief of unification suggests that the standard model should be embedded in a higher ranked gauge group, for example SU(5) or SO(10). Although the quarks and leptons in a higher ranked gauge group belong to same representation, however the mixing in the leptonic sector is drastically different than the mixings in the quark sector. One very interesting scenario is when the mixing is tribimaximal one, which agrees very well with the experimentally allowed oscillation parameter ranges. The initial concept of tribimaximal mixing in the leptonic sector has been proposed by Harrison, Perkins, and Scott [8],

$$U_{TBM} = \begin{pmatrix} \sqrt{\frac{2}{3}} & \sqrt{\frac{1}{3}} & 0 \\ -\sqrt{\frac{1}{6}} & \sqrt{\frac{1}{3}} & -\sqrt{\frac{1}{2}} \\ -\sqrt{\frac{1}{6}} & \sqrt{\frac{1}{3}} & \sqrt{\frac{1}{2}} \end{pmatrix}. \tag{5.1}$$

The different mixing angles for a tribimaximal mixing will give $\sin^2\theta_{12} = 0.33$, $\sin^2\theta_{23} = 0.5$ and $\sin^2\theta_{13} = 0$. For the TBM mixing to exist, the neutrino mass matrix should be of the form

$$m_\nu = \begin{pmatrix} A & B & B \\ B & \frac{1}{2}(A+B+D) & \frac{1}{2}(A+B-D) \\ B & \frac{1}{2}(A+B-D) & \frac{1}{2}(A+B+D) \end{pmatrix} , \tag{5.2}$$

where $A = \frac{1}{3}(2\,m_1 + m_2)$, $B = \frac{1}{3}(m_2 - m_1)$ and $D = m_3$, where m_1, m_2 and m_3 are the neutrino masses. The current neutrino data already give very good measurement of mass squared differences, while the best limit on the absolute neutrino mass scale comes from cosmological data, as given in chapter 2.

Maximal θ_{23} and zero θ_{13} of the TBM can be easily obtained if m_ν possesses $\mu - \tau$ exchange symmetry [9] or the $L_\mu - L_\tau$ symmetry [10]. However, the solar mixing angle $\sin^2\theta_{12}$ is not so easily predicted to be exactly 1/3, as required for exact TBM mixing. Various symmetry groups explaining the flavor structure of the leptons have been invoked in the literature in order to accommodate the neutrino mass and mixing along with charged leptons. In particular, the study of the non-Abelian discrete symmetry group A_4 has received considerable interest in the recent past [11–18]. This group has been shown to successfully reproduce the TBM form of the neutrino mixing matrix, in the basis where the charged lepton mass matrix is diagonal [14]. However, the authors of [14] work in a very special framework where only one of the three possible one dimensional Higgs representations under A_4 is considered and for the A_4 triplet Higgs which contributes to the neutrino mass matrix, a particular vacuum alignment is taken. In this framework, the mixing matrix emerges as independent of the Yukawa couplings, the VEVs and the scale of A_4 breaking. Only the mass eigenstates depend on them.

In the present work, we have consider the most general scenario with all possible one dimensional Higgs representations that can be accommodated within this A_4 model. The Higgs fields which are charged under the symmetry group A_4, are standard model gauge singlets and they are knows as flavons. In our model we have two flavon fields $\phi_{S,T}$ which transform as three dimensional irreducible representation of the group A_4. In addition, we also have three other flavons ξ, ξ', ξ'' which transform as 1, $1'$ and $1''$ respectively. The Lagrangian describing the Yukawa interaction between the different standard model leptons, Higgs and the flavons follows the effective field theoretical description. The different flavon fields take the vacuum expectation values, thereby resulting in a spontaneous breaking of the symmetry group A_4. We explore the conditions on VEVs and Yukawa couplings needed for obtaining exact TBM mixing in this present set-up. We have shown that in the model considered in [14], one gets TBM mixing simply through the alignment of the A_4 triplet Higgs VEV, however the experimentally allowed mass squared differences can be obtained if one has the vacuum expectation value of an additional singlet Higgs. To get the correct Δm^2_{21} and Δm^2_{31}, the product of the VEV and Yukawa of this singlet is determined completely by the VEV and Yukawa of the triplet.

We have consider the presence of additional one dimensional Higgs representations under A_4, construct the neutrino mass matrices and study their phenomenology. In

Lepton	$\mathrm{SU(2)_L}$	A_4	
l	2	3	
$\overline{e}_R$	1	1	
$\overline{\mu}_R$	1	$1''$	
$\overline{\tau}_R$	1	$1'$	
Scalar			VEV
H_u	2	1	$< H_u^0 >= v_u$
H_d	2	1	$< H_d^0 >=v_d$
ϕ_S	1	3	(v_S, v_S, v_S)
ϕ_T	1	3	$(v_T, 0, 0)$
ξ	1	1	u
ξ'	1	$1'$	u'
ξ''	1	$1''$	u''

Table 5.1: List of fermion and scalar fields used in this model. Two lower rows list additional one dimensional Higgs fields considered in the present work. In section 4, we also allow for a different VEV alignment for ϕ_S.

particular, we check which ones would produce TBM mixing and under what conditions. In this A_4 scenario, we have also studied the deviation from TBM and the corresponding effect on the neutrino masses. If just only one Higgs transforming as one dimensional Higgs representation under A_4 is allowed, the model of [14] is the only viable model. We further show that in the simplest version of this model, one necessarily gets the normal mass hierarchy. Inverted hierarchy can be possible if we have at least two or all three Higgs scalars with nonzero VEVs.

We proceed as follows. In section 5.2 we give a brief overview of the A_4 model considered. In section 5.3 we begin with detailed phenomenological analysis of the case where there is just one singlet Higgs under A_4. We next increase the number of contributing one dimensional Higgs representations, give analytical and numerical results. In section 5.4 we study the impact of the misalignment of the VEVs of the triplet Higgs. We end in section 5.5 with our conclusions.

5.2 Overview of the Model

The detail group theory of the discrete symmetry group A_4 has been discussed in chapter 2. The particle contents of our model has been shown in Table 5.1. There are five $\mathrm{SU(3)_C} \times \mathrm{SU(2)_L} \times \mathrm{U_Y(1)}$ singlet Higgs, three (ξ, ξ' and ξ'') of which transform as the different one dimensional representations under A_4 and two (ϕ_T and ϕ_S) of which transform as triplets under the symmetry group A_4. The standard model lepton doublets are assigned to the triplet representation of A_4,

$$l = (L_e, L_\mu, L_\tau)^T,$$

where L_α denotes the standard model lepton doublets. The right handed charged leptons e_R, μ_R and τ_R are assumed to belong to the 1, $1'$ and $1''$ representation respectively. The standard Higgs doublets H_u and H_d remain invariant under A_4. The form of the A_4 invariant Yukawa part of the Lagrangian is

$$\begin{aligned}\mathcal{L}_Y &= y_e \overline{e}_R(\phi_T l) + y_\mu \overline{\mu}_R(\phi_T l)' + y_\tau \overline{\tau}_R(\phi_T l)'' + x_a \xi(ll) + x_a' \xi'(ll)'' + x_a'' \xi''(ll)' \\ &\quad + x_b(\phi_S ll) + h.c. + ...\end{aligned} \tag{5.3}$$

where, following [14] we have used the compact notation, $y_e \overline{e}_R(\phi_T l) \equiv y_e \overline{e}_R(\phi_T l) H_d/\Lambda$, $x_a \xi(ll) \equiv x_a \xi(l H_u l H_u)/\Lambda^2$ and so on, and Λ is the cut-off scale of the theory. Here we adopt an effective field theory approach. We assume that ϕ_S does not couple to charged leptons and ϕ_T does not contribute to the Majorana mass matrix. These two additional features can be obtained by introducing extra abelian symmetries for example Z_3 [14]. After the spontaneous breaking of A_4 followed by $\mathrm{SU(2)_L \times U(1)_Y}$, we get the mass terms for the charged leptons and neutrinos. Assuming the vacuum alignment

$$\langle \phi_T \rangle = (v_T, 0, 0) \ , \tag{5.4}$$

the charged lepton mass matrix is given as

$$m_{cl} = \frac{v_d v_T}{\Lambda} \begin{pmatrix} y_e & 0 & 0 \\ 0 & y_\mu & 0 \\ 0 & 0 & y_\tau \end{pmatrix} \quad , \tag{5.5}$$

Note that we could also obtain a diagonal charged lepton mass matrix even if we assume that $\overline{e}_R$, $\overline{\mu}_R$ and $\overline{\tau}_R$ transform as $1''$, $1'$ and 1, and $\langle \phi_T \rangle = (0, v_T, 0)$ with appropriate change in the Yukawa Lagrangian. Similarly, $\overline{e}_R$, $\overline{\mu}_R$ and $\overline{\tau}_R$ transforming $1'$, 1 and $1''$, and $\langle \phi_T \rangle = (0, 0, v_T)$ could give us the same m_{cl}.

In the most general case, where all three one dimensional A_4 Higgs as well as ϕ_S are present and we do not assume any particular vacuum alignment, the neutrino mass matrix looks like

$$m_\nu = m_0 \begin{pmatrix} a + 2b_1/3 & c - b_3/3 & d - b_2/3 \\ c - b_3/3 & d + 2b_2/3 & a - b_1/3 \\ d - b_2/3 & a - b_1/3 & c + 2b_3/3 \end{pmatrix} \ , \tag{5.6}$$

where $m_0 = \frac{v_u^2}{\Lambda}$ $b_i = 2x_b \frac{v_{S_i}}{\Lambda}$, $a = 2x_a \frac{u}{\Lambda}$, $c = 2x_a'' \frac{u''}{\Lambda}$ and $d = 2x_a' \frac{u'}{\Lambda}$ and we have written the VEVs as

$$\langle \phi_S \rangle = (v_{S_1}, v_{S_2}, v_{S_3}), \quad \langle \xi \rangle = u, \quad \langle \xi' \rangle = u', \quad \langle \xi'' \rangle = u'', \quad \langle H_{u,d} \rangle = v_{u,d} \ . \tag{5.7}$$

For simplicity, in this work we have considered all the Yukawa couplings as well as the parameters a, b, c and d as real.

5.3 Number of One Dimensional Higgs Representations and their VEVs

In this section we work under the assumption that the triplet Higgs ϕ_S has VEVs along the direction

$$\langle \phi_S \rangle \quad = \quad (v_S, v_S, v_S) \ . \tag{5.8}$$

This produces the neutrino mass matrix

$$m_\nu = m_0 \begin{pmatrix} a + 2b/3 & c - b/3 & d - b/3 \\ c - b/3 & d + 2b/3 & a - b/3 \\ d - b/3 & a - b/3 & c + 2b/3 \end{pmatrix} \ , \tag{5.9}$$

where $b = 2x_b \frac{v_S}{\Lambda}$. In the following we discuss the phenomenology of the different forms of m_ν possible as we change the number of one dimensional Higgs or put their VEVs to zero. We assume that m_ν is real.

5.3.1 No One Dimensional A_4 Higgs

If there were no Higgs which transforms as one dimensional irreducible representation under A_4, or if the VEV of all three of them $(\xi, \xi', \ \xi'')$ were zero, one would get the neutrino mass matrix

$$m_\nu = m_0 \begin{pmatrix} 2b/3 & -b/3 & -b/3 \\ -b/3 & 2b/3 & -b/3 \\ -b/3 & -b/3 & 2b/3 \end{pmatrix} \ . \tag{5.10}$$

On diagonalizing this one obtains the eigenvalues

$$m_1 = m_0 \, b, \quad m_2 = 0, \quad m_3 = m_0 \, b \tag{5.11}$$

and the mixing matrix

$$U = \begin{pmatrix} \sqrt{\frac{2}{3}} & \sqrt{\frac{1}{3}} & 0 \\ -\sqrt{\frac{1}{6}} & \sqrt{\frac{1}{3}} & -\sqrt{\frac{1}{2}} \\ -\sqrt{\frac{1}{6}} & \sqrt{\frac{1}{3}} & \sqrt{\frac{1}{2}} \end{pmatrix} . \tag{5.12}$$

Therefore, we can see that the tribimaximal pattern of the mixing matrix is coming directly from the term containing the triplet Higgs ϕ_S and does not depend on the terms containing the one Higgs scalars ξ, ξ', ξ'' [1], which are charged under different one dimensional Higgs representations of the group A_4. However, in the absence of the one

[1]The mixing pattern does not depend explicitly even on the magnitude of the VEV of ϕ_S.

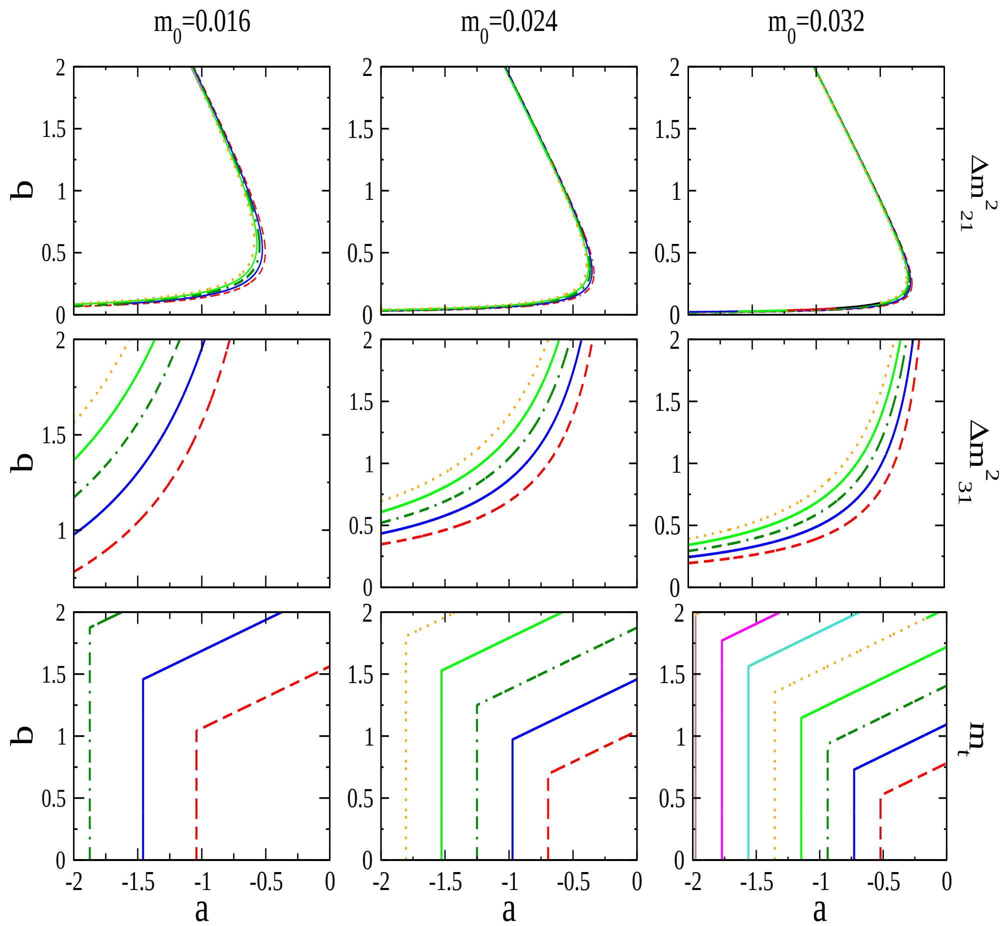

Figure 5.1: Contour plot of $\Delta m^2_{21}, \Delta m^2_{31}$ and sum of absolute neutrino masses m_t in the $a-b$ plane, for three different values of m_0 (m_0=0.016, m_0=0.024 and m_0=0.032) for the case with ξ and ϕ_S. The first row shows contour plots for different values of Δm^2_{21} (in 10^{-5} eV^2), with red dashed lines for 6.5 blue solid lines for 7.1, green dashed lines for 7.7, green solid lines for 8.3, and orange dotted lines for 8.9. The second row shows contour plots for different values of Δm^2_{31} (in 10^{-3} eV^2), with red dashed lines for 1.6, blue solid lines for 2.0, green dashed lines for 2.4, green solid lines for 2.8, and orange dotted lines for 3.2. The third row shows contour plots for m_t (in eV), with red dashed lines for 0.05, blue solid lines for 0.07, green dashed lines for 0.09, green solid lines for 1.1, orange dotted lines for 1.3, turquoise solid lines for 1.4, magenta solid lines for 1.6, and brown solid lines for 1.8.

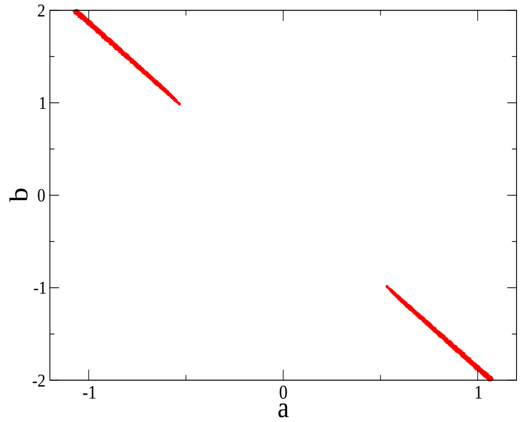

Figure 5.2: Scatter plot showing regions in $a-b$ parameter space for the model considered in [14], which are compatible with the 3σ allowed range of values of the mass squared differences given in [20]. The parameter m_0 is allowed to vary freely.

dimensional Higgs contributions to m_ν, the predicted neutrino masses turn out to be very wrong. In this case, $\Delta m^2_{21} = -b^2\, m^2_0$ and $\Delta m^2_{31} = 0$, in strong disagreement with the oscillation data.

5.3.2 Only One One-Dimensional A_4 Higgs

If we take only one Higgs at a time, which transforms as one dimensional irreducible representation under A_4, then there are three possibilities. The resulting mass matrices are shown in column 2 of Table 5.2. One could get exactly the same situation with three one dimensional Higgs ξ, ξ' and ξ'' and demanding that the VEV of two of them are zero while that of the third is nonzero. The m_ν given in Table 5.2 can be exactly diagonalized and the eigenvalues and eigenvectors are shown in column 3 and 4 of the Table, respectively. It is evident that only the case where ξ is present gives rise to a viable mixing matrix, which is exactly tribimaximal [14]. Only the first case has the form for m_ν given in Eq. (5.2). Each of the m_ν given in Table 5.2 possesses an S_2 symmetry. While the case with ξ exhibits the $\mu-\tau$ exchange symmetry, the one with ξ'' remains invariant under $e-\mu$ permutation and the one with ξ' under $e-\tau$ permutation. This would necessarily demand that while for the first case θ_{23} would be maximal and $\theta_{13} = 0$, for the second and third cases θ_{23} would be either 90° or 0 respectively, and θ_{13} maximal, and hence disallowed by the neutrino oscillation data.

Since only the case with ξ reproduces the correct form for the mixing matrix, we do not discuss the remaining two cases any further. The mass squared differences in this

Higgs	Neutrino mass matrix	Eigenvalues	Mixing Matrix
ξ	$m_0 \begin{pmatrix} a+\frac{2b}{3} & -\frac{b}{3} & -\frac{b}{3} \\ -\frac{b}{3} & \frac{2b}{3} & a-\frac{b}{3} \\ -\frac{b}{3} & a-\frac{b}{3} & \frac{2b}{3} \end{pmatrix}$	$\begin{pmatrix} m_0(a+b), \\ m_0 a, \\ m_0(b-a) \end{pmatrix}$	$\begin{pmatrix} \sqrt{\frac{2}{3}} & \frac{1}{\sqrt{3}} & 0 \\ -\frac{1}{\sqrt{6}} & \frac{1}{\sqrt{3}} & -\frac{1}{\sqrt{2}} \\ -\frac{1}{\sqrt{6}} & \frac{1}{\sqrt{3}} & \frac{1}{\sqrt{2}} \end{pmatrix}$
ξ''	$m_0 \begin{pmatrix} \frac{2b}{3} & c-\frac{b}{3} & -\frac{b}{3} \\ c-\frac{b}{3} & \frac{2b}{3} & -\frac{b}{3} \\ -\frac{b}{3} & -\frac{b}{3} & c+\frac{2b}{3} \end{pmatrix}$	$\begin{pmatrix} m_0(c+b), \\ m_0 c, \\ m_0(b-c) \end{pmatrix}$	$\begin{pmatrix} -\frac{1}{\sqrt{6}} & \frac{1}{\sqrt{3}} & -\frac{1}{\sqrt{2}} \\ -\frac{1}{\sqrt{6}} & \frac{1}{\sqrt{3}} & \frac{1}{\sqrt{2}} \\ \sqrt{\frac{2}{3}} & \frac{1}{\sqrt{3}} & 0 \end{pmatrix}$
ξ'	$m_0 \begin{pmatrix} \frac{2b}{3} & -\frac{b}{3} & d-\frac{b}{3} \\ -\frac{b}{3} & d+\frac{2b}{3} & -\frac{b}{3} \\ d-\frac{b}{3} & -\frac{b}{3} & \frac{2b}{3} \end{pmatrix}$	$\begin{pmatrix} m_0(d+b), \\ m_0 d, \\ m_0(b-d) \end{pmatrix}$	$\begin{pmatrix} -\frac{1}{\sqrt{6}} & \frac{1}{\sqrt{3}} & -\frac{1}{\sqrt{2}} \\ \sqrt{\frac{2}{3}} & \frac{1}{\sqrt{3}} & 0 \\ -\frac{1}{\sqrt{6}} & \frac{1}{\sqrt{3}} & \frac{1}{\sqrt{2}} \end{pmatrix}$

Table 5.2: The mass matrix taking one Higgs at a time, its mass eigenvalues, and its mixing matrix.

case are

$$\Delta m^2_{21} = (-b^2 - 2ab)m_0^2, \quad \Delta m^2_{31} = -4\,a\,b\,m_0^2\ , \tag{5.13}$$

where $m_0 = v_u^2/\Lambda$. Since it is now known at more than 6σ C.L. that $\Delta m^2_{21} > 0$ [19,20], we have the condition that $-2ab > b^2$. We have considered the parameters a and b as real. Since b^2 is a positive definite quantity the above relation implies that $-2ab > 0$, which can happen if and only if $sgn(a) \neq sgn(b)$. Inserting this condition into the expression for Δm^2_{31} gives us $\Delta m^2_{31} > 0$ necessarily in this model. Therefore inverted neutrino mass hierarchy is impossible to get in the effective A_4 model originally proposed by Altarelli and Feruglio [14]. The conclusion is also valid for complex parameter a and b with a relative phase ϕ. However, going to the seesaw-realization given in [14], normal as well as inverted hierarchy is possible to realize.

The sum of the absolute neutrino masses, effective mass in neutrinoless double beta decay and prediction for tritium beta decay are given respectively as

$$m_t = |m_1| + |m_2| + |m_3|, \quad \langle m_{ee}\rangle = m_0(a + 2b/3), \quad m^2_\beta = m_0^2\Big(a^2 + \frac{4ab}{3} + \frac{2b^2}{3}\Big) \tag{5.14}$$

In Fig. 5.1 we show the contours for the observables Δm^2_{21}, Δm^2_{31} and m_t in the $a-b$ plane, for three different fixed values of m_0. The details of the figure and description of the different lines can be found in the caption of the figure.

In Fig. 5.2 we present a scatter plot showing the points in the $a-b$ parameter space which are compatible with the 3σ [20] allowed range of the mass squared differences. We have allowed m_0 to vary freely and taken a projection of all allowed points in the $a-b$ plane. While a is related to the VEV of the singlet ξ, b is given in terms of the VEVs of the triplet ϕ_S. The TBM form for the mixing matrix comes solely from the vacuum alignment of ϕ_S and ξ is not needed for that. The singlet ξ is necessary only for producing the correct values of Δm^2_{21} and Δm^2_{31}. However, it is evident from Fig. 5.2 that for a given value of a needed to obtain the right mass squared differences, the value of b is almost fixed. The relation between a and b can be obtained by looking at the ratio $\frac{\Delta m^2_{21}}{\Delta m^2_{31}} = \frac{-b^2-2ab}{-4ab} \simeq 0.03$, where 0.03 on the right-hand-side (RHS) is the current experimental value. This gives us the relation $b \simeq -1.88a$. Therefore, in addition to the alignment $\langle\phi_S\rangle = (v_S, v_S, v_S)$ to get TBM, one also needs a particular relation between the product of Yukawa couplings and VEVs of ϕ_S and ξ in order to reproduce the correct phenomenology. Even if one includes the 3σ uncertainties on Δm^2_{21} and Δm^2_{31}, $|b|$ is fine tuned to $|a|$ within a factor of about 10^{-2}.

5.3.3 Two One-Dimensional A_4 Higgs

If we take two Higgs fields at a time, belonging to two different one dimensional A_4 representations and allow for nonzero VEVs for them, then the m_ν obtained for the three possible cases are shown in the first three rows of Table 5.3. One can again see that of the three possible combinations, only the ξ', ξ'' combination gives a viable TBM matrix. The other two mass matrices exhibit $e-\tau$ (ξ, ξ'')and $e-\mu$ (ξ, ξ') symmetry respectively and are ruled out. Note that we have chosen $a = c$ for the ξ, ξ'' combination, $a = d$ for the ξ, ξ' combination and $c = d$ for the ξ', ξ'' combination for the results given in Table 5.3. This is a reasonable assumption to make since the phenomenology of the three cases does not change drastically unless the VEVs of the singlet Higgs vary by a huge amount. In particular, by changing the relative magnitude of the VEVs, we do not expect the structure of the mixing matrix for the first two rows of Table 5.3 to change so much so that they could be allowed by the current data. In the limit that $c = d$, it is not hard to appreciate that the resultant matrix with ξ' and ξ'' would exhibit $\mu-\tau$ symmetry, though the ξ' and ξ'' terms alone have $e-\tau$ and $e-\mu$ symmetry respectively.

Since the ξ', ξ'' combination is the only one which gives exact TBM mixing in the approximation that $c = d$, we perform a detailed analysis only for this case. Putting $c = d$ is again contrived and would also lead to a certain fixed relation between them and b, as in the only ξ case. This would mean additional fine tuning of the parameters, unless explained by symmetry arguments. Hence, we allow the two VEVs to differ from each other so that $c = d + \epsilon$. If ϵ is small we can solve the eigenvalue problem keeping only the first order terms in ϵ. The results for this case are shown in the final row of the Table

5.3. The deviation of the mixing angles from their TBM values can be seen to be

$$D_{12} \simeq 0, \quad D_{23} \simeq -\frac{\epsilon}{4d}, \quad U_{e3} \simeq -\frac{\epsilon}{2\sqrt{2}d} \ , \tag{5.15}$$

where $D_{12} = \sin^2\theta_{12} - 1/3$ and $D_{23} = \sin^2\theta_{23} - 1/2$. We show in the left hand panels of Fig. 5.3 the mixing angles $\sin^2\theta_{12}$ (upper panel), $\sin^2\theta_{13}$ (middle panel) and $\sin^2\theta_{23}$ (lower panel) as a function of ϵ. We vary ϵ from large negative to large positive values and solve the exact eigenvalue problem numerically allowing the other parameters, m_0, b and d, to vary freely. For $\epsilon = 0$ of course we get TBM mixing as expected. For very small values of ϵ, the deviation of the mixing angles from their TBM values is reproduced well by the approximate expressions given in Eq. (5.15). For large ϵ of course the approximate expressions fail and we have significant deviation from TBM. The values of $\sin^2\theta_{12}$ and $\sin^2\theta_{13}$ increase very fast with ϵ, while $\sin^2\theta_{23}$ decreases with it. We have only showed the scatter plots up to the 3σ allowed ranges for the mixing angles given in [20]. The mass dependent observables can be calculated upto first order in ϵ as

$$\Delta m^2_{21} \simeq m_0^2\,(b + d + \frac{\epsilon}{2})(3d - b + \frac{3\epsilon}{2}), \quad \Delta m^2_{31} \simeq (4bd + 2b\epsilon)m_0^2 \ , \tag{5.16}$$

$$\langle m_{ee}\rangle = m_0\frac{2b}{3}, \quad m_t = \sum_i |m_i|, \quad m_\beta^2 \simeq m_0^2(\frac{2b^2}{3} + 2d^2 - \frac{4bd}{3} + 2d\epsilon - \frac{2b\epsilon}{3}) \ . \tag{5.17}$$

Of course, epsilon can be larger and we show numerical results for those cases.

Normal Hierarchy

The right panels of Fig. 5.3 show Δm^2_{21} (upper panel), Δm^2_{31} (middle panel) and m_t (lower panel) as a function of ϵ assuming $m_1 < m_2 \ll m_3$. We show Δm^2_{21} and Δm^2_{31} only within their 3σ [20] allowed range. We notice that while Δm^2_{21} and Δm^2_{31} are hardly constrained by ϵ, there appears to some mild dependence of m_t on it.

Fig. 5.4 gives the scatter plots showing the allowed parameter regions for this case. The upper, middle and lower panels show the allowed points projected on the $b - c$, $d - c$ and $b - d$ plane, respectively.

Inverted Hierarchy

For this case it is possible to obtain even inverted hierarchy. We show in Fig. 5.4 the scatter plots showing the allowed parameter regions for inverted hierarchy. We have allowed m_0 to vary freely and show the allowed points projected on the $c - b$, $c - d$ and $d - b$ planes. One can check that only for the points appearing in this plot, $m_3 < m_1 < m_2$.

Higgs	Neutrino mass matrix	Eigenvalues	Eigenvectors
ξ,ξ''	$m_0\begin{pmatrix} a+\frac{2b}{3} & c-\frac{b}{3} & -\frac{b}{3} \\ c-\frac{b}{3} & \frac{2b}{3} & a-\frac{b}{3} \\ -\frac{b}{3} & a-\frac{b}{3} & c+\frac{2b}{3} \end{pmatrix}$	a=c; $\begin{pmatrix} m_0(b-a), \\ 2m_0a, \\ m_0(a+b) \end{pmatrix}$	$\begin{pmatrix} -\frac{1}{\sqrt{6}} & \frac{1}{\sqrt{3}} & -\frac{1}{\sqrt{2}} \\ \sqrt{\frac{2}{3}} & \frac{1}{\sqrt{3}} & 0 \\ -\frac{1}{\sqrt{6}} & \frac{1}{\sqrt{3}} & \frac{1}{\sqrt{2}} \end{pmatrix}$
ξ,ξ'	$m_0\begin{pmatrix} a+\frac{2b}{3} & -\frac{b}{3} & d-\frac{b}{3} \\ -\frac{b}{3} & d+\frac{2b}{3} & a-\frac{b}{3} \\ d-\frac{b}{3} & a-\frac{b}{3} & \frac{2b}{3} \end{pmatrix}$	a=d; $\begin{pmatrix} m_0(b-a), \\ 2m_0a, \\ m_0(a+b) \end{pmatrix}$	$\begin{pmatrix} -\frac{1}{\sqrt{6}} & \frac{1}{\sqrt{3}} & -\frac{1}{\sqrt{2}} \\ -\frac{1}{\sqrt{6}} & \frac{1}{\sqrt{3}} & \frac{1}{\sqrt{2}} \\ \sqrt{\frac{2}{3}} & \frac{1}{\sqrt{3}} & 0 \end{pmatrix}$
ξ',ξ''	$m_0\begin{pmatrix} \frac{2b}{3} & c-\frac{b}{3} & d-\frac{b}{3} \\ c-\frac{b}{3} & d+\frac{2b}{3} & -\frac{b}{3} \\ d-\frac{b}{3} & -\frac{b}{3} & c+\frac{2b}{3} \end{pmatrix}$	c=d; $\begin{pmatrix} m_0(b-c), \\ 2m_0c, \\ m_0(c+b) \end{pmatrix}$	$\begin{pmatrix} \sqrt{\frac{2}{3}} & \frac{1}{\sqrt{3}} & 0 \\ -\frac{1}{\sqrt{6}} & \frac{1}{\sqrt{3}} & -\frac{1}{\sqrt{2}} \\ -\frac{1}{\sqrt{6}} & \frac{1}{\sqrt{3}} & \frac{1}{\sqrt{2}} \end{pmatrix}$
		$c=d+\epsilon$; $\begin{pmatrix} m_0(b-d-\frac{\epsilon}{2}), \\ m_0(2d+\epsilon), \\ m_0(d+b+\frac{\epsilon}{2}) \end{pmatrix}$	$\begin{pmatrix} \sqrt{\frac{2}{3}} & \frac{1}{\sqrt{3}} & -\frac{\epsilon}{2\sqrt{2}d} \\ -\frac{1}{\sqrt{6}}-\frac{\sqrt{3}\epsilon}{4\sqrt{2}d} & \frac{1}{\sqrt{3}} & -\frac{1}{\sqrt{2}}+\frac{\epsilon}{4\sqrt{2}d} \\ -\frac{1}{\sqrt{6}}+\frac{\sqrt{3}\epsilon}{4\sqrt{2}d} & \frac{1}{\sqrt{3}} & \frac{1}{\sqrt{2}}+\frac{\epsilon}{4\sqrt{2}d} \end{pmatrix}$

Table 5.3: Here we take two one dimensional A_4 Higgs at a time, and analytically display eigenvalues and eigenvectors of the neutrino mass matrix.

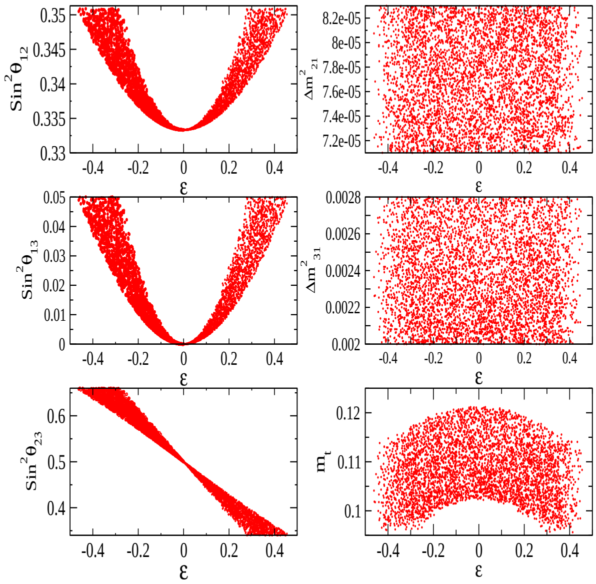

Figure 5.3: The left panels show $\sin^2\theta_{12}$, $\sin^2\theta_{13}$ and $\sin^2\theta_{23}$ vs ϵ and the right panels show Δm^2_{21}, Δm^2_{31} and m_t vs ϵ respectively. Here ξ' and ξ'' acquire VEVs. The other parameters c, b and m_0 are allowed to vary freely.

5.3.4 Three One-Dimensional A_4 Higgs

Finally, we let all three Higgs which transform as different one dimensional irreducible representations under the symmetry group A_4 contribute to m_ν. In this case one has to diagonalize the most general mass matrix given in Eq. (5.9). This matrix has four independent parameters. If we assume that the VEVs of ξ, ξ' and ξ'' are such that $a = c = d$, then the eigenvalues and mixing matrix are given in the first row of Table 5.4. This gives us a mass matrix, which give us two of the mass eigenstates as degenerate. To get the correct mass splitting in association with TBM mixing, it is essential that (i) we should have contribution from the VEVs of the one dimensional Higgs and (ii) the contribution from the the three one dimensional Higgs ξ, ξ' and ξ'' in m_ν should not be identical. If we assume that $a = c \neq d$, then one can easily check that m_ν has $e-\tau$ exchange symmetry, and hence the resulting mass matrix is disallowed. This is because for $a = c$, as discussed before we get $e-\tau$ exchange symmetry and the ξ' term has an in-built $e-\tau$ symmetry. Similarly for $a = d \neq c$, one gets $e-\mu$ symmetry in m_ν and is hence disfavored. Only when we impose the condition $c = d$, we have $\mu-\tau$ symmetry in m_ν, since the ξ term and the sum of the ξ' and ξ'' terms are now separately $\mu-\tau$ symmetric.

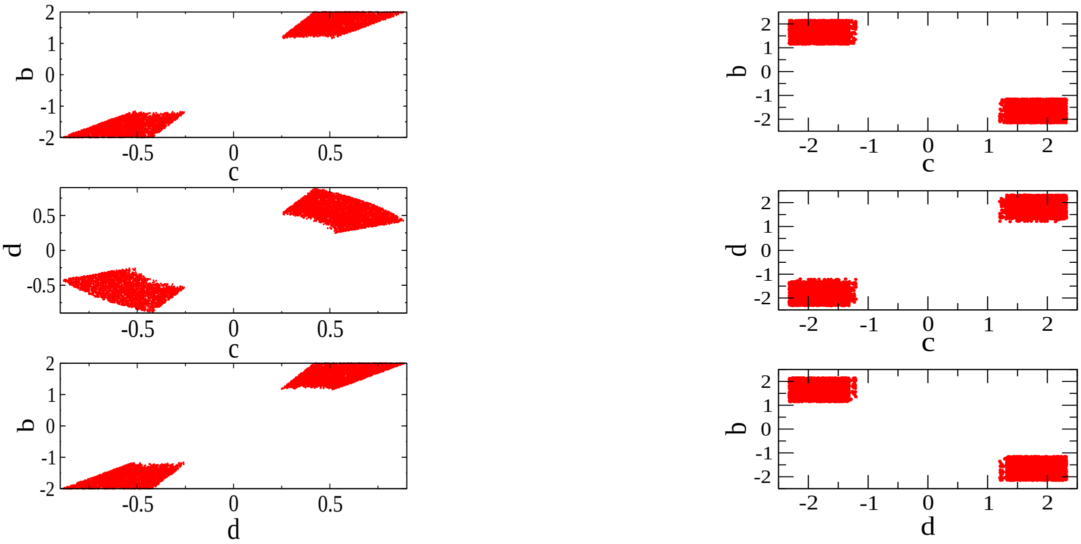

Figure 5.4: In the left pannel, scatter plot showing the 3σ [20] allowed regions for the $b-c-d$ parameters for the case where ξ' and ξ'' acquire VEVs. The top, middle and lower panels show the allowed points projected on the $c-b$, $c-d$ and $d-b$ plane, respectively. The parameter m_0 was allowed to take any value. Here we have assumed normal hierarchy. In the right pannel, the scatter plot for inverted hierarchy.

Therefore, the case $a \neq c = d$ gives us the TBM matrix and the mass eigenvalues are shown in Table 5.4.

Since $a \neq c = d$ is the only allowed case for the three one dimensional Higgs case, we find the eigenvalues and the mixing matrix for the case where c and d are not equal, but differ by ϵ. We take $c = d + \epsilon$ and for small values of ϵ give the results in the last row of Table 5.4, keeping just the first order terms in ϵ. The deviation from TBM is given as follows

$$D_{12} \simeq 0, \qquad D_{23} \simeq \frac{\epsilon}{4(a-d)}, \qquad U_{e3} \simeq \frac{\epsilon}{2\sqrt{2}(a-d)} \ . \tag{5.18}$$

The mass squared differences are

$$\Delta m^2_{21} \simeq m_0^2\,(2a+b+d+\frac{\epsilon}{2})(3d-b+\frac{3\epsilon}{2}), \quad \Delta m^2_{31} \simeq 2\,m_0^2\,b(2d-2a+\epsilon)\ . \tag{5.19}$$

From the expression of the mass eigenvalues given in the Table 5.4, one can calculate the

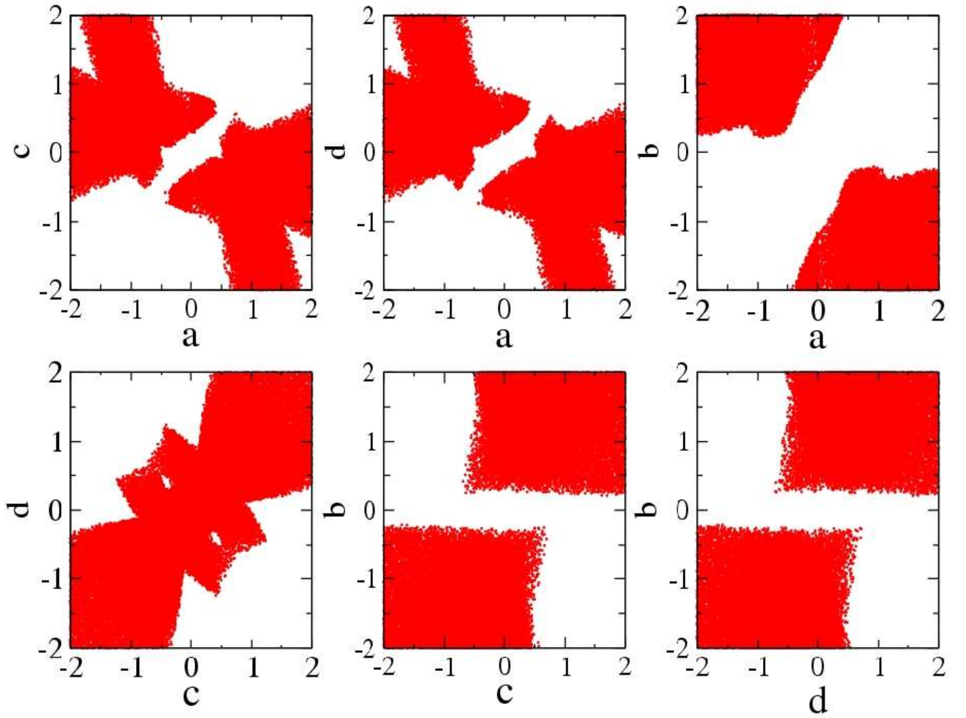

Figure 5.5: Scatter plot showing the 3σ [20] allowed regions in the model parameter space for the case where ξ, ξ' and ξ'' all acquire VEVs. The upper panels show allowed regions projected onto the $a-c$, $a-d$, $a-b$ planes. The lower panels show allowed regions projected onto the $c-d$, $c-b$, $d-b$ planes. Normal hierarchy is assumed.

observables m_t, m_β^2 and $\langle m_{ee}\rangle$

$$\langle m_{ee}\rangle = m_0\,(a+\frac{2b}{3}),\quad m_t=\sum_i |m_i|,\quad m_\beta^2 \simeq m_0^2\,(a^2+\frac{4ab}{3}+\frac{2b^2}{3}+2d^2-\frac{4bd}{3}+2d\epsilon-\frac{2b\epsilon}{3}) \tag{5.20}$$

Normal Hierarchy

Let us begin by restricting the neutrino masses to obey the condition $m_1 < m_2 \ll m_3$ and allow a, b, c and d to take any random value and find the regions in the a, b, c and d space that give Δm_{21}^2, Δm_{31}^2 and the mixing angles within their 3σ [20] allowed ranges. This is done by numerically diagonalizing m_ν. The results are shown as scatter plots in

Higgs	Neutrino mass matrix	Eigenvalues	Eigenvectors
ξ, ξ', ξ''	$m_0 \begin{pmatrix} a+\frac{2b}{3} & c-\frac{b}{3} & d-\frac{b}{3} \\ c-\frac{b}{3} & d+\frac{2b}{3} & a-\frac{b}{3} \\ d-\frac{b}{3} & a-\frac{b}{3} & c+\frac{2b}{3} \end{pmatrix}$	$a = c = d$; $\begin{pmatrix} m_0 b, \\ 3m_0 a, \\ m_0 b \end{pmatrix}$	$\begin{pmatrix} \sqrt{\frac{2}{3}} & \frac{1}{\sqrt{3}} & 0 \\ -\frac{1}{\sqrt{6}} & \frac{1}{\sqrt{3}} & -\frac{1}{\sqrt{2}} \\ -\frac{1}{\sqrt{6}} & \frac{1}{\sqrt{3}} & \frac{1}{\sqrt{2}} \end{pmatrix}$
		$a \neq c = d$; $\begin{pmatrix} m_0(a+b-c), \\ m_0(a+2c), \\ m_0(b+c-a) \end{pmatrix}$	$\begin{pmatrix} \sqrt{\frac{2}{3}} & \frac{1}{\sqrt{3}} & 0 \\ -\frac{1}{\sqrt{6}} & \frac{1}{\sqrt{3}} & -\frac{1}{\sqrt{2}} \\ -\frac{1}{\sqrt{6}} & \frac{1}{\sqrt{3}} & \frac{1}{\sqrt{2}} \end{pmatrix}$
		$a = c \neq d$; $\begin{pmatrix} m_0(b+d-a), \\ m_0(2a+d), \\ m_0(a+b-d) \end{pmatrix}$	$\begin{pmatrix} -\frac{1}{\sqrt{6}} & \frac{1}{\sqrt{3}} & -\frac{1}{\sqrt{2}} \\ \sqrt{\frac{2}{3}} & \frac{1}{\sqrt{3}} & 0 \\ -\frac{1}{\sqrt{6}} & \frac{1}{\sqrt{3}} & \frac{1}{\sqrt{2}} \end{pmatrix}$
		$a = d \neq c$; $\begin{pmatrix} m_0(b+c-a) \\ m_0(2a+c), \\ m_0(a+b-c) \end{pmatrix}$	$\begin{pmatrix} -\frac{1}{\sqrt{6}} & \frac{1}{\sqrt{3}} & -\frac{1}{\sqrt{2}} \\ -\frac{1}{\sqrt{6}} & \frac{1}{\sqrt{3}} & \frac{1}{\sqrt{2}} \\ \sqrt{\frac{2}{3}} & \frac{1}{\sqrt{3}} & 0 \end{pmatrix}$
		$a \neq c = d + \epsilon$; $\begin{pmatrix} m_0(a+b-d-\frac{\epsilon}{2}), \\ m_0(a+2d+\epsilon), \\ m_0(b+d-a+\frac{\epsilon}{2}) \end{pmatrix}$	$\begin{pmatrix} \sqrt{\frac{2}{3}} & \frac{1}{\sqrt{3}} & a_4 \\ -\frac{1}{\sqrt{6}}+a_2 & \frac{1}{\sqrt{3}} & -\frac{1}{\sqrt{2}}-a_5 \\ -\frac{1}{\sqrt{6}}+a_3 & \frac{1}{\sqrt{3}} & \frac{1}{\sqrt{2}}-a_6 \end{pmatrix}$

Table 5.4: The mass matrix taking all three one dimensional A_4 Higgs, its mass eigenvalues and its mixing matrix. The correction factors in the last row are: $a_2 = \frac{\sqrt{3}\epsilon}{4\sqrt{2}(a-d)}$, $a_3 = -\frac{\sqrt{3}\epsilon}{4\sqrt{2}(a-d)}$ and $a_4 = \frac{\epsilon}{2\sqrt{2}(a-d)}$, $a_5 = \frac{1\epsilon}{4\sqrt{2}(a-d)}$, $a_6 = \frac{\epsilon}{4\sqrt{2}(a-d)}$.

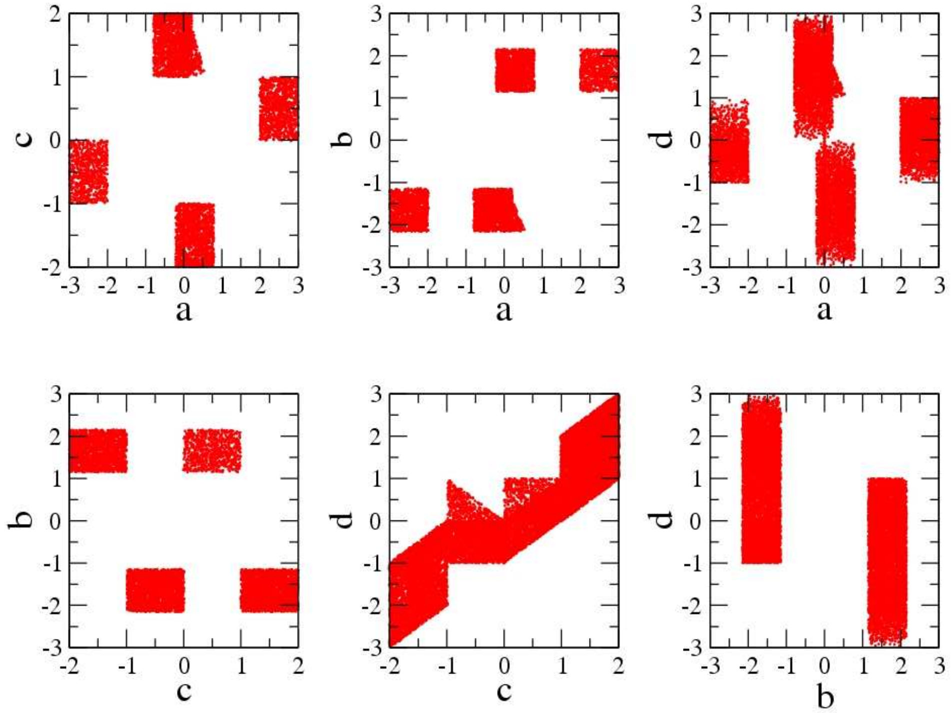

Figure 5.6: Same as Fig. 5.5 but for inverted hierarchy.

Fig. 5.5. To help see the allowed zones better, we have projected the allowed points on the $a-c$, $a-d$ and $a-b$ plane shown in the upper panels, and $c-d$, $c-b$ and $d-b$ plane in the lower panels. There are several things one can note about the VEVs and hence the structure of the resultant m_ν

- $a = 0$ is allowed, since this gives a m_ν which has contributions from ξ' and ξ'', discussed in section 3.3,
- $b = 0$ is never allowed since b is needed for TBM mixing as pointed out before,
- $a = b$, $a = c$ and $a = d$ are never allowed,
- $c = d$ is allowed and we can see from the lower left-hand panel how much deviation of c from d can be tolerated,
- $c = 0$ and $d = 0$ can also be tolerated when $a \neq 0$.

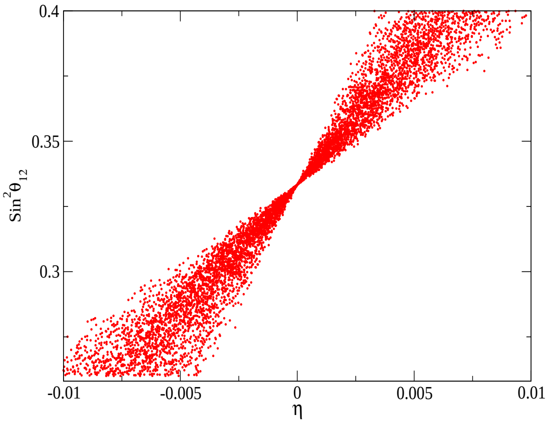

Figure 5.7: Variation of $\sin^2\theta_{12}$ with η for the case where we allow for a misalignment of the triplet Higgs such that $\langle\phi_S\rangle = (v_{S1}, v_S, v_S)$ and $a \neq c = d$.

All these features are consistent with the results of Table 5.4.

Inverted Hierarchy

In this case too its possible to get inverted hierarchy. The corresponding values of the parameters of m_ν which allow this are shown as scatter plots in Fig. 5.6. Here m_0 has been allowed to take any value, and we show the points projected on the $a-c$, $a-b$, $a-d$ plane in the upper panels and $c-b$, $c-d$, $b-d$ plane in the lower panels. Each of these points also satisfy the 3σ experimental bounds given in [20]. Note that for $a = 0$ we get the same regions in b, c and d, as in the right-pannel of Fig. 5.4.

5.4 Vacuum Alignment of the Triplet Higgs

In case we do not confine ourselves to $\langle\phi_S\rangle = (v_S, v_S, v_S)$, we would have the general m_ν given in Eq. (5.6). Since we have argued in the previous section that the only viable scenario where one allows for all three Higgs singlet is when $a \neq c \simeq d$, we will assume that this condition for the singlet terms holds. We further realize that to reproduce a mixing matrix with $\theta_{13} \sim 0$ and $\theta_{23} \sim 45°$, it might be desirable to keep $\mu - \tau$ symmetry in the mass matrix. Therefore, we show our results for the case $\langle\phi_S\rangle = (v_{S_1}, v_S, v_S)$. The mass matrix is then given as

$$m_\nu = m_0 \begin{pmatrix} a+2b_1/3 & d-b/3 & d-b/3 \\ d-b/3 & d+2b/3 & a-b_1/3 \\ d-b/3 & a-b_1/3 & d+2b/3 \end{pmatrix} . \tag{5.21}$$

Of course for $b_1 = b$ one would recover the case considered in the previous section and TBM mixing would result. The possibility of $b_1 \neq b$ gives rise to deviation from TBM mixing. In order to solve this matrix analytically we assume that $b_1 = b + \eta$ and keep only the first order terms in η. The mass eigenvalues obtained are

$$m_1 = m_0\,(a+b-d+\frac{\eta}{3}), \quad m_2 = m_0\,(a+2d), \quad m_3 = m_0\,(-a+b+d+\frac{\eta}{3}), \quad , \tag{5.22}$$

and the mixing matrix is

$$\begin{pmatrix} \sqrt{\frac{2}{3}}\Big(1-\frac{\eta}{3(3d-b)}\Big) & \sqrt{\frac{1}{3}}\Big(1+\frac{2\eta}{3(3d-b)}\Big) & 0 \\ -\sqrt{\frac{1}{6}}\Big(1+\frac{2\eta}{3(3d-b)}\Big) & \sqrt{\frac{1}{3}}\Big(1-\frac{\eta}{3(3d-b)}\Big) & -\sqrt{\frac{1}{2}} \\ -\sqrt{\frac{1}{6}}\Big(1+\frac{2\eta}{3(3d-b)}\Big) & \sqrt{\frac{1}{3}}\Big(1-\frac{\eta}{3(3d-b)}\Big) & \sqrt{\frac{1}{2}} \end{pmatrix} . \tag{5.23}$$

Therefore, the only deviation from TBM comes in θ_{12} and we have

$$D_{12} \simeq \frac{4\eta}{9(3d-b)} . \tag{5.24}$$

We show in Fig. 5.7 variation of $\sin^2\theta_{12}$ with η. As expected, $\sin^2\theta_{12}$ is seen to deviate further and further from its TBM value of 1/3 as we increase the difference between v_S and v_{S1}. The other two mixing angles are predicted to be exactly at their TBM values due to the presence of $\mu-\tau$ symmetry in m_ν. They would also deviate from TBM once we allow for either $v_{S_2} \neq v_{S_3}$ or $c \neq d$, and in the most general case, both.

5.5 Conclusions

In this work we have seen the implication of A_4 flavor symmetry on the neutrino oscillation data while emphasizing mostly on tribimaximal mixing pattern. We stick to a most generic setup and we consider all the possibilities, where the one dimensional Higgses ξ, ξ', ξ'' belong to 1, $1'$, $1''$ representation under the symmetry group A_4. Other than this, we also haves two A_4 triplets $\phi_{T,S}$. We analyze the different cases by taking one, two and all three one dimensional A_4 Higgs fields at a time and show only few of them can give viable neutrino mass and mixing. To get tribimaximal mixing one would require VEV alignments of the triplet and also specific relations between different VEV's and Yukawa couplings.

Also we have shown, while the triplet alone is sufficient to provide the tribimaximal mixing, to get the viable neutrino mass splitting the one dimensional representation must be present. We have analyzed the possibilities to get normal and/or inverted hierarchy for these different viable scenarios. The most simple case with A_4 singlet ξ will lead to normal hierarchy, while inclusion of other one dimensional representation allows for inverted hierarchy as well. Finally we address the deviation from the tribimaximal mixing and give one illustrative example where the deviation is realized due to deviation from the triplet vacuum alignments.

Bibliography

[1] M. C. Gonzalez-Garcia, M. Maltoni and J. Salvado, JHEP **1004**, 056 (2010) [arXiv:1001.4524 [hep-ph]].

[2] K. Eguchi *et al.*, [KamLAND Collaboration], Phys.Rev.Lett.**90** (2003) 021802; T. Araki *et al.* [KamLAND Collaboration], Phys. Rev. Lett. **94**, 081801 (2005). I Shimizu, talk at 10th International Conference on Topics in Astroparticle and Underground Physics, TAUP 2007,Sendai, Japan, 2007.

[3] B. T. Cleveland *et al.*, Astrophys. J. **496**, 505 (1998); J. N. Abdurashitov *et al.* [SAGE Collaboration], Zh. Eksp. Teor. Fiz. **122**, 211 (2002) [J. Exp. Theor. Phys. **95**, 181 (2002)]; W. Hampel *et al.* [GALLEX Collaboration], Phys. Lett. B **447**, 127 (1999); S. Fukuda *et al.* [Super-Kamiokande Collaboration], Phys. Lett. B **539**, 179 (2002); B. Aharmim *et al.* [SNO Collaboration], Phys. Rev. C **72**, 055502 (2005); B. Collaboration, arXiv:0708.2251 [astro-ph].

[4] Y. Ashie *et al.* [Super-Kamiokande Collaboration], Phys. Rev. D **71**, 112005 (2005).

[5] E. Aliu *et al.* [K2K Collaboration], Phys. Rev. Lett. **94**, 081802 (2005).

[6] D. G. Michael *et al.*. [MINOS Collaboration], Phys. Rev. Lett. **97**, 191801 (2006).

[7] M. Apollonio *et al.*, Eur. Phys. J. C **27**, 331 (2003).

[8] P. F. Harrison, D. H. Perkins and W. G. Scott, Phys. Lett. B **458**, 79 (1999); P. F. Harrison, D. H. Perkins and W. G. Scott, Phys. Lett. B **530** (2002) 167; P. F. Harrison and W. G. Scott, arXiv:hep-ph/0402006.

[9] T. Fukuyama and H. Nishiura, hep-ph/9702253; R. N. Mohapatra and S. Nussinov, Phys. Rev. D **60**, 013002 (1999); E. Ma and M. Raidal, Phys. Rev. Lett. **87**, 011802 (2001); C. S. Lam, Phys. Lett. B **507**, 214 (2001); P.F. Harrison and W. G. Scott, Phys. Lett. B **547**, 219 (2002); W. Grimus and L. Lavoura, Phys. Lett. B **572**, 189 (2003); J. Phys. G **30**, 73 (2004); Y. Koide, Phys. Rev. D **69**, 093001 (2004); A. Ghosal, hep-ph/0304090; W. Grimus *et al.*, Nucl. Phys. B **713**, 151 (2005); R. N. Mohapatra, JHEP **0410**, 027 (2004); R. N. Mohapatra and S. Nasri, Phys.

Rev. D **71**, 033001 (2005); R. N. Mohapatra, S. Nasri and H. B. Yu, Phys. Lett. B **615**, 231 (2005); Phys. Rev. D **72**, 033007 (2005); B. Brahmachari and S. Choubey, Phys. Lett. B **642**, 495 (2006); F. Feruglio,Y. Lin, hep-ph/0712.1528.

[10] S. Choubey and W. Rodejohann, Eur. Phys. J. C **40**, 259 (2005);

[11] E. Ma and G. Rajasekaran, Phys. Rev. D **64**, 113012 (2001).

[12] E. Ma, Mod. Phys. Lett. A **17**, 627 (2002).

[13] K. S. Babu, E. Ma and J. W. F. Valle, Phys. Lett. B **552**, 207 (2003).

[14] G. Altarelli and F. Feruglio, Nucl. Phys. B **720**, 64 (2005); G. Altarelli and F. Feruglio, Nucl. Phys. B **741**, 215 (2006); G. Altarelli , F. Feruglio and Y. Lin, Nucl. Phys. B **775**, 31 (2007).

[15] K. S. Babu and X.-G. He, arXiv:hep-ph/0507217.

[16] E. Ma, Mod. Phys. Lett. A **22**, 101 (2007); E. Ma, Mod. Phys. Lett. A **21**, 2931 (2006); E. Ma, H. Sawanaka and M. Tanimoto, Phys. Lett. B **641**, 301 (2006); B. Adhikary, B. Brahmachari, A. Ghosal, E. Ma and M. K. Parida, Phys. Lett. B **638**, 345 (2006); E. Ma, Phys. Rev. D **73**, 057304 (2006); S. L. Chen, M. Frigerio and E. Ma, Nucl. Phys. B **724**, 423 (2005); E. Ma, Phys. Rev. D **72**, 037301 (2005); E. Ma, Mod. Phys. Lett. A **20**, 2601 (2005); E. Ma, Phys. Rev. D **70**, 031901 (2004).

[17] M. Hirsch, A. S. Joshipura, S. Kaneko and J. W. F. Valle, Phys. Rev. Lett. **99**, 151802 (2007); [arXiv:hep-ph/0703046]. M. Hirsch, J. C. Romao, S. Skadhauge, J. W. F. Valle and A. Villanova del Moral, Phys. Rev. D **69**, 093006 (2004); L. Lavoura and H. Kuhbock, Mod. Phys. Lett. A **22**, 181 (2007); Y. Koide, Eur. Phys. J. C **52**, 617 (2007); S. F. King and M. Malinsky, Phys. Lett. B **645**, 351 (2007); X. G. He, Y. Y. Keum and R. R. Volkas, JHEP **0604**, 039 (2006); A. Zee, Phys. Lett. B **630**, 58 (2005); F. Bazzocchi, S. Kaneko and S. Morisi, arXiv:0707.3032 [hep-ph]. B. Adhikary and A. Ghosal, Phys. Rev. D **75**, 073020 (2007); I. K. Cooper, S. F. King and C. Luhn, Phys. Lett. B **690**, 396 (2010) [arXiv:1004.3243 [hep-ph]]; K. S. Babu and S. Gabriel, arXiv:1006.0203 [hep-ph].

[18] M. Honda and M. Tanimoto, arXiv:0801.0181 [hep-ph].

[19] S. Choubey, arXiv:hep-ph/0509217; S. Goswami, Int. J. Mod. Phys. A **21**, 1901 (2006); A. Bandyopadhyay, S. Choubey, S. Goswami, S. T. Petcov and D. P. Roy, Phys. Lett. B **608**, 115 (2005); G. L. Fogli *et al.*, Prog. Part. Nucl. Phys. **57**, 742 (2006).

[20] M. Maltoni, T. Schwetz, M. A. Tortola and J. W. F. Valle, New J. Phys. **6**, 122 (2004) [arXiv:hep-ph/0405172].

Chapter 6

S_3 Flavor Symmetry and Lepton Mass and Mixing

6.1 Introduction

In the previous chapter we have seen the implication of the discrete symmetry group A_4 in explaining the tribimaximal mixing matrix. Another discrete group which has been extensively discussed in the literature as a family symmetry group is the S_3 permutation group [1–7]. In this chapter we show how the S_3 symmetry group can be used to generate appropriate neutrino mass and mixing, and as well as the charged lepton mass hierarchy. To explain neutrino mass and mixing, we have extended our particle content by $\mathrm{SU(2)_L}$ triplet Higgs fields and the standard model singlets.

The S_3 group has the S_2 permutation group as its subgroup. If one identifies this subgroup with the $\mu - \tau$ exchange symmetry, then it is straightforward to get vanishing θ_{13} and maximal θ_{23} for the neutrinos. However, since the same group acts on the charged leptons as well, this would lead to μ and τ masses of the same order. In addition this would lead to a highly non-diagonal mass matrix for the charged leptons, which is undesirable in this case. Therefore, the S_3 group should be broken in such a way that $\mu - \tau$ permutation symmetry remains intact for the neutrinos but gets badly broken for the charged leptons.

In the following, we propose a model with $S_3 \times Z_4 \times Z_3$ family symmetry. The additional Z_3 symmetry is required for obtaining the correct form of the charged lepton mass matrix. We preserve the $\mu - \tau$ symmetry in the neutrino sector while breaking it maximally for the charged leptons. In particular, we introduce two $\mathrm{SU(2)_L}$ triplet Higgs in our model for generating the neutrino masses. The charged lepton masses are generated by the standard Higgs doublet. The particle content of our model has been tabulated in Tab. (6.1). We postulate two additional S_3 doublets of Higgs which are $\mathrm{SU(2)_L \times U(1)_Y}$ singlets, to generate the desired lepton mass matrices. The S_3 group is broken spontaneously when the singlet Higgs acquire VEVs. The VEVs are aligned in such a way that the residual $\mu-\tau$ symmetry is intact for the neutrinos but broken maximally for the charged leptons. We explicitly minimize our scalar potential and discuss the VEV alignment. We show that under the most general case, the minimization condition of our scalar potential predicts a very mild breaking of the $\mu-\tau$ symmetry for the neutrinos.

Since the Higgs triplet Δ interacts with the gauge bosons via their kinetic terms, they can be produced at the LHC and then can be traced via their subsequent decays. The most crucial feature of the Higgs triplet is the presence of the doubly charged Higgs. The doubly charged Higgs can decay to different states such as dileptons, gauge bosons, singly charged Higgs H^+. We discuss the doubly charged decay modes, specially the decay to the dileptonic mode and relate the doubly charged decay with the neutrino phenomenology. In our model the mixing between the two doubly charged Higgs is very closely related with the extent of the $\mu-\tau$ symmetry in the neutrino sector. In the exact $\mu-\tau$ limit the mixing angle θ between the two doubly charged Higgs is $\theta=\frac{\pi}{4}$, whereas mild breaking of the $\mu-\tau$ symmetry results in a mild deviation rom $\theta\sim\frac{\pi}{4}$. This close connection between the $\mu-\tau$ symmetry and the doubly charged mixing angle significantly effects the doubly charged Higgs-dileptonic vertices. In the exact $\mu-\tau$ limit, the vertex factors $H_2^{++}-\mu-\tau$ and $H_2^{++}-e-e$ are zero, hence the doubly charged Higgs H_2^{++} never decays to $\mu^++\tau^+$ or to $2e^+$ states. Other than this, the non observation of the $e\mu$ and $e\tau$ states in the dileptonic decay of the doubly charged Higgs would possibly disfavor the inverted mass hierarchy of the standard model neutrino. We study the phenomenological viability and testability of our model both in the exact as well as approximate $\mu-\tau$ symmetric cases. We have also very briefly commented about lepton flavor violation in our model. We give predictions for the mass squared differences, mixing angles, absolute neutrino mass scale, beta decay and neutrino-less double beta decay.

The chapter is organized as follows. In section 6.2 we introduce the particle content of our model and write down the mass matrices for the neutrinos and charged leptons. In section 6.3 we present the phenomenological implications of our model in the exact and approximate $\mu-\tau$ symmetric case. We discuss in detail the possible collider phenomenology and lepton flavor violating channels which could be used to provide smoking gun evidence for our model. Section 6.4 is devoted to justifying the alignment needed for the Higgs VEVs. We end in section 6.5 with our conclusions.

6.2 The Model

We present in Table 6.1 the particle content of our model and their transformation properties under the discrete groups S_3 , Z_4 and Z_3. The Higgs H is the usual $\mathrm{SU(2)_L}$ doublet,

$$H=\begin{pmatrix} H^+ \\ H^0 \end{pmatrix}\ , \tag{6.1}$$

Field	H	l_1	D_l	$\overline{e_R}$	$\overline{\mu_R}$	$\overline{\tau_R}$	Δ	ϕ_e	ξ
S_3	1	1	2	1	1	1	2	2	2
Z_4	i	-1	1	1	$-i$	1	-1	i	-1
Z_3	1	1	1	1	ω	ω^2	1	ω	1

Table 6.1: Transformation properties of matter and flavon fields under the flavor groups.

which transforms as singlet under S_3. The Higgs Δ_1 and Δ_2 are $\mathrm{SU(2)_L}$ triplets with hypercharge $Y = +2$,

$$\Delta_i = \begin{pmatrix} \Delta_i^+/\sqrt{2} & \Delta_i^{++} \\ \Delta_i^0 & -\Delta_i^+/\sqrt{2}\ , \end{pmatrix} , \tag{6.2}$$

which transform as a doublet

$$\Delta = \begin{pmatrix} \Delta_1 \\ \Delta_2 \end{pmatrix} , \tag{6.3}$$

under S_3. Other than these fields, we also have two additional S_3 scalar doublets ϕ_e and ξ,

$$\phi_e = \begin{pmatrix} \phi_1 \\ \phi_2 \end{pmatrix}, \quad \xi = \begin{pmatrix} \xi_1 \\ \xi_2 \end{pmatrix} , \tag{6.4}$$

which are singlets under $\mathrm{SU(2)_L} \times \mathrm{U_Y(1)}$. The $\mathrm{SU(2)_L} \times \mathrm{U_Y(1)}$ lepton doublets are distributed in the S_3 multiplets as follows:

$$D_l = \begin{pmatrix} L_2 \\ L_3 \end{pmatrix} , \tag{6.5}$$

transforms as a doublet under S_3, where $L_2 = L_\mu = (\nu_{\mu L}, \mu_L)^T$ and $L_3 = L_\tau = (\nu_{\tau L}, \tau_L)^T$, while

$$L_1 = L_e = \begin{pmatrix} \nu_{eL} \\ e_L \end{pmatrix} , \tag{6.6}$$

transforms as a singlet. The right-handed fields e_R, μ_R and τ_R transform as 1 under S_3. The corresponding charges of the particles under Z_4 and Z_3 has been summarized in Table 6.1.

6.2.1 Neutrino Masses and Mixing

Given the field content of our model and their charge assignments presented in Table 6.1, the most general $S_3 \times Z_4 \times Z_3$ invariant Yukawa part of the Lagrangian (leading order) giving the neutrino mass can be written as

$$-\mathcal{L}_\nu^y = \frac{y_2}{\Lambda}(D_l D_l)^{\underline{1}}(\xi\Delta)^{\underline{1}} + \frac{y_1}{\Lambda}(D_l D_l)^{\underline{2}}(\xi\Delta)^{\underline{2}} + 2y_3 l_1 D_l \Delta + \frac{y_4}{\Lambda} l_1 l_1 \xi \Delta + h.c. + ... \tag{6.7}$$

where Λ is the cut-off scale of the theory and the underline sign in the superscript represents the particular S_3 representation from the tensor product of the two S_3 doublets[1]. Since $(D_l D_l)$ and $\xi\Delta$ are 2×2 products which could give either 1 or 2, and since we can obtain 1 either by 1×1 or 2×2, we have two terms coming from $(D_l D_l \xi\Delta)$. The $(D_l D_l)(\xi\Delta)$ as $1'\times1'$ term does not contribute to the neutrino mass matrix. In this model the presence of the Z_4 symmetry prevents the appearance of the usual 5 dimensional $D_l D_l HH$ and $l_1 l_1 HH$ Majorana mass term for the neutrinos. In fact, the neutrino mass matrix is completely independent of H due to the Z_4 symmetry. In addition, there are no Yukawa couplings involving the neutrinos and the flavon ϕ_e due to Z_4 or/and Z_3 symmetry. The S_3 symmetry is broken spontaneously when the flavon ξ acquires a vacuum VEV:

$$\langle\xi\rangle = \begin{pmatrix} u_1 \\ u_2 \end{pmatrix} . \tag{6.8}$$

The $\mathrm{SU(2)_L}\times\mathrm{U_Y(1)}$ breaks at the electroweak scale by the VEV of the SU(2) doublet Higgs H. The VEV of the Higgs triplet is

$$\langle\Delta\rangle = \begin{pmatrix} \langle\Delta_1\rangle \\ \langle\Delta_2\rangle \end{pmatrix}, \qquad \text{where } \langle\Delta_i\rangle = \begin{pmatrix} 0 & 0 \\ v_i & 0 \end{pmatrix} . \tag{6.9}$$

The neutrino get masses due to the VEV of the Higgs triplet field Δ and as well as the standard model gauge singlet field ξ. The mass matrix of the neutrino is given as

$$m_\nu = \begin{pmatrix} 2y_4\frac{w}{\Lambda} & 2y_3v_2 & 2y_3v_1 \\ 2y_3v_2 & 2y_1\frac{u_2v_2}{\Lambda} & 2y_2\frac{w}{\Lambda} \\ 2y_3v_1 & 2y_2\frac{w}{\Lambda} & 2y_1\frac{u_1v_1}{\Lambda} \end{pmatrix} , \tag{6.10}$$

where $w = u_1v_2 + u_2v_1$. For the VEV alignments

$$v_1 = v_2, \quad \text{and} \quad u_1 = u_2 , \tag{6.11}$$

the neutrino mass matrix reduces to the form

$$m_\nu = \begin{pmatrix} 2y_4\frac{2u_1v_1}{\Lambda} & 2y_3v_1 & 2y_3v_1 \\ 2y_3v_1 & 2y_1\frac{u_1v_1}{\Lambda} & 2y_2\frac{2u_1v_1}{\Lambda} \\ 2y_3v_1 & 2y_2\frac{2u_1v_1}{\Lambda} & 2y_1\frac{u_1v_1}{\Lambda} \end{pmatrix} . \tag{6.12}$$

We discuss about the VEV alignments in section 6.4. Denoting $\frac{u_1}{\Lambda}$ as u_1' the mass matrix becomes

$$m_\nu = 2v_1 \begin{pmatrix} 2y_4u_1' & y_3 & y_3 \\ y_3 & y_1u_1' & 2y_2u_1' \\ y_3 & 2y_2u_1' & y_1u_1' \end{pmatrix} , \tag{6.13}$$

[1] The term $(l_l D_l \Delta)$ denotes $(l_l^T C i\tau_2 D_l \Delta)$, where C is the charge conjugation operator.

where $u'_1 = \frac{u_1}{\Lambda}$ and it is less than 1. Redefining $2y_4u'_1$ as y_4, $y_1u'_1$ as y_1 and $2y_2u'_1$ as y_2, the final form of the mass matrix is

$$m_\nu = 2v_1 \begin{pmatrix} y_4 & y_3 & y_3 \\ y_3 & y_1 & y_2 \\ y_3 & y_2 & y_1 \end{pmatrix} . \tag{6.14}$$

In the above matrix, for the VEV $u_1 = 0$, we would obtain the matrix

$$m_\nu = 2v_1y_3 \begin{pmatrix} 0 & 1 & 1 \\ 1 & 0 & 0 \\ 1 & 0 & 0 \end{pmatrix} . \tag{6.15}$$

This is a very well known form of the neutrino mass matrix which returns inverted neutrino mass spectrum with eigenvalues $\{-2\sqrt{2}v_1y_3, 2\sqrt{2}v_1y_3, 0\}$, and bimaximal mixing with $\theta_{23} = \theta_{12} = \pi/4$ and $\theta_{13} = 0$. The family symmetry considered in the literature for obtaining the form of the mass matrix given by Eq. (6.15) is $L_e - L_\mu - L_\tau$ [8]. However, exact bimaximal mixing is ruled out by the solar neutrino and KamLAND data [9]. Besides, as one can see from the eigenvalues of this neutrino mass matrix, that $\Delta m^2_{21} = 0$. This is untenable in the light of the experimental data. In order to generate the correct Δm^2_{21} and deviation of θ_{12} from maximal that is consistent with the data, one has to suitably perturb m_ν (for instance, in [10] the authors have build a model in the framework of the Zee-Wolfenstein ansatz). In the S_3 model that we consider here, this is very easily obtained if we allow non-zero VEV for ξ. The strength of the additional terms is linearly proportional to u_1/Λ and could be relatively small.

In what follows, we will consider all values of u_1/Λ from very small to ~ 1. The eigenvalues of the most general matrix given by Eq. (6.14) are[2]

$$m_i = v_1 \Big(y_1 + y_2 + y_4 - \sqrt{y_1^2 + y_2^2 + y_4^2 + 8y_3^2 + 2y_1y_2 - 2y_1y_4 - 2y_2y_4} \Big) , \tag{6.16}$$

$$m_j = v_1 \Big(y_1 + y_2 + y_4 + \sqrt{y_1^2 + y_2^2 + y_4^2 + 8y_3^2 + 2y_1y_2 - 2y_1y_4 - 2y_2y_4} \Big) , \tag{6.17}$$

$$m_3 = 2v_1 \Big(y_1 - y_2 \Big) . \tag{6.18}$$

In the above, $i, j = 1, 2$ and the only difference between m_i and m_j comes in the sign of the quantity within square root. We know that the solar neutrino data provides evidence for $\Delta m^2_{21} > 0$ at more than 6σ [9]. Therefore, the choice of m_1 and m_2 in Eqs. (6.16) and (6.17) is determined by the condition $m_2 > m_1$ *viz.*, the larger eigenvalue corresponds to

[2]For all analytical results given in this section we have assumed the model parameters to be real for simplicity. We check the phenomenological viability and testability of our model in the next section for complex Yukawa couplings.

m_2. The eigenvectors are given as

$$U_i = \begin{pmatrix} -\frac{y_1+y_2-y_4+\sqrt{a}}{2y_3 b} \\ \frac{1}{b} \\ \frac{1}{b} \end{pmatrix}~, \quad U_j = \begin{pmatrix} -\frac{y_1+y_2-y_4-\sqrt{a}}{2y_3 c} \\ \frac{1}{c} \\ \frac{1}{c} \end{pmatrix}~, \quad U_3 = \begin{pmatrix} 0 \\ -\frac{1}{\sqrt{2}} \\ \frac{1}{\sqrt{2}} \end{pmatrix}~, \tag{6.19}$$

where U_i corresponds to the eigenvalue given in Eq. (6.16) and U_j to that in Eq. (6.17). Whether $U_1 \equiv U_i$ or U_j depends on whether m_i is smaller or larger than m_j. The quantities b and c are the normalization constants given by

$$b^2 = 2 + \frac{(y_1 + y_2 - y_4 + \sqrt{a})^2}{(2y_3)^2}~, \tag{6.20}$$

and

$$c^2 = 2 + \frac{(y_1 + y_2 - y_4 - \sqrt{a})^2}{(2y_3)^2}~, \tag{6.21}$$

and a is given as

$$a = y_1^2 + y_2^2 + y_4^2 + 8y_3^2 + 2y_1y_2 - 2y_1y_4 - 2y_2y_4~. \tag{6.22}$$

From Eqs. (6.16), (6.17) and (6.18) we obtain

$$\begin{aligned} \Delta m^2_{21} &= 4\, v_1^2\, (y_1 + y_2 + y_4)\, \sqrt{a}~, \\ \Delta m^2_{31} &= v_1^2\, (3y_1 - y_2 + y_4 - \sqrt{a})(y_1 - 3y_2 - y_4 + \sqrt{a})~. \end{aligned} \tag{6.23}$$

The mixing angles can be seen from Eq. (6.19) to be

$$\begin{aligned} \theta^\nu_{13} &= 0~, \\ \tan\theta^\nu_{23} &= 1~, \\ \tan\theta^\nu_{12} &= \frac{(y_1 + y_2 - y_4 - \sqrt{a})\, b}{(y_1 + y_2 - y_4 + \sqrt{a})\, c}~. \end{aligned} \tag{6.24}$$

In the above, neither the ratio of the two mass squared differences $\Delta m^2_{21}/\Delta m^2_{31}$, nor the mixing angles depend on the value of the triplet VEV v_1. They only depend on the Yukawa couplings. Only the absolute mass square differences Δm^2_{21} and Δm^2_{31} individually depend on the triplet VEV. The effective neutrino mass predicted for neutrino-less double beta decay is given as

$$|m_{\nu_{ee}}| = |2v_1y_4|~, \tag{6.25}$$

while the effective mass squared observable in beta decay m^2_β and the total neutrino mass crucial for cosmology m_t are given as

$$m^2_\beta = \sum_i |m_i|^2|U_{ei}|^2~, \quad \text{and} \quad m_t = \sum_i |m_i|~, \tag{6.26}$$

respectively.

6.2.2 Charged Lepton Masses and Mixing

In this section we discuss the charged lepton masses. The Yukawa Lagrangian up to order $1/\Lambda^3$ giving the charged lepton mass is

$$\begin{aligned}
-\mathcal{L}_e^y &= \frac{\gamma}{\Lambda}\overline{\tau}_R H^\dagger(D_l\phi_e) + \frac{\gamma^b}{\Lambda^3}\overline{\tau}_R H^\dagger(D_l\phi_e)_{\underline{1}}(\xi\xi)_{\underline{1}} + \frac{\gamma'}{\Lambda^3}\overline{\tau}_R H^\dagger(D_l\phi_e)_{\underline{2}}(\xi\xi)_{\underline{2}} \\
&+\frac{\gamma'''}{\Lambda^3}\overline{\tau}_R H^\dagger(D_l\phi'_e)_{\underline{1}}(\phi_e\phi_e)_{\underline{1}} + \frac{\gamma^a}{\Lambda^3}\overline{\tau}_R H^\dagger(D_l\phi'_e)_{\underline{2}}(\phi_e\phi_e)_{\underline{2}} + \frac{\gamma''}{\Lambda^2}\overline{\tau}_R H^\dagger l_1(\phi_e\xi) \\
&+\frac{\beta'}{\Lambda^2}\overline{\mu}_R H^\dagger(D_l\phi_e\phi_e) + \frac{\beta''}{\Lambda^3}\overline{\mu}_R H^\dagger l_1(\phi_e\phi_e\xi) + \frac{\alpha''}{\Lambda^3}\overline{e}_R H^\dagger l_1(\phi_e\phi_e\phi_e) \\
&+\frac{\alpha'}{\Lambda^3}\overline{e}_R H^\dagger(D_l\phi'_e)_{\underline{1}}(\phi'_e\phi'_e)_{\underline{1}} + \frac{\alpha}{\Lambda^3}\overline{e}_R H^\dagger(D_l\phi'_e)_{\underline{2}}(\phi'_e\phi'_e)_{\underline{2}} + h.c + ...
\end{aligned} \tag{6.27}$$

While Z_4 symmetry was sufficient to get the desired m_ν, the extra Z_3 symmetry had to be introduced in order to obtain the correct form for the charged lepton mass matrix. The presence of the Z_4 symmetry ensures that the flavon doublet ϕ_e couples to charged leptons only. This is a prerequisite since we wish to break S_3 such that the $\mu-\tau$ symmetry remains intact for the neutrinos while it gets maximally broken for the charged leptons. For neutrinos the $\mu-\tau$ symmetry was kept intact by the choice of the vacuum alignments given in Eq. (6.11). To break it maximally for the charged leptons we choose the VEV alignment [7]

$$\langle\phi_e\rangle = \begin{pmatrix} v_c \\ 0 \end{pmatrix} . \tag{6.28}$$

Once S_3 is spontaneously broken by the VEVs of the flavons and $\mathrm{SU(2)_L \times U(1)_Y}$ by the VEV of the standard model doublet Higgs, we obtain the charged lepton mass matrix (leading terms only)[3]

$$m_{cl} = \begin{pmatrix} \alpha''\lambda^2 & 0 & 0 \\ \beta''\lambda u'_1 & \beta'\lambda & 0 \\ \gamma'' u'_2 & \gamma' {u'_2}^2 & \gamma \end{pmatrix} v\lambda , \tag{6.29}$$

where $v = \langle H\rangle$ is the VEV of the standard Higgs, $\lambda = v_c/\Lambda$, $u'_1 = u_1/\Lambda$ and $u'_2 = u_2/\Lambda$ The charged lepton masses and mixing matrix are obtained from

$$m^2_{l_{diag}} = U_l\, m_l m_l^\dagger\, U_l^\dagger , \tag{6.30}$$

giving the masses as

$$m_\tau \simeq \gamma\lambda v, \quad m_\mu \simeq \beta'\lambda^2 v, \quad m_e \simeq \alpha''\lambda^3 v . \tag{6.31}$$

[3]While this form of charged lepton mass matrix has been obtained using $Z_4 \times Z_3$ symmetry, similar viable forms can be obtained using other Z_n symmetries. For example, we have explicitly checked that $Z_6 \times Z_2$ and $Z_8 \times Z_2$ symmetries also give viable structure for m_{cl}.

For $\lambda \simeq 2 \times 10^{-2} \simeq \frac{\lambda_c^2}{2}$ where λ_c is the Cabibbo angle, the correct mass hierarchy of τ to μ to e as well as their exact numerical values can be obtained by choosing $\gamma = 0.36$, $\beta' = 1.01$ and $\alpha'' = 0.25$ and $v \sim 10^2$ GeV. In this present scenario the masses of the charged leptons do not depend on the VEV of ξ, however the mixing angles involved depend on this parameter. We have chosen $u_1' = u_2' \simeq \mathcal{O}(10^{-1})$, which is justified from large y_1 and y_2 in Fig.6.2 and large y_4 in Fig.6.3 and the perturbative nature of the Yukawa couplings. The large redefined y_1 and y_2 in Fig.6.2 and large redefined y_4 in Fig.6.3 suggest that $u_{1,2}'$ should not be much less than unity, which leads to the natural choice $u_{1,2}' \sim \mathcal{O}(10^{-1})$. For $u_1' = u_2' = u' \simeq 10^{-1}$ and γ', γ'' and β'' of the order unity, we get the charged lepton mixing angles as

$$\sin\theta_{12}^l \simeq \lambda^2, \quad \sin\theta_{23}^l \simeq 0.1\lambda, \quad \sin\theta_{13}^l \simeq 0.1\lambda^2 \ . \tag{6.32}$$

Since $U = U_l^\dagger U_\nu$, where U is the observed lepton mixing matrix and U_ν is the matrix which diagonalizes m_ν given by Eq. (6.12), the contribution of charged lepton mixing matrix would be very tiny. For $\sin\theta_{13}$ the maximum contribution from the charged lepton is $\mathcal{O}(10^{-4})$. In any case, in what follows we show all results for $U = U_l^\dagger U_\nu$.

6.3 Phenomenology

6.3.1 Exact $\mu - \tau$ Symmetry Limit

We have already presented in Eqs. (6.23) and (6.31) the expressions for the neutrino mass squared differences and charged lepton masses, while in Eqs. (6.24) and (6.32) we have given the mixing angles in the lepton sector in terms of model parameters. We argued that for $\lambda \simeq 2 \times 10^{-2} \simeq \frac{\lambda_c^2}{2}$, we obtain the charged lepton mass hierarchy in the right ballpark.

Since neutrino masses are directly proportional to v_1, it is phenomenologically demanded that the magnitude of this VEV should be small. In fact, since $\Delta m_{31}^2 \propto v_1^2$, we take $v_1^2 \sim 10^{-4} - 10^{-3}$ eV^2, and find that all experimentally observed neutrino masses and mixing constraints are satisfied. It is not unnatural to expect such a small value for v_1^2. For instance, in the most generic left-right symmetric models,

$$v_1 \equiv v_L \sim v^2/v_R \ , \tag{6.33}$$

where v is the electroweak scale and v_R is the VEV of the $\mathrm{SU(2)_R}$ Higgs triplet. It is natural to take $v_R \sim 10^{13} - 10^{15}$ GeV for which we get $v_1 \sim 1 - 10^{-2}$ eV.

Allowing v_1^2 to take any random value between $10^{-4} - 10^{-3}$ eV^2 we have checked that the neutrino mass spectrum obtained is hierarchical. For larger values of v_1 of course one would get larger values for the absolute neutrino mass scale and for $v_1 \sim 1$ eV, we expect a quasi-degenerate neutrino mass spectrum. In all our plots we keep v_1^2 between

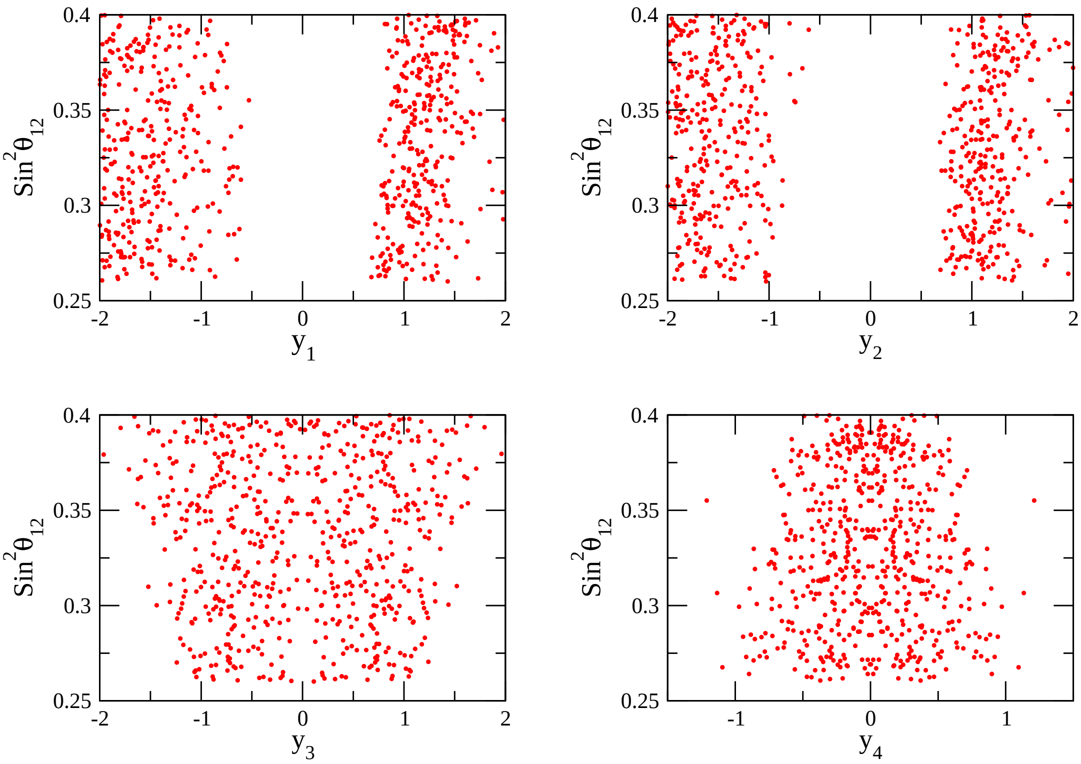

Figure 6.1: Scatter plots showing the range of the solar mixing angle $\sin^2\theta_{12}$ as a function of the model parameters in m_ν in the exact $\mu-\tau$ symmetry limit and for normal hierarchy. In each of the panels all other parameters except the one appearing in the x-axis are allowed to vary freely.

$10^{-4} - 10^{-3}$ eV^2. In Figure 6.1 we show the prediction for $\sin^2\theta_{12}$ as a function of the model parameters y_i's. In each panel we show the dependence of $\sin^2\theta_{12}$ on a given y_i, allowing all the others to vary randomly. Here we have assumed normal mass hierarchy for the neutrinos. For the charged lepton sector we have assumed a fixed set of model parameters which give viable charged lepton masses and we took $\lambda \simeq 2 \times 10^{-2}$. We note that for normal hierarchy ($\Delta m^2_{31} > 0$):

- $y_1 = 0$ and $y_2 = 0$ are not allowed.
- There is almost negligible dependence of $\sin^2\theta_{12}$ on y_1 and y_2 for $|y_1| > 1$ and $|y_2| > 1$ respectively.
- The range of $\sin^2\theta_{12}$ decreases with $|y_3|$ and $|y_4|$.

Figure 6.2 gives the scatter plots showing allowed ranges for the model parameters in two-dimensional parameter spaces, taking two parameters at a time and allowing the

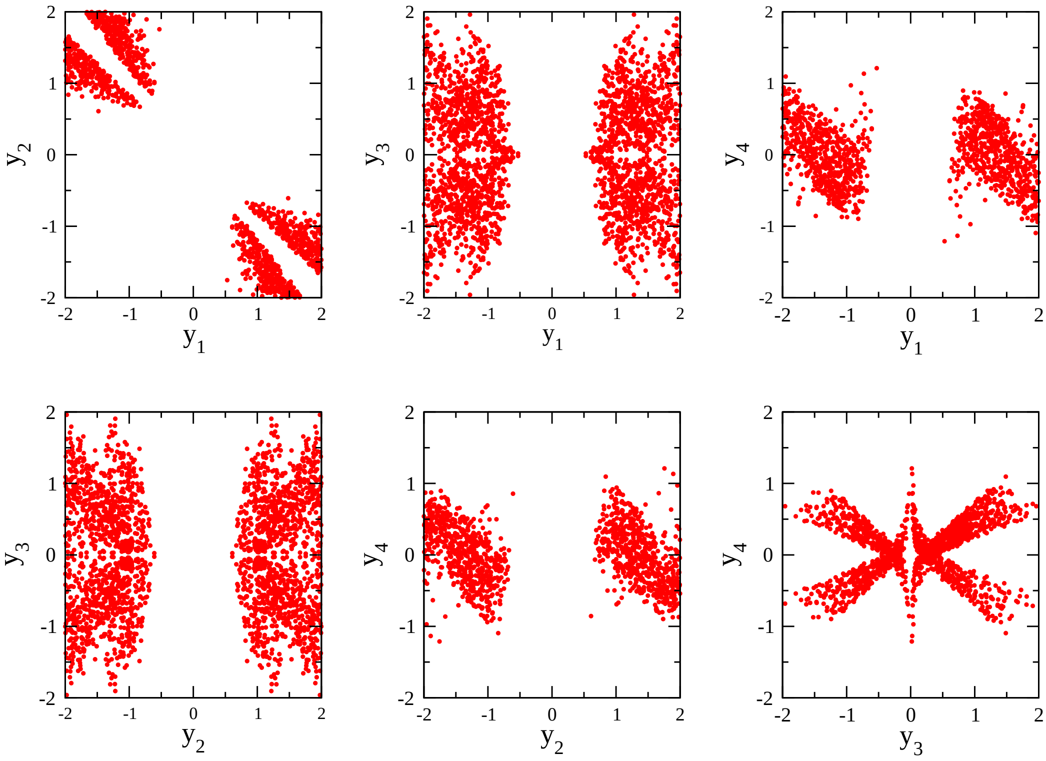

Figure 6.2: Scatter plots showing allowed ranges of the m_ν model parameters for the normal mass hierarchy in the exact $\mu-\tau$ symmetry limit. In each of the panels all other parameters except the one appearing in the x and y-axes are allowed to vary freely.

rest to vary freely. We have considered normal hierarchy in this figure. We note from the figure that for normal hierarchy:

- $y_1 = 0$ and $y_2 = 0$ are not allowed as we had seen before. With $y_1 = 0$ we would have obtained neutrino mass matrix Eq.(6.14) with two texture zeros in $\mu-\mu$ and $\tau-\tau$ elements and with $e-\mu$ and $e-\tau$ entries same in the mass matrix it will not be possible to get a normal-hierarchy [11]. However, as we will see from Figure 6.3 inverted hierchy can occur in this case. With $y_2 = 0$ one gets neutrino mass matrix with one texture zero in $\mu-\tau$ element which is not viable for normal ordering [12]. The allowed values of y_1 for normal hierarchy are highly correlated with the allowed values of y_2 and they are necessarily of opposite signs. One obtains a rough linear dependence between the allowed values of y_1 and y_2.

- $y_4 = 0$ is allowed and there is very little correlation of allowed values of y_4 with y_1 and y_2. For $y_4 = 0$, one gets a neutrino mass matrix Eq.(6.14) with one texture zero in $e-e$ element which can produce normal hierarchy only [12]. This predicts

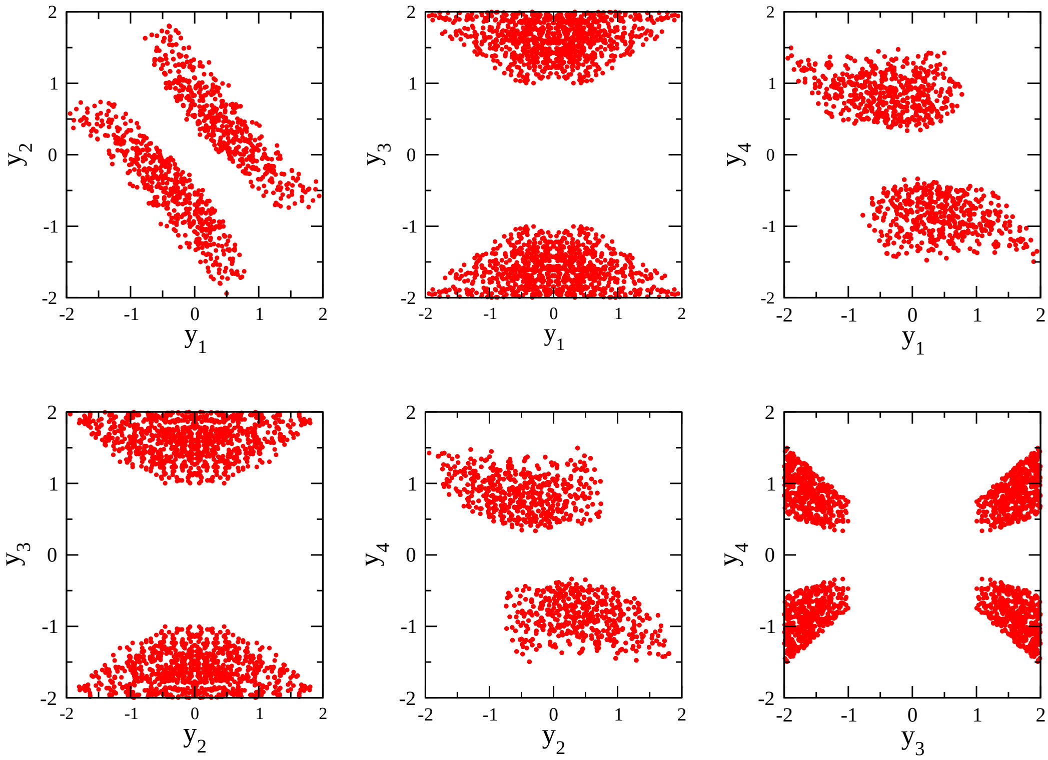

Figure 6.3: Same as Figure 6.2 but for inverted hierarchy.

$|m_{\nu_{ee}}| = 0$.

- y_3 and y_4 are strongly correlated.

In Figure 6.3 we show the corresponding allowed ranges for the model parameters for inverted hierarchy. In each of the panels, the parameters that do not appear on the x and y-axes are allowed to vary randomly. From a comparison of Figures 6.2 and 6.3 we can observe that the allowed areas in the parameter space is almost complementary[4]. We find that for the inverted hierarchy:

- $y_1 = 0$ and $y_2 = 0$ *simultaneously* are still not allowed, though now we can have $y_1 = 0$ or $y_2 = 0$ separately when the other parameter is within a certain favorable (non-zero) range. As for normal hierarchy, allowed values of y_1 and y_2 are highly correlated. As before there is a linear dependence between them.

[4]Of course the same set of model parameter values would *never* give both normal and inverted hierarchy simultaneously. However, we have shown two-dimensional projections of the model parameter space and hence their could be few overlapping points in the two figures.

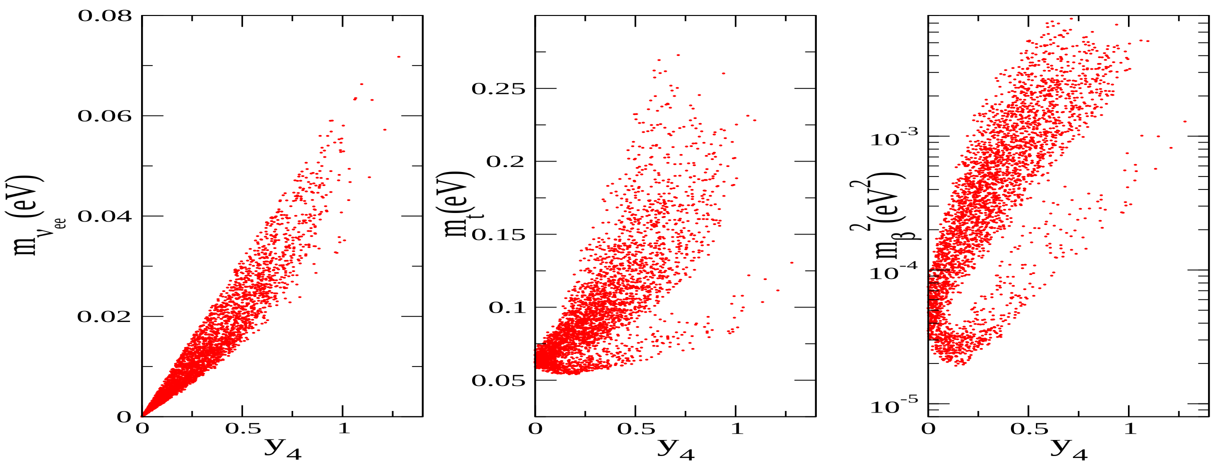

Figure 6.4: Scatter plots showing variation of $|m_{\nu_{ee}}|$, m_t and m_β^2 with the model parameter y_4.

- $y_3 = 0$ and $y_4 = 0$ are not allowed here.

  In the left panel of Figure 6.4 we show the variation of the effective neutrino mass $m_{\nu_{ee}}$ with the model parameter y_4. The effective mass predicted for neutrino-less double beta decay in our model is $|m_{\nu_{ee}}| = |2v_1 y_4|$. We have allowed v_1 to vary freely in the range $10^{-1} - 10^{-2}$. From Figure 6.4 one can clearly see that our model predicts $|m_{\nu_{ee}}| \lesssim 0.07$ eV. The next generation of neutrino-less double experiments are expected to probe down to $|m_{\nu_{ee}}| = 0.01 - 0.05$ eV [13]. The middle panel of this figure shows the total predicted neutrino mass m_t and right panel shows m_β^2. We find that the total neutrino mass m_t (in eV) varies within the range $0.05 < m_t < 0.28$, while the effective mass squared observable in beta decay $m_\beta^2 \simeq \mathcal{O}(10^{-4} - 10^{-2}) eV^2$. The KATRIN experiment will be sensitive to $m_\beta > 0.3$ eV [14].

6.3.2 Mildly Broken $\mu - \tau$ Symmetry Limit

So far we have *assumed* that the S_3 breaking in the neutrino sector is such that the residual $\mu - \tau$ symmetry is exact. This was motivated by the fact that S_2 is a subgroup of S_3 and we took a particular VEV alignment given in Eq. (6.11). We will discuss about VEV alignment in section 6.4. In this subsection we will assume that the $\mu - \tau$ symmetry is mildly broken. This could come from explicit $\mu - \tau$ breaking terms in the Lagrangian. In the next section we will see that in our model this comes after the minimization of the scalar potential due to the deviation of the VEV alignments from that given in Eq. (6.11). Small breaking of the VEV alignments could also come from radiative corrections and/or higher order terms in the scalar part of the Lagrangian. Any breaking of $\mu - \tau$

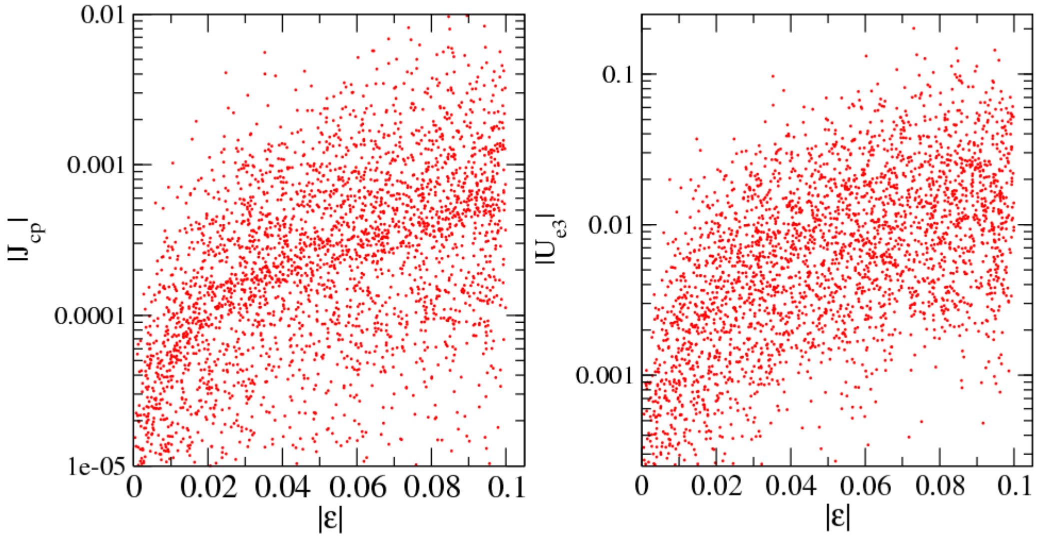

Figure 6.5: The Jarlskog invariant J_{CP} (left panel) and $\sin\theta_{13}$ as a function of the $\mu - \tau$ symmetry breaking parameter $|\epsilon|$.

symmetry will allow θ_{23} to deviate from maximal and θ_{13} from zero. Any non-zero θ_{13} will open up the possibility of low energy CP violation in the lepton sector. For the sake of illustration we consider a particular $\mu - \tau$ symmetry breaking for m_ν which results from the deviation of the VEV alignment from Eq. (6.11). We will see in the next section that this deviation is small and could come from $v_1 \neq v_2$ and/or $u_1 \neq u_2$. For the sake of illustration we consider only the breaking due to $v_1 \neq v_2$. We will see that from the minimization of the scalar potential one can take $v_1 = v_2(1+\epsilon)$. As a result the neutrino mass matrix (6.10) becomes

$$m_\nu = 2v_2 \begin{pmatrix} y_4 u'(2+\epsilon) & y_3 & y_3(1+\epsilon) \\ y_3 & y_1 u' & y_2 u'(2+\epsilon) \\ y_3(1+\epsilon) & y_2 u'(2+\epsilon) & y_1 u'(1+\epsilon) \end{pmatrix} . \tag{6.34}$$

We show the values of $|U_{e3}| \equiv \sin\theta_{13}$ predicted by the above m_ν as a function of the symmetry breaking parameter $|\epsilon|$ in the right panel of Figure 6.5. We have considered complex Yukawa coupling in this case. The left panel panel of this figure shows the Jarlskog invariant

$$J_{CP} = \mathrm{Im}\Big\{U_{e1}\, U_{\mu 2}\, U^*_{e2}\, U^*_{\mu 1}\Big\} \ , \tag{6.35}$$

as a function of $|\epsilon|$. We note that the model predicts values of $\sin\theta_{13}\lesssim 10^{-1}$ and $J_{CP}\lesssim 10^{-2}$ with the exact value determined by the extent of symmetry breaking. This could give $\sin^2 2\theta_{13} \lesssim 0.04$, which is just within the sensitivity reach of the forthcoming reactor experiments like Double Chooz [15] and long baseline accelerator experiments like T2K [16] and NOνA [17]. These values of θ_{13} and J_{CP} could give a large positive signal in the next generation high performance long baseline experiments using neutrino beams from Neutrino Factories, Superbeams and Beta-beams [18].

6.3.3 Collider Signature and Lepton Flavor Violation

Recent discussion on the analysis of the scalar potential and the Higgs mass spectrum for models with one triplet Higgs can be found in [19]. In our model with two Higgs triplets we get mixing between the two doubly charged Higgs Δ_1^{++} and Δ_2^{++}. The physical Higgs fields can be obtained from the scalar potential and are given by

$$\begin{aligned} H_1^{++} &= \Delta_1^{++}\cos\theta \,+\, \Delta_2^{++}\sin\theta \ , \\ H_2^{++} &= -\Delta_1^{++}\sin\theta \,+\, \Delta_2^{++}\cos\theta \ , \end{aligned} \tag{6.36}$$

where the mixing angle θ is

$$\tan 2\theta = \frac{e_2(u_1^2+u_2^2) + e_2' u_1 u_2}{h_6'(u_2^2-u_1^2) - h_6|v_c|^2} \ . \tag{6.37}$$

The parameters e_2, e_2', h_6 and h_6' are defined in Eq. (6.48). In the exact $\mu-\tau$ limit, which can be realized by setting $h_6 = 0$ and $h_6' = 0$ [5], the mixing angle θ is of course $\pi/4$. Even when h_6 and h_6' are $\neq 0$, since the couplings involved in Eq. (6.37) are expected to be of comparable strengths and since $v_c^2 << u_1^2$ (from the observed masses and mixing [6]) and $u_2^2 - u_1^2$ is expected to be small [7] we obtain nearly maximal mixing. In the approximate limit where we take $u_1 \simeq u_2 = u$ and neglect $|v_1|^2$, $|v_c|^2$ and v^2 in comparison to u^2, the square of the masses of the doubly charged Higgs are given by

$$M^2_{H_1^{++}} \simeq -a + u^2\ [(4e_1 + 2e_1') - (2e_2 + e_2')] \ , \tag{6.38}$$

$$M^2_{H_2^{++}} \simeq -a + u^2\ [(4e_1 + 2e_1') + (2e_2 + e_2')] \ . \tag{6.39}$$

[5] We will see this in the next section.

[6] $v_c^2/\Lambda^2 \sim 10^{-4}$ from charged lepton masses and from neutrino phenomenology $u_{1,2}^2/\Lambda^2 \sim 10^{-2}$, hence $v_c^2 \ll u_{1,2}^2$

[7] from neutrino phenomenology. Also see next section.

The quantities e_1, e'_1, e_2 and e'_2 are dimensionless coefficients in the scalar potential and will be explained in the next section. We will see in the next section that a in Eqs. (6.38) and (6.39) has a mass dimension 2 and comes as the co-efficient of the $\Delta_{1,2}^{++}\Delta_{1,2}^{--}$ term in the scalar potential. We note that the masses are modified due the mixing between Δ_1^{++} and Δ_2^{++}, and depend on the VEV u. The difference between the square of the masses of the two doubly charged Higgs depends only on u and the coefficients e_2 and e'_2. Measuring this mass squared difference at a collider experiment will provide a handle on the VEV u, which could then be used in conjunction with the lepton mass and mixing data to constrain the new scale Λ. In the most natural limit where we take all coupling constants e_1, e'_1, e_2 and e'_2 to be of the same order, then $M^2_{H_1^{++}} \simeq -a$ and $M^2_{H_2^{++}} \simeq -a + 9e_1u^2$.

The most distinctive signature of the existence of triplet Higgs can be obtained in collider experiments, through the production and subsequent decay of the doubly charged Higgs particle(s) [20–22]. The doubly charged Higgs, if produced, would decay through the following possible channels:

$$\begin{aligned} H^{++} &\rightarrow H^+H^+ \ , \\ H^{++} &\rightarrow H^+W^+ \ , \\ H^{++} &\rightarrow l^+\,l^+ \ , \\ H^{++} &\rightarrow W^+W^+ \ . \end{aligned} \tag{6.40}$$

In our model we have two doubly charged and two singly charged Higgs, however we have suppressed the corresponding indices in Eq. (6.40). Likewise, we have suppressed the flavor indices of the leptons. The first two decay modes depend on the mass difference between the singly and doubly charged Higgs and hence might be kinematically suppressed compared to the last two channels. We therefore do not consider them any further. The decay rate $H_{1,2}^{++} \rightarrow W^+W^+$ is proportional to the square of triplet Higgs VEVs $v_{1,2}$, while the decay rate to dileptons is inversely proportional to them. As a result the ratio of the decay rates for the two channels is proportional to $v_{1,2}^{-4}$ and is given as [21]

$$\frac{\Gamma(H_{1,2}^{++} \rightarrow l_a^+ l_b^+)}{\Gamma(H_{1,2}^{++} \rightarrow W^+W^+)} \approx \Big(\frac{m_\nu}{M_{H_{1,2}^{++}}}\Big)^2 \Big(\frac{v}{v_{1,2}}\Big)^4 \ , \tag{6.41}$$

where $M_{H_{1,2}^{++}}$ is the mass of the doubly charged Higgs and m_ν is the scale of neutrino mass. It has been shown [21] from a detailed calculation that for $M_{H_{1,2}^{++}} \simeq 300$ GeV and $v_{1,2} \lesssim 10^{-4}$ GeV, decay to dileptons will dominate. For our model $v_1^2 \approx v_2^2 \simeq 10^{-3} - 10^{-4}$ eV^2 and hence we can safely neglect decays to W^+W^+. The decay rate to dileptons is given as [20–22]

$$\Gamma(H_{1,2}^{++} \rightarrow l_a^+ l_b^+) = \frac{1}{4\pi(1+\delta_{ab})}|F_{ab}|^2 M_{H_{1,2}^{++}} \ , \tag{6.42}$$

while the branching ratio for this decay mode is

$$BR_{ab} = BR(H_{1,2}^{++} \to l_a^+ l_b^+) = \frac{2}{(1+\delta_{ab})} \frac{|F_{ab}|^2}{\Sigma_{ab}|F_{ab}|^2} , \tag{6.43}$$

where F_{ab} are the relevant vertex factors which directly depend on the form of the neutrino mass matrix. Using Eq. (6.7), we have tabulated in Table 6.2 the vertex factors for all possible interaction channels in our model. We see that apart from e-μ or e-τ combinations given in the table, all vertices have extra suppression factor of $\frac{u_{1,2}}{\Lambda}$. All other vertices arising from Eqs. (6.7) and (6.27) will involve the flavon fields ξ and/or ϕ and will be suppressed by higher orders in Λ. We therefore do not give them here. We had argued from Eq. (6.37) that in the exact $\mu - \tau$ symmetric limit $\theta = \pi/4$. One can then immediately see from Table 6.2 that $H_2^{++}ee$ and $H_2^{++}\mu\tau$ couplings are zero. Therefore, in the exact $\mu-\tau$ symmetric limit, the decay of H_2^{++} to ee and $\mu\tau$ is strictly forbidden. We have noted above that even when we do not impose exact $\mu - \tau$ symmetry, $\theta \approx \pi/4$ and hence these decay channels will be suppressed. The branching ratio of all the other decay modes are determined by the corresponding Yukawa couplings. Generally speaking, since all the vertices other than $H_{1,2}^{++}e\mu$ and $H_{1,2}^{++}e\tau$ are $\frac{u_{1,2}}{\Lambda}$ suppressed, branching ratio of these channels will be larger than all others, assuming equal values of y_1,y_2,y_3 and y_4. However, y_3 and y_4 could be small for normal hierarchy while inverted hierarchy could be produced for very small y_1 and y_2. This will give a handle on determining the neutrino parameters in general and the neutrino mass hierarchy in particular [22]. For instance, if the decay modes of doubly charged Higgs to $e\mu$ and $e\tau$ are not observed at a collider experiment, then it would imply small y_3, which would disfavor the inverted hierarchy.

Signature of doubly charged Higgs could in principle also be seen in lepton flavor violating processes. However, in the framework of our model the additional contribution to $l_i \to l_j\gamma$ are smaller than what is expected in the standard model. One can check from Table 6.2 that the only additional diagram which does not have any Λ (or $u_{1,2}/\Lambda$) suppression contributes to $\tau \to \mu\gamma$. However, even this diagram will be suppressed due to $M_{H_{1,2}^{++}} \gg M_W$ [23]. The presence of $H_{1,2}^{++}$ will allow the decay modes of the form $l_l \to l_i l_j l_k$ at the tree level, where l_i, l_j and l_k are leptons of any flavor. The branching ratios for $\mu \to eee$ and $\tau \to eee$ in our model for exact $\mu - \tau$ symmetry is given by [24]

$$BR(\mu \to eee) \simeq \frac{1}{16\, G_F^2} \frac{u_1^2}{\Lambda^2} \frac{|y_4^* y_3|^2}{M_{H_1^{++}}^4} . \tag{6.44}$$

Thus we see that even this process is suppressed by u_1^2/Λ^2 compared to other models with triplet Higgs. Branching ratio for all other lepton flavor violating decay modes such as $\tau \to \mu\mu\mu$ are further suppressed. The only decay mode which comes unsuppressed is $\tau \to ee\mu$, for which the branching ratio is given by

$$BR(\tau \to ee\mu) \simeq \frac{1}{4\, G_F^2} \frac{|y_3|^4}{M_{H_{1,2}^{++}}^4} . \tag{6.45}$$

Vertices	Vertex factors F_{ab}
$e\mu\ H_1^{++}$	$2y_3 sin\theta C P_L$
$e\mu H_2^{++}$	$2y_3 cos\theta C P_L$
$e\tau H_1^{++}$	$2y_3 cos\theta C P_L$
$e\tau H_2^{++}$	$2y_3 sin\theta C P_L$
$ee H_1^{++}$	$y_4 \frac{(sin\theta u_1 + cos\theta u_2)}{\Lambda} C P_L$
$ee H_2^{++}$	$y_4 \frac{(cos\theta u_1 - sin\theta u_2)}{\Lambda} C P_L$
$\mu\tau H_1^{++}$	$y_2 \frac{(sin\theta u_1 + cos\theta u_2)}{\Lambda} C P_L$
$\mu\tau H_2^{++}$	$y_2 \frac{(cos\theta u_1 - sin\theta u_2)}{\Lambda} C P_L$
$\tau\tau H_1^{++}$	$y_1 \frac{u_1}{\Lambda} cos\theta C P_L$
$\tau\tau H_2^{++}$	$y_1 \frac{u_1}{\Lambda} sin\theta C P_L$
$\mu\mu H_1^{++}$	$y_1 \frac{u_2}{\Lambda} sin\theta C P_L$
$\mu\mu H_2^{++}$	$y_1 \frac{u_2}{\Lambda} cos\theta C P_L$

Table 6.2: Doubly charged Higgs triplet and lepton vertices and the corresponding vertex factors F_{ab}, where a and b are generation indices. The charged lepton mass matrix is almost diagonal in our model. In this analysis we have considered that mass basis and flavor basis of the charged leptons are the same.

The current experimental constraint on this decay mode is $BR(\tau \to ee\mu) < 2 \times 10^{-7}$ [25], which constrains our model parameter y_3 as (assuming $M_{H_{1,2}^{++}} \sim 300$ GeV)

$$|y_3| \lesssim 10^{-1}\ . \tag{6.46}$$

In our model y_3 is predicted to be large for the inverted hierarchy while it could be tiny for the normal hierarchy. On the face of it then it appears that the bound given by Eq. (6.46) disfavors the inverted hierarchy for our model. However, recall that the allowed values of y_3 shown in Figs. 6.2 and 6.3 were presented assuming v_1^2 to lie between $10^{-3} - 10^{-4}$ eV^2. However, v_1^2 could be higher and since what determines the mass squared differences Δm_{21}^2 and Δm_{31}^2 is the product of v_1^2 and the Yukawas, higher v_1^2 would imply smaller values of the latter. For instance, we could have taken $v_1^2 \sim 10^{-1} - 10^{-2}$ eV^2 and in that case inverted hierarchy would still be allowed. The bound given by Eq. (6.46) has been obtained assuming $M_{H_{1,2}^{++}} \sim 300$ GeV. For more massive doubly charged Higgs the braching ratio would go down. On the other hand, if one uses bounds from lepton flavor violating decays to constrain the Yukawas, then one would obtain corresponding limits on the value of v_1. We conclude that with improved bounds on lepton flavor violating decay modes, one could test our model and/or the neutrino mass hierarchy predicted by our model.

6.4 The Vacuum Expectation Values

In this section we discuss about the necessary conditions which have to be satisfied, in order to achieve the VEV alignments required for $\mu - \tau$ symmetry. Up to terms of dimension four, the $S_3 \times Z_4 \times Z_3$ invariant scalar potential (cf. Table 6.1) is given by

$$V = \sum_i V_i \tag{6.47}$$

where

$$\begin{aligned}
V_1 &= -aTr[\Delta'\Delta] + b(Tr[\Delta'\Delta])^2 \\
V_2^a &= [-c(\xi\xi) + h.c] + c'(\xi'\xi) \\
V_2^b &= [d(\xi\xi)^{\underline{1}}(\xi\xi)^{\underline{1}} + h.c] + d'(\xi'\xi')^{\underline{2}}(\xi\xi)^{\underline{2}} + [d''(\xi'\xi)^{\underline{1}}(\xi\xi)^{\underline{1}} + h.c] \\
V_3^a &= [e_1 Tr[(\Delta'\Delta)^{\underline{1}}](\xi\xi)^{\underline{1}} + h.c] + e_1' Tr[(\Delta'\Delta)^{\underline{1}}](\xi'\xi)^{\underline{1}} \\
V_3^b &= [e_2 Tr[(\Delta'\Delta)^{\underline{2}}](\xi\xi)^{\underline{2}} + h.c] + e_2' Tr[(\Delta'\Delta)^{\underline{2}}](\xi'\xi)^{\underline{2}} \\
V_3^c &= h_6' Tr[\Delta'\Delta]^{\underline{1}'}(\xi'\xi)^{\underline{1}'} + h_6''(\xi'\xi)^{\underline{1}'}(\phi_e'\phi_e)^{\underline{1}'} \\
V_4 &= f_1 Tr[(\Delta'\Delta)^{\underline{1}}(\Delta'\Delta)^{\underline{1}}] + f_2 Tr[(\Delta'\Delta)^{\underline{1}'}(\Delta'\Delta)^{\underline{1}'}] + f_3 Tr[(\Delta'\Delta)^{\underline{2}}(\Delta'\Delta)^{\underline{2}}] \\
V_5 &= -h_1(\phi_e'\phi_e) + h_2(\phi_e'\phi_e')^{\underline{1}}(\phi_e\phi_e)^{\underline{1}} + h_3(\phi_e'\phi_e')^{\underline{2}}(\phi_e\phi_e)^{\underline{2}} \\
V_6 &= h_4 Tr[\Delta'\Delta]^{\underline{1}}(\phi_e'\phi_e)^{\underline{1}} + h_5 Tr[\Delta'\Delta]^{\underline{2}}(\phi_e'\phi_e)^{\underline{2}} + h_6 Tr[\Delta'\Delta]^{\underline{1}'}(\phi_e'\phi_e)^{\underline{1}'} \\
V_7^a &= [l_1(\xi\xi)^{\underline{1}}(\phi_e'\phi_e)^{\underline{1}} + h.c] + l_1''(\xi'\xi)^{\underline{1}}(\phi_e'\phi_e)^{\underline{1}} \\
V_7^b &= [l_2(\xi\xi)^{\underline{2}}(\phi_e'\phi_e)^{\underline{2}} + h.c] + l_2'(\xi'\xi)^{\underline{2}}(\phi_e'\phi_e)^{\underline{2}} + l_4(H^\dagger H)(\phi_e'\phi_e) \\
V_8 &= a_1 Tr[\Delta'\Delta](H^\dagger H) + [a_2(H^\dagger H)(\xi\xi) + h.c] - \mu^2(H^\dagger H) + \lambda(H^\dagger H)^2 \\
&\quad + r(H^\dagger\tau_i H)Tr[\Delta'\tau_i\Delta] + a_2''(H^\dagger H)(\xi'\xi)
\end{aligned} \tag{6.48}$$

The underline sign in the superscript represents the particular S_3 representation from the tensor product of the two S_3 doublets. The superscripts "2" without the underline represent the square of the term. The quantities with primes are obtained following Eq. (2.55)

$$\xi' = \sigma_1(\xi)^\dagger = \begin{pmatrix} \xi_2^\dagger \\ \xi_1^\dagger \end{pmatrix}, \quad \phi_e' = \sigma_1(\phi_e)^\dagger = \begin{pmatrix} \phi_2^\dagger \\ \phi_1^\dagger \end{pmatrix}, \quad \Delta' = \sigma_1(\Delta)^\dagger = \begin{pmatrix} \Delta_2^\dagger \\ \Delta_1^\dagger \end{pmatrix}. \tag{6.49}$$

The potential given by Eqs. (6.47) and (6.48) has to be minimized. The singlets ξ and ϕ_e pick up VEVs which spontaneously breaks the S_3 symmetry at some high scale, while Δ picks up a VEV when $\mathrm{SU(2)_L \times U(1)_Y}$ is broken at the electroweak scale. The VEVs have already been given in Eqs. (6.8), (6.9), and (6.28). For the sake of keeping the algebra simple we take the VEVs of Δ and ϕ_e to be complex but the VEVs of ξ to be real.

We denote $v_1 = |v_1|e^{i\alpha_1}, v_2 = |v_2|e^{i\alpha_2}$, where v_1 and v_2 are the VEVs of Δ_1 and Δ_2. Substituting this in Eqs. (6.47) and (6.48) we obtain

$$V = (-a + 4e_1u_1u_2 + e_1'(u_1^2 + u_2^2) + h_4|v_c|^2 + a_1v^2)(|v_2|^2 + |v_1|^2) + (b + f_1 + f_2)(|v_2|^2 + |v_1|^2)^2$$

$$
\begin{aligned}
&-4cu_1u_2 + c'(u_1^2+u_2^2) + 8du_1^2u_2^2 + d'(u_1^4+u_2^4) + 4d''u_1u_2(u_1^2+u_2^2) + 2(f_3-2f_2)|v_1|^2|v_2|^2 \\
&+2|v_1||v_2|[e_2(u_1^2+u_2^2) + e_2'u_1u_2]\ \cos(\alpha_2-\alpha_1) + (-h_1+4l_1u_1u_2)|v_c|^2 + l_1''|v_c|^2(u_1^2+u_2^2) \\
&+h_3|v_c|^4 + 4a_2v^2u_1u_2 + [-h_6|v_c|^2 + h_6'(u_2^2-u_1^2)](|v_2|^2-|v_1|^2) - h_6''(u_2^2-u_1^2)|v_c|^2 \\
&+a_2''v^2(u_1^2+u_2^2) + l_4v^2|v_c|^2 - \mu^2v^2 + \lambda v^4 \qquad (6.50)
\end{aligned}
$$

where we have absorbed r in the redefined a_1. The minimization conditions are:

$$\frac{\partial V}{\partial(\alpha_2-\alpha_1)} = 0\ , \qquad (6.51)$$

$$\frac{\partial V}{\partial(|v_1|)} = 0\ , \qquad (6.52)$$

$$\frac{\partial V}{\partial(|v_2|)} = 0\ , \qquad (6.53)$$

$$\frac{\partial V}{\partial u_1} = 0\ , \qquad (6.54)$$

$$\frac{\partial V}{\partial u_2} = 0\ , \qquad (6.55)$$

$$\frac{\partial V}{\partial|v_c|} = 0\ . \qquad (6.56)$$

From Eq. (6.51) we obtain the condition,

$$2|v_1||v_2|[e_2(u_1^2+u_2^2) + e_2'u_1u_2]\ \sin(\alpha_2-\alpha_1) = 0\ . \qquad (6.57)$$

Hence

$$\alpha_2 = \alpha_1\ , \qquad (6.58)$$

as long as $|v_1|, |v_2|$ and $[e_2(u_1^2+u_2^2) + e_2'u_1u_2]$ are $\neq 0$. Eq. (6.52) leads to the condition,

$$
\begin{aligned}
&-2a|v_1| + 4B(|v_2|^2+|v_1|^2)|v_1| + 2|v_1|[4e_1u_1u_2 + e_1'(u_1^2+u_2^2)] + 2|v_2|[e_2(u_2^2+u_1^2) + e_2'u_1u_2] \\
&+4F|v_1||v_2|^2 + 2h_4|v_1||v_c|^2 + 2a_1|v_1|v^2 + 2h_6|v_c|^2|v_1| - 2h_6'|v_1|(u_2^2-u_1^2) = 0\ , \qquad (6.59)
\end{aligned}
$$

where we have defined $B = (b + f_1 + f_2)$, $F = f_3 - 2f_2$ and we have used $\alpha_2 = \alpha_1$. Using Eq. (6.53) we obtain,

$$\begin{aligned}
&-2a|v_2| + 4B(|v_2|^2 + |v_1|^2)|v_2| + 2|v_2|[4e_1u_1u_2 + e_1'(u_1^2 + u_2^2)] + 2|v_1|[e_2(u_2^2 + u_1^2) + e_2'u_1u_2] \\
&+4F|v_2||v_1|^2 + 2h_4|v_2||v_c|^2 + 2a_1|v_2|v^2 - 2h_6|v_c|^2|v_2| + 2h_6'|v_1|(u_2^2 - u_1^2) = 0 \; . \qquad (6.60)
\end{aligned}$$

Multiplying Eq. (6.59) by $|v_2|$ and Eq. (6.60) by $|v_1|$ and subtracting one from the other we obtain,

$$(2e_2(u_1^2 + u_2^2) + 2e_2'u_1u_2 + 4F|v_1||v_2|)(|v_1|^2 - |v_2|^2) = 4|v_1||v_2|[h_6|v_c|^2 - h_6'(u_2^2 - u_1^2)] \quad (6.61)$$

In the limit $h_6 = 0$ and $h_6' = 0$ we get $|v_2| = |v_1|$ (if e_2, e_2' and $F \neq 0$ simultaneously), which is required for exact μ-τ symmetry in the neutrino sector. However, there is no *a priori* reason to assume that h_6, and h_6' are zero. In the most general case keeping non-zero h_6 and h_6', we obtain

$$|v_1|^2 = |v_2|^2 + \frac{4|v_1||v_2|[h_6|v_c|^2 - h_6'(u_2^2 - u_1^2)]}{2e_2(u_1^2 + u_2^2) + 2e_2'u_1u_2 + 4F|v_1||v_2|} \; . \qquad (6.62)$$

Since $|v_1||v_2| \ll u_1u_2$ [8] and $(u_1^2 + u_2^2)$ we neglect the $4F|v_1||v_2|$ term from the denominator. For $u_1 \simeq u_2 = u$ and $e_2 \simeq e_2'$, one obtains

$$|v_1|^2 = |v_2|^2 + \frac{2|v_1||v_2|h_6|v_c|^2}{3e_2u^2} \; . \qquad (6.63)$$

For a fixed v_2, this is a quadratic equation in v_1 which allows the solution $v_1 \simeq v_2(1 + \epsilon)$ where $\epsilon = \frac{h_6v_c^2}{3e_2u^2}$. For h_6 and e_2 of the same order and $\frac{u}{\Lambda} = 10^{-1}$, $\frac{v_c}{\Lambda} = 10^{-2}$ we obtain $\epsilon \simeq 10^{-2} \ll 1$. This would give rise to a very mild breaking of the $\mu - \tau$ symmetry. We have discussed this case in section 6.3.2.

Using Eqs. (6.54) and (6.55) and repeating the same exercise we get the deviation from $u_1 = u_2$ as

$$u_1^2 = u_2^2 + \frac{A}{B} \qquad (6.64)$$

where A and B are

$$A = 4u_1u_2[h_6''|v_c|^2 - h_6'(|v_2|^2 - |v_1|^2)] \qquad (6.65)$$

$$\begin{aligned}
B \;=\; &(-4c + 16du_1u_2 - 4d'u_1u_2 + 4d''(u_1^2 + u_2^2) + 4e_1(|v_1|^2 + |v_2|^2) + 2e_2'|v_1||v_2| + 4l_1|v_c|^2 \\
&+4a_2v^2) \; . \qquad (6.66)
\end{aligned}$$

[8] $v_{1,2}^2 \sim 10^{-3}/10^{-4}\text{eV}^2$, $u_{1,2}/\Lambda \sim 10^{-1}$ from neutrino phenomenology. Hence the hierarchy between the VEV's is justified.

Using the same arguments as above, it is not hard to see that the deviation from $u_1 = u_2$ is also mild. Again, $u_1 = u_2$ is satisfied when $h'_6 = 0$ and $h''_6 = 0$. Since $h_6 = 0$ is also required for $|v_1| = |v_2|$ to be satisfied, we conclude that exact $\mu - \tau$ symmetry for neutrinos demands that $h_6 = 0$, $h'_6 = 0$ and $h''_6 = 0$ simultaneously.

Finally, from the last minimization condition (6.56) we get the solution,

$$|v_c|^2 = \frac{1}{4h_3} \Big[2h_6(|v_2|^2 - |v_1|^2) + 2h''_6(u_2^2 - u_1^2) - 2l''_1(u_1^2 + u_2^2) + 2h_1 \\ -2h_4(|v_1|^2 + |v_2|^2) - 8u_1u_2l_1 - 2l_4v^2\Big] \, . \tag{6.67}$$

We next use use the condition (6.67) to estimate the cut-off scale Λ. Since h_1 define in Eq. (6.48) gives the square of the mass of the ϕ_e fields, it could be large. The other couplings h_3, l_1, l_4, h_4, h''_6, l''_1 and h_6 are dimensionless and can be assumed to have roughly the same order of magnitude which should be much much smaller than h_1. Dividing both sides of Eq. (6.67) by Λ^2 and using $|v_1|^2 \simeq |v_2|^2 = 10^{-3}$ eV^2, $\frac{v_c}{\Lambda} \simeq 2 \times 10^{-2}$, $\frac{u_{1,2}}{\Lambda} \simeq 10^{-1}$ and hence $(\frac{v_{1,2}}{\Lambda})^2 \ll (\frac{v_c}{\Lambda})^2 < (\frac{u_2^2-u_1^2}{\Lambda^2}) < (\frac{u_{1,2}}{\Lambda})^2$, we get [9]

$$\Lambda^2 \simeq \frac{h_1}{4l_1 + 2l''_1} \times 10^2 \text{ GeV}^2 \, . \tag{6.68}$$

The coupling h_1 has mass dimension 2 and in principle could be large. As an example, if we take h_1 in TeV range, for example if we take $\sqrt{h_1} = 10$ TeV, then the cut-off scale of the theory is fixed as 10^2 TeV, where we have taken l_1 and $l''_1 \simeq \mathcal{O}(1)$. From $\frac{u_1}{\Lambda} = \frac{u_2}{\Lambda} \sim 10^{-1}$ and $\frac{v_c}{\Lambda} \sim 10^{-2}$, we then obtain $u_{1,2} = 10$ TeV and $v_c = 1$ TeV. The constraints from the lepton masses themselves do not impose any restriction on the cut-off scale and the VEVs. One can obtain estimates on them only through limits on the masses of the Higgs. For instance, from Eqs. (6.38) and (6.39) one could in principle estimate u by measuring the difference between doubly charged Higgs masses. This could then be combined with the neutrino data to get Λ, and finally use the charged lepton masses to get v_c.

Since we consider a model with triplet Higgs to generate Majorana neutrino masses, it is pertinent to make some comments regarding breaking of lepton number and possible creation of a massless goldstone called Majoron [26]. It is possible to break lepton number explicitly by giving a lepton number to the fields ξ. In that case one would not break lepton number spontaneously and there would be no Majoron.

These VEV alignments have been obtained by assuming no effect of renormalization group running. However, it is understood that the running from the high scale where S_3 is broken to the electroweak scale where the masses are generated, will modify the

[9] h_6,h''_6=0 is motivated from $\mu - \tau$ symmetry, which together with $(\frac{v_1}{\Lambda})^2 \ll (\frac{v_c}{\Lambda})^2 < (\frac{u_1}{\Lambda})^2$ can also lead to Eq. 6.68. Even for a mild breaking of $\mu - \tau$ which leads to $(u_2^2 - u_1^2) \ll u_{1,2}^2$, the equation is valid.

VEV alignments. Another way the VEV alignments could get modified is through higher dimensional terms in the scalar potential. Due to the Z_4 as well as Z_3 symmetry that we have imposed, one cannot get terms of dimension five in the scalar potential. The possible next order terms in V would therefore be terms of dimension six. These terms would be suppressed by Λ^2 and are therefore expected to be much less important in V.

6.5 Conclusions

In this work, we have attempted to provide a viable model for the lepton masses and mixing by imposing a $S_3 \times Z_4 \times Z_3$ family symmetry. Our model has two $\mathrm{SU(2)_L}$ Higgs triplets arranged in the doublet representation of S_3. In addition we also have two sets of S_3 flavon doublets which are singlets with respect to the standard model. We have assigned the standard model fermions in suitable representation of S_3. We have obtained viable neutrino mass and mixing as well as the charged lepton mass hierarchy due to the VEV alignments. We have analyzed the normal and inverted mass hierarchy in detail. We gave predictions for $\sin^2\theta_{12}$, Δm^2_{21}, Δm^2_{31}, effective mass in neutrino-less double beta decay, the observed mass squared in direct beta decay and total mass of the neutrinos relevant to cosmological data. We have analyzed the potential and have shown in the most general case, one would obtain mild deviation from $\theta_{23} = \frac{\pi}{4}$ and $\theta_{13} = 0$. This will open up the possibility of CP violation in the leptonic sector. Production and subsequent decay of the doubly charged Higgs at particle colliders is a smoking gun signal for the existence of triplet Higgs. We relate the $\mu - \tau$ or mildly broken $\mu - \tau$ symmetry in the neutrino sector with the doubly charged Higgs decay modes in Colliders. We showed that in our model since the triplet VEV is required to be very small, decay to dileptons would predominate. In our model the mixing between the two doubly charged Higgs is very closely related with the extent of the $\mu - \tau$ symmetry in the neutrino sector. In the exact $\mu - \tau$ limit the mixing angle θ between the two doubly charged Higgs is $\theta = \frac{\pi}{4}$, whereas mild breaking of the $\mu - \tau$ symmetry results in a mild deviation $\theta \sim \frac{\pi}{4}$. This close connection between the $\mu - \tau$ symmetry and the doubly charged mixing angle significantly effects the doubly charged Higgs-dileptonic vertices. In the exact $\mu - \tau$ limit, the vertex factors $H_2^{++} - \mu - \tau$ and $H_2^{++} - e - e$ are zero, hence the doubly charged Higgs H_2^{++} never decays to $\mu^+ + \tau^+$ or to $2e^+$ states. Other than this, the non observation of the $e\mu$ and $e\tau$ states in the dileptonic decay of the doubly charged Higgs would possibly disfavor the inverted mass hierarchy of the standard model neutrino. Hence, the lepton flavors involved in the final lepton pair could be used to distinguish this model from the other models with triplet Higgs as well as to distinguish the inverted and normal hierarchy. Our model predicts lepton flavor violating processes such at $\tau \to ee\mu$ at the tree level. This and other lepton flavor violating processes could therefore be used to constrain the model as well as the neutrino mass hierarchy.

Bibliography

[1] E. Ma, Phys. Rev. D **44**, R587 (1991); Y. Koide, Phys. Rev. D **60**, 077301 (1999); M. Tanimoto, Phys. Lett. B **483**, 417 (2000); J. Kubo, Phys. Lett. B **578**, 156 (2004) [Erratum-ibid. B **619**, 387 (2005)]; F. Caravaglios and S. Morisi, arXiv:hep-ph/0503234; S. Morisi and M. Picariello, Int. J. Theor. Phys. **45**, 1267 (2006).

[2] P. F. Harrison and W. G. Scott, Phys. Lett. B **557**, 76 (2003).

[3] W. Grimus and L. Lavoura, JHEP **0508**, 013 (2005).

[4] R. N. Mohapatra, S. Nasri and H. B. Yu, Phys. Lett. B **639**, 318 (2006).

[5] N. Haba and K. Yoshioka , Nucl. Phys. B **739**,254 (2006).

[6] C. Y. Chen and L. Wolfenstein, Phys. Rev. D **77**, 093009 (2008); S. Kaneko, H. Sawanaka, T. Shingai, M. Tanimoto and K. Yoshioka, arXiv:hep-ph/0703250; Y. Koide, Eur. Phys. J. C **50**, 809 (2007); Y. Koide, Phys. Rev. D **73**, 057901 (2006); T. Teshima, Phys. Rev. D **73**, 045019 (2006); F. Caravaglios and S. Morisi, arXiv:hep-ph/0503234; L. Lavoura and E. Ma, Mod. Phys. Lett. A **20**, 1217 (2005); T. Araki, J. Kubo and E. A. Paschos, Eur. Phys. J. C **45**, 465 (2006); N. Haba, A. Watanabe and K. Yoshioka , Phys. Rev. Lett **97**, 041601 (2006).

[7] F. Feruglio and Y. Lin, Nucl. Phys. B **800**, 77 (2008) [arXiv:0712.1528 [hep-ph]].

[8] S. T. Petcov, Phys. Lett. B **110**, 245 (1982); for more recent studies see, e.g., R. Barbieri *et al.*, JHEP **9812**, 017 (1998); A. S. Joshipura and S. D. Rindani, Eur. Phys. J. C **14**, 85 (2000); R. N. Mohapatra, A. Perez-Lorenzana and C. A. de Sousa Pires, Phys. Lett. B **474**, 355 (2000); W. Grimus and L. Lavoura, Phys. Rev. D **62**, 093012 (2000); K. S. Babu and R. N. Mohapatra, Phys. Lett. B **532**, 77 (2002); H. J. He, D. A. Dicus and J. N. Ng, Phys. Lett. B **536**, 83 (2002) H. S. Goh, R. N. Mohapatra and S. P. Ng, Phys. Lett. B **542**, 116 (2002);

[9] S. Choubey, arXiv:hep-ph/0509217; S. Goswami, Int. J. Mod. Phys. A **21**, 1901 (2006); A. Bandyopadhyay, S. Choubey, S. Goswami, S. T. Petcov and D. P. Roy, Phys. Lett. B **608**, 115 (2005); G. L. Fogli *et al.*, Prog. Part. Nucl. Phys. **57**, 742

(2006); M. Maltoni, T. Schwetz, M. A. Tortola and J. W. F. Valle, New J. Phys. **6**, 122 (2004) [arXiv:hep-ph/0405172].

[10] B. Brahmachari and S. Choubey, Phys. Lett. B **642**, 495 (2006).

[11] P. H. Frampton, S. L. Glashow and D. Marfatia, Phys. Lett. B **536**, 79 (2002); Z. Z. Xing, Phys. Lett. B **530**, 159 (2002); B. Desai, D. P. Roy and A. R. Vaucher, Mod. Phys. Lett. A **18**, 1355 (2003).

[12] A. Merle and W. Rodejohanm, Phys. Rev. D **73**, 073012 (2006).

[13] F. T. Avignone, Nucl. Phys. Proc. Suppl. **143**, 233 (2005).

[14] A. Osipowicz *et al.* [KATRIN Collaboration], arXiv:hep-ex/0109033.

[15] K. Anderson *et al.*, arXiv:hep-ex/0402041.

[16] Y. Itow *et al.*, arXiv:hep-ex/0106019.

[17] D. S. Ayres *et al.* [NOvA Collaboration], arXiv:hep-ex/0503053.

[18] A. Bandyopadhyay *et al.* [ISS Physics Working Group], arXiv:0710.4947 [hep-ph].

[19] P. Dey, A. Kundu and B. Mukhopadhyaya, arXiv:0802.2510 [hep-ph].

[20] A. Abada*et al*, JHEP 0712:061 (2007); A. G. Akeroyd, M. Aoki and H. Sugiyama, Phys. Rev. D **77**, 075010 (2008).

[21] P. Fileviez*et al.* Phys. Rev. D **78**, 015018 (2008).

[22] J. Garayoa and T. Schwetz, JHEP 0803:009 (2008).

[23] S. M. Bilenky and S. T. Petcov, Rev. Mod. Phys. **59**, 671 (1987) [Erratum-ibid. **61**, 169.1989 ERRAT,60,575 (1989 ERRAT,60,575-575.1988)]; R. N. Mohapatra, Phys. Rev. D **46**, 2990 (1992).

[24] M. Kakizaki, Y. Ogura and F. Shima, Phys. Lett. B **566**, 210 (2003).

[25] W. M. Yao *et al.* [Particle Data Group], J. Phys. G **33** (2006) 1.

[26] G. B. Gelmini and M. Roncadelli, Phys. Lett. B **99**, 411 (1981); Y. Chikashige, R. N. Mohapatra and R. D. Peccei, Phys. Lett. B **98**, 265 (1981); J. Schechter and J. W. F. Valle, Phys. Rev. D **22**, 2227 (1980); T. P. Cheng and L. F. Li, Phys. Rev. D **22**, 2860 (1980).

Chapter 7

Conclusion

In this thesis we have looked into different aspects of beyond standard model physics and its connection to neutrino masses and mixings. From a series of outstanding experiments like solar and atmospheric neutrino experiments, KamLAND, K2K, MINOS we have the information about the standard model neutrino mass splittings and its very peculiar mixing angles. Combined with cosmological bound specially from WMAP data, the sum of the light neutrino masses are bounded within eV range, while the observed solar and atmospheric mass splittings from the different oscillation experiments are $\Delta m^2_{21} \sim 10^{-5}$ $\mathrm{eV}^2$and $\Delta m^2_{31} \sim 10^{-3}$ eV^2 respectively. Hence, the standard model neutrinos have extremely tiny mass, which is 10^{12} order smaller as compared to the top quark mass. The aesthetic belief of unification suggests that the standard model should be embedded in a higher ranked gauge group, for example SU(5) or SO(10). Although the quarks and leptons in a higher ranked gauge group belong to same representation, however the mixing in the leptonic sector is drastically different than the mixings in the quark sector. Unlike the mixing in the quark sector, in the leptonic sector two of the mixing angles θ_{12} and θ_{23} are quite large ($\sin^2\theta_{12} \sim 0.32$, $\sin^2\theta_{23} \sim 0.46$) while at present there is an upper bound on the third mixing angle θ_{13} as $\sin^2\theta_{13} < 0.05$. The observed mixing angles are in very close agreement with the tribimaximal mixing pattern where the solar mixing angle is $\sin^2\theta_{12} = 0.33$, reactor mixing angle $\sin^2\theta_{13} = 0.0$ and the atmospheric mixing angle is maximal $\sin^2\theta_{23} = 0.5$. The maximal mixing angle θ_{23} and $\theta_{13} = 0$ point towards a possible $\mu - \tau$ symmetry in the neutrino sector. Going beyond the standard model, seesaw mechanism can explain small neutrino masses very naturally, without fine tuning of Yukawa to extremely small values. The Majorana mass of the standard model in this scheme is generated from the dimension-5 *Weinberg* operator $\frac{LLHH}{M}$, and is hence naturally suppressed by the large mass scale M of the integrated out heavy modes. However, the mixings in the leptonic sector still remain unexplained. The mixing angles in the leptonic sector can be explained very naturally if one imposes flavor symmetry.

We have discussed the standard model, its drawbacks and the minimal supersymmetric standard model in chapter 1. Chapter 2 was devoted to neutrino mass and mixing, the different seesaw realizations. In chapter 3 [1] we built a model on type-III seesaw and have studied its detail phenomenology. In type-III seesaw, SU(2) triplet fermion gets integrated out and generate the dimension-5 *Weinberg* operator. The triplet fermions which transform as an adjoint representation of SU(2), contain two charged fermionic states ($\Sigma^{\pm}$) and one charge neutral Majorana fermionic state (Σ^0). Being SU(2) triplet, the triplet fermions offers a distinctive feature as compared to the type-I seesaw mechanism, where the gauge singlet Majorana neutrino generate the *Weinberg* operator. The gauge singlet right handed neutrino field of type-I seesaw interacts with the lepton and Higgs via the Yukawa Lagrangian, while its interaction with the gauge bosons is suppressed by the standard model neutrino-gauge singlet right handed neutrino mixing. Compared to this, the $\mathrm{SU(2)_L}$ triplet fermion interacts directly with the standard model gauge bosons through their kinetic term, as well as with the leptons and the Higgs via the Yukawa Lagrangian. Hence for the 100 GeV mass range, the triplet fermions can be produced copiously at LHC, opening up the possibility to test the seesaw at LHC. Since the standard model neutrino masses are $M_\nu \simeq -Y_\Sigma^T M^{-1} Y_\Sigma v^2$, hence for triplet fermion mass $M = \mathcal{O}(10^2)$ GeV, the Yukawa coupling Y_Σ between the triplet fermions-Higgs doublet-leptonic doublet gets constrained as $Y_\Sigma \sim 10^{-6}$ by the eV neutrino mass. This in a way tentamounts to fine tuning of the Yukawas, and smothers out the very motivation for the seesaw mechanism, which was to explain the smallness of the neutrino mass without unnaturally reducing the Yukawa couplings. We show that the large Yukawa coupling and few hundred GeV triplet fermions are still possible with the addition of another $\mathrm{SU(2)_L} \times \mathrm{U(1)_Y}$ Higgs doublet to this existing setup [1].

In our model we have considered three sets of right handed triplet fermionic fields Σ_i, and one additional Higgs doublet Φ_2. In addition, we also have introduced one discrete Z_2 symmetry, softly broken by the Higgs potential. The additional Higgs field Φ_2 (Z_2 odd) has the same SU(2) and $\mathrm{U(1)_Y}$ transformations as the standard model Higgs doublet Φ_1(Z_2 even), only differing in its Z_2 charge assignment. Hence in the Yukawa Lagrangian, the additional Higgs field Φ_2 interacts only with the standard model leptons (Z_2 even) and the triplet fermions (Z_2 odd), whereas the standard model Higgs Φ_1 interacts with all other standard model fermionic fields. Due to the very specific nature of the Yukawa Lagrangian, the standard model neutrino and the triplet fermionic neutral component mixing is governed by the vacuum expectation value v' of the additional Higgs doublet. Hence small vacuum expectation value $v' \sim 10^{-4}$ GeV generates eV neutrino mass, even with large $\mathcal{O}(1)$ Yukawa coupling Y_Σ. The charged lepton and quark masses in this model are determined by the large vacuum expectation value $v \sim 100$ GeV of the standard model Higgs doublet.

The choice of the small vacuum expectation value of the additional Higgs field has a significant impact on determining the Higgs mass spectra and the mixing angle between the neutral Higgses. With two Higgs doublets the Higgs sector in our model is enriched with five physical degrees of freedom (H^0, h^0, A^0, $H^\pm$). Working within the framework of a softly broken Z_2 symmetry, the mass of the light Higgs h^0 is determined by the standard model Higgs vacuum expectation value ($v \sim 10^2$ GeV) as well as by the extent of the Z_2 symmetry breaking coupling λ_5, whereas all the other Higgs masses are governed by the standard model Higgs vacuum expectation value v. Hence, in our model it is possible to accommodate a light Higgs state h^0. However, the presence of the light Higgs does not violate the LEP bound, due to the vanishingly small $Z-Z-h^0$ coupling. Due to the order of magnitude difference between the two vacuum expectation values v and v', the mixing angle α between the two neutral Higgs h^0 and H^0 is proportional to the ratio of the two vacuum expectation values ($\tan\beta = \frac{v'}{v}$) and is extremely small $\tan 2\alpha \sim \tan\beta \sim 10^{-6}$.

We have studied in detail the production and subsequent decay of the triplet fermions at LHC. Triplet fermion production at the LHC is mostly governed by the gauge boson mediated partonic subprocesses. Once produced, the triplet fermion can decay to different final state particles such as to a lepton+Higgs or to a lepton+ gauge boson. In our model, due to the large Yukawa coupling Y_Σ and small value of the mixing angle α as well as $\tan\beta$, the triplet fermions ($\Sigma^\pm$, Σ^0) decay predominantly into standard model leptons along with the neutral and charged Higgses h^0, A^0, $H^\pm$. The other decay modes where triplet fermions decay into a standard model lepton along with the neutral Higgs H^0 or the standard model gauge bosons is highly suppressed. The dominant decay of the triplet fermion into a standard model lepton and a Higgs h^0, A^0, $H^\pm$ is more than 10^{11} times larger compared to the one Higgs doublet type-III seesaw scenario.

The different decay modes of the triplet fermions are inherently linked with the neutrino phenomenology. In particular, the exact or approximate $\mu - \tau$ symmetry in the neutrino sector distinguishes among the different leptonic states when the triplet fermion decays into a standard model lepton and a Higgs. The $\mu - \tau$ symmetry in the neutrino sector provide equal opportunity to μ and τ states to be the leptonic final states, whereas it forbids the third generation of charged triplet fermions to decay into electron state e in the decay of 3rd generation of triplet fermions..

We have also looked into different Higgs decay modes and the possible collider signatures of our model. In the Higgs sector, the different Higgs decay modes are governed by the Yukawa couplings and also by the small mixing angle α as well as $\tan\beta$. The neutral Higgs predominantly decays to $2b$ while the dominant decay mode for the charged Higgs $H^\pm$ is $H^\pm \to W^\pm h^0$. Other than this, a distinctive feature of our model is the displaced vertex of the Higgs h^0. Unlike the type-III seesaw with one Higgs doublet, in our model the triplet fermions do not have any displaced vertex. The type-III seesaw with two Higgs doublet can be verified at LHC via the different collider signatures which this model offers. We have calculated the effective cross sections for these channels.

In charper 4 [2], we have build a model of R-parity violating supersymmetry and discussed the neutrino mass generation. The observed data on solar and atmospheric neutrino mass splitting constrains the number of triplet fermion generation to be minimally two. However the R-parity violating supersymmetric framework enables a viable description of the neutrino mass and mixing even with one generation of triplet matter chiral superfield which has R-parity -1 [2]. R-parity which is a discrete symmetry is defined as $R_p = (-1)^{3(B-L)+2S}$ and has been implemented in the minimal supersymmetric extension of the standard model to forbid the baryon number ($\hat{U}^c\hat{D}^c\hat{D}^c$) and the lepton number violating ($\hat{L}\hat{L}\hat{E}^c$, $\hat{L}\hat{Q}\hat{D}^c$) operators. Non-observation of proton decay constrains the simultaneous presence of lepton and baryon number violation, however leaving some space for the individual presence of either of these two. To accommodate the Majorana mass term of the standard model neutrino, lepton number violation is required. Spontaneous violation of R-parity meets both ends, it generates neutrino mass and satisfies the proton decay constraint, as in this scheme, the R-parity violating operators are generated very selectively. In our model R-parity is spontaneously broken by the vacuum expectation value of the different sneutrino fields. As a consequence, only the lepton number violating bilinear operators are generated while working in the weak basis. Sticking to the framework of the perturbative renormalizable field theory, the baryon number violating operators ($\hat{U}^c\hat{D}^c\hat{D}^c$) would never be generated, hence naturally satisfying the proton decay constraint. Because of the R-parity violation, the standard model neutrinos ν_i mix with the triplet fermion Σ^0, as well as with the Higgsino $\tilde{h}_u^0$ and gauginos $\tilde{\lambda}_{3,0}^0$. Hence, in our model we have a 8×8 color and charge neutral fermionic mass matrix. With one generation of the triplet matter chiral superfield and the R-parity violation, two of the standard model neutrino masses can be generated as a consequence of the conventional seesaw along with the gaugino seesaw, while the third neutrino still remains massless. Hence, in this scenario viable neutrino masses and mixings are possible to achieve. In addition, the standard model charged leptons ($l^{\pm}$), triplet fermions ($\Sigma^{\pm}$) and the charginos ($\tilde{\lambda}^{\pm}, \tilde{h}_{u,d}^{\pm}$) mixing is also determined by the different R-parity violating vacuum expectation values, as well as the different couplings of the superpotential. Hence, the charged lepton mass matrix is an extended 6×6 matrix. In our model the spontaneous violation of R-parity is not associated with any global $U(1)$ lepton number breaking, since we break lepton number explicitly. Hence, the spontaneous R-parity violation is not associated with generation of any Majoron. We have explicitly analyzed the scalar potential and the minimization condition and have shown that the different R-parity violating sneutrino vacuum expectation values u, $\tilde{u}$ in our model share a proportionality relation. From the neutrino phenomenology these vacuum expectation values are bounded to be small $u, \tilde{u} < 10^{-3}$ GeV, where we have considered gaugino masses of the order of few hundred GeV. We have discussed very briefly about the possible collider signatures which this model can offer.

While the smallness of the neutrino mass can be explained via the seesaw mechanism, the very particular mixing of the standard model neutrinos can be well explained by invoking a suitable flavor symmetry. Among the widely used flavor symmetry groups, A_4 and S_3 are very promising ones. We have discussed in detail about the group theoretical aspects of the flavor symmetry groups A_4 and as well as S_3 in chapter 2, while in chapter 5 [3] we have build a model based on the group A_4. We have considered the most generic scenario with all possible one dimensional Higgs representations that can be accommodated within this A_4 model. The Higgs fields which are charged under the symmetry group A_4, are standard model gauge singlets and they are knows as flavons. In our model [3] we have two flavon fields $\phi_{S,T}$ which transform as three dimensional irreducible representation of the group A_4. In addition, we also have three other flavons ξ, ξ', ξ'' which transform as 1, $1'$ and $1''$ respectively. The Lagrangian describing the Yukawa interaction between the different standard model leptons, Higgs and the flavons follows the effective field theoretical description. The different flavon fields take the vacuum expectation values, thereby resulting in a spontaneous breaking of the symmetry group A_4. We have explored the conditions on VEVs and Yukawa couplings needed for obtaining exact TBM mixing in this present set-up. In particular, we have checked which combinations of the different one dimensional Higgs fields ξ, ξ' and ξ'' would produce TBM mixing and under what conditions. We have explicitly shown that the A_4 triplet field ϕ_S can alone generate the tribimaximal mixing in the neutrino sector if all the vacuum expectation values v_{s_i} of its component fields are equal. However it gives the atmospheric mass splitting $\Delta m^2_{31} = 0$, and hence is clearly incompatible with the neutrino oscillation data. To generate viable neutrino mass splittings in association with tribimaximal mixing, the one dimensional representations has to be included. Although the representation 1 which was originally proposed by Altarelli and Feruglio is the minimalistic choice to recover the correct mass, this particular choice ends up with a severe fine-tuning between the different parameters of the theory. The product of the VEV and Yukawa of this singlet is determined completely by the VEV and Yukawa of the triplet. Other than this, the normal hierarchy ($\Delta m^2_{31} > 0$) between the standard model neutrino masses is the only allowed possibility. Inverted hierarchy can be possible if we have at least two or all three Higgs scalars with nonzero VEVs. The extreme fine-tuning in the parameter space is also gets reduced if one introduces two or three flavon fields at a time. Deviation from the particular relations between the different Higgs vacuum expectation values and Yukawas will lead to deviation from tribimaximal mixing. In the charged lepton sector the diagonal charged lepton mass matrix emerges as a consequence of an additional discrete symmetry Z_3, as well as the vacuum alignment of the flavon field ϕ_T.

In chapter 6 we have constructed a flavor model based on the symmetry group S_3 [4], which reproduces the observed neutrino mass and mixing, as well as the standard model charged lepton mass hierarchy. We use two SU(2) Higgs triplets (Δ) with hypercharge $Y = 2$, arranged in a doublet of S_3, and the standard model singlet Higgs (ϕ_e, ξ) which are also put as doublets of S_3. Due to the appropriate charge assignment under additional discrete symmetry groups Z_4 and Z_3, the flavon ϕ_e enters only in the charged lepton Yukawa, whereas the other flavon ξ enters both in the neutrino as well as in the charged lepton Yukawa. The Higgs triplets Δ and the flavon field ξ take vacuum expectation value, and generate standard model neutrino masses. To reproduce the observed lepton masses and mixings, the symmetry group S_3 has to be broken such that the neutrino sector contains the exact/approximate Z_2 symmetry along the $\nu_\mu - \nu_\tau$ direction, while it is broken down maximally in the charged lepton sector. This particular feature is achieved by the vacuum alignments of the different Higgs fields Δ, ϕ_e and ξ. Exact $\mu - \tau$ symmetry in the neutrino mass matrix is achieved as a consequence of the vacuum alignments $\langle\Delta_1\rangle = \langle\Delta_2\rangle$ and $\langle\xi_1\rangle = \langle\xi_2\rangle$, otherwise resulting in mildly broken $\mu - \tau$ symmetry. The mild breaking of $\mu - \tau$ symmetry opens up the possibility of CP violation in the leptonic sector. We have analyzed the potential and we show that under the most general case, the minimization condition predicts a very mild breaking of the $\mu - \tau$ symmetry for the neutrinos. The charged lepton sector offers very tiny contribution to the physically observed PMNS mixing matrix, while the main contribution comes from the neutrino mixing matrix. In the neutrino sector both normal and inverted hierarchy are allowed possibilities.

Since the Higgs triplet Δ interacts with the gauge bosons via their kinetic terms, they can be produced at the LHC and then can be traced via their subsequent decays. The doubly charged Higgs can decay to different states such as dileptons, gauge bosons, singly charged Higgs H^+. In our model the mixing between the two doubly charged Higgs is very closely related with the extent of the $\mu - \tau$ symmetry in the neutrino sector. In the exact $\mu - \tau$ limit the mixing angle θ between the two doubly charged Higgs is $\theta = \frac{\pi}{4}$, whereas mild breaking of the $\mu - \tau$ symmetry results in a mild deviation $\theta \sim \frac{\pi}{4}$. This close connection between the $\mu - \tau$ symmetry and the doubly charged mixing angle significantly effects the doubly charged Higgs-dileptonic vertices. In the exact $\mu - \tau$ limit, the vertex factors $H_2^{++} - \mu - \tau$ and $H_2^{++} - e - e$ are zero, hence the doubly charged Higgs H_2^{++} never decays to $\mu^+ + \tau^+$ or to $2e^+$ states. Other than this, the non observation of the $e\mu$ and $e\tau$ states in the dileptonic decay of the doubly charged Higgs would possibly disfavor the inverted mass hierarchy of the standard model neutrino. The presence of Higgs triplet predicts lepton flavor violating processes such at $\tau \to ee\mu$ at the tree level. This and other lepton flavor violating processes could therefore be used to constrain the model as well as the neutrino mass hierarchy.

Bibliography

[1] **Two Higgs doublet type III seesaw with $\mu - \tau$ symmetry at LHC,**
P. Bandyopadhyay, S. Choubey and M. Mitra,
JHEP **0910**, 012 (2009) [arXiv:0906.5330 [hep-ph]].

[2] **Spontaneous R-parity violating type III seesaw,**
S. Choubey and M. Mitra,
JHEP **1005**, 021 (2010) [arXiv:0911.2030 [hep-ph]].

[3] **$\mathbf{A_4}$ flavor symmetry and neutrino phenomenology,**
B. Brahmachari, S. Choubey and M. Mitra,
Phys. Rev. D **77**, 073008 (2008) [arXiv:0801.3554 [hep-ph]].

[4] **Lepton masses in a minimal model with triplet Higgs bosons and S_3 flavor symmetry,**
M. Mitra and S. Choubey,
Phys. Rev. D **78**, 115014 (2008) [arXiv:0806.3254 [hep-ph]].